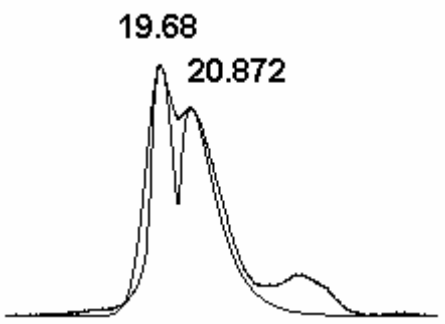

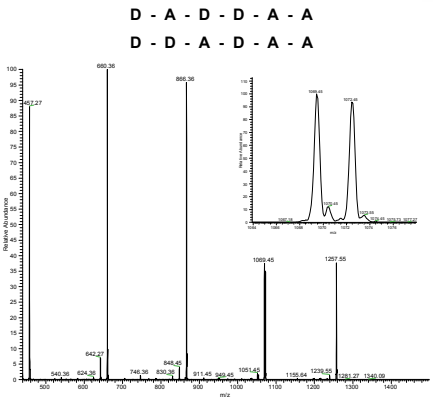

MASS SPECTROMETRIC ANALYSIS OF CHITOOLIGOSACCHARIDES AND THEIR INTERACTION WITH PROTEINS

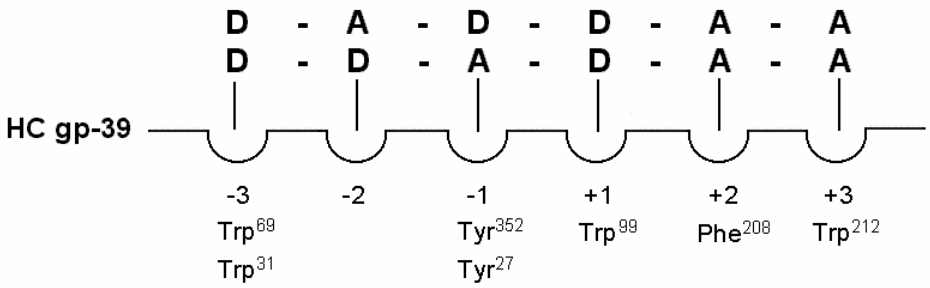

SVEN BAHRKE

Universität Potsdam
Institut für Chemie
Arbeitsgruppe Prof. Dr. M. G. Peter

Mass Spectrometric Analysis of Chitooligosaccharides and their Interaction with Proteins

Dissertation
zur Erlangung des akademischen Grades
„doctor rerum naturalium“
(Dr. rer. nat.)
in der Wissenschaftsdisziplin „Naturstoffchemie“

eingereicht an der
Mathematisch-Naturwissenschaftlichen Fakultät
der Universität Potsdam

von
Sven Bahrke

Potsdam, den 9.3.08

Die vorliegende Arbeit wurde an der Universität Potsdam, Institut für Chemie, Abteilung Naturstoffchemie unter Leitung von Prof. M. G. Peter angefertigt.

Danken möchte ich an dieser Stelle meiner Familie, den Mitarbeitern der Arbeitsgruppe von Prof. Dr. M. G. Peter sowie Dr. Sophie Haebel vom Interdisziplinären Zentrum für Massenspektrometrie von Biopolymeren.

Teile dieser Arbeit wurden bereits an folgender Stelle veröffentlicht:

1) S. Bahrke, J. M. Einarsson, J. Gislason, M. G. Peter (2007) Protein-ligand interactions of chitooligosaccharides with the chitolectin HC gp-39 and with chitinases, 8th International Conference of the European Chitin Society, EUCHIS, Antalya, Turkey, Sep. 8 - 11, 2007.
2) F. H. Cederkvist, A. Zamfir, M. Mormann, M. P. Parmer, M. Fröesch, S. Bahrke, K. M. Vårum, M. G. Peter, V. G. H. Eijsink, J. Peter – Katalinić, M. Sørlie (2007) Chitinase – chitooligosaccharide interactions as seen through the eyes of mass spectrometry, 8th International Conference of the European Chitin Society, EUCHIS, Antalya, Turkey, Sep. 8 - 11, 2007.
3) S. Haebel, S. Bahrke, M.G. Peter (2007) Quantitative sequencing of complex Mixtures of heterochitooligosaccharides by vMALDI-linear ion trap mass spectrometry. *Anal. Chem.* **79**, 5557.
4) F. H. Cederkvist, A. D. Zamfir, S. Bahrke, V. G. H. Eijsink, M. Sørlie, J. Peter-Katalinić, M. G. Peter (2006) Identification of a high-affinity binding oligosaccharide by (+)nanoelectrospray quadrupole time-of-flight tandem mass spectrometry of a non-covalent enzyme-ligand complex. *Angew. Chem. Int. Edn.* **45**, 2429.
5) D. Ciechańska, S. Bahrke, S. Haebel, H. Struszczyk, M. G. Peter (2005) Incorporation of glucose into chitosan by *Acetobacter xylinum*. *Adv. Chitin Sci.* (Eds.: H. Struszczyk, A. Domard, M. G. Peter, H. Pospieszny), Poznań, Institute of Plant Protection, **8**, 140.
6) M. G. Peter, S. Bahrke, S. Haebel (2005) Isolation and structure analysis of aminoglucan heterooligosaccharides (Poster), 1st Brazilian Conference on Mass Spectometry, BrMASS, Campinas, SP, Brazil, Nov. 20 – 22, 2005.
7) S. Haebel, S. Bahrke, P. Sümmchen, M. G. Peter (2005) Simultaneous sequencing and quantification of the components of an isobaric mixture of linear heterochitooligosaccharides by MALDI-LTQ mass spectrometry (Poster), 2nd Glycanforum, Berlin, Germany, Nov. 24 – 25, 2005.
8) M. G. Peter, S. Bahrke, S. Haebel, S. Sveinsdottir, J. M. Einarsson (2004) Isolation, structure analysis, and applications of chitooligosaccharides, III Iberoamerican Symposium on Chitin and Chitosan, Cordoba, Spain, Sep. 26 – 29, 2004.
9) F. R. Thormodsson, J. M. Einarsson, J. Gislason, S. Bahrke, M. G. Peter (2004) Growth promoting effect of chitooligosaccharides on chondrocytes in culture (Poster),

6th International Conference of the European Chitin Society, EUCHIS, Poznań, Poland, Aug. 31 – Sep. 3, 2004.

10) S. Bahrke, D. Ciechanska, S. Haebel, H. Struszczyk, M. G. Peter (2004) Incorporation of glucose into chitosan by Acetobacter xylinum (Poster), 6th International Conference of the European Chitin Society, EUCHIS, Poznań, Poland, Aug. 31 – Sep. 3, 2004

Zur Publikation vorbereitete Manuskripte:

1) S. Bahrke, N. C. How, J. M. Einarsson, M. G. Peter, Quantitative analysis and preparation of heterochitooligomers, homologs, and isomers.
2) S. Bahrke, J. M. Einarsson, J. Gislason, M. G. Peter, The potency of heterochitooligomers to inhibit family 18 chitinases depends on DP, FA, and sequence of D and A units.
3) S. Bahrke, J. M. Einarsson, J. Gislason, M. G. Peter, Partially acetylated chitooligosaccharides bind with high affinity to the 39 kDa human cartilage glycoprotein HC gp-39.

Weitere Publikationen und Konferenzbeiträge:

1) S. Bahrke, J. M. Einarsson, J. Gislason, S. Haebel, M. C. Letzel, J. Peter-Katalinić, M. G. Peter (2002) Sequence analysis of chitooligosaccharides by matrix-assisted laser desorption ionisation post source decay mass spectrometry. *Biomacromol.* **3**, 696.
2) S. Bahrke, S. Haebel, M. G. Peter, M. C. Letzel, J. M. Einarsson, J. Gislason, J. Peter-Katalinić (2003) Sequence analysis of chitooligosaccharides by MALDI PSD mass spectrometry (Poster), Symposium "Glycane und Glycomimetica in Medizin und Pharmazie", Charité – Universitätsmedizin, Berlin, Germany, 14.11.03.

Patente:

1) J. M. Einarsson, J. Gislason, M. G. Peter, S. Bahrke (2004) Pharmaceutical composition comprising chitooligomers, PCT Int. Appl. 03026677 WO Application Date 04-03-03.
2) J. Gislason, J. M. Einarsson, N. C. How, S. Bahrke (2006) Compositions of partially deacetylated chitin derivatives, PCT Int. Appl. WO 2006134614 Application Date 06-12-21

Abbreviations

0-…

^{1}H-NMR	proton nuclear magnetic resonance
2D	two dimensional
^{3}J	three bond coupling constant
4-MU	4-methylumbellyferone / 4-methylumbellyferyl derivative
^{13}C-NMR	nuclear magnetic resonance of the 13-carbon nuclide

A

A	*N*-acetylglucosamine (acetylated)
A*	trideuterio *N*-acetylglucosamine
Ac_2O-d_6	hexadeuterio acetic acid anhydride
AKT	protein kinase B
AMAC	2 aminoacridone
AMCase	acidic mammalian chitinase
AMCR	3-(acetylamino)-6-aminoacridine
amu	atomic mass unit

B

B_{max}	concentration of the inhibitor that reduces the protein activity by 100%
Brp-39	breast regressing protein 39 kDa

C

CEC	cation exchange chromatography
Chi A	chitinase A from *Serratia marcescens*
Chi B	chitinase B from *Serratia marcescens*
ChO	chitooligosaccharide
CID	collision induced dissociation

D

D	glucosamine (deacetylated)
DP	degree of polymerisation

E

ERK 1	extracellular-signal regulated kinase, isoform 1
ERK 2	extracellular-signal regulated kinase, isoform 2
ESI	electro spray ionization

F

F	fluorescence intensity
F_A	molar fraction of A units
FAB	fast atom bombardment
FWHM	full width at half maximum

G

GAG	glucosaminoglycan

H

H	hexose
HC gp-39	human cartilage glycoprotein molecular weight 39 kDa
HCT	human chitotriosidase
HPAEC-PAD	high performance anion exchange chromatography with pulsed amperometric detection

I

IC_{50}	concentration of inhibitor that reduces protein activity by 50%
IEC	ion exchange chromatography
IL-4	interleucin-4

K

K_a	association constant
K_d	dissociation constant
K_i	dissociation constant for inhibitor binding
K_m	Michaelis constant

L

M

MALDI-TOF MS	matrix assisted laser desorption ionisation time-of-flight mass spectrometry
MALDI-QTOF MS	matrix assisted laser desorption ionisation quadrupole time-of-flight mass spectrometry
MAP kinase	mitogen-activated protein kinase
MGP-40	40-kDa mammary gland protein
MS^2	MS/MS (tandem mass spectrometry)
MUC9	mucin 9

N

nanoESI-QTOF MS	nano electrospray ionization quadrupole time-of-flight mass spectrometry

P

PI 3 K	phosphoinositide-3 kinase
PSD	post source decay

R

RI	refractive index

S

SI-CLP	stabilin-1 interacting chitinase-like protein
STD-NMR	saturation-transfer difference nuclear magnetic resonance

T

T	tag
Th 2	T cell-helper

TIM barrel	triosephosphate isomerase barrel

U

U	unit

V

W

w_h	peak width at half peak height

Y

Z

Contents

2.5 *Partially Acetylated Chitooligosaccharides Bind with High Affinity to the 39 kDa Human Cartilage Glycoprotein HC gp-39*. S. Bahrke, J. M. Einarsson, J. Gislason, M. G. Peter, Manuscript prepared for publication.

2.6 *Identification of a High-Affinity Binding Oligosaccharide by (+)Nanoelectrospray Quadrupole Time-of-Flight Tandem Mass Spectrometry of a Non-Covalent Enzyme-Ligand Complex.* F. H. Cederkvist, A. D. Zamfir, S. Bahrke, V. G. H. Eijsink, M. Sørlie, J. Peter-Katalinić, M. G. Peter, *Angew. Chem. Int. Edn.* **2006**, *45*, 2429.

2.7 *Growth Promoting Effect of Chitooligosaccharides on Chondrocytes in Culture.* F. R. Thormodsson, J. M. Einarsson, J. Gislason, S. Bahrke, M. G. Peter, (Poster), 6th International Conference of the European Chitin Society, EUCHIS, Posnań, Poland, Aug. 31- Sep. 3, 2004.

2.8 *Protein-Ligand Interactions of Chitooligosaccharides with the Chitolectins HC gp-39 and with Chitinases.* S. Bahrke, J. M. Einarsson, J. Gislason, M. G. Peter, 8 th International Conference of the European Chitin Society, EUCHIS, Antalya, Turkey, Sep. 8 – 11, 2007.

1.0 Introduction

1.1 Structure of Chitooligosaccharides

Oligosaccharides, which are composed of β-1,4-linked *N*-acetylglucosamine and / or glucosamine, are named chitooligosaccharides (ChO's).[1] Homochitooligosaccharides are oligomers of *N*-acetylglucosamine / GlcNAc (A) or glucosamine / GlcN (D). They are obtained by hydrolysis of chitin ($F_A = 1.00$) or chitosan ($F_A = 0.00$), respectively.[2] Hydrolysis of chitin or chitosan of $0.00 < F_A < 1.00$ gives heterochitooligosaccharides which are always obtained as complex mixtures containing compounds of different oligomers (i. e. different DP), homologs (i. e. different F_A, but same DP), and isomers (different sequence of D and A units, but same DP and F_A).[2, 3] The number of homologs comprising one oligomer is DP + 1; the number of isomers comprising one homolog D_xA_y is $(x + y) ! / (x ! * y !)$.[2] Table 1 shows that the number of all compounds comprising one oligomer is increasing exponentially with the DP.

Table 1. Number of isobars comprising heterochitooligosaccharides (F_A 0.50 to 0.67) of DP3, 6, 9 and 12.

DP	Homolog (F_A)	Number of Isomers
3	D_1A_2 (0.67)	3
6	D_3A_3 (0.50)	20
9	D_4A_5 (0.56)	126
12	D_6A_6 (0.50)	924

The hydrolysis of chitin or chitosan is either performed enzymatically or chemically. The hydrolysis of α-chitin proceeds slowly as it is insoluble in common solvents. Thus, chitin is commonly solubilized by deacetylation to chitosan previous to the hydrolysis. In order to deacetylate chitin under homogeneous conditions, α-chitin is transformed to colloidal chitin, microcrystalline chitin or organic co-solvents are added to the deacetylation reaction mixture. Deacetylation of chitin affords chitosan, which is soluble in diluted acids.

For the partial enzymatic hydrolysis of chitosan chitinases,[4] chitosanases,[5] or other glycosyl hydrolases (e.g. lysozyme,[6] hemicellulases,[6] cellulases[7]), proteases (e.g. papain,[6] pronase[8]) or esterases (e.g. lipases[6]) can be employed.

For the chemical partial hydrolysis of chitosan commonly concentrated hydrochloric acid is employed.[9] In less cases phosphoric acid is used. The degradation with HCl gas is performed

as a solid phase reaction with HCl gas flushing through a tube filled with chitosan.[10] The degradation with the nitrosyl cation (prepared in situ from a mixture of sodium nitrite and hydrochloric acid) gives anhydromannosyl derivatives of chitooligosaccharides. This reaction is easy to control as specifically amino groups are attacked under mild conditions.[11] The oxidative hydrolysis employing hydrogen peroxide or the ozonolysis of chitosan give partially oxidised reaction products (lactones, gluconic acids or glucuronic acids).[12] The hydrofluorolysis of chitosan (in dry hydrogen fluoride liquid) gives α-1-fluoro chitooligosaccharides which are the base of further activated chitooligosaccharides.[13] The hydrolysis of chitosan under acetylation conditions (sulfuric acid / acetic anhydride) gives per-*N*,*O*-acetylated chitooligosaccharides.[14]

The chemical synthesis of heterochitooligosaccharides has not yet been described. Only the synthesis of protected chitooligosaccharides up to DP 12 is reported.[15] The effort in time and chemicals is high, especially if libraries of heterochitooligosaccharides are demanded. Combinatorial solid phase synthesis could be an efficient alternative for the preparation of defined heterochitooligosaccharides, which, however has not yet been realized in the case of heterochitooligosaccharides. For a general description of the method of combinatorial solid phase synthesis of carbohydrates see [16], [17], [18].

Alternatively to a completely synthetic route, chitooligosaccharides are obtained by chemo-enzymatic synthesis. The chemo-enzymatic synthesis aims on the reversion of the enzymatically catalysed hydrolysis reaction. For this purpose either organic co-solvents are added to the reaction mixture, which allow keeping monomers and small oligomers in solution but precipitating oligosaccharides of higher DP. [19, 20] Alternatively catalytically impaired glycosyl hydrolases are employed in combination with activated educts mimicking the transition state of the hydrolysis reaction.[21]

1.2 Analysis of Chitooligosaccharides

The analysis of ChOs is important for e.g. quality control or the evaluation of the results of biological tests.

1.2.1 Separation of chitooligosaccharides

Chromatographic methods were applied for the separation of oligomers and homologs. Separations of mixtures composed of homooligomers of either glucosamine or

N-acetylglucosamine by GPC affords rather pure oligomers.[2, 9] Mixtures of heterochitooligosaccharides obtained from the hydrolysis of chitosan with chitinase B from *S. marcescens* were separated by GPC.[3] Analysis by ^{1}H and ^{13}C-NMR revealed mixtures of oligosaccharides of different DP, F_A and sequences indicating that the resolution is decreased due to overlapping peaks of oligomers and homologs.[22, 23]

Cation exchange chromatography (CEC) separates molecules according to their overall charge. In solutions of pH < 6.2, when the amine groups of the glucosamine residues are protonated, chitosan is a positively charged polymer; so are GlcN containing chitooligomers.[24]

Amino phases which are widely used for the separation of sugars were successfully employed for the separation of *N*-acetylglucosamine homooligomers and moreover for the separation of heterochitooligomers of DP ≤ 5, although the performance of that material is not comparable to CEC or GPC materials.[25, 26]

Quaternary ammonium phases were used in alkaline solutions for anion exchange chromatography of amino sugars. In alkaline solutions the free electron pairs of the hydroxyl oxygen, the amino nitrogen and the amide nitrogen as well as deprotonated forms of these functional groups interact with the quaternary ammonium groups of the stationary groups resulting in a separation of heterochitooligomers and homologs.[27]

ChOs of DP ≤ 6 have been sequentially degraded by using exo-glucosaminidases and exo-*N*-acetylglucosaminidases. The fragments were reacetylated and identified by chromatography [28, 29] as well as mass spectrometry, [25] allowing to conclude the sequences of heterochitooligosaccharides.

The structure analysis of a partial hydrolysate of chitosan by NMR gave information concerning the reducing and non-reducing end monomer units as well as their nearest to neighbours allowing for the determination of diads and triads.[30, 31]

1.2.2 Mass Spectrometry

FAB- and MALDI-TOF MS were extensively employed for the analysis of mixtures of *N*-acetylglucosamine homooligomers, glucosamine homooligomers and lipochitooligosaccharides. But also mixtures of heterochitooligomers of DP ≤ 17 were studied and mapped by MALDI-TOF MS.[32, 33, 34] Besides for the analysis of oligomers and homologs, MALDI-TOF PSD MS was successfully employed for the sequence analysis of heterochitooligosaccharides of DP ≤ 12 after tagging of the reducing end.[2]

It should be mentioned that the mass spectrometric methods described so far give only qualitative results for mixtures of oligomers, homologs and isomers. A quantitative method was developed in the course of the present thesis (see Chapter 2).

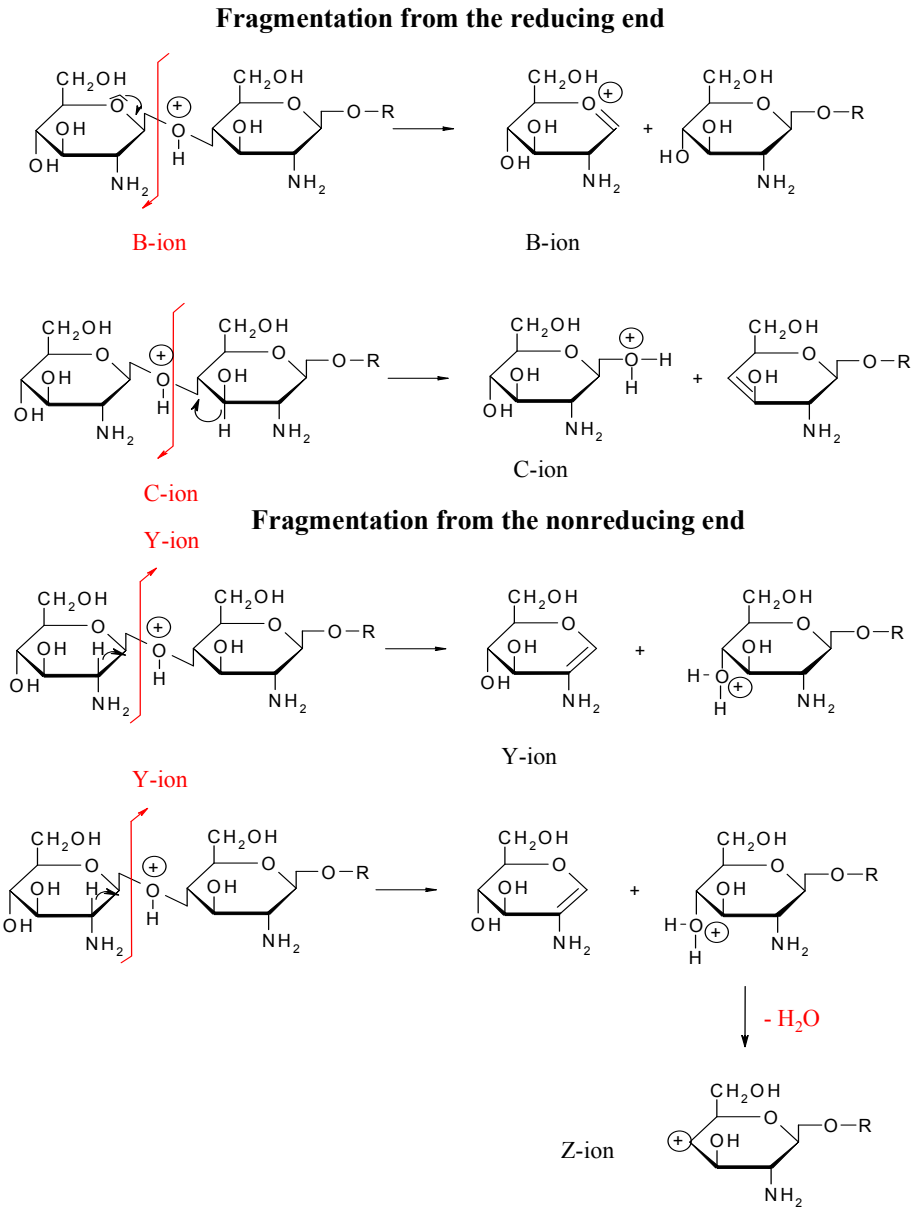

Figure 1. Fragmentation of chitosan homooligosaccharides in FAB or CID mass spectrometry in analogy to B. Domon et al.[35] showing the formation of B-, C-, Y- and Z-type ions. Less frequent ring fragmentations are not depicted.

In FAB- or CID- fragmentation, oligosaccharides fragment almost exclusively by cleavage of the glycosidic bond yielding Y- and Z-type ions if the charge is retained on the reducing end or B- and C-type ions if the charge is retained on the non-reducing end, respectively (Figure

1). Due to overlapping m/z values for ions of identical monosaccharide composition, we cannot distinguish between fragmentations of native chitooligosaccharides from the reducing or non-reducing end. Thus for sequencing, the introduction of a tag at the reducing end of the molecule is essential to distinguish B- from Z-type and C- from Y-type ions.[2, 35]

1.2.3 NMR Spectroscopy

NMR spectroscopy was employed for structure analysis of depolymerised chitosan.[36] The method yields information about the reducing and nonreducing end monosaccharide moieties as well as the variations in the nearest neighbours.[37] Therefore, information on the frequency of diads and triads is obtained.[37, 38, 39] The method is limitied to ChO's of low DP (< 5) and sample amounts of above 20 mg.[37, 39]

1.3 Properties and Biological Functions of Chitooligosaccharides

Chitooligomers of DP ≤ 10 are water-soluble. The water-solubility of chitooligosaccharides of DP > 10 depends on F_A and pH. Chitooligosaccharides are hygroscopic (especially DP 1 and 2 oligomers) and tend to be infested by fungi and to less extent bacteria. Moreover, ChO's like other sugars are sensitive to auto oxidation and should be stored at ambient temperature under dry inert conditions. For long-term storage the temperature should be kept below – 20°C. The shelf life of ChO's is significantly increased when they are stored in mixture with antioxidants like vitamin C or salts like sodium chloride.

The water-solubility of ChO's ("water-soluble chitosan") offers an interesting range of applications as these molecules show an increased bioavailability compared to the polymer chitosan. Whereas chitosan is currently not registered as an agent in medicine due to inconsistent product properties of different charges (e. g. with respect to the molecular mass), the smallest chitosan oligomer, glucosamine, is used as an analgesic for the treatment of rheumatic diseases like arthritis, osteoarthritis or osteoporosis. Glucosamine is the precursor for the biosynthesis of glucosaminoglycans, and it stimulates chondrocytes to produce GAG's, which are a main component of cartilage.[40] Several biological functions of chitosan could rather be attributed to ChO's. Chitosan coated bone, joint prostheses or implants made of chitosan containing ceramics promote the growth of human osteoblasts and extracellular matrix proteins. Chitooligosaccharides released through enzymatic hydrolysis e.g. by lysozyme are involved in this process accelerating the bone regeneration.

Chitooligosaccharides are thought to be primers for hyaluronan biosynthesis. Hyaluronic acid is thought to be the earliest evolutionary form of glucosaminoglycans. It is an important polysaccharide in cartilage, synovial fluid, vitreous humor of the eye and in the skin of vertebrates.[41] It may also play an important role in tissue organisation, morphogenesis, cancer metastasis, wound healing, and inflammation.[42] Hyaluronic acid is secreted from cells by an enzyme complex named hyaluronic acid synthases,[42] that are evolved from chitin or cellulose synthases. Supplying a mouse hyaluronan acid synthase with UDP-glucosamine and UDP-*N*-acetylglucosamine gave hyaluronan acid in vitro.[43] When the mouse hyaluronan acid synthases are incubated with UDP-*N*-acetylglucosamine alone, *N*-acetylglucosamine homooligosaccharides are obtained.[43]

Chitooligosaccharides are active as immune stimulators through activation of macrophages.[44, 45, 46] Chitooligosaccharides (especially A_5 and A_6) inhibit the production of nitric oxide (NO) by activated macrophages thus reducing cytotoxicity in cell proliferation during the inflammation processes in wound healing.[47, 48]

Other biological effects include antimetastatic and antiviral activities of chitooligosaccharides.[49, 50] Glucosamine homooligomers of DP ≥ 30 possess antimicrobial activity against several bacteria. Pigs that were fed with the vitamin C salts of chitooligosaccharides (0.1 – 0.4 % of the total mass of nutrition, 54 days) showed increased levels of lactic acid bacteria and *E. coli* in the gastro-intestinal tract, resulting in an improved food conversion ratio. Additionally, an increased antibody production and macrophage activity was measured indicating a strengthening of the humoral immunity in pigs.[51]

Chitooligosaccharides, in combination with a hypocaloric diet, were reported to reduce body weight, serum triglycerides and the total as well as low density lipoprotein cholesterol, but to increase the high density lipoprotein cholesterol. In addition, a lowering of the blood pressure was observed.[52, 53, 54]

Chitooligosaccharides are produced in vivo during the development of vertebrates (e. g. Xenopus, zebra fish and mouse). The chitinase-like DG42/ hyaluronan acid synthase subfamily synthesizes both, chitooligosaccharides and hyaluronan acid during cell differentiation.[55] ChOs have been shown to be vital for a normal anterior/ posterior axis formation in the late gastrula [56] (for a revue see [57]).

In plants, chitooligosaccharides elicit defence reactions like the induction of chitinases or of metabolites of the shikimate pathway (e.g. lignin). Chitooligosaccharides stimulate the production of secondary metabolites in plant cell cultures. Besides, chitooligosaccharides induce cell division in the cortex of leguminosae by nodulation factors. In plants, oligomers of

DP5 - 7 are more active than DP1 - 4. The reason has been related to the ability of special lectins (chitolectins, chitinase-like proteins, CLPs) to bind chitooligosaccharides.[58, 59, 60, 61]

1.4 Enzymes Degrading Chitinous Material

1.4.1 Occurrence, Properties and Biological Functions of Chitinases

Chitin has a structural function for fungi, insects, molluscs and crustaceans. In these organisms the chitin fibrils have to be remodelled or degraded for normal development. The controlled hydrolysis of chitin is performed by chitinases and *N*-acetylglucosaminidases. Besides, organisms that do not contain chitin produce chitinases.

Bacteria

Bacteria use chitin for nutrition thus requiring a large supply of small fragments. For that reason bacterial chitinases act processively and produce mainly A_2 as the end product of hydrolysis.[62]

Many marine bacteria contain chitinases as their hosts, zooplankton, molluscs and crustaceans produce large amounts of chitin. Also soil contains chitin-degrading bacteria like *Serratia marcescens*. This bacterium produces extracellular chitinases, which are able to degrade chitin within the fungal cell wall.

Rhizobia are symbiotic plant bacteria produce lipo-chitooligosaccharides consisting of A_3 to A_6, containing fatty acid and sugar substitutions at the *N*-acetylglucosamine residues. These lipo-chitooligosaccharides are named Nod factors as they elicit the morphogenesis of nitrogen-fixing nodules on the roots of specific host plants, where the substitution pattern of the Nod factor determines host specificity. On the other hand, Nod factors elicit plant defence responses including an increase in chitinase activity. The pathways of degradation by plant root chitinases depend on the substitution pattern of the Nod factors and differ between root chitinases of different legumes. It is proposed that host recognition takes place not only by the specificity of Nod factor receptors, but also by hydrolysis of Nod factors by chitinases. In this way, the induction of chitinases might regulate nodule formation and prevent secondary infection.[63, 64]

Fungi

In most fungi, chitin is located in the inner cell wall. Fungal cell walls grow through hyphae, which elongate by apical deposition of wall polysaccharides. To allow apical growth and formation of hyphal branches, the cell wall needs to be softened, requiring chitinases. Moreover, many soil fungi have an inducible chitinolytic system for nutrition purpose, which is repressed in the presence of glucose.[65, 66]

Plants

Plants use chitinases in their defence against chitinous pathogens. For that purpose plant chitinases have to damage the cell wall of a pathogen within a short time, so that they attack the chitin chains randomly and form larger chitooligosaccharides.

Invertebrates

Invertebrates need chitinases during the process of moulting. The exoskeleton of insects consists mainly of chitin and protein. Prior to moulting, the old cuticle has to be broken down employing a mixture of chitinases and trypsin-like proteases.[67, 68]

Fish

In vertebrates, chitinases serve for food processing and defence against parasites and generally against pathogens. Fish have chitinolytic activities in their blood and the digestive tract. It has been suggested that fish gastric chitinolytic enzymes are mainly used for food processing as toothless fish show the highest gastric chitinase activity. In blood, chitinolytic enzymes are mostly found in the white blood cells, suggesting that these enzymes contribute to the defence against pathogens.[69, 70]

Mammals, including Man

In mammals, including *Homo sapiens*, high chitinolytic activity was determined in the blood serum, stomach and intestine, whereas lung, tongue and kidney showed lower, though significant levels.

The chitinolytic activity is presently attributed to two distinct chitinases. One of them, human chitotriosidase HCT (named by its ability to cleave A_3), is found at increased plasma levels in patients suffering from Gaucher disease, a rare genetic disorder that is caused by a mutation in the glucocerebrosidase gene. [71] This chitinase is found at high levels in the human blood, expressed in macrophages (and at decreased levels in the lung). [72] It putatively serves for the

defence against pathogens, like fungi or nematodes, which synthesize chitin during several stages of their life cycle. [73, 74] However, a recessively inherited deficiency in chitotriosidase activity is frequently encountered, suggesting that this enzyme no longer fulfils an important defence function under normal circumstances or, alternatively, that other enzymes may compensate the lack of functional human chitotriosidase. [71, 74]

This role could be taken by the other known mammalian chitinase, which was found at increased levels in the stomach of mice. [75] The predominant pH optimum for the chitinolytic activity of this enzyme is 2.3 (in contrast to human chitotriosidase, which is catalytically impaired at this low pH), thus it is named acidic mammalian chitinase (AMCase). [75] Due to the low pH optimum and its main occurrence in the stomach, AMCase is putatively involved in the processing of food. [75] However, it could be additionally important for the defence against pathogens, at least in cases where human chitotriosidase is catalytically impaired. [76]

The overproduction of AMCase was recently linked to asthma development. [77, 78] Asthma is a chronic disease characterized by exaggerated Th2 airway inflammation. [77, 79] In a mouse model of ovalbumin-induced bronchial asthma, the administration of anti-AMCase antibody leads to a decrease of Th2 inflammation.[80]

1.4.2 Families of Enzymes Degrading Chitinous Material

Glycosyl hydrolases are grouped into families according to similarities in their amino acid sequences. Presently, 111 families are listed in the CAZY database.[81] Chitinolytic enzymes are found in family 5 (chitosanases), family 8 (chitosanases), family 18 (chitinases and endo-β-*N*-acetylglucosaminidases), family 19 (chitinases), family 20 (β-hexosaminidases and chitobiases), and family 46, 75, 80 (chitosanases).[5] Besides, also proteases etc. can be considered as chitinolytic, which are not regarded for the comments below.

1.4.3 Family 5 Chitosanases

Chitosanases, in contrast to chitinases, show a maximum of activity on high-deacetylated chitosan. The catalytic mechanism of chitosanases requires two acidic amino acid residues. Tanabe et al. [82] characterized two chitosanases, ChoI and ChoII, from *Streptomyces griseus* HUT 6037. These enzymes hydrolyse not only chitosan but also carboxymethylcellulose with retention of the anomeric form. Both enzymes require a D unit located at subsite –1 for successful hydrolyses, with no preference for A or D at subsite +1.

1.4.4 Family 8 Chitosanases

The best characterized chitosanase belong to this family was found in *Bacillus* sp. No.7M.[83] This chitosanases requires D units located at both, subsite –1 and subsite +1, for successful hydrolyses of the glycosidic bond. Other extensively studied chitosanases belonging to this family are produced by *Bacillus circulans* WL-12[84] and *Paenibacillus fukuinensis* strain D2[85].

1.4.5 Family 18 Chitinases

The family 18 of glycosyl hydrolases contains chitinases from insects, fungi, mammals, bacteria, viruses and plants, and endo-β-*N*-acetylglucosaminidases, which cleave between two *N*-acetylglucosamine units in glycans and glycoproteins. [86] Several of the family 18 chitinases possess a chitin binding besides the catalytic domain. [87] Examples are chitinases A and B from the bacterium *Serratia marcescens* that possess a fibronectin type III domain. Deletion of the binding domain does not affect the substrate affinity of the enzyme, but influences the rate of hydrolysis. [88]

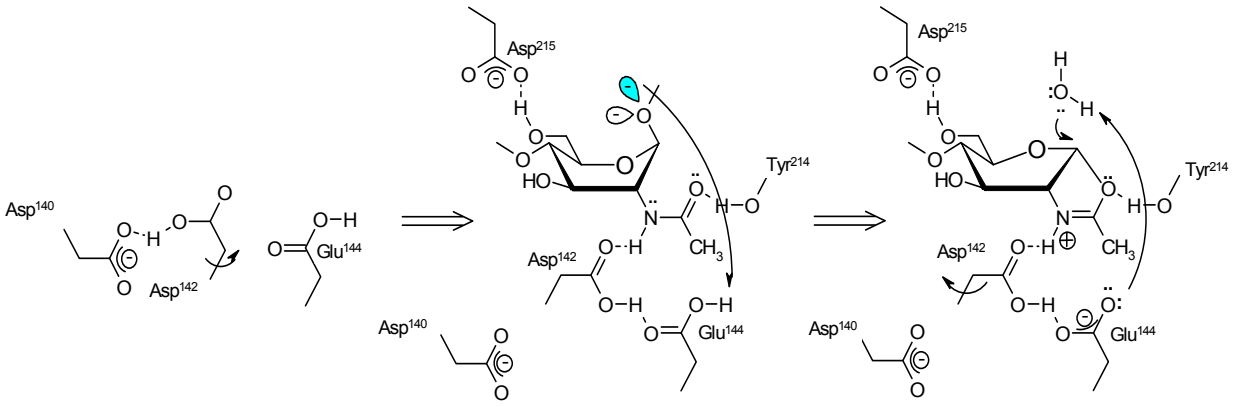

Figure 2. The mechanism of catalysis of family 18 chitinases for the example of chitinase B from Serratia marcescens. The core of the catalytic centre is formed by the ensemble of deprotonated Asp[140], Asp[142] and Glu[144]. Glu[144] protonates the glycosidic bond of the saccharide. Asp[142] supports the formation of the oxazolinium ion and thus the anchimeric assistance of the acetamido group of the A unit in subsite –1 via stabilization of the nitrogen proton. The formation of the oxazolinium ring is additionally supported by Tyr[214]. Deprotonated Glu[144] stabilizes the proton of a water molecule, which attacks C-1, opens the oxazolinium ring to form the final hydrolysis product. During catalysis the sugar moiety bound to subsite –1 takes up different conformations: chair (solution) – skewed boat (binding state) – half-chair (oxazolinium ion). The mechanism of catalysis is unique for all family 18 chitinases including the essential glutamate residue. Only the indices of amino acid residues differ within family 18 chitinases. The figure was essentially taken from literature [89].

The catalytic domain of all family 18 chitinases consists of a $(\beta/\alpha)_8$-barrel with a deep substrate-binding cleft formed by the loops following the C-termini of the eight parallel β-strands. A glutamic residue at the C-terminus of β-strand 4 has been identified as the essential

proton donor for catalysis as was shown by site-directed mutagenesis.[89] The unique mechanism of chitin / chitosan hydrolysis by family 18 chitinases is shown in Figure 2.

1.4.6 Chitinase A from *Serratia marcescens*

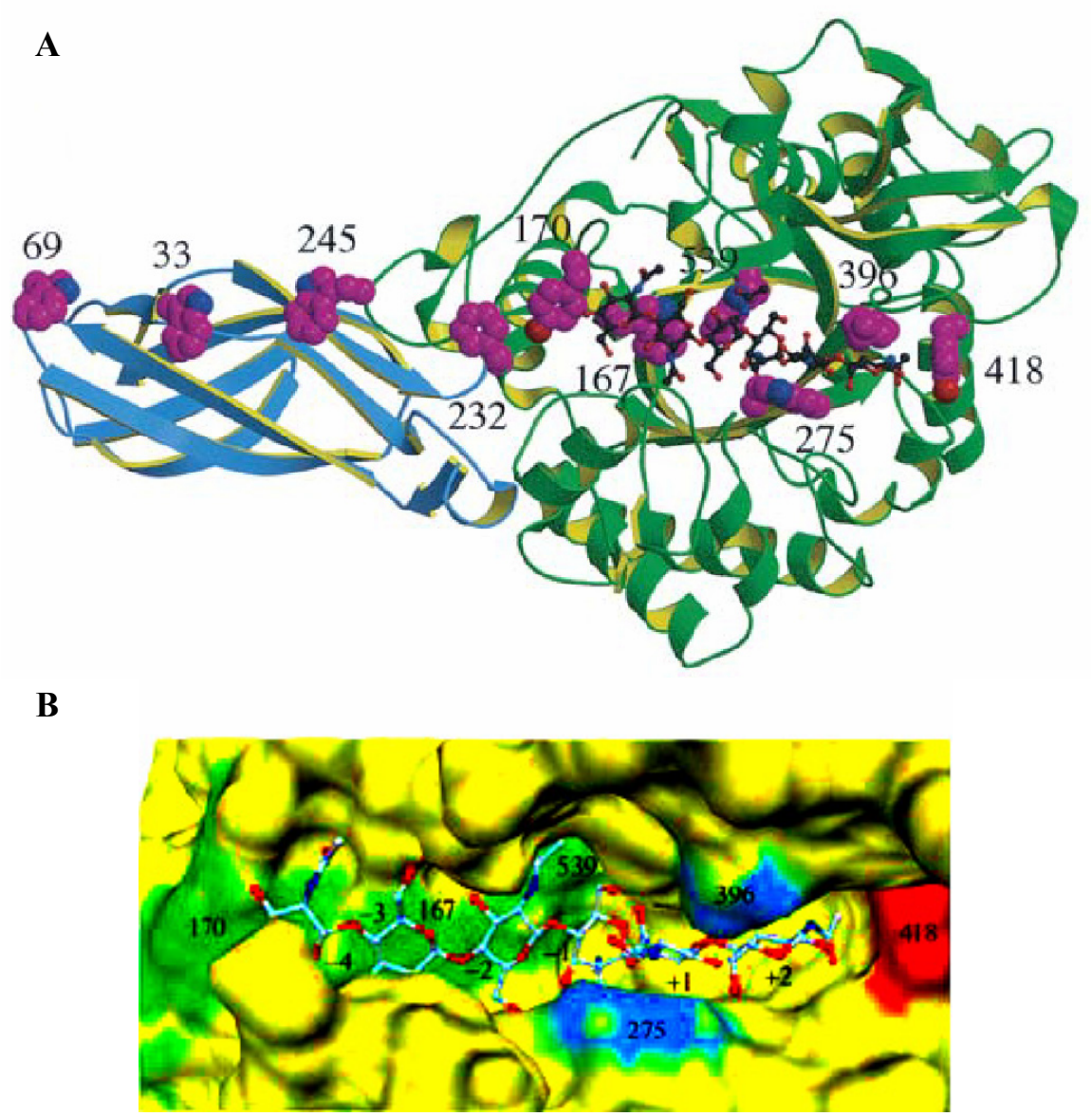

Figure 3. Three-dimensional structure and molecular surface of chitinase A mutant E315L. Data based on crystal structure analysis with the A_6 substrate in the binding cleft. (A) The N-terminal chitin-binding domain is shown in blue and the C-terminal catalytic domain in green. Aromatic residues that line the substrate-binding cleft are shown in space-filling mode. (B) Surface representation of the substrate binding cleft in ball-and-stick mode. The aromatic residues that interact with the substrate are highlighted. Tyr^{418} (red) interacts with the N-acetyl group of the reducing-end A unit. Phe^{396} and Trp^{275} (cyan) are on opposite sides of the cleft and stack against the hydrophobic faces of GlcNAc sites +2 and +1 respectively. Trp^{539}, Trp^{167} and Tyr^{170} (green) are at the bottom of the cleft and are positioned to interact with the hydrophobic faces of the A units at sites –1, –3 and –5 respectively.
Figures A – B were taken from literature [90].

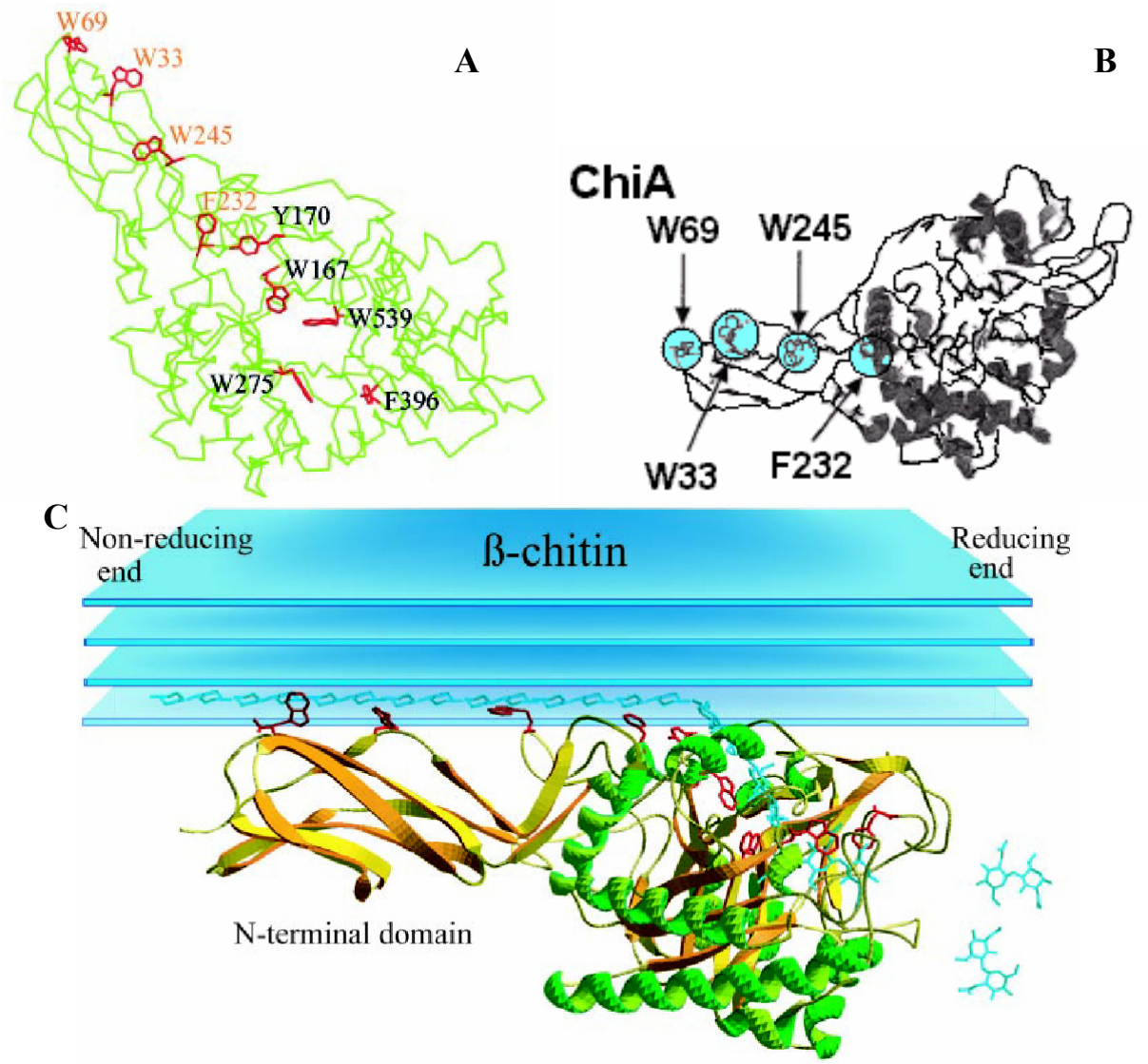

Figure 4. (A) Positions of aromatic residues in chitinase A from Serratia marcescens. A-carbon chain (green) of chitinase A with the side chains of aromatic residues (red). Four linearly aligned aromatic residues outside of the catalytic are labelled with orange letters. (B) Exposed aromatic residues of chitinase A. Exposed aromatic residues are shown on ribbon-drawings of the 3D structure of chitinase A (PDB ID: 1EDQ). Green indicates the bound chitin oligomer. (C) Model for crystalline β-chitin hydrolysis by chitinase A. Ribbon-drawing of the catalytic domain and the N-terminal chitin-binding domain with the side chains of aromatic residues (red) and a bound chitin chain (blue) which ranges from the chitin-binding domain (non-reducing end) into the catalytic domain (reducing end). Dimers (blue) are cut off from the reducing end. Figures A and C were taken from literature [91], figure B was taken from literature [92].

Chitinase A from *Serratia marcescens* contains the consensus sequences SXGG and DXXDXDXE of family 18 bacterial chitinases. The catalytic domain consists of a conserved $(\beta/\alpha)_8$ TIM barrel with a deep substrate-binding cleft.[91] The glutamic residue 315 at the C-terminus of β-strand 4 has been identified as the essential proton donor for catalysis.[90] Figures 3 – 4 display the structure of the family 18 chitinase A from *Serratia marcescens* and its catalytically impaired mutant E315L, as deduced from crystallographic data.[90] Figure 3B

shows a chitin hexamer modelled into the catalytic domain, [90] and Figure 4C shows a chitin chain which is bound with its non-reducing end to the N-terminal chitin binding domain and reaches with its reducing end into the catalytic domain where between subsites –1 and +1 disaccharide units are cut off. [91]

The catalytic domain of chitinase A forms a deep substrate-binding cleft [91], which is on one hand aligned with aromatic residues of the amino acids tryptophan, phenylalanin and tyrosin.[90] On the other hand, the binding cleft contains exposed residues of amino acids that are able to form hydrogen bonds with the substrate (mainly carboxylic and hydroxyl groups).[90] Glu^{315} takes a special role, as it is essential for hydrolysis by protonation of the glycosidic bond. [90] Positions of the binding cleft that are able to host segments of the substrate, e.g. monosaccharide units, are called subsites.

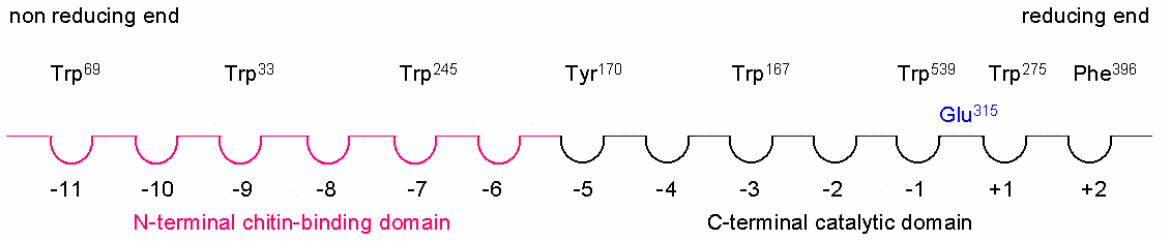

Figure 5. Schematic drawing of the N-terminal chitin-binding domain (red) and the C-terminal catalytic domain (black) of chitinase A with subsites ranging from –11 (non-reducing end) to +2 (reducing end). The catalytic site (with Glu^{315}) is positioned asymmetrically in the binding cleft between subsites –1 and +1. The catalytic domain ends at subsite +2. The drawing was made according to the discussions of the subsites of the C-terminal catalytic domain in reference [90] and the N-terminal chitin-binding domain in reference [91].

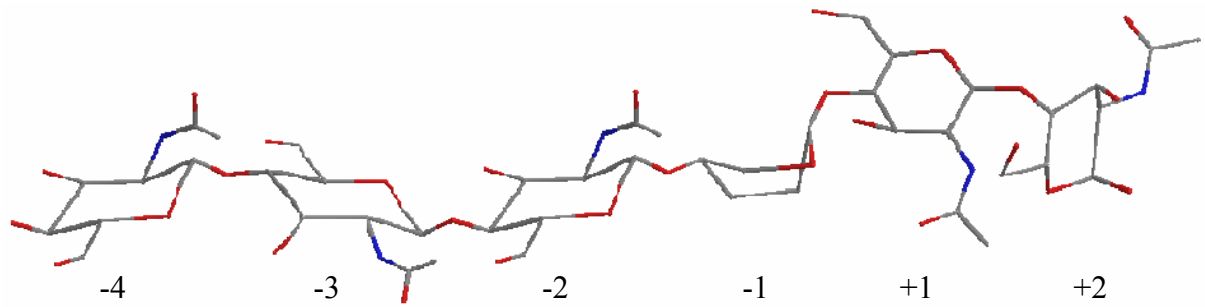

Figure 6. Schematic drawing of the arrangement of the monosaccharide units of a chitin hexasaccharide bound to chitinase A. The sugar moiety bound to subsite –1 takes up different conformations during catalysis: chair (unbound), twisted boat (bound), half-chair (oxazolinium ion).[93, 94] The twisted boat conformation of the A unit bound to subsite –1 results in an edgewise binding of the A units in subsites +1 and +2. [93, 94](Chem3D Pro 11.0 ®, carbon atoms: black, oxidation atoms: red, nitrogen atoms: blue)

Figures 5 – 6 show schematically the subsites of chitinase A. Negative subsites host the non-reducing end of the oligosaccharide chain, positive subsites the reducing end. The hydrolysis

reaction takes place between subsites –1 and +1. Glu^{315} is placed asymmetrically in the catalytic cleft which, according to crystallographic data of complexes with *N*-acetylglucosamine hexa- and octamers can at least accommodate seven *N*-acetylglucosamine units as crystal structures.[90] The disaccharide at +1 and +2 is the leaving group, i.e. the aglycon. Thus, chitinase A degrades chitin from the reducing end.[91] Hydrolysis occurs with retention of the anomeric configuration.[94] Double displacement at the glycosyl C-1 is accomplished by a substrate-assisted mechanism in which the carbonyl oxygen of the *N*-acetyl group at C-2 of the –1 *N*-acetylglucosamine, rather than a protein residue or a water molecule, acts as the nucleophile.[93] The glycosyl oxygen (O-1) of the –1 *N*-acetylglucosamine becomes protonated by the active site glutamic residue, and an oxazolinium intermediate is formed. This positively charged intermediate is stabilized through interaction with a conserved aspartic residue (Asp^{313} in chitinase A), located two amino acids upstream from the glutamic residue.[95] The substrate-assisted mechanism is facilitated by an induced conformational change in which the *N*-acetylglucosamine at –1 adopts a skewed-boat conformation, which results in a 90° twist of the linkage with the *N*-acetylglucosamine at +1.[90, 93, 94]

Substrate binding is controlled by a series of aromatic residues. The aglycon disaccharide is inserted edgewise into the cleft and, in chitinase A, interacts with three aromatic residues, Tyr^{418} and Phe^{396} at the +2 site and Trp^{275} at the +1 site.[90] Although Tyr^{418} appears to mark the end of the cleft, it does not interfere with the extension of the reducing end beyond the +2 site.[90] Trp^{275} and Phe^{396} form opposite sites of the cleft, stacking against the hydrophobic faces of the *N*-acetylglucosamine units.[90] The *N*-acetylglucosamine units of the aglycon part of the substrate have its hydrophobic faces aligned with the aromatic amino acid residues in the cleft floor, -1 (Trp^{539}), -3 (Trp^{167}), -5 (Trp^{170}).[90, 91, 96, 97] The sugars in the even-numbered subsites, -2 and -4, have their hydrophobic surfaces exposed.[91, 96]

Besides the C-terminal catalytic cleft, chitinase A possesses an N-terminal domain, named chitin-binding domain, which has a fibronectin type III fold. The chitin-binding domain contains four tryptophan residues (Trp^{33}, Trp^{69}, Trp^{232} and Trp^{245}), which are positioned correctly to correspond to binding sites for additional odd-numbered *N*-acetylglucosamine units.[91] The N-terminal chitin-binding domain extends the C-terminal catalytic domain beyond subsite –5 (Figure 5). The mutagenesis of Trp^{33} and Trp^{69} of the chitin-binding domain of chitinase A revealed that these amino acids are important for the degradation of chitin (crystalline β-chitin), but not for the degradation of chitooligosaccharides (Figure 4C).[91, 98] In contrast to the aromatic amino acid residues in the deep catalytic cleft, the

aromatic amino acid residues of the chitin-binding domain are exposed to the surrounding solution. Secondly, the number and intensity of hydrophobic and hydrogen bond interactions increases continuously from negative towards positive subsites with a maximum at the core of the catalytic cleft (subsites –1 and +1). Consequently, chitinase A contacts the chitin chain first with the chitin binding domain at the reducing end, which is moving along the gradient of increasing hydrophobic and hydrogen bond interactions to subsites +1 and +2. Hydrolysis takes place between subsites –1 and +1, and the reducing end disaccharide in subsites +1 and +2 is cleaved off. Afterwards, the enzyme moves by two *N*-acetylglucosamine units towards the non-reducing end and hydrolysis is repeated.[91, 98]

In case that the chitin (or chitosan) chain contains D units, hydrolysis is only processed successfully by family 18 chitinases like ChiA if an A unit is positioned in subsite –1. The cleaving rate for D-X bonds is 0, in contrast to A-X bonds (X = aglycon disaccharide unit). Thus, occasionally the enzyme moves four or more units towards the non-reducing end before the next successful hydrolytic event. Chitinase A is a processively acting enzyme with mainly exo-activity (cut-off of A_2). [90] However, also endo-activity was observed to some extent, meaning that the enzyme attacks the chitin chain randomly. Upon binding, the chitin chain extends beyond subsite +2. Chitinase A binds longer oligosaccharides with the reducing end preferentially located at subsite +2. But also in this case the analysis of hydrolysis products indicated that A units extend beyond subsite +2 to some extend (e.g. A_6, binding mode –3 to +2). [90] Binding a D residue at subsite –1 is non-productive and actually results in the case of chitooligosaccharides in competitive inhibition of the enzyme.

1.4.7 Chitinase B from *Serratia marcescens*

Chitinase B from *Serratia marcescens* contains the conserved motif DXXDXDXE of family 18 bacterial chitinases. The catalytic domain consists of a conserved $(\beta/\alpha)_8$ TIM barrel with a deep substrate-binding cleft. [99] The catalytic Glu^{144} is located at the end of β-strand 4 of the TIM barrel. This amino acid residue is the essential proton donor for catalysis. [100]

Figures 7 and 8 display the structure of the family 18 chitinase B from *Serratia marcescens* (PDB ID: 1E16) and its catalytically impaired mutant E144Q.

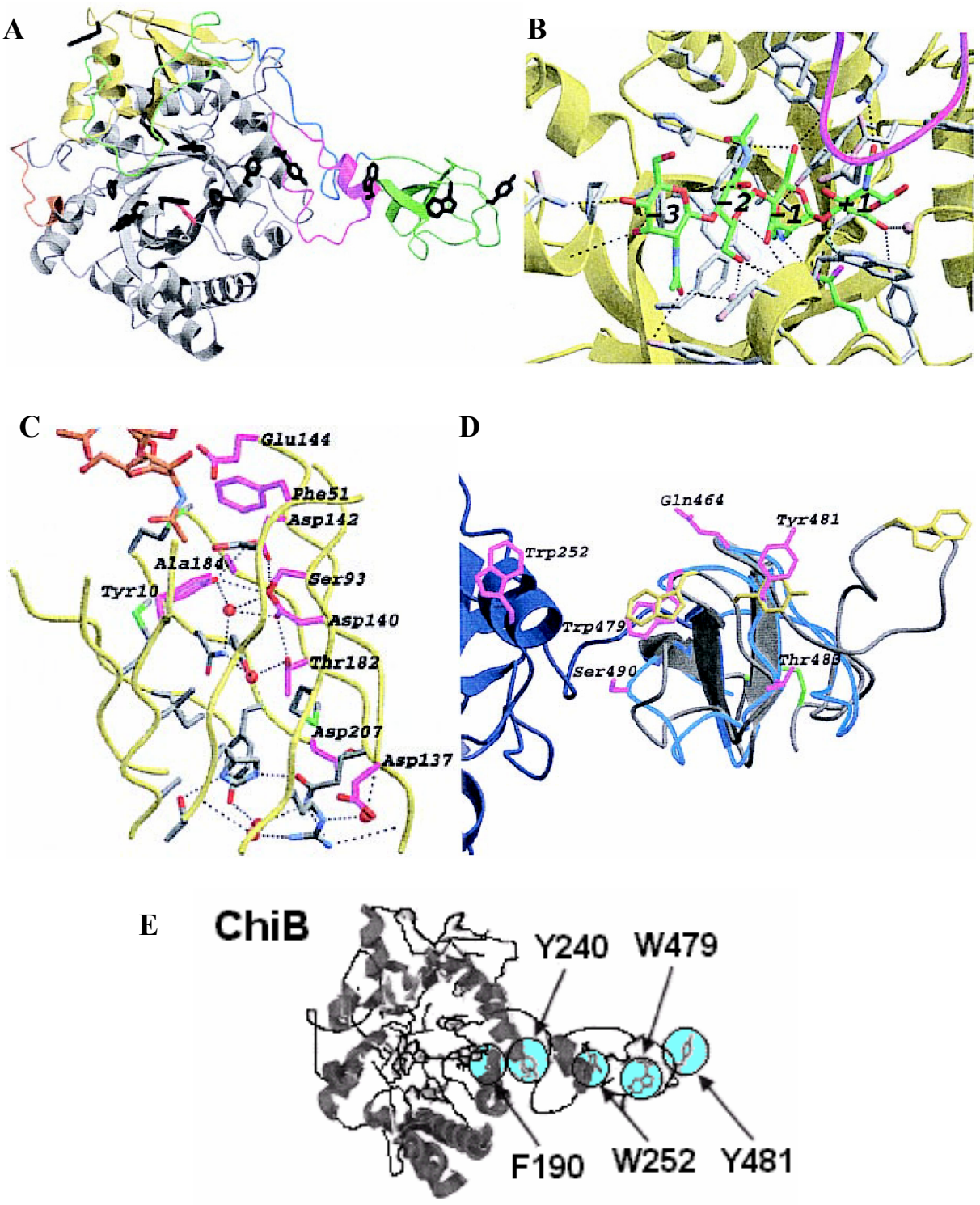

Figure 7. Three-dimensional structure and molecular surface of chitinase B, as deduced from crystallographic data.[92, 100] *(A) The structure of chitinase B, colour-coded to identify various domains. The TIM barrel (grey), the α/β-domain (yellow), the support loop (red), the linker (blue), and the chitin-binding domain (green). (B) and (C) Details of the catalytic domain of chitinase B.*[100] *(B) Active site with the modelled chitotetraose shown in a stick representation with the carbon coloured green. The chitinase B backbone is shown as a yellow ribbon. Side chains within 5 Å of the chitotetraose are depicted by grey sticks. Possible hydrogen bonds are drawn as black dashed lines. The four water molecules that are predicted to be replaced by the substrate are shown as blue transparent spheres.*[100] *The A residues are labelled from -3 to +1, corresponding to their location with respect to the active site residue. The loop around residue 316, partially covering the active site, is shown in magenta.*[100] *(C) Structure*

of the interior of the chitinase B TIM barrel. The strands forming the TIM barrel are shown as yellow ribbon. Side chains of residues lining the inside of the barrel are shown as sticks. Side chains conserved in chitinase A and B are coloured magenta. Water molecules in the structure are shown as red spheres. [100] *Hydrogen bonds are shown as black dashed lines. Conserved residues are labelled according to the chitinase B sequence. Part of the chitotetraose model is shown as sticks, with carbon atoms coloured orange.* [100] *(D) and (E) Details of the chitin-binding domain of chitinase B. (D) Superposition of the chitinase-binding domain of chitinase B (blue ribbon) and the cellulose-binding domain of endoglucanase Cel5 (grey ribbon).* [100] *The conserved β-strands show an almost exact overlap. Most of the support loop of the catalytic domain of chitinase B is shown as a dark-blue ribbon. Trp^{252} also is shown in magenta.* [100] *The substrate- binding residues for the cellulose-binding domain are shown in yellow, and the equivalent residues in the chitinase-binding domain are shown in magenta. The disulfide bond between the termini of the cellulose-binding domain is shown in green. Polar residues lining the path of aromatic residues in chitinase B are shown in magenta. Labels correspond to the chitinase B sequence. (D) Chitinase B consists of a catalytic domain with a TIM barrel fold and a small C-terminal domain. Five aromatic residues are linearly aligned on the surface of chitinase B, Tyr^{481} and Trp^{479} are in the C-terminal domain, and Trp^{252}, Tyr^{240} and Phe^{190} in the catalytic domain.*
Figures A – D were taken from literature [100]. Figure E was taken from literature [92].

The catalytic domain of chitinase B forms a deep substrate-binding cleft which is closing to a tunnel-like structure upon substrate binding due to Asp^{316} and Trp^{97}. Figure 8 (C) and (D) illustrates the closing of the "roof" upon substrate binding. [101] The binding cleft of chitinase B is aligned with aromatic residues of amino acids and secondly contains exposed residues of amino acids that are able to form hydrogen bonds with the substrate. Glu^{144} is essential for hydrolysis by protonation of the glycosidic bond. The catalytic domain of chitinase B has six clearly identifiable subsites, running from –3 to +3. [101]
Additionally, chitinase B contains a chitin – binding domain, which is connected, to the catalytic domain via a linker beyond subsite +3. The spatial arrangement of the catalytic and chitin-binding domain indicates that chitinase B degrades chitin chains from their non-reducing end.[92]
The catalytic domain is locked beyond subsite –3.[100] Figures 9 and 10 show schematically the subsites of chitinase B. Negative subsites host the non-reducing end of the oligosaccharide chain, positive subsites the reducing end. The hydrolysis reaction takes place between subsites -1 and +1. The catalytic cleft is able to host nine A units with core subsites -3 to +3.[92] In the case of chitin hydrolysis, preferentially a disaccharide unit bound to subsites -1 and -2 is the leaving group, subordinately a trisaccharide unit bound to subsites -1, -2 and -3 is cut off, i.e. the glycon part of the substrate.[22, 102] In conclusion, chitinase B cleaves chitin from the non-reducing end.

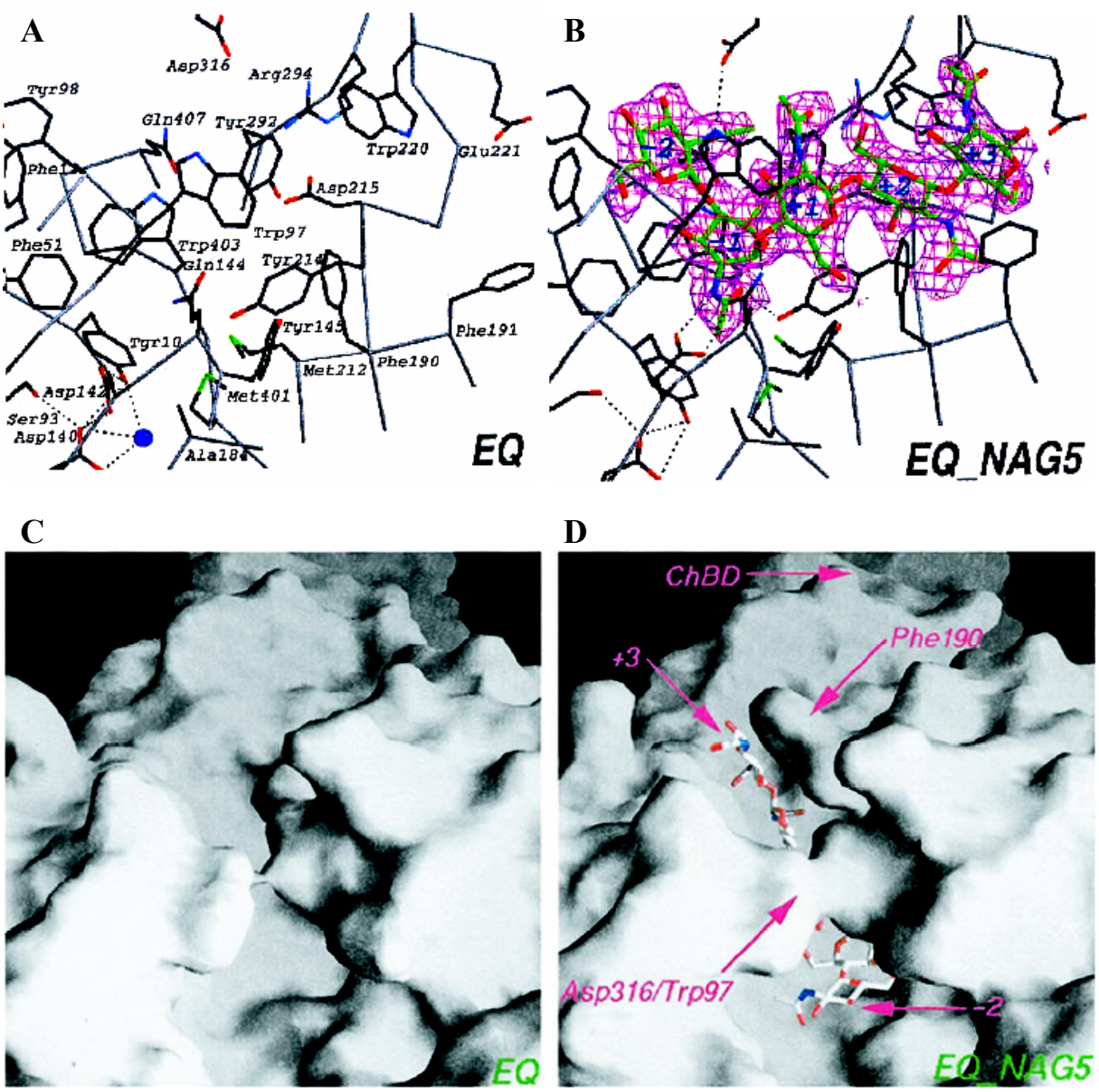

Figure 8. Three-dimensional structure and molecular surface of chitinase B mutant E144Q. Data based on crystallographic data. (A) and (B) Structure of chitinase B / complexes. The structures of EQ (E144Q) and EQ_NAG5 (NAG5 = A_5) are shown as they would occur along the reaction coordinate. Side chains interacting with the sugars are shown as sticks (carbons in black) together with relevant stretches of the backbone (grey). A_5 is drawn in a stick model with green carbons. Important water molecules are shown as blue spheres. The unbiased electron density map of A_5 is contoured in magenta. Important hydrogen bonds are drawn as dotted lines. Amino acid side chains in EQ, and the sugars bound to subsites -2 to +3 in EQ_A_5 are labelled. (C) and (D) Molecular surface representation of the EQ and EQ_A_5 structures. The monosaccharide moieties are shown in a stick representation. (D) Arrows highlight the flip of Phe^{190}, the tunnel formed by residues Asp^{316} and Trp^{97} (note the difference to unbound EQ in (C)), the A_5 binding subsites +3 and -2, and the chitin-binding domain. Figures A – D were taken from literature [101].

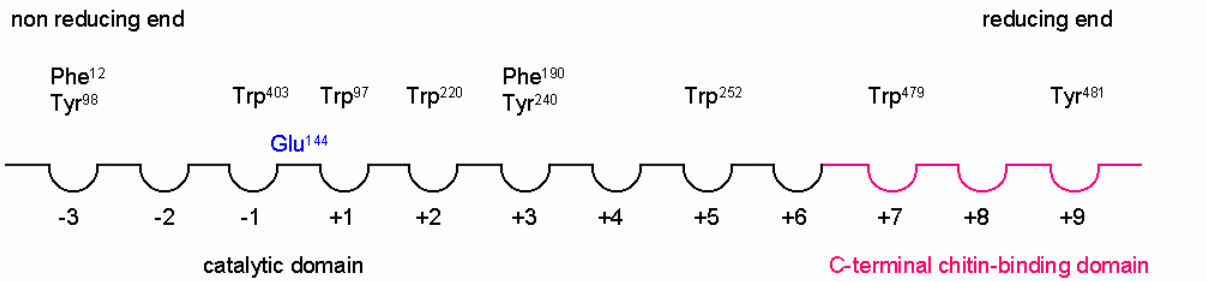

Figure 9. Schematic drawing of the C-terminal chitin-binding domain (red) and the N-terminal catalytic domain (black) of chitinase B with subsites ranging from -3 (non-reducing end) to +9 (reducing end). The catalytic site (with Glu^{144}) is positioned asymmetrically in the binding cleft between subsites –1 and +1. The catalytic domain is locked beyond subsite -3. The drawing was made according to the discussions of the N-terminal chitin-binding domain with the core subsites –3 to +3 in reference [101] and the discussion of additional subsites including of the C-terminal catalytic domain in reference [92].

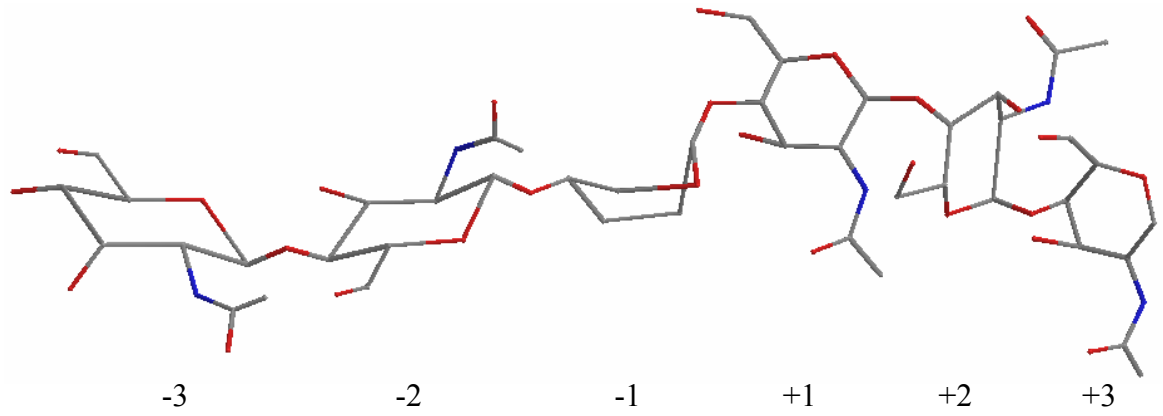

Figure 10. Schematic drawing of the arrangement of the monosaccharide units of a chitin hexasaccharide bound to chitinase B. The sugar moiety bound to subsite –1 takes up different conformations during catalysis: chair (unbound), twisted boat (bound), half-chair (oxazolinium ion).[93, 94] The twisted boat conformation of the A unit bound to subsite –1 results in an edgewise binding of the A units in subsites +1 to +3.[93, 94](Chem3D Pro 11.0 ®, carbon atoms: black, oxidation atoms: red, nitrogen atoms: blue)

The substrate is hydrolysed with anomeric retention, the released -1 sugar remains in the β-configuration. Details of the catalytic mechanism of family 18 chitinases, which is also valid for chitinase B, are described in chapter 1.4.5 and Figure 2.[95]

The substrate-assisted mechanism is facilitated by an induced conformational change in which the *N*-acetylglucosamine at subsite –1 adopts a skewed-boat conformation, which results in a 90° twist of the linkage with the A unit at subsite +1. Substrate binding is predominantly facilitated by a series of aromatic residues.[100] The catalytic domain contains the following amino acid residues contributing significantly to hydrophobic interactions: Phe^{12} / Tyr^{98} (-3), Trp^{403} (-1), Trp^{97} (+1), Trp^{220} (+2), Phe^{190} / Tyr^{240} (+3), and Trp^{252} (+5).[99, 100, 101] Binding of substrate induces several conformational changes that result

in favourable protein-substrate interactions. Trp^{97} and Trp^{220} move toward each other, creating a hydrophobic sandwich with the sugars at the +1 and +2 positions. Asp^{316} rotates 152°, which leads to the formation of a hydrogen bond with Trp^{97} on the opposite side of the substrate. These movements together lead to a partial closure of the roof of the catalytic domain tunnel.[101] Additionally, Phe^{190} rotates –91° around to form a hydrogen bond with the sugar at subsite +3. [101] These data for chitinase B from *S. marcescens* were obtained from crystallographic measurements; principally conformational changes upon non-covalent protein – oligosaccharide interactions can be also obtained by STD-NMR measurements as was demonstrated for the interaction between the plant chitinase hevamin and the chitin trimer.[103]

Besides the catalytic domain with a TIM barrel fold, chitinase B possesses a small C-terminal chitin-binding domain. Five aromatic residues are linearly aligned on the surface of the chitinase B molecule. Phe^{190} / Tyr^{240} (+3) and Trp^{252} (+5) belong to the catalytic domain[101] whereas Trp^{479} (+7) and Tyr^{481} (+9) are part of the chitin-binding domain.[92] Replacement of these aromatic residues by alanin employing site-directed mutagenesis shows that besides Phe^{190} all four amino acid residues, Tyr^{240}, Trp^{252}, Trp^{479}, and Tyr^{481} are essential for a successful binding of β-crystalline chitin.[92]

Besides the contribution of aromatic amino acid residues to hydrophobic interactions, several polar amino acid residues mediate hydrogen bonds, which synergistically contribute to the binding of the saccharide. In contrast to the aromatic amino acid residues in the deep catalytic cleft the amino acid residues of the chitin-binding domain are exposed to the solution.[92] The number of hydrophobic amino acid residues increases continuously from the subsites of the chitin-binding domain to the subsites of the catalytic domain with a maximum for subsite -1.[92] Consequently, chitinase B contacts the chitin chain first with the chitin-binding domain at the non-reducing end. The chitin chain is moving along the gradient of increasing hydrophobic and hydrogen bond interactions towards subsites -1 and -2. Hydrolysis between subsites -1 and +1 cleaves of the glycon part, which was bound to subsites -1 and -2. As adjacent monomer units are related by a 180° rotation, the enzyme moves two *N*-acetylglucosamine units towards the reducing end and hydrolysis is repeated resulting in the production of A_2.[22, 102] But chitinase B produces also odd numbered chitooligosaccharides, which is in agreement with its third subsite -3 at the glycon leaving side. In case that the chitin chain contains D units, hydrolysis is only processed successfully if an A unit is positioned in subsite –1. [22, 102] Glycosidic bonds are cleaved with relative rates AA-X : DA-X : YD-X ca. 3 : 1 : 0, and bonds of the type YYA-X are cleaved very slowly (X = aglycon part; Y = D or A unit). [102]

Thus, occasionally the enzyme moves 2n (n > 1) monomer units towards the reducing end before the next successful hydrolytic event occurs. Chitinase B is a processive enzyme with typical exo-activity with respect to water-soluble chitin due to its closed, tunnel-like catalytic domain.[101] For chitosan being the substrate, a clear exo-activity is not observed as only A units in subsite -1 lead to product formation resulting in movement of 2n monomer units so that 2n-3 monomer units extend beyond subsite -3. Thus, the porch loop locks the non-reducing end efficiently only in the case of water-soluble chitin.[92] Nevertheless, chitinase B acts strictly processive also in the case of chitosan. [102] Chitinase B binds longer chitooligosaccharides with the non-reducing end preferentially located at subsite -2. The analysis of the hydrolysis products of A_6 by MALDI-TOF MS (performed by the author of the present thesis) demonstrates that the non-reducing end may be equally bound to subsite -3 in the case of chitooligomers, revealing chitotriosidase activity of chitinase B. Binding a D unit at subsite -1 is non-productive and actually results in the case of chitooligosaccharides to competitive inhibition of the enzyme.[104] Moreover, an A unit is highly favoured at subsite -2 for successful catalysis, as the order of hydrolysis rates of different types of glycosidic bonds shows.

1.4.8 Comparison of Chitinase A and B

Chitinase A and B both convert chitin into chitin dimers and monomers. However, the two enzymes play different roles in the degradation of chitin as the combination of both enzymes results in a synergistic effect on the degradation rate.[3] Differences between chitinase A and B can be explained by a structural comparison of both enzymes. Whereas the support loop and the chitin-binding domain extend the catalytic domain of chitinase B on the reducing side of the active site, the fibronectin III-like chitin-binding domain of chitinase A extends the catalytic domain at the non-reducing side. Thus, chitinase B degrades chitin from the non-reducing end, exhibiting chitobiosidase and chitotriosidase activity, whereas any chitobiosidase activity displayed by chitinase A results in degradation of the chitin chain from the reducing end.[100]

Figure 11 shows a superposition of the structures of chitinase A and B revealing that the chitin-binding domains of chitinase A and B extend the catalytic cleft in opposite directions resulting in a degradation of the chitin chain from opposite directions, too.

The non-reducing side of the catalytic domain of chitinase B is locked by the porch loop. Additionally, chitinase B contains an insertion of 17 amino acids, which is part of a mobile loop that extends of the catalytic cleft. Upon substrate binding a tunnel-like structure is

formed which is typical for exo-chitinases.[101] A porch loop analogue is absent in chitinase A, meaning that the catalytic domain is open on both sides. Thus, the cleft of chitinase A has a more groove-like character, typical for endo-enzymes.[90] However, strict exo-activity for chitinase B is only observed for water-soluble chitin as the D units in the substrate result occasionally in an extension of the non-reducing end beyond subsite -3 and thus beyond the porch loop.[100]

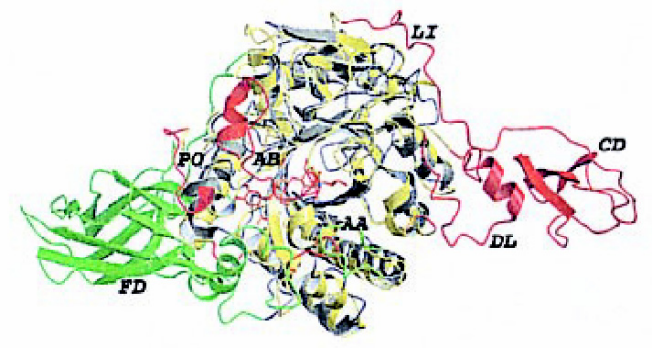

Figure 11. Superposition of the structures of chitinase A and B both in ribbon representation. Chitinase A is coloured grey, chitinase B yellow. Residues that correspond to insertions in chitinase A with respect to chitinase B are coloured green; residues that correspond to insertions in chitinase B with respect to chitinase A are coloured red. AA, active site covering loop in chitinase A; AB active site covering loop in chitinase B; CD, chitin-binding domain in chitinase B; DL support loop in chitinase B; FD, fibronectin chitin-binding domain in chitinase A; LI, linker in chitinase B; PO, porch loop in chitinase B. The figure was taken from literature [100].

1.4.9 Human Chitotriosidase

Human chitotriosidase (HCT) or human macrophage chitinase is an active family 18 chitinase that is found in human blood. It shows a broad pH optimum around seven. [75] The enzyme is able to hydrolyse A_3, which lead to the name chitotriosidase. [105] It occurs in two major forms of 39 kDa and 50 kDa, where the 50 kDa form can be transformed into the 39 kDa form by proteolysis. [106] The chitinase putatively plays a role in defence against chitinous human pathogens, which is supported by the fact that humans deficient in chitotriosidase activity are more susceptible to nematodal infections.[73, 74]

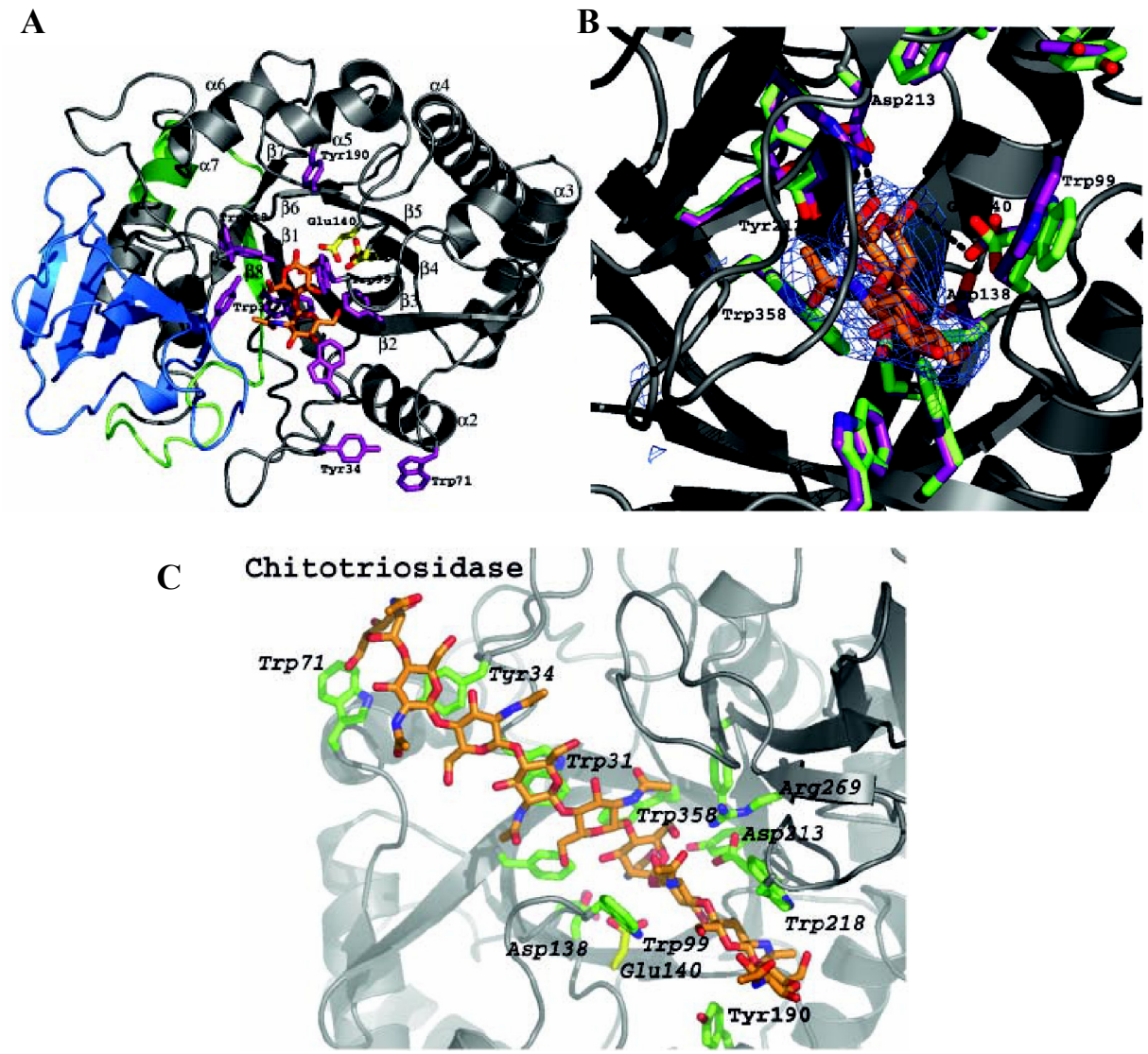

Figure 12. Structure of human chitotriosidase. (A) The backbone of chitotriosidase as shown as a grey ribbon. The α/β domain is coloured blue. Residues 344 – 372, which are deleted in the inherited mutated form of the enzyme are coloured green. Asp[136], Asp[138] and Glu[140] are shown as a sticks model with carbons coloured yellow. Solvent-exposed aromatic side chains lining the active site cleaved are shown as purple sticks. A_2 as shown in a sticks representation with orange carbon atoms. (B) Details of the active site. The HCT backbone is shown as a grey ribbon. Solvent-exposed aromatics and residues interacting with A_2 are shown as sticks with carbons coloured green for the apo-structure and carbons coloured purple for the chitotriosidase-A_2 complex. A simulated-annealing $F_0 - F_c$, φ_{calc} map for A_2 as observed in the chitotriosidase- A_2 complex is shown in blue, contoured at 3σ. A_2 is shown in a sticks representation with orange carbon atoms. (C) Comparison of active site details. The substrate-binding pocket of HCT is displayed. Protein backbones are represented by a grey ribbon. A model of A_9 is shown as a sticks drawing with orange carbons. Side chains in the active site cleft are shown as sticks with green carbons, except for the catalytic glutamic acid, which is shown with yellow carbons. Figures A – C were taken from literature [76].

Like all other family 18 chitinases, HCT has the DXXDXDXE motif at the end of strand β4 with Glu[140] being the essential catalytic acid. [76] Figure 12 displays the structure of HCT with emphasis on the catalytic domain. Up to now only crystal structures of complexes between

HCT and A_2 are available. Through superposition of the chitinase B mutant – A_5 and the chitinase A mutant – A_8 [107] complexes onto the HCT-A_2 structure, a model of a HCT complex with A_9 can be produced. [76] Whereas A_2 occupies subsites -2 and -1, A_9 occupies continuously subsites -6 to +3 without any steric hindrance. The non-reducing end is placed at subsite -6, the reducing end at subsite +3 with the catalytic centre between subsites -1 and +1. [76] It should be pointed out that it is not yet proven by crystallographic data that the reducing end (subsites +1, +2, +3) of chitooligosaccharide substrates is bound edgewise to HCT like for chitinase A and B, and that the sugar moiety bound to subsite –1 takes a skew boat conformation. However, the computer model based on these assumptions shows no steric clashes so that this model is very likely.[76]

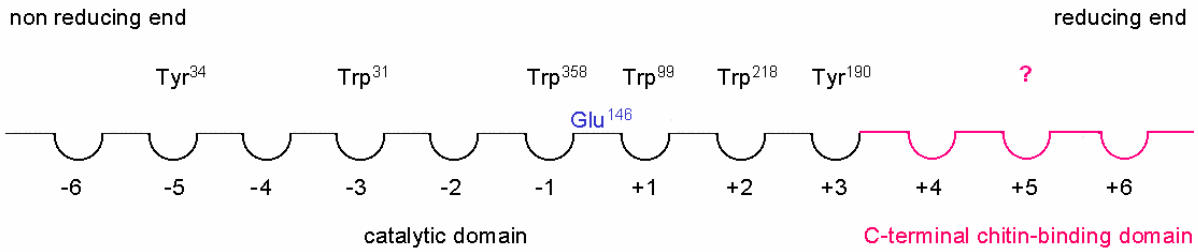

Figure 13. Schematic drawing of the catalytic domain (black) of human chitotriosidase with subsites ranging from -6 (non-reducing end) to +3 (reducing end). The catalytic site (with Glu^{146}) is positioned asymmetrically in the binding cleft between subsites -1 and +1. The drawing was made according to the discussions of the catalytic domain with core subsites -3 to +3 in reference [76] and the discussion of additional subsites including of a C-terminal chitin-binding domain in reference [76], which extends the catalytic domain of the 50 kDa-form of human chitotriosidase beyond subsite +3.
The number of subsites of the chitin-binding domain is unknown and set fictively to three in the figure. As well the aromatic amino acid residues of the subsites of the chitin-binding domain are unknown.

The active site of human chitotriosidase is aligned with several solvent-exposed aromatic side chains that stack against the hydrophobic face of the sugars, Tyr^{34} (-5), Trp^{31} (-3), Trp^{358} (-1), and Trp^{99}, Trp^{218} and Tyr^{190} (+1, +2 and +3), see Figure 13. [100] The pattern and conservation of these exposed aromatic residues is most reminiscent of that observed in chitinase A. However, in contrast to chitinase A, the 39 kDa form of human chitotriosidase possesses no chitin-binding domain whereas the chitin-binding domain, thus present in the 50 kDa form, is located toward the C-terminus, similar to what is observed for chitinase B and AMCase. [75, 76] But the structure of this domain is not similar to that of chitinase B. It shows rather similarities with the sequences of similar domains in nematodal and insect chitinases. [108] In contrast to both bacterial enzymes chitinase A and B, which show ego-activity towards water-soluble chitin, human chitotriosidase possesses not a deep active site cleft, which is partially

closed by overhanging loops. The cleft is even more open compared to chitinase A.[76, 90] Moreover, the active sites of chitinase A and B are blocked at opposite ends, whereas the human chitotriosidase active site cleft is fully extended over one face of the enzyme,[76] indicating that human chitotriosidase acts as an endo-chitinase with respect to water-soluble chitin, which would be consistent with its proposed role as a defence protein against chitin-containing pathogens (Figure 14).[71, 106, 109]

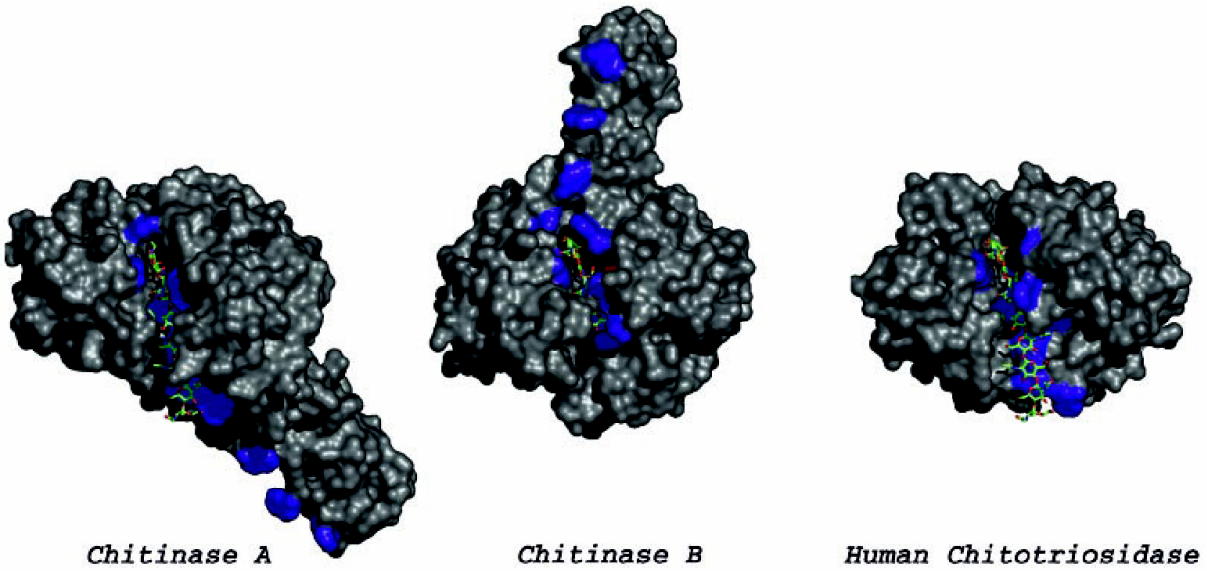

Figure 14. Comparison of the structures of HCT with chitinase A and B from Serratia marcescens. Molecular surfaces are shown for currently known complexes of chitinases with chitooligosaccharides: chitinase A with A_8, chitinase B with A_5, and HCT with a model of A_9. The catalytic glutamic acid is coloured red, and exposed aromatic side chains lining the active site cleft are coloured blue. The chitooligosaccharides are shown as sticks with green carbons. The figure was taken from literature [76].

The putative role that HCT plays in the defence against chitinous human pathogens implies that although chitinases in the pathogenic organisms themselves may be targets for the design of inhibitors, it would be desirable to exclude inhibitors that show strong activity against HCT as they might have negative side effects. The human enzyme appears to have significant differences in the active site as compared with chitinases of pathogens, which could be used for the design of inhibitors that show different specificity toward human and pathogen chitinases.[76, 110]

1.4.10 Acidic Mammalian Chitinase

A second mammalian chitinase, acidic mammalian chitinase (AMCase) was recently found. The mRNA of this chitinase is expressed in the gastrointestinal tract and lung of human.[108] AMCase, a member of the family 18 of glycosyl hydrolases, shows an 8-stranded α/β (TIM)

barrel catalytic core structure. [111] Like HCT, AMCase contains an N-terminal catalytic domain of 39 kDa and a C-terminal chitin-binding domain separated by a hinge region. [108, 111] AMCase is able to hydrolyse glycosidic bonds not only at physiological pH but also around pH 2. The profound acid stability of AMCase is in agreement with the fact that this chitinase is found in the stomach of mammalian.[75]

1.4.11 Family 19 Chitinases

The family 19 of glycosyl hydrolases covers mainly chitinases from plants and only to a minor extend chitinases from bacteria. Family 19 chitinases differ not only in the amino acid sequence of the catalytic domain from family 18 chitinases but also in the catalytic mechanism of the hydrolysis of chitin.[112, 113, 114]

For family 18 chitinases is characteristic that they produce chitooligomers with a β-configured A unit at the reducing end and either D or A at the non-reducing end.[115] In contrast, family 19 chitinases produce chitooligosaccharides with either D or A at the reducing end in the α-configuration and A at the non-reducing end. [116]

The X-ray crystal structure of a family 19 chitinase isolated from barley shows structural similarities with hen egg-white lysozyme, suggesting an analogous catalytic mechanism. [116, 117, 118]

Two acidic residues Glu^{67} and Glu^{89} are essential for catalysis. The catalytic mechanism of family 19 chitinases is called single displacement mechanism (in contrary to the double displacement mechanism of family 18 chitinases) due to the inversion of the anomeric configuration and the need for two largely separated acidic residues within the active site. [116] The single displacement mechanism requires one acidic residue to act as a general acid and the other as a general base (Glu^{89} in the case of barley chitinase [116]), activating water for a concerted nucleophilic attack at C-1. The chitooligosaccharide substrate binds with all sugars in a chair conformation favouring protonation of the β-1,4-glycosidic oxygen atom by Glu^{67}. Asn^{199} forms a hydrogen bond with the *N*-acetyl group, preventing the formation of an oxazolinium ion intermediate.

A conformational change of a flexible loop region of the active site brings the deprotonated Glu^{89} close to the oxocarbenium cation. Glu^{89} and Ser^{120} coordinate with a water molecule, which is activated for nucleophilic attack resulting in an inversion of the configuration at C-1.[116, 117, 119]

1.4.12 Family 20 Glycosyl Hydrolases – Chitobiases and β-Hexosaminidases

The family 20 of glycosyl hydrolases consists of chitobiases (β-*N*-acetylglucosaminidases) and β-hexosaminidases. Both enzymes cleave monosaccharides from the non-reducing end of a poly- or oligosaccharide. Whereas chitobiases cleave exclusively A_2, β-hexosaminidases remove either *N*-acetylglucosamine or *N*-acetylgalactosamine from glycoproteins, glycolipids and proteoglycans.[120] Both enzymes hydrolyse glycosidic bonds with retention of the configuration at C1.[121, 122]

1.4.13 Family 46 Chitosanases

Family 46 chitosanases were isolated from:

Streptomyces sp. strain N174 [123]

Nocardioides sp. strain N106 [124]

Amycolatopsis sp. strain CsO-2 [125]

Streptomyces coelicolor A3 (2), SCO0677 or SCF91.37 [126]

Streptomyces coelicolor A3 (2), SCO2024 or SC3A3.02 [127]

Bacillus subtilis [128, 129]

Bacillus amyloliquefaciens [130]

Bacillus KFB-C04, thermostable chitosanase, [131] alias *Bacillus* sp. strain CK4 [132]

Chlorella virus PBCV-1 [133, 134]

Chlorella virus CVK2 [135]

Bacillus ehimensis [136, 137]

Bacillus coagulans [138]

Burkholderia gladioli [139, 140]

Bacillus circulans MH-K1 [141]

For successful hydrolysis family 46 chitosanases require stringently a D unit positioned at subsite +1 whereas the specificity for subsite -1 is less pronounced (either A or D). Hydrolysis is performed under inversion of the configuration at C1, indicating that the catalytic mechanism is analogous to that proposed for family 19 chitinases (single displacement mechanism).

1.4.14 Family 75 Chitosanases

Family 75 chitosanases were isolated from *Nectria haematococca var. brevicona* [142], *Aspergillus oryzae* [143], *Aspergillus fumigatus* [144], and *Metarhizium anisopliae* [145]. These four

enzymes are significantly homologous to each other. Details about the cleaving specificity of these enzymes are not known today.

1.4.15 Family 80 Chitosanases

Family 80 chitosanases were isolated from *Matsuebacter chitosanotabidus* [146] and Sphingobacterium *multivorum* [147]. Details about the cleaving specificity of these enzymes are not known today.

1.5 Lectins

Lectins are complex proteins or glycoproteins that have specific recognition and binding functions for complex carbohydrate structures of glycoconjugates which enables them to bind specifically to cells or cell membranes and to initiate or mediate biochemical reactions. Lectins are ubiquitary, they are found in plants, microorganisms and animals, also mammals including humans.[148]

Due to the fact that many plant lectins are highly toxic for insects by clotting their blood cell they may be considered as defence substances against insects.[149]

Lectins function as mediators of biological signalling, similar to hormones.[150] E.g. wheat germ agglutinin is known to bind to the insulin receptor giving the fat cell the same message that insulin gives, namely to produce fat.[151, 152]

Besides this hormone-like function, wheat germ agglutinin initiates allergic reactions in the gut causing the release of interleukin-4, interleukin-13 and histamine from human basophiles producing allergic symptoms.[153]

Microorganisms contain lectins for interactions with their hosts. E.g. *Rhizobium trifolii* gets stuck to the roots of clover via lectin – polysaccharide interactions in order to establish a symbiosis. Microbes use lectins for attachment to their host cells.[154]

In animals, lectins take several functions, mainly in the recognition of cells or glycoproteins. Selectins and galectins are involved in cell routing and cell-cell interactions; heparin- and hyaluronic acid – binding lectins are involved in cell – matrix interactions. In humans, lectins take in general the same functions as in animals although less experimental data are available.[155] The human galectin-1 has an anti-inflammatory function, and it acts protectively as part of the immune system.[156] In the same direction goes the effect, that specialized lectins (e.g. opsolins) coat foreign antigens to make them susceptible to phagocytosis by white blood

cells. Liver lectins capture microorganisms, which are filtered off from the blood stream. Human lectins bind to the glycan chains of membrane-bound glycoproteins mediating biological activity. The biological activity either results from a blocking of the glycan chains that are not able to interfere with cells or receptors. Alternatively, the lectin-glycoprotein complex binds to a receptor.

1.6 Chitolectins

Family 18 of glycosyl hydrolases contains homologous proteins without hydrolytic activity due to the lack of one or more of the highly conserved carboxylic groups of catalytically active family 18 chitinases. Chitolectins function as receptors of chitin, chitosan or chitooligomers. Of special interest are mammalian, in particular human chitolectins.

1.6.1 Human Cartilage Glycoprotein-39

The human cartilage protein, molecular mass 39 kDa (HC gp-39) possesses a variety of other names: YKL-40 on base of its three N-terminal amino acids tyrosine Y, lysine K, leucine L; breast regressing protein 39 kDa (brp-39); 38-kDa heparin-binding glycoprotein (gp38k); chitinase-3-like-1 (CHI3L1); and Chondrex. In this thesis the protein is named HC gp-39. It is abundant in liver and found at lower levels in kidney, brain and placenta. Although its mRNA is not observed in healthy cartilage, HC gp-39 is over expressed in osteoarthritis, [157] rheumatoid arthritis, [158] cancer (some kinds of breast and colon cancer), [159, 160, 161, 162, 163] liver fibrosis,[164] inflamed tissues, [165] spinal fluids following neural damage, [166] arteriosclerosis [167] and more generally, pathologies with increased tissue remodelling. [168]

Epitopes of HC gp-39 are recognised by the immune system of patients suffering from rheumatoid arthritis; [169] the serum concentration of HC gp-39 is positively correlated with the disease progression. [170] Thus, it could be used as a biomarker for these pathogenic conditions. HC gp-39 is a possible auto antigen in rheumatoid arthritis with the capability to induce T-cell-mediated autoimmune response. [171] Peptides derived from HC gp-39 can induce immunologic tolerance in patients suffering from persistent rheumatoid arthritis. [172]

HC gp-39 is secreted by articular chondrocytes, [173] synovial fibroblasts, [174] smooth muscle cells[175] and neutrophile granulocytes [169] as well as macrophages. [176, 177, 178] It promotes the proliferation of connective tissue cells acting synergistically with the insulin-like growth factor, possibly resulting in scar tissue formation. [178] The protein appears to be induced in

osteoarthritis patients and generally in aging humans. [179] It has been reported that HC gp-39 plays a role as an auto antigen in rheumatoid arthritis and that it is expressed in diseased human osteoarthritic cartilage and osteocytes, but not in non-diseased tissue. [180]
It was reported that ChO treatment of persons suffering from rheumatoid arthritis has a positive effect on the course of the diseases. [181] Putatively ChO's reduce the expression of HC gp-39, which plays a key role in rheumatoid arthritis.
Recently it was shown that HC gp-39 is a potent growth factor, inducing cell proliferation through activation of protein kinase B and kinase ½ mitogen-activated protein kinase signalling pathways. HC gp-39 initiates MAP kinase and PI-3K signalling cascades in human connective-tissue cells (chondrocytes, fibroblasts), leading to a phosphorylation of ERK1 / ERK2 and AKT. Both pathways are required for the cells to complete progression through the mitotic cycle. [178] HC gp-39 may function to maintain or promote the integrity of the connective-tissue elements in a pro-apoptotic environment. [178] Similar activity has been shown for an orthologous protein from guinea pig and a homolog in Drosophila.[182] It is supposed that chitooligosaccharides could influence the growth of chondrocytes[183], osteoblasts[183] and macrophages via its ligand nature for HC gp-39.
Chondrocytes are cartilage cells that produced collagen and proteoglycans, which are the basic components of cartilage. (Figure S10, Appendix) The growth stimulating effect of ChO's on chondrocytes results in a regeneration of cartilage through normalisation of proteoglycans and collagen.
Besides 53% sequence identity to human chitotriosidase (HCT),[184, 185] the binding site of HC gp-39 is similar to the binding site of chitinase A from *Serratia marcescens*.[96] In family 18 chitinases, the glutamate is the catalytic acid, which protonates the glycosidic bond. The neighbouring aspartate plays a key role in orienting the *N*-acetyl group of the -1 sugar for nucleophilic attack on the anomeric carbon. In HC gp-39, these residues correspond to Leu[140] and Ala[138]; consequently HC gp-39 possesses no chitinase activity.[186]
HC gp-39 is capable of binding chitooligosaccharides, [186] as its binding cleft is lined with solvent-exposed aromatic residues, which are important for interacting with the hydrophobic faces of the pyranose rings in chitooligosaccharides according to catalytically active family 18 chitinases (Figures 15 – 21). [187, 188]
The X-ray structure analysis of co-crystals of HC gp-39 with A_8 reveals six binding sites, - 4 to +2.[187] Further, two additional subsites, -5 and -6, were identified.[188] The X-ray structure analysis of co-crystals of HC gp-39 with A_5 revealed an additional subsite +3. [188] In HC gp-39, A_5 binds with equal frequencies to subsites -2 to +3 and subsites -3 to +2. [188] The X-ray

structure analysis of co-crystals of HC gp-39 with A_2 gave evidence for the occupation of subsites -5 and -6. Similar results were produced for A_3. [188] Chitooligosaccharides are bound to HC gp-39 in similar conformation and location as observed previously for complexes of chitooligosaccharides with chitinases. That means, the -1 sugar is in the boat conformation. The distorted conformation is stabilised by multiple interactions involving Trp^{99}, Trp^{352}, Arg^{263}, and Tyr^{141}. [188] Intriguingly, although six subsites, from -1 to -6, are available for chitooligosaccharides to bind in a linear fashion the distorted conformation is preferred. All together nine subsites, -6 to +3, were identified. [187, 188] The majority of the favourable interaction between the protein and sugar is due to the interaction between sugar rings and the aromatic residues at -6 (Trp^{71}), -5 (Trp^{34}), -3 (Trp^{31}), -1 (Trp^{352}), +1 (Trp^{99}), and +3 (Trp^{212}).[188] Figure 19 summarizes the facts. Additionally, hydrogen bonds are found with the +2 *N*-acetyl group (water mediated interactions with Thr^{184} and Thr^{179}), the -1 sugar (Trp^{99}, Asn^{100}, Asp^{207}, Arg^{263}), the -2 sugar (Trp^{352}, Asn^{100}, and water mediated interactions with Arg^{263}, Glu^{290} and Glu^{97}), the -3 *N*-acetyl group (Asn^{100}) and the -4 O-6 hydroxyl group (Glu^{70}). [187, 188] Based on a definite binding site for A_4 (-2 to +2) and the lack of definite binding sites for A_5 (-3 to +2 vs. -2 to +3) and A_6 (-4 to +2 vs. -3 to +3), it would appear that the energetic surface distal to the -3 and +2 subsites is shallow and not well defined. [187, 188]

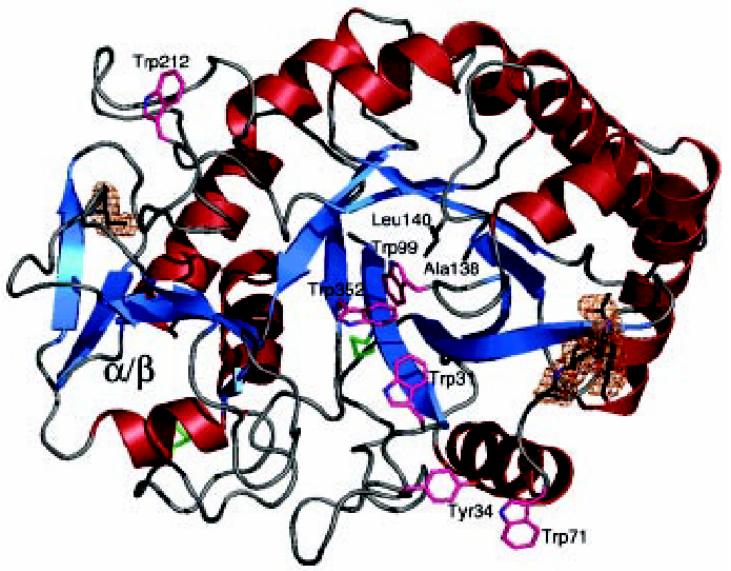

Figure 15. The structure of HC gp-39 is shown as a coloured ribbon (helices, red; strands, blue). Ile^{311} and the A_2 N-linked glycan on Asn^{60} are shown as stick models with black carbons, together with the final 2 $F_0 - F_c$, φ_{calc} map (orange) contoured at 1.0 σ. The side chains of Leu^{140} and Ala^{138} are shown as black sticks. The two disulfide bonds are shown in green. Solvent-exposed aromatic residues lining the putative binding cleft and conserved with HCT are shown as sticks with magenta carbons. The figure was taken from the literature [187].

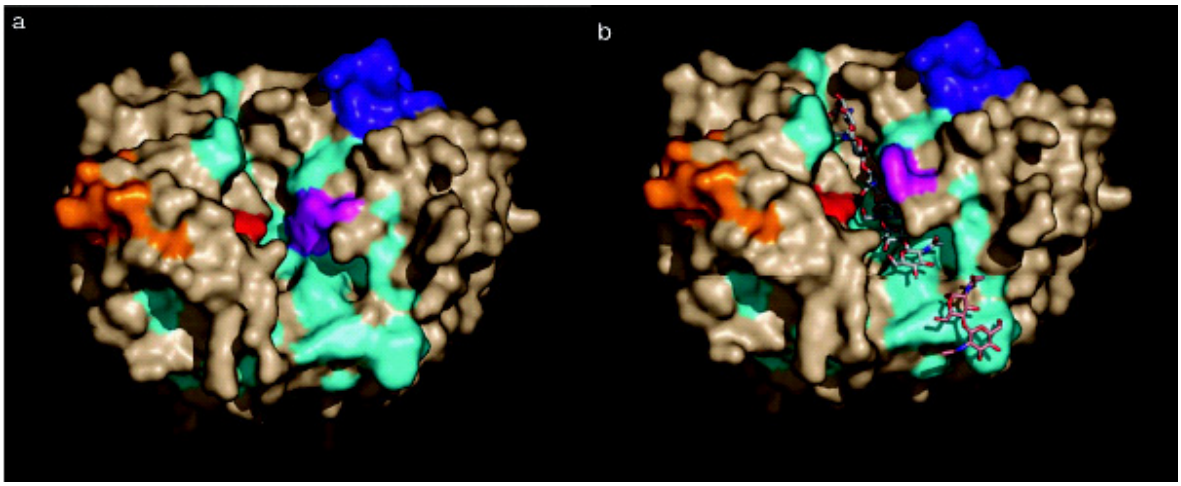

Figure 16. Surface representation of the structures of HC gp-39 (a) and of HC gp-39 in complex with chitooligosaccharides (b). The protein surface is coloured as follows: aromatic amino acid residues are shown in cyan, Trp^{99} is depicted in violet, the putative heparin-binding site GRRDKQH (residues 143 – 149) is coloured blue and the epitope 259 – 271 is coloured in red (residues 259 – 269) and orange (residues 266 – 271). The bound A_5 and A_2 are shown in white and pink sticks, respectively. The figure was taken from the literature [188].

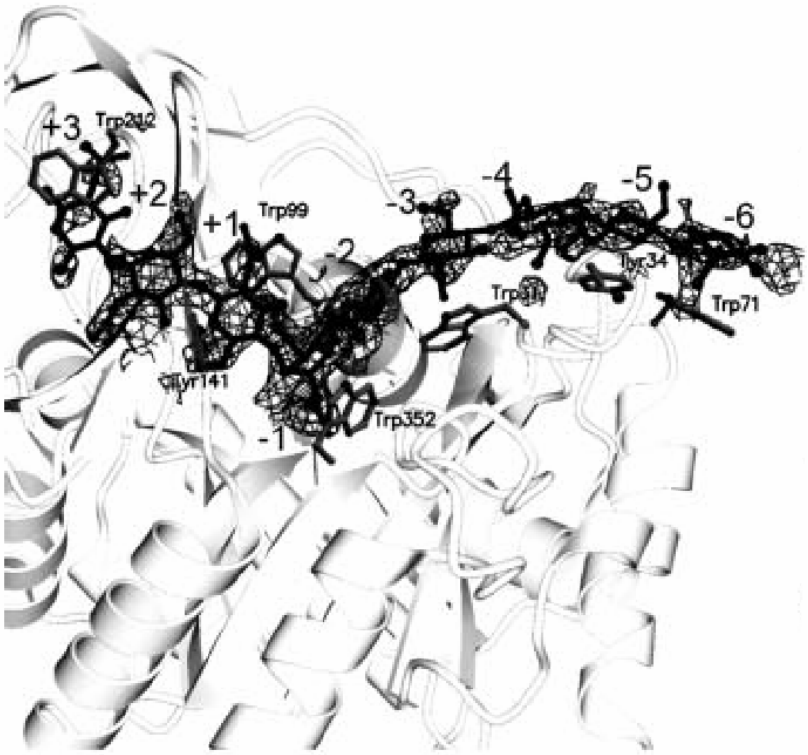

Figure 17. Model of HC gp-39 with a long chitin oligosaccharide and the lining of aromatic amino acid residues. The boat confirmation of the A unit is visible in the –1 subsite. The oligosaccharide is shown in black in a ball-and-stick representation; the structure of the protein is shown as a ribbon representation in grey colour. The aromatic residues lining the carbohydrate binding site are shown in ball-and-stick representation. The figure was taken from the literature [188].

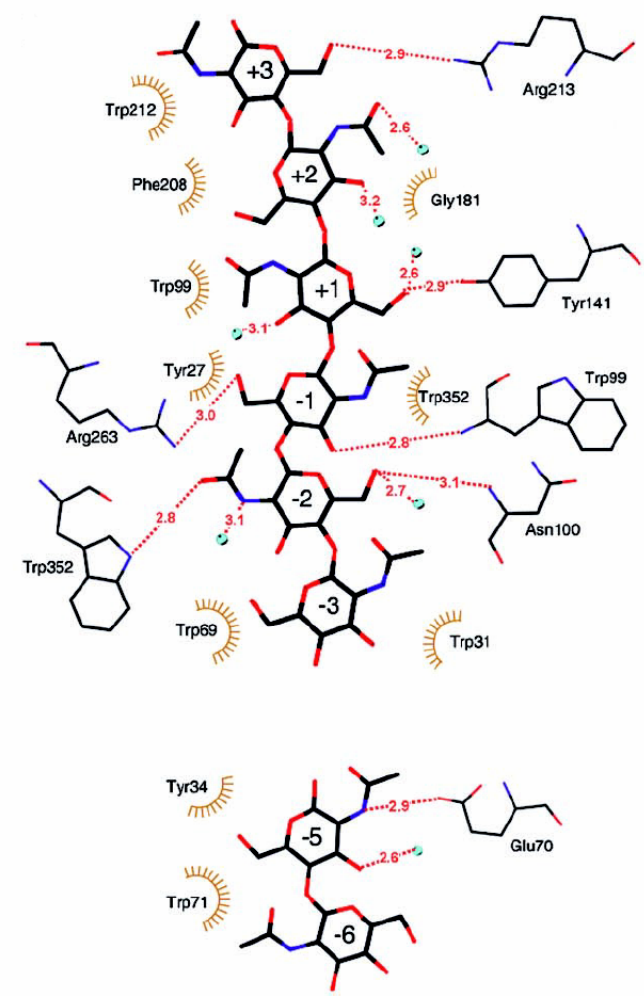

Figure 18. Schematic representation of the chitin-binding site showing protein carbohydrate interactions at subsides –3 to +3, – 6, and –5. The bound chitin oligosaccharide and the amino acid side chains are shown in thick and thin black lines. The hydrogen-bonding interactions are shown as red dashed lines with atomic distances in Å. Amino acid residues contributing to hydrophobic interactions with the bound chitin oligomer are schematically drawn as brown half-circles. Water molecules are shown as blue spheres. The figure was taken from the literature [188].

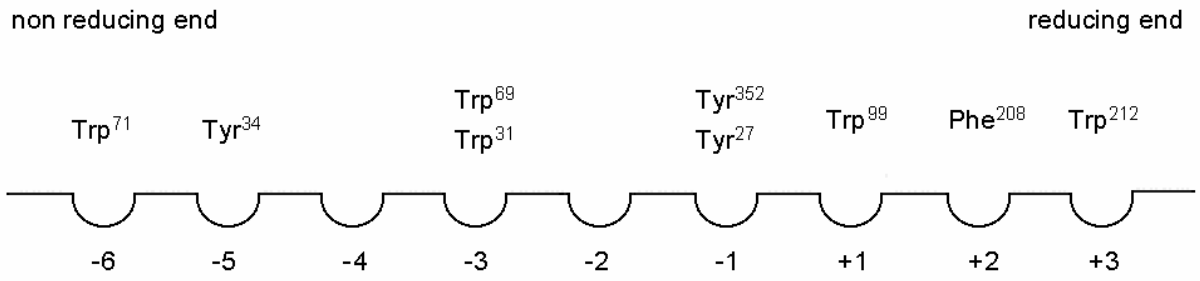

Figure 19. Schematic drawing of the chitin-binding domain of the catalytically inactive chitolectin HC gp-39 with subsites ranging from -6 (non-reducing end) to +3 (reducing end). The former catalytic site is positioned asymmetrically in the binding cleft between subsites -1 and +1. The chitin-binding domain is not locked at any subsite. The drawing was made according to the discussion of the subsites of the chitin-binding domain of HC gp-39 in reference [188].

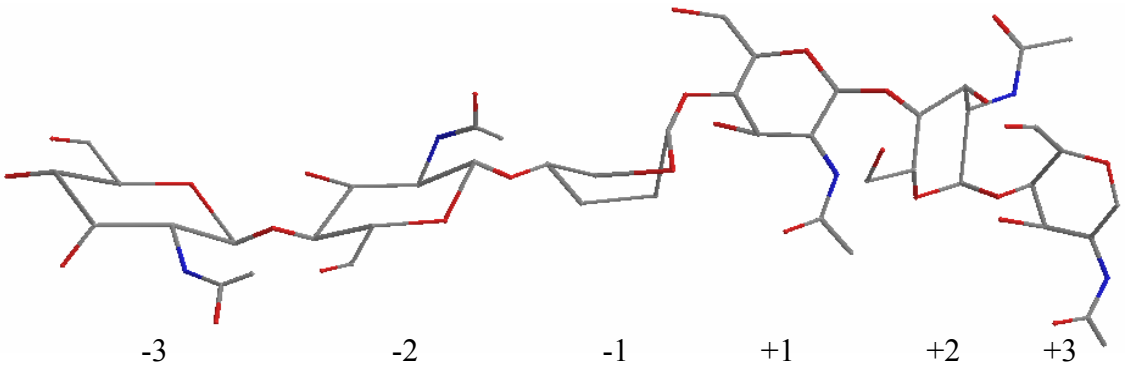

Figure 20. Schematic drawing of the arrangement of the monosaccharide units of a chitin hexasaccharide bound to HC gp-39. The sugar moiety bound to subsite -1 takes up a twisted boat conformation which results in an edgewise binding of the A units in subsites +1 to +3. [143, 144] *Chitooligosaccharides with DP > 3 preferably bind to HC gp-39 involving subsites -1, +1 and +2 resulting in an edgewise arrangement even though enough subsites exist which allow for a non-edgewise binding. Only A_2 and A_3 prefer to bind to the distal subsites -6, -5 and -4. (Chem3D Pro 11.0 ®, carbon atoms: black, oxidation atoms: red, nitrogen atoms: blue)*

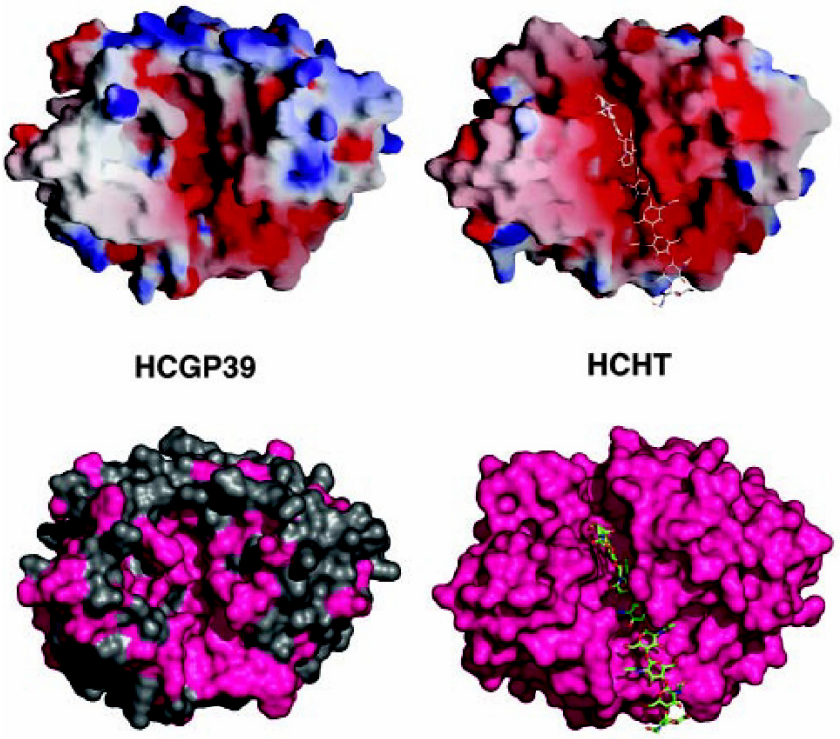

Figure 21. Structural comparison of HC gp-39 with human chitotriosidase. The top panel shows the electrostatic surface potential (red, < –7.5 kT; blue, > +7.5 kT). The bottom panel highlights the sequence conservation (magenta conserved; grey, non-conserved). For HCT a model of A_9 is additionally shown as a stick model. The figure was taken from the literature [187].

It was reported that chitooligosaccharides induce a conformational change of HC gp-39. [187] Two regions of the protein are in the focus. On one hand the region involving His^{209}, Trp^{212} and Arg^{213} (subsites +2 / +3), on the other hand Trp^{99} and Asn^{100} (subsite +1). Whereas for the 209 – 213 region a significant conformational change is under discussion, it is undoubtedly

found for the 99 – 100 region. [189] It is speculated that the 99 – 100 region (subsite +1) functions as a "gate"; Trp^{99} including its side chain in the +1 position has a "pinched" conformation when the chitooligosaccharide is not bound and a "stacked" conformation while interacting with the oligosaccharide. [189] Due to the difference in the orientation of Trp^{99}, the chitin-binding groove is wider in HC gp-39 than in human chitotriosidase. [188] In the plant chitinase hevamine, which acts as a defence endo-chitinase, the residue corresponding to Trp^{99} is a glycin, a substitution that ensures a completely open chitin-binding groove and full accessibility of the central subsites located near the catalytic residues. [188]

The physiological function of a ligand-binding induced conformational change of HC gp-39 is still not clearly investigated as well as the function of a putative gate at subsite +1 or the preferred binding of A_2 and A_3 to the distal subsites -6 and -5.

The observation that *N*-acetylglucosamine oligomers bind to HC gp-39 suggests that HC gp-39 could participate in specific signalling processes perceiving the presence of newly synthesized hyaluronic acid chains; [190, 191] short *N*-acetylglucosamine oligomers are putative primers for the biosynthesis of hyaluronic acid. The *N*-acetylglucosamine oligomers are kept at the reducing end of nascent glycans.[188, 192]

Additionally to the X-ray analysis of co-crystals of *N*-acetylglucosamine oligomers and HC gp-39, the interactions between both species were studied by affinity assays. The equilibrium binding was analysed fluorometrically, using the intrinsic tryptophan fluorescence in aqueous solution, which is increasing upon oligosaccharide binding due to a rearrangement of the solvent environment. The fluorescence data showed a binary interaction with dissociation constants of 331 μM for A_4 and 6.7 μM for A_6, indicating a tighter interaction with increasing DP.[187]

HC gp-39 possesses a second binding site, which is located in a surface loop and putatively binds heparan sulfate. [193] Heparan sulfate contains both, *N*-acetylglucosamine and glucosamine units. [194] Proteoglycans containing heparan sulfate are present at the cell surface and in the extracellular matrix where they are involved in cell adhesion, organ genesis and wound healing. Furthermore, they play a role as growth factors (cytokines). [194, 195]

Recently was found that three isoforms of HC gp-39, which differ in their glycosylation patterns, are able to bind collagen form I with relatively low affinity (K_d = 1 μM). The chondrocyte derived species was found to stimulate the rate of type I collagen fibrillo-genesis, whereas the cartilage major form had an inhibitory effect. The ability of HC gp-39 to regulate fibrillo-genesis suggests a physiological role in the laying down of new collagen fibrils during development and connective tissue remodelling.[196]

1.6.2 Other Human Chitolectins

Besides HC gp-39, further chitolectins were detected in humans. Closely related to HC gp-39 (chitinase-3-like protein 1) is YKL-39 (chitinase-3-like protein 2). In contrast to the broad range of HC gp-39 expression, YKL-39 production is predominantly demonstrated for chondrocytes and synoviocytes. [197] This protein is expressed in healthy articular chondrocytes (like HC gp-39), but whereas HC gp-39 is significantly down regulated in late stage osteoarthritic chondrocytes, YKL-39 is significantly up regulated. [197, 198] Two biological activities of YKL-39 might contribute to the progression of arthritis. One is the induction of autoimmune response, and second is the participation in tissue remodelling. [198] Immunisation with purified YKL-39 induced arthritis in different strains of mice.[199]

Stabilin-interacting chitinase-like protein (SI-CLP) is the most recently identified human chitolectin. This protein is an interacting partner and sorting ligand for stabilin-1, which is expressed in macrophages and endothelial cells in liver, spleen, lymph node and bone marrow. [108, 111, 200] It was found, that macrophages treated with interleucin-4 (IL-4) secrete SI-CLP; treatment with a combination of IL-4 and dexamethasone blocked secretion and resulted in intracellular accumulation of SI-CLP. [108] SI-CLP is found in patients with chronic inflammatory disorders of the respiratory tract. [108] As SI-CLP is up regulated by glucocorticoids it is a promising marker for the individual response to glucocorticoids and prediction of side effects of corticoid treatment. [111]

Human oviductin MUC9 shows a striking level of sequence identity with HC gp-39 (46%) and family 18 chitinases (up to 35%).[108] It is exclusively secreted by oviductal epithelium with highest expression levels in time of ovulation, which indicates a regulatory role during fertilization. [201] Oviductins are heavily glycosylated (up to 45% of the molecular mass). The protein interacts with the zona pellucida of the oocyte during its passage through the oviduct until implantation of the embryo. [201, 202] Putatively, human oviductin binds with its chitinase-like domain to specific oligosaccharides of the oocyte, shielding it from proteases by their bulky oligosaccharide side chains.[202]

1.6.3 Non-Human Chitolectins

Besides in humans, catalytically inactive chitinase-like proteins are expressed in other mammals, but also insects and plants. E.g. YM1 is secreted by murine activated peritoneal macrophages elicited by oral infection of mice with nematodes. [108, 203] The induced expression of YM1 by activated macrophages and the profound cellular changes paralleling its appearance suggest that YM1 may bear functional significance to the development of either host defence against or tolerance to nematode. [203] The structure of YM1 showed a good

agreement with chitinase A from *S. marcescens* in the catalytic TIM barrel ($(\beta/\alpha)_8$ barrel) and the small α+β folding domain. [193] In addition to chitinase A, concanavalin B and narbonin also share structure similarity with YM1. [193, 204] With respect to human chitotriosidase YM1 is poorly conserved and does not show a well-defined cleft, additionally it is more negatively charged. [203] YM1 has been identified as an animal lectin with a binding specificity toward carbohydrates containing D units. Additionally, YM1 possesses an ability to bind heparin / heparan sulfate. [203]

MGP-40 (mammary gland protein 40 kDa) is another mammalian chitolectin. It was isolated from goat dry secretions. [189] This protein is implicated as a protective signalling factor that determines which cells are to survive the drastic tissue remodelling that occurs during involution. [189] It has been indicated that certain cancers could surreptitiously utilize the proposed normal protective signalling by proteins of this family to extend their own survival and thereby allow them to invade the organ and metastasis. [189] In view of this, MGP-40 could form an important target for drug design against breast cancer. [189] The structure of MGP-40 is consistent with the $(\beta/\alpha)_8$ barrel topology of the family 18 chitinases. [205] Detailed analysis of the crystal structure of MGP-40 suggests that it is able to bind chitooligosaccharides. [189, 205]

Plants also produce proteins that contain the family 18 conserved regions without showing any hydrolytic activity; examples are narbonin from *Vicia narbonensis L.* seeds[206] and concavalin B. [207, 208] The functions of these proteins are yet unknown.

1.7 Aims of this Thesis

In nature, chitinous materials often co-occur with proteins which either hydrolyse chitin or chitosan like chitinases, or proteins that are evolved from chitinases but which are catalytically impaired and function as biological signalling mediators – the chitolectins. One aim of this thesis is to measure quantitatively the binding of chitooligosaccharides to chitinases and chitolectins. In detail, the family 18 chitinases A and B from *Serratia marcescens* were selected to determine the affinities of heterochitooligosaccharides with respect to DP, F_A and sequence. *N*-acetylglucosamine oligomers of DP > 2 are substrates of chitinases as well as chitin or chitosan. Glucosamine oligomers, composed solely of D units, are not hydrolysed by chitinases. However, these compounds are supposed to bind poorly to chitinases. Heterooligosaccharides, composed of A and D units, have the potential to bind to chitinases with sufficient affinities due to their content of A units. On the other hand, they

offer the advantage of being resistant against hydrolysis due to the presence of several D units. A combination of both properties is the predisposition for substances to act as chitinase inhibitors. Chitinase inhibitors play important roles e.g. as insecticides (some insects need chitinases to destroy the cuticle during metamorphosis) or as agents against malaria (filariae need chitinases to escape from the peritrophic membrane of hosting insects).

The second scope of the present thesis is to determine quantitatively the affinities of heterochitooligosaccharides to the human chitolectin HC gp-39 with respect to DP, F_A and sequence.
HC gp-39 is of increased interest due to its well-investigated structure of the chitin-binding domain on one hand, and its involvement in cellular signalling processes on the other hand. The predominant amino sugar monomer units of the human body are *N*-acetylglucosamine and *N*-acetylgalactosamine which both occur in glucosaminoglycans and proteoglycans. *N*-acetylglucosamine forms together with its derivative *N*-acetylmuramine the backbone of the bacterial cell wall, and it contributes to the glycosylation pattern of glycoproteins. Glycoproteins cover together with glycolipids all cell surfaces. Free glucosamine rarely occurs in the human body. It is a component of heparin and heparan besides *N*-acetylglucosamine. Up to now, no human polysaccharide or oligosaccharide structure is described containing sequences of D and A units as characteristic for chitinous material. The finding of HC gp-39 and other human chitolectins promises that further chitinous structures could be involved in cellular signalling processes in humans. The presence of lectins containing chitooligosaccharide binding sites suggests that exogenous chitooligosaccharides (taken up with nutrients) have the potential to influence biological processes in humans. Chitosan is degraded in the human body to extent. It is resistant against hydrolysis at physiological pH values (stomach: ca. 1, cells: ca. 5 – 6, cancer cells ca. 3 – 4). The chitinases present in the human body do not hydrolyse D-D bonds. Additionally, chitosan and especially chitin are poorly soluble under physiological conditions and even in digestive fluids. They are not resorbed but mostly excreted undigested.
Chitooligosaccharides are soluble in digestive fluids and in human blood. Their low molecular mass compared to the corresponding polymers promises an increased resorption rate. Thus, chitooligosaccharides appear to be the preferred form for the transportation of chitinous activity into the human body. The highest biological activities are expected from *N*-acetylglucosamine homooligomers as the binding pockets of chitolectins are optimised for A units. A units occur in the human body significantly more often than D units. D units occur in

heparan sulphate, a glucosaminoglycan. A units, GlcNAc, are part of N-glycans and therefore frequently occur in the human body – on cell surfaces as well as glycosylated proteins.[209] Additionally, GlcNAc is a compound of glucosaminoglycans.[210] Putatively, chitin homooligomers of DP < 6 are primers of the hyaluronan biosynthesis in vertebrates.[211, 212]
On one hand the highest bioactivity is expected for *N*-acetylglucosamine homooligomers, on the other hand these oligomers show the lowest biostability. *N*-acetylglucosamine homooligomers are less stable under acidic conditions than glucosamine homooligomers due to the anchimeric assistance by the acetamido group at C-2 with respect to hydrolysis of the glycosidic bond. Additionally, *N*-acetylglucosamine homooligomers of DP > 2 are preferred substrates for the human family 18 chitinases HCT and AMCase but also for lysozyme. Heterochitooligosaccharides, composed of A and D units, promise on one hand a sufficient biostability in human due to its D units and on the other hand a sufficient affinity to HC gp-39 (and other chitolectins) to influence biological signalling due to its A units.
For affinity studies either pure oligomers, homologs, isobars or well-characterized mixtures of heterooligosaccharides have to be applied to obtain sound results. Thus, the third and fourth scopes of this thesis were to establish rapid and less substance consuming methods for the quantitative analysis of complex mixtures of heterochitooligosaccharides (containing oligomers, homologues and isobars), and moreover to establish methods for the preparation of pure oligomers, homologues and isobars based on chromatographic separation techniques. Moreover, it was the aim to conclude from the oligomer, homologue and sequence composition of partial depolymerisates of chitosan or chitosan copolymers to the monomer arrangement in the polymer.

2.0 Off-Prints

Quantitative Analysis and Preparation of Heterochitooligomers, Homologs and Isomers

Sven Bahrke[†], *Ng Chuen How*[‡], *Jón Einarsson*[‡], *Jóhannes Gislason*[‡], *and Martin G. Peter*[*,†]

[†]Institut für Chemie, Universität Potsdam, Karl-Liebknecht-Str. 24 – 25, 14415 Potsdam, Germany,

[‡]Genis ehf, Myrargata 2, 101 Reykjavik, Iceland

Received Date

Abstract Heterochitooligosaccharides possess intriguing biological activities. The activity is hereby coupled to the structure (DP, F_A and sequence of D and A units). The present work provides a series of chromatographic and mass spectrometric methods which enable the researcher to analyse rapidly mixtures of heterochitooligomers, homologs and isomers. The combinations of GPC (Biogel P4™, RI detection) and IEC (Resource S™, UV detection) as well as GPC and MALDI-TOF MS after derivatisation of the free amino groups with hexadeutero acetic anhydride were successfully used for this purpose. The sequence IEC (SP Sepharose™) followed by GPC (Biogel P4™) proved to be optimal for the preparation of

[*] To whom all correspondence should be addressed. Institut für Chemie, Universität Potsdam, Karl-Liebknecht-Str. 24 – 25, 14415 Potsdam, Germany, e-mail: Martin.Peter@uni-potsdam.de

pure homologs of DP2 – 10 in the scale of milligrams. Alternatively, a multistep chromatographic separation by GPC (Biogel P4™) afforded salt-free homologs. For the quantitative analysis and preparation of isomers in microgram scale IEC on Mono S™ stationary phases (UV detection) was employed.

Keywords

Chromatography, mass spectrometry, heterochitooligosaccharides, homologs, isomers.

Introduction

Chitin is the name for the sugar copolymer composed of *N*-acetylglucosamine (A) and glucosamine (D), which is insoluble in diluted acids. The deacetylation of chitin gives chitosan, which is soluble in diluted acetic acid. In nature we usually find chitin (exceptionally for some fungi). The monomer units of both polymers, chitin and chitosan, are connected via β-(1,4)-linkages.[1]

Chitin and chitosan are enzymatically degradable by either chitinases or chitosanases usually giving complex mixtures of heterochitooligomers – homologs and – isomers which are composed of *N*-acetylglucosamine (A) and glucosamine (D). They are prepared by either chemical or enzymatic degradation of chitosan or chitin. The degree of polymerisation (DP) varies from 2 to 20 units in a segment, and each segment differs in the mole fraction of A residues (F_A, i.e. homologs) and in the sequences of D and A residues (i.e. isomers). A heterochitooligomer of DP3 for example includes 4 homologs (D_3, D_2A_1, D_1A_2, A_3) each of which represents either a pure isomer (D_3 = DDD; A_3 = AAA) or a mixture of isomers (D_2A_1 = DDA, DAD, ADD; D_1A_2 = DAA, ADA, AAD).[2]

Chitooligosaccharides possess a number of intriguing biological activities such as promotion of chondrocyte growth[1], immune stimulation through activation of macrophages[3], chemotactic migration of polymorphonuclear cells[4], morphogenetic activity in vertebrates[5,6] and growth regulator or elicitor action in plants.[7,8,9] Hereby, the biological activity alters with DP, F_A and the sequence of D and A units as was demonstrated for the affinities of ChOs to chitinase B (*Serratia marcescens*)[10]. Also the differences in the interactions of *N*-acetylglucosamine homooligomers (DP $\geq$ 4) with the chi-lectin HC gp-39 were studied.[11,12]

Therefore it is necessary to know in detail the quantitative composition of mixtures of oligomers, homologs and isomers. Moreover, in many cases it is desirable to apply pure homologs or even isomers for biological studies to obtain clear results.

Chromatographic methods were applied for the separation of mixtures of oligomers, homologs and isomers.

Gel permeation chromatography (GPC) separates molecules of different dimensions and herewith molecular masses. Gel chromatographic separations of mixtures of chitosan or chitin homooligomers give pure oligomers.[2,13,14] Mixtures of heterochitooligomers obtained by enzymatic depolymerization with chitinase B (*Serratia marcescens*) were separated employing GPC followed by NMR analysis of the fractions.[15,16]

Cation exchange chromatography separates ChOs according to their charge numbers.[14] Separations of complex mixtures of ChOs give fractions of identical charge numbers but different DP.[17,18]

Further chromatographic methods were employed for the analysis and preparation of heterochitooligosaccharides. Amino stationary phases were employed for the separation of

chitin oligomers.[14,19,20] But also mixtures of heterochitooligomers of DP ≤ 5 elute from this material. However, the peak resolution for the separation of heterochitooligomers is not comparable to that obtained employing GPC or IEC materials, respectively.[14] As well amide stationary phases were used for the separation of chitin oligomers.[21] Anion exchange materials in alkaline eluents were successfully employed for the separation of homologs.[21]

MALDI-TOF and FAB MS have been extensively employed for the analysis of mixtures of (hetero)chitooligosaccharides.[2,23,24,25,26,27] Hereby, these mass spectrometric methods have proved to be rapid tools for the qualitative analysis of even complex mixtures of oligomers (DP 1 – 20) and homologs.

The objectives of the present research are to develop a method combining GPC and IEC for the analysis and preparation of heterochitooligomers and homologs. Secondly, a method based on IEC is developed for the analysis and preparation of isomers. And finally a mass spectrometric method is developed allowing for the rapid quantitative analysis of mixtures of heterochitohomologs. This method demands a derivatisation of the free amino groups with Ac_2O-d_6. The acetylation of heterochitooligomers (partial re-*N*-acetylation employing Ac_2O in MeOH/H_2O[26], per-*N*-acetylation for subsequent HPLC analysis[14, 28], per-acetylation in combination with hydrolysis[29,30]) and especially the acetylation of chitosan (partial re-acetylation of chitosan[31], formation of chitin hydrogel[32]) is described in many variants in the literature. Applying deuterated reagents for the acetylation (deutero per-*N*-acetylation), a change in the rate of the reaction or a consecutive change in the degrees of substitutions of the reaction products does not appear as the isotopic effect is neglectible. The *N*-acetylation is usually accompanied to some degree by *O*-acetylation. The standard method for the selective *O*-deacetylation of chito-oligomers (in the presence of *N*-acetyl groups) is the treatment with diluted KOH. However, different reagents are described (ammonia[26,32,33], cyanide[34], sodium methanolate[35],hydrazine acetate[36]).

Materials and Methods

Materials

Sample 1 (mixture of chitosan homooligomers): hydrolysate of deacetylated chitosan (F_A 0.02, Euphausia superba) with HCl aq. fum.; filtration 0.8 and 0.2 µm pore size, ultra-filtration 3 and 0.5 kDa.

Sample 2 (mixture of ChOs): hydrolysate of deacetylated chitosan (F_A 0.48, *Pandalus borealis*) with a family 18 chitinase from *Penicillium sp*.; filtration 0.8 and 0.2 µm pore size, ultra-filtration 3 and 1 kDa.

Sample 3 (mixture of ChOs): see sample 1; ultra-filtration only 3 kDa.

Sample 1 was prepared in our laboratory. Samples 2 and 3 are a generous gift of *Genis ehf, Reykjavik, Iceland*

Chitin oligomers (A_n) *Seikagaku, Tokyo, Japan*

HCl (37%, fuming, p.a.), NaOH (p.a.), ethanol (99.9+%), ammonium acetate p.a *Merck KG, Darmstadt, Germany*

NaCl (p.a.) *Riedel-de-Haën, Seelze, Germany*

3,5-Dinitro salicylic acid (98+%), 2,5-dihydroxy benzoic acid (Gentisic acid, 99+%) *Fluka Chemie, Buchs, Switzerland*

Glacial acetic acid (99+%) *Sigma-Aldrich, Taufkirchen, Germany*

Methanol (99.9%), glucose (anhydrous, p.a.) *Acros, Geel, Belgium*

Hexadeutero acetic anhydride and tetradeutero acetic acid *Chemotrade, Leipzig, Germany*

All other chemicals were purchased from *Sigma/Aldrich* (*Munich, Germany*) in p.a. quality.

Methods

Gel Permeation Chromatography of Heterochitooligosaccharides. The separations for analytical purpose are performed on a system consisting of two columns in series (each Ø =

2.5 cm, length = 100 cm, GE Healthcare XK25, Uppsala, Sweden) filled with Biogel P4, fine grade (BioRad, Munich, Germany) which are coupled to a refractive index detector (Shimadzu RID 6A, Duisburg, Germany) and a fraction collector (Pharmacia, Uppsala, Sweden). The mobile phase (0.05 M ammonium acetate buffer pH 4.2) was run through the columns with a flow rate of 25 $mL*h^{-1}$ using a peristaltic pump (Pharmacia P1, Uppsala, Sweden). The sample amount is 50 mg.

The run of a standard mixture of chitosan homooligomers (sample 1) on the column gives a separation up to DP 14. The resolution of the peaks for the DP6 and 7 oligomers is $R_S = 1.10$.

(The chromatogram of sample 1 including the determination of peak parameters is shown in Supporting Information Figure S-1).

In order to prove how the RI signal is depending on the DP and F_A of ChOs, equal masses of D_4, D_9 and A_3 were analysed by RI detection. For all three oligomers the peak areas were identical within the error margin, indicating that the RI signal is proportional to the mass of the ChOs, independently from the DP and F_A.

The experimental results are confirmed by theoretical calculations: The refractive index (n_r) is a function of the molar mass (M_m), the density (ρ) and the molar refraction (R_m): $n_r^2 = (M_m/ \rho + 2 R_m)/ (M_m/ \rho - R_m) \Leftrightarrow R_m* \rho/ M_m = (n_r^2 - 1)/ (n_r^2 + 2)$.[37] Assuming that ρ is nearly constant for oligomers and homologs, the quotient R_m/ M_m determinates n_r. R_m is the sum of the molar bond refractions $r_{b,m}$. Table 1 shows the calculated molar refractions for D_4, D_9 and A_3.[37] The quotient R_m/ M_m [$mL*g^{-1}$] is constant for the oligomers D_4 and D_9 as well as the acetylated species A_3. Thus, n_r is independent of the DP and F_A but linearly depending on the mass of the ChO.

Table 1. Calculated molar refractions R_m for D_4, D_9 and A_3. The quotient R_m/ M_m (molar refraction / molar mass) is constant for oligomers and homologs (D_4, D_9, A_3). The last column shows the deviations $\Delta(R_m/M_m)$ of D_9 and A_3 with respect to D_4.

ChO	R_m [$mL*mol^{-1}$]	R_m / M_m [$mL*g^{-1}$]	$\Delta R_m / M_m$ [$mL*g^{-1}$]
D_4	142.82	0.2157	-.-
D_9	316.72	0.2158	0.0001
A_3	135.88	0.2166	0.0019

Separations for preparative purposes are either conducted under the conditions above, or – if the sample amount increases 250 mg - the conditions are changed: The column dimensions are increased to Ø = 5.0 cm, total length = 200 cm, the flow rate is increased to 50 $mL*h^{-1}$. Under these conditions GPC fractionations of ChOs were successfully performed up to a sample amount of 0.75 g. Preparative fractionations include separations of crude mixtures of ChOs obtained by enzymatic degradation of chitosan, re-chromatography of GPC fractions or separations of IEC fractions of compounds with identical charge numbers but different DP.

Cation Exchange Chromatography of Heterochitooligosaccharides. For analytical purpose, fractions from the GPC separation of sample 2 are objected to cation exchange chromatography. The separations are performed on a system consisting of an HPLC instrument (Jasco, Gross-Umstadt, Germany) with a UV detector (detection wavelength 210 nm) and a Resource S™ stationary phase (Pharmacia, Uppsala, Sweden) with a bed volume of 1 mL. Under a flow rate of 1 $mL*min^{-1}$ the following gradient was run: eluent A, HCl pH 3.5; eluent B, HCl pH 3.5 + 1 M NaCl. Gradient: 0-5 min 0% B, 5-45 min 0-50% B, 45-46

min 50-100% B, 46-55 min 100% B, 55-56 min 100-0% B, 56-70 min 0% B. The gradient run from 46 - 70 min is for washing and equilibration of the column.

For the optimisation of the separations of compounds with charge numbers of 5 or higher the gradient is adjusted as follows: 0-10 min 0% B, 10-75 min 0-50% B, followed by the washing and conditioning procedure.

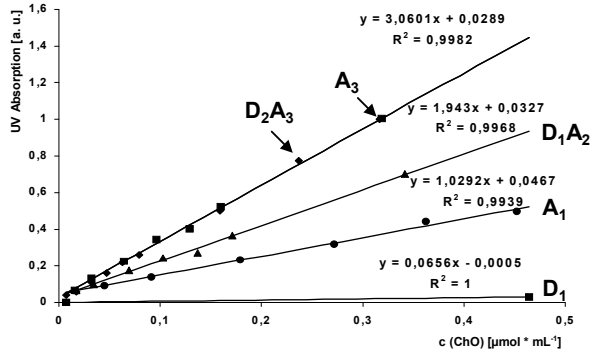

Figure 1. The figure shows the plots of the UV absorptions of D_1, A_1, D_1A_2, A_3 and D_2A_3 versus the concentration in the range of 0.0 to 0.6 µmol*mL^{-1}. The plots are fitted to linear functions. The equations and coefficients of determination are given in the Figure. The slopes of the graphs are increasing with increasing number of A units. The slopes vary to a low extend with the number of D units (D_1 and D_2A_3 vs. A_3).

The dependency of the UV signal from the DP, F_A and amount of the ChOs was determined. Hence, concentration-dependent UV absorption data were taken for D_1, A_1, D_1A_2, A_3 and D_2A_3 (Figure 1). The UV absorptions are linearly increasing with the molar concentration of ChOs. The slopes within the range of 0.0 to 0.6 µmol*mL^{-1} are 0.0656 a.u.*mL*µmol^{-1} for D_1, 1.0292 a.u.*mL*µmol^{-1} for A_1, 1.9430 a.u.*mL*µmol^{-1} for D_1A_2, 3.0610 a.u.*mL*µmol^{-1} for A_3 and 3.0610 a.u.*mL*µmol^{-1} for D_2A_3. The slopes are nearly identical for ChOs of the same number of A units (e.g. A_3 and D_2A_3) indicating that the UV absorption of D units is neglectable. This observation is supported by the slope of the plot for D_1 (0.0650 a.u.*mL*µmol^{-1}) which is almost zero. The ratio of the slopes for A_1, D_1A_2 and A_3 / D_2A_3 is 1.0292 : 1.9430 : 3.0610 which is within the error margin of the measurements (weighing error) equal to 1 : 2 : 3, indicating that the UV absorption of ChOs linearly depends on the number of A units. The linear range of the UV absorption for ChOs is 0.05 to 4.5 µmol*mL^{-1}*n_A^{-1}, where n_A is the number of A units of the ChO. (The plot of the UV absorption vs. the concentration of A_3 in the range of 0.05 to 5 µmol*mL^{-1} is shown in Supporting Information Figure S-2).

The UV signal is proportional to the number of A units in the oligosaccharide chain. The chromophor – the amide bond – has an absorption maximum at ca. 220 nm.[38] The UV absorption of a linear combination of n identical but non-conjugated chromophors in the molecule is comparable to the same number n of individual chromophors.

The heterochitooligosaccharide chain may occur in twisted conformations (tangle-like) besides a linear arrangement of the monomer units (rod-like), depending on DP and F_A of the ChO as well as the pH and the ionic strength of the solution. A decrease of the linearity of the

oligosaccharide chain will decrease the UV absorption as the chromophors partially hide each other. The UV signal is almost independent from the number of D units as the UV absorption of the amino group is neglectable compared to the UV absorption of the amide bond due to missing $\pi \rightarrow \pi^*$ and $n \rightarrow \pi^*$ electron transitions.[39]

For the quantitative determination of a ChO, the peak area of the UV absorption has to be divided by the number of A units of the corresponding ChO. As the UV signal is proportional to the molar amount of the ChO, the corrected peak area has to be multiplied with the molar weight of the ChO, followed by multiplication with 100 and division by the total mass of the sample to obtain the relative mass of a ChO in %. Figure 2 shows exemplarily the cation exchange chromatogram of GPC fraction 5 of sample 2. The peak containing D_2A_3 has an area of 683 a.u.*min, the peak containing D_3A_3 has an area of 371 a.u.*min, the peak containing D_4A_2 has an area of 76 a.u.*min and the peak containing D_5A_2 has an area of 74 a.u.*min. The corrected peak areas (division by the number of A units) are: D_2A_3 228 a.u.*min, D_3A_3 124 a.u.*min, D_4A_2 38 a.u.*min and D_5A_2 37 a.u.*min. The peak areas are proportional to the molar amounts of the homologs. The relative masses are obtained by multiplication with the corresponding molar masses to give: D_2A_3 216459 a.u.*min*g*mol^{-1}, D_3A_3 137696 a.u.*min*g*mol^{-1}, D_4A_2 40601 a.u.*min*g*mol^{-1} and D_5A_2 45492 a.u.*min*g*mol^{-1}. The total mass of GPC fraction 5 is 216459 + 137696 + 40601 + 45492 = 440248 a.u.*min*g*mol^{-1}. The relative masses of the homologs are set in relation to the total mass of the GPC fraction:

D_2A_3 216459 a.u.*min*g*mol^{-1}*100 / 440248 a.u.*min*g*mol^{-1} = 49.2 %;

D_3A_3 137696 a.u.*min*g*mol^{-1}*100 / 440248 a.u.*min*g*mol^{-1} = 31.3 %; D_4A_2 40601 a.u.*min*g*mol^{-1}*100 / 440248 a.u.*min*g*mol^{-1} = 9.2 %; D_5A_2 45492 a.u.*min*g*mol^{-1} * 100 / 440248 a.u.*min*g*mol^{-1} = 10.3 %. The gel permeation chromatogram of sample 2 gives the information that GPC fraction 5 is 16.3 % of 50 mg = 8.2 mg. Consequently, the following masses are obtained for the compounds of GPC fraction 5: D_2A_3 4.0 mg, D_3A_3 2.6 mg, D_4A_2 0.8 mg and D_5A_2 0.8 mg.

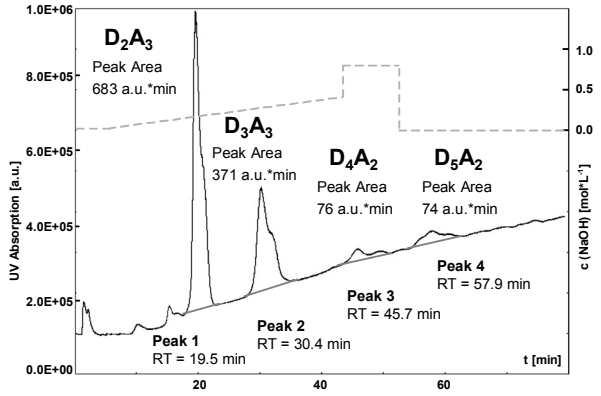

Figure 2. The figure shows the cation exchange chromatogram of GPC fraction 5 (sample 2). The NaCl gradient employed for elution of the ChOs is displayed as a dashed line. The peaks are labelled with the substance found by MALDI-TOF MS in the corresponding fractions as well as the retention time [min] and the peak area [a.u.*min]. The ChOs are separated by charge number (according to the number of protonated free amino groups D units). The separation was performed in HCl of pH 3.5.

For the preparative separation of GPC fractions, principally the same method was used as described for the analysis of GPC fractions. The lyophilised fractions of 10 mg in average were separated in batches of up to 1 mg on Mono S™ cation exchange resin (1 mL bed volume). The HPLC fractions were collected manually and desalted by dialysis (Floatalyzer™, SpektraPor, Germany). The purity of the homologs was verified by MALDI-TOF MS. The salt content was analysed by the DNS assay.

Mixtures of ChOs were separated for preparative purpose by cation exchange chromatography employing SP Sepharose. Stationary phase: SP Sepharose, 45-165 µm (wet) exclusion limit approx. 4000000 Da, S1799, (Sigma). Column size: Ø 5 cm, length 24 cm, respective 470 mL bed volume (XK 50, Pharmacia Biotech, Uppsala, Sweden). Sample amount: 7.5 g. Mobile phase: A hydrochloric acid of pH 3.5 B 1 M sodium chloride in hydrochloric acid of pH 3.5. Gradient: 0 – 1.25 h 0% B; 1.25 – 17.7 h 0 – 30% B; 17.7 – 35.3 h 100% B; 35.3 – 62 h 0% B. The eluent was run at 2 mL*min^{-1}. Fractions of 20 mL were collected and lyophilised. Each fraction was analysed by MALDI-TOF MS. Appropriate fractions were combined. Equipment: peristaltic pump (Pharmacia P1, Uppsala, Sweden), UV detector (detection at 235 nm, SpectroMonitor 3100, Milton Roy, Ivyland, USA), fraction collector (SuperFrac, Pharmacia Biotech, Uppsala, Sweden). The fractions were lyophilised.

Cation Exchange Chromatography of Heterochitoisomers. For analytical purpose, a MonoS™ PC 1.6/5 column, bed volume 0.1 mL (GE Healthcare, Uppsala, Sweden) is used on a SMART System™ (GE Healthcare, Uppsala, Sweden). 20 µg of the pure heterochitohomolog are dissolved in 20 mM formic acid of pH 3.8 (A), objected to the column and eluted with 0.6 M NaCl in 20 mM formic acid of pH 3.8 (B). Gradient: 0-16%B, 0-46 min. Flow rate: 60 µL*min^{-1}. The chromatogram is monitored at 214 nm (UV).

The peaks of the chromatograms for the separation of isomers are typically not baseline separated. For the separation of two D_3A_3 isomers (peak 1 and 2, Figure 3) the resolution is 0.4. Thus, peak fitting (PeakFit™ program, Systat Inc., San Jose, USA) is applied for the calculation of peak areas. The peaks of the chromatogram of the separation of three D_2A_3 isomers are successfully fitted to a hybrid of two Gaussian functions (Figure 4) whereas the peaks of the separation of two D_3A_3 isomers are optimally fitted to Peak Pulse functions (Figure 3).

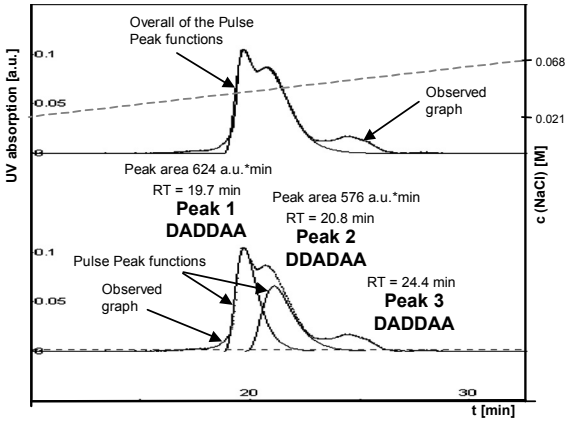

Figure 3. The figure shows the cation exchange chromatogram of a mixture of the two D_3A_3 isomers DADDAA and DDADAA. The three peaks of the chromatogram are not baseline separated. Thus, the chromatogram is fitted to Pulse Peak functions for peak 1 and 2. The upper part of the figure compares the overall of the Pulse Peak functions with the observed

graph indicating a perfect fit for peak 1 and 2. All three peaks are labelled with the isomer detected by MALDI-TOF tandem MS (sequence analysis with quantitation after derivatisation of the ChO with AMAC) and the retention time. For peak 1 and 2 additionally the peak areas are given as calculated on base of the fit to Pulse Peak functions. The NaCl gradient employed for the elution of the isomers is given as a dashed line.

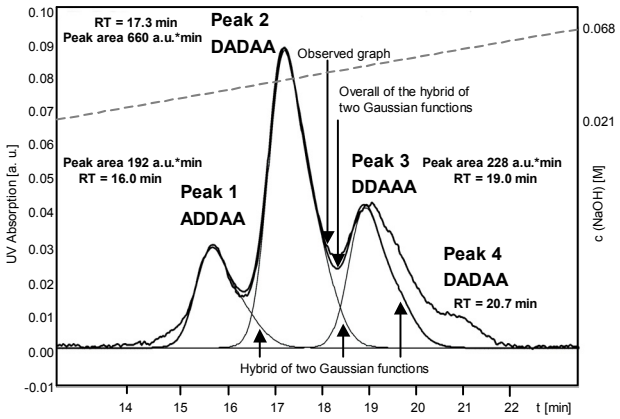

Figure 4. The figure shows the cation exchange chromatogram of a mixture of the three D_2A_3 isomers ADDAA, DADAA and DDAAA. The four peaks of the chromatogram are not baseline separated. Thus, the chromatogram is fitted to hybrids of two Gaussian functions for peaks 1, 2 and 3. The overlay of the observed graph with the overall of the hybrid Gaussian functions indicates a perfect fit for peaks 1 – 3. All four peaks are labelled with the isomer detected by MALDI-TOF tandem MS (sequence analysis with quantitation after derivatisation of the ChO with AMAC) and the retention time. For peaks 1 - 3 additionally the peak areas are given as calculated on base of the fit to the hybrids of two Gaussian functions. The NaCl gradient employed for the elution of the isomers is given as a dashed line.

As isomers possess identical numbers of A units the peak areas are directly proportional to the relative molar amounts of the isomers. Moreover, the isomers possess identical molar masses so that the peak areas are proportional to the relative masses of the isomers. A mixture of D_2A_3 isomers is obtained from GPC fractionation of sample 2 followed by cation exchange chromatographic separation of GPC fraction 5 (see *Methods, Gel Permeation Chromatography of Heterochitooligosaccharides* and *Cation Exchange Chromatography of Heterochitohomologs*). 4.0 mg of D_2A_3 are calculated. The peaks of the cation exchange chromatogram of D_2A_3 possess the following areas: ADDAA 19%, DADAA 55% and

DDAAA 26%. Consequently, the relative masses of the isomers are ADDAA 19%, DADAA 55% and DDAAA 26% and the absolute masses of the D_2A_3 isomers of GPC fraction 5 of sample 1 are ADDAA 0.8 mg, DADAA 2.2 mg and DDAAA 1.0 mg.

For preparative purpose 200 µg of the pure homolog are objected to a Tricorn Mono S™ 5/50 GL column (GE Healthcare, Uppsala, Sweden) with 1 mL bed volume. The column is run with 20 mM formic acid (pH 3.8) and a gradient of 0 – 0.12 M NaCl (0 – 50 min) on a Jasco HPLC system (Jasco, Gross-Umstadt, Germany) with UV detector (detection wavelength 210 nm). Flow rate: 1 $mL*min^{-1}$. Fractions are collected manually. For washing the column is run with 20 mM formic acid / 0.6 M NaCl for 5 min. For desalting, the fractions are run against 1L of bidest. water (Floatalyzer™, SpektraPor, Breda, The Netherlands). The purity of the fractions is analysed by MALDI-TOF tandem MS after derivatisation with AMAC. The salt content of the fractions is determined by the DNS assay.

Quantitative Analysis of Homologs by MALDI-TOF Mass Spectrometry. The mass spectrometric signal intensities of native ChOs depend on the number of A units. E.g. the signal intensity of D_5 is reduced by 70 % compared to the signal intensity of A_5 for equimolar amounts of both components. The DP influences the mass spectrometric signal intensities less. (Figure S-3 of the Supporting Information shows exemplarily the MALDI-TOF MS of equimolar amounts of D_5 and D_6.) Consequently, the ChOs are derivatised with Ac_2O-d_6 to form per-*N*-acetylated compounds. The amino groups of former D units are transformed to trideutero-*N*-acetamido groups. These groups allow to distinguish between former D units and A units but do not cause any differences in signal intensities between A units and former D units so that the mass spectrometric signal intensity is proportional to the molar amount of the ChO derivative.

For per-*N*-acetylation 1 mg of the sample is dissolved in 1 mL of water. 5 µL of the solution (i.e. 5 µg of oligosaccharide) is transferred into an Eppendorf tube. 5 µL of a mixture of HOAc-d_4, Ac_2O-d_6 and methanol (v/v 1:4:6) are added. The solution is agitated for 30 sec in a vortexer and afterwards left for 1 h at 25 – 30 °C. Finally the reaction mixture is dried in a vacuum centrifuge, 50 µL of water are added to re-dissolve the residue, followed by lyophilisation of the solution using a freeze-drying machine.

As the per-*N*-acetylation is accompanied by an *O*-acetylation, the per-*N*-acetylated ChO derivatives are selectively *O*-deacetylated. 10 µL of 10 mass-% NH_3 are added to the dry ChO derivative. The solution is vortexed for 30 sec and afterwards left for 30 min at r.t. . Finally the reaction mixture is dried in a vacuum centrifuge, 50 µL of water are added to re-dissolve the residue, followed by lyophilisation of the solution using a freeze-drying machine.

After the derivatisation procedure the MALDI-TOF mass spectra are recorded. Ca. 15 nmol of the ChO are dissolved in 200 µL of water / methanol (v/v 50:50). 0.5 µL of the solution are mixed on the target with 2 µL of a solution of 15 $mg*mL^{-1}$ of DHB in 30 vol.-% aqueous ethanol. The drop is dried under a gentle stream of air. The mass spectra are recorded on a Bruker Reflex II (Bruker Daltonik, Bremen, Germany). All spectra are recorded in the positive ion mode. For ionisation a nitrogen laser (337 nm, 3 ns pulse width, 3 Hz) is used. The spectra are measured in the reflector mode with external calibration. Each spectrum is the average of at least 60 acquisitions.

For the calculation of the amounts of ChOs in the mixture, generally the peak areas of the mass spectrometric signals and all species of pseudomolecular ions (protonated, sodiated and potassiated) have to be regarded. Preliminary experiments showed that calculations based on peak areas or peak intensities give the same results (deviation 2%) as well as calculations based on either protonated, sodiated or potassiated species. Thus, for all calculations of the present work peak intensities and sodiated pseudomolecular ions were regarded exclusively.

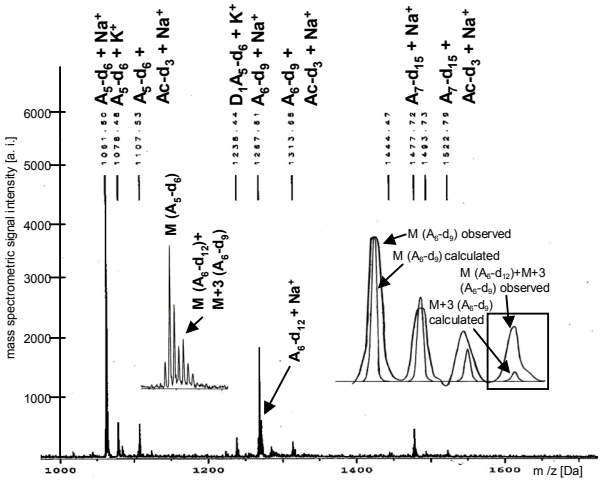

Figure 5. The figure shows the MALDI-TOF MS of GPC fraction 5 (sample 2) after derivatisation with Ac_2O-d_6 followed by selective *O*-deacetylation with NH_3. The following compounds are detected: A_5-d_6, A_6-d_9, A_6-d_{12} and A_7-d_{15}. Minor compounds are A_5-d_6 + Ac-d_3, A_6-d_9 + Ac-d_3, A_7-d_{15} + Ac-d_3 (over-acetylation, *O*-acetylation) and D_1A_5-d_6 (sub-acetylation). The main pseudomolecular ions are sodium adducts, minor species are potassium adducts. Inset 1 shows that the pseudomolecular ion (M) of A_6-d_{12} is overlapping with the isotopic pattern of A_6-d_9 (M+3). Thus, the calculated isotopic pattern of A_6-d_9 is overlayed with the observed isotopic pattern and the signal intensity of M+3 A_6-d_9 (calculated) is subtracted from the signal intensity of M A_6-d_{12} (observed) as inset 2 shows.

Figure 5 shows that to a little extent *O*-trideuteroacetylation (M + 45 Da), sub-deuteroacetylation (M – 45 Da) and incomplete deuteration (M – 1) are observed. In general, the ratio of the signal intensities of these species with respect to the signal intensity of the sodiated pseudomolecular peak is constant for each homolog. Thus, the error is below 2% if the signal intensities of these species are not regarded. However, for an increase of precision the signal intensities of these species are added to the signal intensity of the pseudomolecular ion. The masses of homologs differ by 3 Da after the derivatisation procedure. E.g. D_4A_2 becomes A_6-d_{12} (1271 Da) and D_3A_3 becomes A_6-d_9 (1268 Da). Occasionally, the MALDI-TOF mass spectra are complicated due to overlapping isotopic patterns of the homolog derivatives, e.g. A_6-d_9 and A_6-d_{12}, inset Figure 5. In this case the isotopic pattern of the lower mass component (here A_6-d_9) is calculated (Bruker Xmass 5.0™ software, Bruker Daltonics, Bremen, Germany) and the area of the M+3 peak of A_6-d_9 is subtracted from the M peak of A_6-d_{12} to obtain the exact amount of A_6-d_{12} (inset Figure 5).

The mass spectrometric signal intensity is proportional to the molar amount of the ChO. Thus, the signal intensity has to be multiplied with the molar weight of the ChO, followed by multiplication with 100 and division by the total mass of the sample to obtain the relative mass of a ChO in %. Figure 5 shows exemplarily the MALDI-TOF MS of GPC fraction 5 of sample 1 after the derivatisation procedure. The signal intensities (assigned with the Bruker Xmass 5.0™ software) are: A_5-d_6 (ex D_2A_3) 125 i.u., A_6-d_9 (ex D_3A_3) 51 i.u., A_6-d_{12} (ex

D_4A_2) 17 i.u. and A_7-d_{15} (ex D_5A_2) 13 i.u. The signal intensity for A_6-d_{12} is corrected by subtraction of the signal intensity of the M+3 peak of A_6-d_9 (cf. Figure 5). The signal intensities are proportional to the molar amounts. The relative masses are obtained by multiplication of the molar amounts with the corresponding molar masses to give: D_2A_3 118671 i.u.*g*mol^{-1}, D_3A_3 56632 i.u.*g*mol^{-1}, D_4A_2 18163 i.u.*g*mol^{-1} and D_5A_2 15984 i.u.*g*mol^{-1}. The total mass of GPC fraction 5 is 118671 + 56632 + 18163 + 15984 = 209450 i.u.*g*mol^{-1}. The relative masses of the homologs are set in relation to the total mass of the GPC fraction: D_2A_3 118671 i.u.*g*mol^{-1} * 100 / 209450 i.u.*g*mol^{-1} = 56.7 %;

D_3A_3 56632 i.u.*g*mol^{-1} * 100 / 209450 i.u.*g*mol^{-1} = 27.0 %; D_4A_2 18163 i.u.*g*mol^{-1} * 100 / 209450 i.u.*g*mol^{-1} = 0.7 %; D_5A_2 15984 i.u.*g*mol^{-1} * 100 / 2094507 i.u.*g*mol^{-1} = 7.6 %. The gel permeation chromatogram of sample 2 gives the information that GPC fraction 5 is 16.3 % of 50 mg = 8.2 mg. Consequently, the following masses are obtained for the compounds of GPC fraction 5: D_2A_3 4.7 mg, D_3A_3 2.2 mg, D_4A_2 0.7 mg and D_5A_2 0.6 mg. In order to determinate absolute masses of ChOs directly by mass spectrometry, the homolog or mixture of homologs is per-*N*-acetylated with Ac_2O-d_6. A standard solution of the corresponding chitin oligomer is prepared. 1 µmol of the chitin oligomer is dissolved in 1 mL of water. 5 µL of the standard solution are added to the lyophilisate obtained by the deutero per-*N*-acetylation of ChOs. The resulting solution is analysed by MALDI-TOF MS. The signals are quantified. The signal intensity of the reference reflects 5 nmol of substance, the amount of the analyte is calculated from the signal intensity with respect to the signal intensity of the standard.

Results and Discussion

Combination of GPC and IEC for the Quantitative Analysis of Oligomers, Homologs and Isomers. 50 mg of a complex mixture of heterochitooligosaccharides containing oligomers, homologs and isomers was separated on Biogel P4. (The MALDI-TOF mass spectrum of sample 2 is shown in Supporting Information Figure S-4). Fractions were collected automatically and analysed by MALDI-TOF MS.[40] The chromatogram (Figure 6) shows unlike for the separation of the standard a mixture of chitosan oligomers (cf. *Materials and Methods*) peak overlappings. The analysis of the GPC fractions by MALDI-TOF MS (Figure 6) reveals that the fractions are still mixtures of oligomers and homologs. But the compositions of the fractions are less complex than the starting sample. GPC fraction 5 for example contains DP5, 6 and 7 oligomers which are composed of D_2A_3, the homologs D_3A_3 and D_4A_2, and D_5A_2 (The results of the GPC of sample 2 including the results of the MALDI-TOF mass spectra of the GPC fractions are summarized in Supporting Information Table S1.) Each homolog represents a mixture of isomers. The fit of the chromatogram to Gaussian functions reveals a decrease of resolution compared to the separation of the standard. For the separation of the DP6 and 7 chitosan homooligomers a resolution of 1.10 is calculated whereas for the separation of peak 5 (mainly containing D_2A_3, DP5 and D_3A_3, DP6) and peak 6 (mainly containing D_3A_3, DP6 and D_4A_3, DP7) a resolution of 0.6 is observed. The resolution of the separation of heterochitooligosaccharides is decreased as unlike for homooligosaccharides the molecular masses of several homologs are overlapping resulting in similar molecular sizes. (Figure S-5 in the Supporting Information shows the situation for the example of DP5 to 7 homologs. The molecular masses of D_1A_4, A_5, D_6, D_5A_1, and D_4A_2, D_3A_3, D_2A_4, D_1A_5, A_6, D_7, D_6A_1, D_5A_2 and D_4A_3 range between 984.4 and 1271.5 Da, the average difference is 24 Da which is too little for a baseline separation by GPC.)

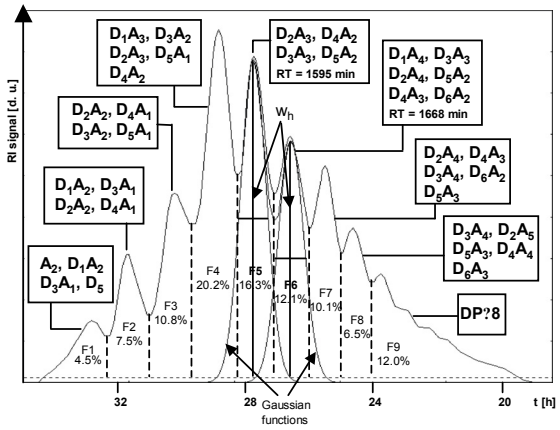

Figure 6. Gel permeation chromatogram of sample 2. Fractions were collected according to the baseline drops in the chromatogram. The peaks are labelled with the compounds detected in the corresponding fractions by MALDI-TOF MS. The relative peak areas [%] were calculated according to the RI signal intensities using baseline drops. Exemplarily peak 5 and 6 are fitted to Gaussian functions. The resolution is determined based on the peak widths at half peak heights (w_h) to 0.6.

For a quantification of the results the peak areas based on RI signals are calculated. As the RI signals of ChOs are independent of the DP and F_A, the peak areas are directly proportional to the mass of ChOs (cf. *Materials and Methods*). Peak edges were defined by baseline drop according to the collection of the fractions (Figure 6). The relative amounts calculated on base of peak areas are in good agreement with the relative amounts of the fractions obtained from weighing. (The relative amounts of GPC fractions 1 – 9 are summarized in Supporting Information Table S1.)

The fractions from GPC are applied to cation exchange chromatography on Resource S™ stationary phases. The components of the fractions are separated according to the charge number. Figure 2 shows exemplarily the chromatogram of the cation exchange separation of GPC fraction 5. This fraction contains D_2A_3, D_3A_3, D_4A_2 and D_5A_2. (The MALDI-TOF mass spectrum of GPC fraction 5 is shown in the Supporting Information Figure S-6.)

The cation exchange chromatogram shows 4 main peaks. The MALDI-TOF mass spectra of the fractions show that fraction 1 contains D_2A_3 (charge number 2), fraction 2 contains D_3A_3 (charge number 3), fraction 3 contains D_4A_2 (charge number 4) and fraction 4 contains D_5A_2 (charge number 5). GPC fractions containing oligomers of identical charge numbers (e.g. D_4A_1 and D_4A_3 (both GPC fraction 6) are not separated by IEC. In this case the relative molar amounts and relative masses are estimated from the relative signal intensities of the MALDI-TOF mass spectra.

For a quantitation of results the peak areas based on UV signals are calculated. The UV signal intensity of ChOs is proportional to the number of A units and the molar amount of ChOs. The absorption of D units is neglectable (cf. *Materials and Methods*). Consequently, for the calculation of the mass of a homolog the peak area of an UV signal is divided by the number of acetyl groups followed by multiplication with the molar weight of the corresponding homolog. Table 2 summarizes the relative masses of DP4 – 8 homologs as calculated from the cation exchange chromatograms of GPC fractions 3, 4, 5 and 7.

Table 2. Results of the quantitative analysis of sample 2 employing GPC followed by IEC. The relative masses are calculated from the peak areas as described under *Methods*. Column 3 (7) gives the relative masses with respect to the total mass of the corresponding GPC fraction, column 4 (8) gives the relative masses with respect to the total mass of sample 2.

GPC Fraction	Homolog	Mass [%] resp. GPC	Mass [%] resp. Sample 2	GPC Fraction	Homolog	Mass [%] resp. GPC	Mass [%] resp. Sample 2
F1	A_2	15	0.7	F5	D_2A_3	49	8.0
	D_1A_2	35	1.6		D_3A_3	31	5.1
	D_3A_1	50	2.3		D_4A_2	9	1.5
F2	D_1A_2	53	4.0		D_5A_2	10	1.8
	D_4A_1	5	0.4	F6	D_1A_4	0	0.0
	D_2A_2	35	2.6		D_3A_3	27	3.3
	D_3A_1	7	0.5		D_2A_4	15	1.8
F3	D_2A_2	69	7.5		D_4A_3	40	4.8
	D_3A_2	15	1.6		D_5A_2	18	2.2
	D_4A_1	10	1.1		D_6A_2	0	0.0
	D_5A_1	7	0.8	F7	D_2A_4	20	2.0
F4	D_1A_3	31	6.3		D_4A_3	40	4.0
	D_3A_2	52	10.5		D_3A_4	15	1.5
	D_4A_2	10	2.0		D_5A_3	21	2.1
	D_5A_1	8	1.6		D_6A_2	4	0.4
				F8	D_3A_4	22	1.4
					D_4A_4	52	4.4
					D_5A_3	10	0.7
					D_6A_3	16	1.0

The information taken from the cation exchange chromatograms together with the information taken from the gel permeation chromatograms allows for the calculation of the absolute masses of oligomers and homologs present in a complex mixture of ChOs. For the present example the masses of oligomers up to DP 8 were determined (Tables 2 and 4). Table 4 summarizes the relative masses of the compounds of GPC fractions 1 to 8 of the separation of sample 2 as calculated on base of IEC. The following oligomers (and main homologs) were found in fractions 1-8: DP2: 1% (A_2 0.7%), DP3: 6% (D_1A_2 5.6%), DP4: 19% (D_2A_2 10.1%, D_1A_3 6.3%), DP5: 22% (D_3A_2 12.1%, D_2A_3 8.0%), DP6: 18% (D_3A_3 8.4%), DP7: 16% (D_4A_3 8.8%). Fraction 9 contains oligomers of DP $\geq$ 8 (relative mass: 12%).

For the quantitative analysis of mixtures of isomers, cation exchange chromatography on a ono S™ PC 1.6/5 column is employed. Figure 4 shows the chromatogram of the separation of 20 µg of a mixture of D_2A_3 isomers. 4 peaks are monitored by UV detection. The MALDI-TOF mass spectra of the native compounds indicate pure D_2A_3 for all 4 peaks. The sequence analysis of the corresponding AMAC derivatives reveals that fraction 1 contains mainly ADDAA, fraction 2 DADAA and fraction 3 DDAAA whereas fraction 4 contains again DADAA. For a quantitative determination of the isomers the peaks of the chromatogram are fitted each to a hybrid of two Gaussian functions simulating a peak asymmetry. The peak areas equal the relative molar amounts of the isomers or relative masses, respectively, giving 19% ADDAA, 55% DADAA and 26% DDAAA. Peak 4 is not regarded for this calculation.

In the same way a mixture of two D_3A_3 isomers is separated and quantified. The chromatogram (Figure 3) shows three peaks the first of which mainly contains DADDAA, the second mainly contains DDADAA whereas the third contains again DADDAA. The peaks are fitted to Pulse Peak functions giving the following relative masses: DADDAA 52%, DDADAA 48%. Peak 3 is not regarded for this calculation.

The results obtained by the chromatographic analysis of D_2A_3 and D_3A_3 are compared to the results obtained from the sequence analysis with simultaneous quantification performed by vMALDI-LTQ multistage tandem MS. The relative masses of the D_2A_3 isomers are 15%

ADDAA, 57% DADAA and 26% DDAAA. For D_3A_3 the relative masses are found to 49% DADDAA and 51% DDADAA. These results are in good accordance with the chromatographic results.

The separation of heterochitohomologs by cation exchange chromatography is based on the interaction of the positively charged ammonium groups of the ChOs with the sulfonic acid groups of the cation exchange resin in acidic media. The ammonium groups (weak acid) replace the protons of the sulfonic acid groups (strong acid) of the cation exchange resin.

The retention time of a ChO is proportional to the number of its ammonium groups or D units, respectively. Heterochitoisomers possess identical numbers of D units but differ in the sequence of D and A units. Thus, an additional mechanism effects the separation of these compounds. Regarding the sequence of elution of the three D_2A_3 isomers – ADDAA 16.0 min, DADAA 17.3 min and DDAAA 19.0 min – one may conclude that the retention time of isomers is proportional to the number of D units which are exposed at the nonreducing end (as in this case) or the reducing end. The isomer ADDAA is eluting first as the A units at both ends sterically hinder the interaction between the ammonium groups of the D units and the sulfonic acid groups of the cation exchange resin (Figure 7). The isomer of the sequence DADAA is eluting at second as one D unit is placed at the nonreducing end of the oligosaccharide chain (Figure 7). The isomer of the sequence DDAAA is eluting at last as two neighbouring D units are placed at the nonreducing end. Some of the sulfonic acid groups of the resin have the right distance to fit both ammonium groups and consequently form a strong double ionic interaction (Figure 7). The separation of the two D_3A_3 isomers confirms the theory: DADDAA (one exposed D unit) elutes first, DDADAA (two exposed D units) elutes secondly. For the separations of isomers some compounds are observed to elute in two peaks: one of a large peak area eluting first and a second of a small peak area eluting second. The most plausible explanation for this observation is an additional separation of the α- / β-anomers. The cation exchange material is based on a reverse stationary phase. Derivatised (middle polar) reverse stationary phases like amide phases are known to separate anomeric mixtures of chito-oligomers due to differences in polarities.[21] The β-anomer shows a higher polarity and is thus eluted first from the reversed phase column.

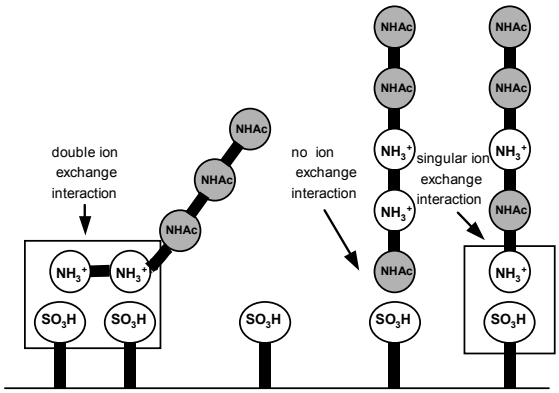

Figure 7. Explanation for the differences in retention times of the three D_2A_3 isomers ADDAA, DADAA and DDAAA on a Mono S™ cation exchange stationary phase. Protonated D units are displayed as white circles, A units as grey circles and the sulfonic acid groups of the strong cation exchanger as white ovals. ADDAA possesses no D unit exposed at the end of the sequence and is thus sterically hindered to exchange the protons of the sulfonic

acid groups. DADAA has one exposed D unit at the non-reducing end supporting a singular cation exchange interaction with the cation exchange resin. DDAAA possesses two exposed D units. As some of the distances of the sulfinic acid groups match the distance of the exposed D units, DDAAA is to some degree able to form double cation exchange interactions. The resulting sequence of elution is ADDAA, DADAA, DDAAA.

The method of the separation of heterochitoisomers by cation exchange chromatography was extended from mixtures of two or three isomers to multi-component samples containing 6 isomers. Figure 8 shows the chromatogram of the separation of 200 µg of D_3A_4 on a Tricorn Mono S™ 5/50 GL column. As determined by vMALDI-LTQ multistage tandem MS, D_3A_4 is a mixture of 45% DADADAA, 31% ADDADAA, 17% ADADDAA 17 %, 3% ADDDAAA, 2% DADDAAA and 2% ADADDAA. The chromatogram shows three main peaks (RT = 78.5 min, 80.6 min and 82.6 min) which are putatively attributed to the three main components. Additionally, two minor peaks and a shoulder (RT = 76.4 min, 83.6 min and 85.9 min) are observed.

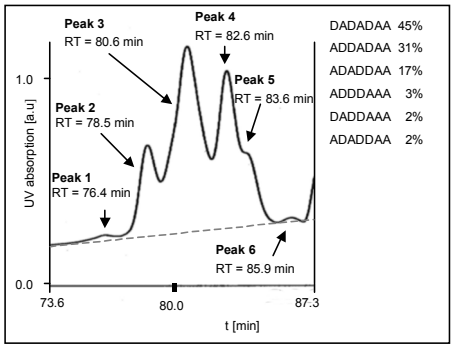

Figure 8. Cation exchange chromatogram of a complex mixture of D_3A_4 isomers. The relative amounts of the compounds as determined by vMALDI-LTQ™ multistage MS (after derivatisation of the ChOs with AMCR) are given in the right part of the figure. Five peaks and one shoulder are observed which are labelled with retention times. The concentrations of NaCl necessary for elution are: peak 1, 0.191 M; peak 2, 0.196 M; peak 3, 0.202 M; peak 4, 0.207 M; peak 5, 0.209 M; peak 6, 0.215 M. The three main peaks may be attributed to the successful separation of the three main isomers DADADAA, ADDADAA and ADADDAA.

Quantitative Analysis of Homologs by MALDI-TOF Mass Spectrometry. Alternatively to the quantitative analysis of the GPC fractions by means of IEC a method based on MALDI-TOF MS can be applied. For native ChOs the signal intensities depend on the number of D units mainly as the hydrophilic interactions (hydrogen bonds) between the free amino groups of the D units and the matrix (DHB) are stronger compared to the acetamido groups of A

units. The dependency of the mass spectrometric signal intensities from the DP (with constant F_A) of ChOs is less marked. Thus, mixtures of chitin oligomers with constant F_A and $\Delta DP < 5$ are successfully quantified by MALDI-TOF MS. ChOs containing D units have to be per-*N*-acetylated previously. For the derivatisation Ac_2O-d_6 is used. Former glucosamine (D) units are transformed to trideutero-*N*-acetylglucosamine units which is the base for an unequivocal mass spectrometric distinction of D and A units after the derivatisation procedure due to a mass difference of 3 Da. The deuterium atoms have no effect on the mass spectrometric signal intensity. The per-*N*-acetylation is occasionally accompanied by *O*-acetylation. The trideuteroacetoxy groups are selectively removed by ammonia. Figure 9 shows exemplarily the steps of the derivatisation procedure for one of the D_2A_2 isomers, ADAD.

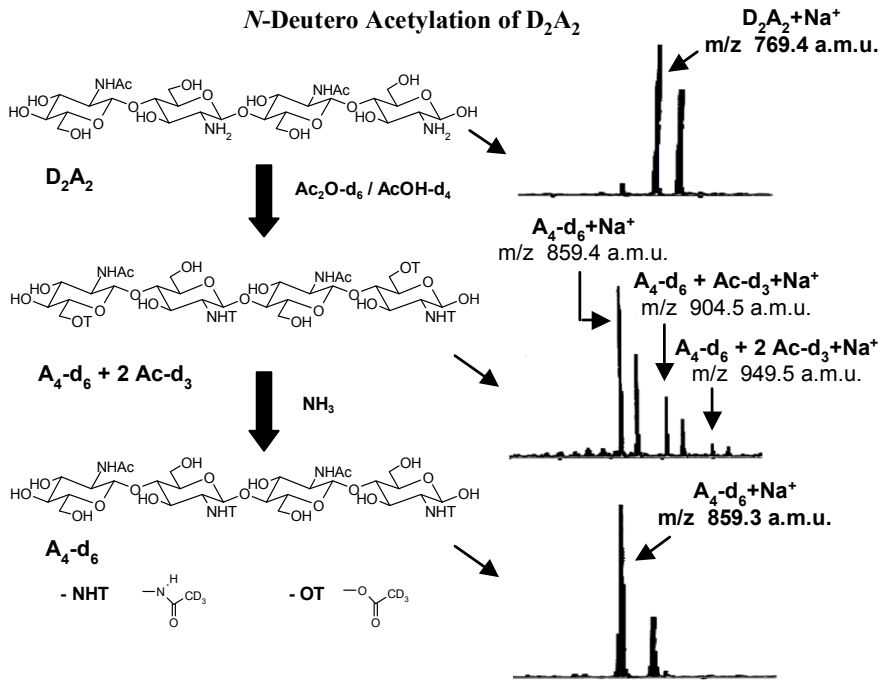

Figure 9. *N*-deuterioacetylation of D_2A_2. The figure shows the MALDI-TOF mass spectra of the native D_2A_2, the A_4-d_6 after per-*N*-deuterioacetylation of D_2A_2 with Ac_2O-d_6 and the A_4-d_6 after *O*-deacetylation with NH_3. Besides the labelled sodiated species potassium adducts are observed which are labelled with $[M+K^+]$. Additionally, the structure of one D_2A_2 isomer (ADAD) is exemplarily given before and after the per-*N*-deuterioacetylation showing *N*-trideuterioacetyl groups (NHT) and *O*-trideuterioacetyl groups (OT). The *O*-acetyl groups are selectively removed by NH_3 to form A_4-d_6 exclusively.

Figure 5 shows the MALDI-TOF mass spectrum of GPC fraction 5 after the derivatisation procedure. (The MALDI-TOF mass spectrum of the native GPC fraction 5 is shown in Supporting Information Figure S-6.) The homologs are identified by the number of trideuterio-*N*-acetylglucosamine units, the relative molar amounts are determined according to the relative intensities of the mass spectrometric signals. In case of overlapping isotopic patterns of homolog derivatives (e.g. A_6-d_9 and A_6-d_{12}, GPC fraction 5, Figure 5) the signal

intensity of the calculated intensity of the M+3 peak of A_6-d_9 is subtracted from the signal intensity of the M peak of A_6-d_{12} (cf. *Materials and Methods, Quantitative Analysis of Homologs by MALDI-TOF Mass Spectrometry*). The signal intensities of chitin oligomers are independent from the DP (for $\Delta DP < 4$.) The mass spectrometric signal intensities are proportional to the molar amounts of ChOs. The relative masses [%] are calculated according to the procedure described under *Materials and Methods, Quantitative Analysis of Homologs by MALDI-TOF Mass Spectrometry*.

Table 3. Results of the quantitative analysis of sample 2 employing GPC followed by MALDI-TOF MS. The relative masses are calculated from the peak areas as described under *Methods*. Column 3 (7) gives the relative masses with respect to the total mass of the corresponding GPC fraction, column 4 (8) gives the relative masses with respect to the total mass of sample 2.

GPC Fraction	Homolog	Mass [%] resp. GPC	Mass [%] resp. Sample 2	GPC Fraction	Homolog	Mass [%] resp. GPC	Mass [%] resp. Sample 2
F1	A_2	19	0.9	F5	D_2A_3	57	9.3
	D_1A_2	31	1.4		D_3A_3	27	4.4
	D_3A_1	51	2.3		D_4A_2	8	1.3
F2	D_1A_2	48	3.6		D_5A_2	8	1.3
	D_4A_1	18	1.4	F6	D_1A_4	3	0.4
	D_2A_2	30	2.3		D_3A_3	32	3.9
	D_3A_1	4	0.3		D_2A_4	9	1.1
F3	D_2A_2	66	7.1		D_4A_3	35	4.1
	D_3A_2	20	2.2		D_5A_2	16	1.9
	D_4A_1	10	1.1		D_6A_2	6	0.7
	D_5A_1	4	0.4	F7	D_2A_4	34	3.5
F4	D_1A_3	35	7.1		D_4A_3	34	4.5
	D_3A_2	54	10.9		D_3A_4	11	1.1
	D_4A_2	6	1.2		D_5A_3	9	0.9
	D_5A_1	5	1.0		D_6A_2	3	0.3
				F8	D_3A_4	19	1.2
					D_4A_4	55	3.6
					D_5A_3	14	0.9
					D_6A_3	12	0.8

Table 3 summarizes the relative masses of the compounds of GPC fractions 1 to 8 of the separation of sample 2 as calculated on base of MALDI-TOF MS. The following oligomers (and main homologs) were found in fractions 1-8: DP2: 1% (A_2 0.9%), DP3: 5% (D_1A_2 5.0%), DP4: 19% (D_2A_2 9.4%, D_1A_3 7.1%), DP5: 25% (D_3A_2 13.1%, D_2A_3 9.3%), DP6: 17% (D_3A_3 8.3%), DP7: 14% (D_4A_3 8.6%). Fraction 9 contains oligomers of DP $\geq$ 8 (relative mass: 12%). The sum of the relative masses of oligomers of DP 4 – 7 is 75%. The sum of the relative masses of the main homologs of DP 4 – 7 is 55.8%.

The comparison of the results obtained by IEC with those obtained by MALDI-TOF MS (Table 4) shows that the masses are in the same range indicating that no systematic errors are occurring. The deviations are in average 0.4 mg for an average mass of the homologs of 5.0 mg. The results obtained by MALDI-TOF MS are more reliable especially for minor compounds as the IEC occasionally shows fluctuations in the baseline which complicate the peak area analysis.

Table 4. Comparison of the results of the quantitative analysis of sample 2 employing GPC followed by either IEC (columns 3 and 4) or MALDI-TOF MS (columns 5 and 6). The masses are calculated with respect to the total mass of sample 2 (50 mg). Column 7 shows the differences of the masses calculated on base of IEC or MS.

Oligomer	Homolog	Mass [%] IEC	Mass [mg] IEC	Mass [%] MS	Mass [mg] MS	Δ Mass [mg]
DP2	A_2	0.7	0.4	0.9	0.5	0.1
DP3	D_1A_2	5.6	2.8	5.0	2.5	0.3
DP4	D_3A_1	2.8	1.4	2.6	1.3	0.1
	D_2A_2	10.1	5.1	9.4	4.7	0.4
	D_1A_3	6.3	3.2	7.1	3.6	0.4
DP5	D_4A_1	1.5	0.8	2.5	1.3	0.5
	D_3A_2	12.1	6.1	13.1	6.6	0.5
	D_2A_3	8.0	4.0	9.3	4.7	0.7
	D_1A_4	0.0	0.0	0.4	0.2	-.-
DP6	D_5A_1	2.4	1.2	1.4	0.7	0.5
	D_4A_2	3.5	1.8	2.5	1.3	0.5
	D_3A_3	8.4	4.2	8.3	4.2	0.0
	D_2A_4	3.8	1.9	4.6	2.3	0.4
DP7	D_5A_2	4.0	2	3.2	1.6	0.4
	D_4A_3	8.8	4.4	8.6	4.3	0.1
	D_3A_4	2.9	1.5	2.3	1.2	0.3
DP8	D_6A_2	0.4	0.2	1.0	0.5	0.3
	D_5A_3	2.8	1.4	1.8	0.9	0.5
	D_4A_4	4.4	2.2	3.6	1.8	0.4
DP9	D_6A_3	1.0	0.5	0.8	0.4	0.1
DP ≥ 8		12.0	6.0	12.0	6.0	0.0

Limitations of the Methods for the Analysis of Homologs and Isomers. GPC has proved to be a useful tool for the quantitative analysis of chitohomooligomers. Biogel P4 resolves homooligomers up to DP12, for oligomers of higher molecular masses equivalent materials (like Biogel P30) are commercially available. The peaks are easily fitted to Gaussian functions. The separation of heterochitooligomers containing oligomers and homologs is much more complicated as the separation of oligomers is overlapping with the separation of homologs resulting in peak overlappings and hidden peaks of minor components which make peak fitting procedures useless. In this case the peak areas of fractions are determined by baseline drop and the components of the fractions have to be quantified by other methods.

The cation exchange chromatography was used for ChOs with charge numbers up to +6. For higher charge numbers the peaks become broader due to increased retention times even though the gradient is set appropriately. Broad peaks decrease the sensitivity of the method.

The main shortcoming of the cation exchange chromatography is the fact that oligomers of identical charge numbers are not separated.

The accuracy of the quantification of mixtures of homologs by MALDI-TOF MS after per-*N*-acetylation is limited by additional signals caused by *O*-deuteroacetylation (M+45), sub-deuteroacetylation (M-45) and sub-deuteration (M-1). These shortcomings are circumvented by addition of the corresponding signal intensities to the signal intensity of the pseudomolecular ion M of the homolog derivative. In case of overlapping isotopic patterns of homolog derivatives the calculated intensity of the M+3 peak is subtracted from the observed intensity of the M+3 peak. The quantitative analysis of oligomers is limited in the range of Δ DP < 5.

Combination of GPC and IEC for the Preparation of Homologs and Isomers in Milligram Scale. Three different ways for the preparation of homologs were tested:

1. Step 1, GPC; Step 2, GPC (re-chromatography)
2. Step 1, GPC; Step 2, IEC (cation exchange chromatography)

3. Step 1, IEC (cation exchange chromatography); Step 2: GPC

The GPC of complex mixtures of ChOs gives a separation according to molecular sizes which are related to the molecular masses. As homologs differ in the molecular masses by 42 Da, a separation of these components is theoretically possible thus difficult due to the little molecular mass difference. Mixtures of ChOs which are prepared by enzymatic hydrolysis of chitosan employing chitinases (as for the sample used for this work) typically contain mainly one or two homologs of an oligomer. This circumstance has a positive effect on the quality of the separation.

0.75 g of sample 3 are separated by GPC on Biogel P4 (column diameter 5 cm, length 200 cm). (The chromatogram of sample 3 is shown in Supporting Information Figure S-7.)

Exemplarily, fraction 6 (yield 7.3 %) was further used with the aim to prepare pure D_2A_3. The MALDI-TOF MS (Figure 10) shows that fraction 6 is still a complex mixture of DP3 to DP 7 oligomers and homologs. Two additional re-chromatographic steps on Biogel P4 (column diameter 2.5 cm, length 200 cm) are necessary (Figure 11) to obtain D_2A_3 in a purity of 94% yield 6.8 mg (equals 0.9% of the mass of sample 3). The purity of the products was analysed by MALDI-TOF MS, the salt content was determined by the DNS assay. As for the whole preparation process only the volatile ammonium acetate buffer is used, the work-up is done by lyophilisation. The disadvantages of the method are time-consuming multiple re-chromatographic steps and the relatively low purity of the product. The advantage is the fact that the components are not contaminated with NaCl during the preparation process.

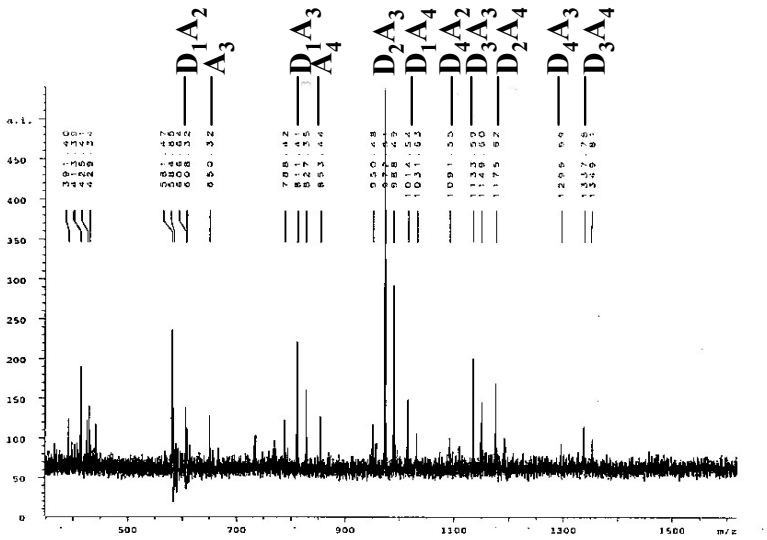

Figure 10. MALDI-TOF mass spectrum of fraction 6 of the GPC of sample 3. Fraction 6 is a complex mixture of oligomers and homologs of DP3 to 7. It was used for the preparation of D_2A_3 employing two re-chromatographic steps on Biogel P4.

The second way for the preparation of ChOs – GPC followed by cation exchange chromatography – was extensively described above under the analytical aspect. For preparative purpose 250 mg of a mixture of ChOs was separated by GPC (Biogel P4, column diameter 2.5 cm, total column length 200 cm) yielding fractions of 10 mg in average. The lyophilised fractions were separated in charges of up to 1 mg on Mono S™ cation exchange resin (1 mL bed volume). Repeated GPC-IEC steps allowed for the preparation of 4.8 mg of D_2A_3 (98% purity), 3.7 mg of D_3A_3 (98% purity), 4.5 mg of D_2A_4 (96% purity), and 1.6 mg

of D_3A_4 (97% purity) after desalting. For desalting dialysis (Floatalizers™) was used. The purity of the products was analysed by MALDI-TOF MS, the salt content was determined by the DNS assay. A disadvantage of the method is the contamination of the product with NaCl during the preparation process. Furthermore, oligomers of identical charge numbers (numbers of D units) are not separated by IEC so that in some cases components of GPC fractions cannot be isolated.

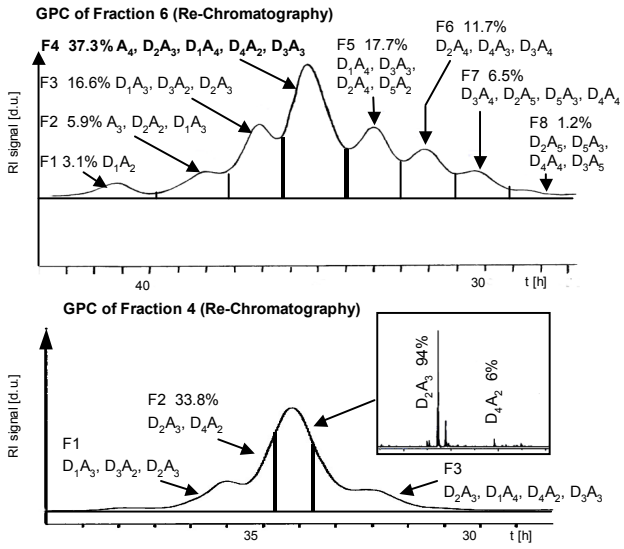

Figure 11. Re-chromatography on Biogel P4. Fraction 6 of the GPC of sample 3 is applied to re-chromatography on Biogel P4 (upper part of Figure 11). The fractions of the chromatogram are labelled with the components detected by MALDI-TOF MS and the relative peak areas calculated by baseline drop according to the collection of the corresponding fractions. Fraction 4 (containing A_4, D_2A_3, D_1A_4, D_4A_2 and D_3A_3; yield 37.3%) was applied to a second re-chromatography on Biogel P4 (lower part of Figure 11) yielding three fractions. Fraction 2 (yield 33.8 %) contains D_2A_3 in a purity of 94% as the signal quantification of the inset MALDI-TOF MS of fraction 2 indicates. D_2A_3 was obtained in an overall yield of 0.9 % (fraction 6, GPC of sample 3 = 7.3 %; fraction 4, GPC of fraction 6 (first re-chromatography) 37.3 % = 2.7 % overall yield; fraction 2 GPC of fraction 4 (second re-chromatography)

33.8 % = 0.9 % overall yield).

The third approach for the preparation of pure homologs starts with the separation of the mixture of ChOs by cation exchange chromatography. Figure 12 shows the chromatogram of the separation of 7.5 g of sample 2 on SP Sepharose (column diameter 5 cm, length 24 cm). Each IEC fraction was analysed by MALDI-TOF MS, indicating that every fraction contains

molecules of identical charge numbers but different DPs (Figure 12). (The results of the MALDI-TOF mass spectra are summarized in Supporting Information Table S2.)

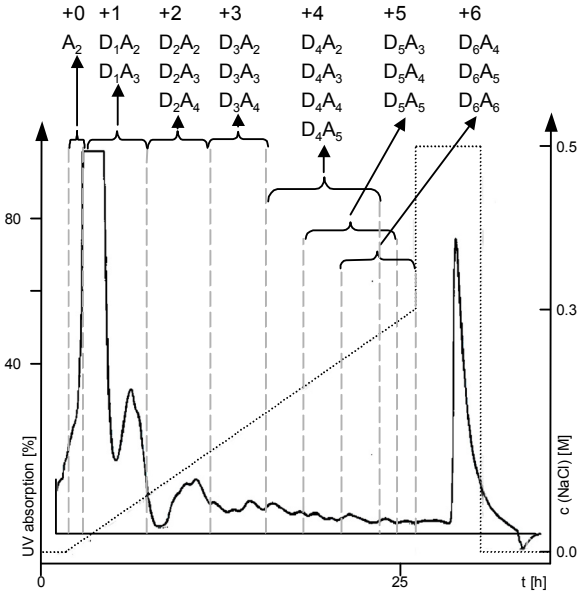

Figure 12. Cation exchange chromatogram of sample 2, an enzymatic hydrolysate of chitosan (F_A 0.48) which was ultrafiltrated to cut out a range of molecular masses between 1000 and 3000 Da. The oligomers and homologs are separated according to the charge number. Fractions of identical charge numbers are marked by dashed lines. The fractions are labelled with the oligomers found by MALDI-TOF MS. The fractions contain molecules of identical charge numbers but different DP. The NaCl gradient employed for the elution of ChOs is displayed as a dotted line.

In the second step the fractions from cation exchange chromatography are separated by GPC according to the molecular sizes to give pure homologs which are desalted in the same step. Figure 13 shows exemplarily the GPC separation of the combined IEC fractions 95 – 100. The predominant compound D_3A_2 is obtained in a yield of 17 mg (0.23% with respect to the starting material) in a purity of 93%. (Additionally, the purities and yields of all homologs that were prepared according to this method are summarized in Supporting Information Table S3.) The ammonium acetate buffer was removed by lyophilisation. The purity of the products was analysed by MALDI-TOF MS, the salt content was determined by the DNS assay. The disadvantage of this method is the inconsistent purity of the products depending on the charge number of the oligomer. The advantages of the method are salt-free products and the fact that less time-consuming steps give high amounts of homologs with an acceptable purity.

The preparation of isomers is performed essentially according to the method described for the separation of isomers for analytical purpose. For the upscaling, a Tricorn MonoS™ 5/50 GL column (1 mL bed volume) was used. The pure homologs (D_2A_3 and D_3A_3, sample 2) each representing a mixture of homologs were separated in batches of 200 µg. As the chromatograms of the separations of D_2A_3 and D_3A_3 show, the peaks are not baseline separated. Thus, material was collected only around the tips of the peaks to guarantee a high purity of the products. The fractions were desalted by dialysis. Repeated separations afforded

0.4 mg of ADDAA and 0.5 mg of DADAA in the case of D_2A_3 and 0.4 mg of each DADDAA and DDADAA in the case of D_3A_3. The purity of the products was analysed by MALDI-TOF tandem MS after derivatisation with AMAC. For the D_2A_3 were no impurities detected, for DADDAA a purity of 99% was found and for DDADAA a purity of 91% was determined. The salt content of the products was analysed by the DNS assay.

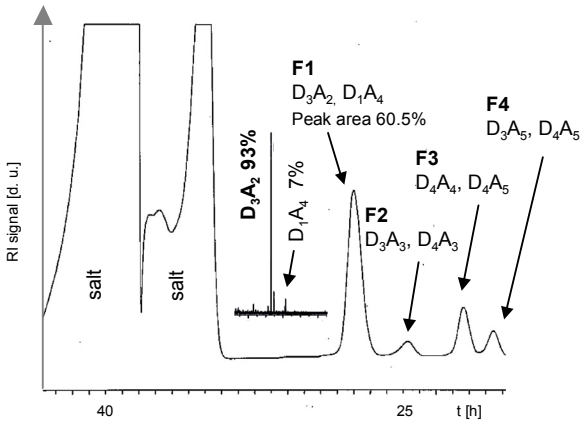

Figure 13. Gel permeation chromatogram of fractions 95-100 of the IEC of sample 2. Besides a high signal intensity for the salt (resulting from the gradient of the previous IEC) four peaks are observed. Fraction 1 corresponding to peak 1 contains D_3A_2 in a purity of 93% as the signal quantification of the inset MALDI-TOF MS indicates. Fraction 1 is obtained in a yield of 60.5 %. The overall yield of D_3A_2 is 0.23 % (yield of IEC fractions 95 – 100 equals 0.38 %).

Conclusions

It could be demonstrated that the combination of two chromatographic techniques – gel permeation chromatography and cation exchange chromatography – is a useful tool for the quantitative analysis of complex mixtures of ChOs containing oligomers, homologs and isomers. Particularly a sample of ChOs obtained by enzymatic degradation of chitosan with a chitinase containing oligomers, homologs and isomers of DP 2 to 11 (determined by MALDI-TOF MS) was analysed. Starting from 50 mg of sample the oligomers and homologs of DP 2 to 8 could be successfully quantitated by the combination of gel permeation chromatography and cation exchange chromatography.

Exemplarily the isomeric composition of two homologs – D_2A_3 and D_3A_3 – containing maximally three components was successfully quantitated employing cation exchange chromatography in combination with computer aided peak fitting. The results obtained from the quantitative analysis employing a combination of gel permeation chromatography and cation exchange chromatography are compared to methods using a combination of gel permeation chromatography and mass spectrometry. A method was successfully developed for the quantitative analysis of mixtures of homologs by MALDI-TOF MS. The problem of

the dependency of the signal intensities from the F_A of the ChOs was circumvented by the per-*N*-acetylation with Ac_2O-d_6 which transmutes the homologs into components of equivalent mass spectrometric properties and allows at the same time to distinguish former D units from A units due to a mass difference of 3 Da caused by the trideuterioacetamido group. As the mass spectrometric signal intensity of the per-*N*-acetylated ChOs is not depending on the DP of the oligomer (within a range of Δ DP < 5), the method was successfully employed for the quantitative analysis of the mixture of ChOs (sample 2) which was analysed before by the combination of GPC and IEC. The composition of oligomers and homologs up to DP 8 was quantitated. The comparison of the results obtained from both methods reveals a good agreement. The mass spectrometric method offers some advantages with respect to the amount of sample and time consumed for the analysis. Especially for oligomers and homologs of DP > 7 the precision of the mass spectrometric method is superior. Finally, oligomers of identical charge numbers (GPC fractions) are quantitated without any restriction.

The results of the quantitative analysis of the mixtures of isomers are compared to the results obtained from the earlier established method employing a sequencing by vMALDI-LTQ multistage MS and previous sequencing with AMCR. The results of both methods are in good agreement. The comparison helps to prevent systematic errors. The mass spectrometric method is advantageous since more complex mixtures of isomers can be quantitated.

The combination of gel permeation chromatography and cation exchange chromatography proved to be a useful tool for the preparation of homologs with purities up to 98%. Three combinations of methods were compared: GPC-GPC-GPC; GPC-IEC; IEC-GPC. The combination IEC-GPC proved to be superior for most applications with respect to the quality of the products (purity and salt content), the time effort and the potential for an up-scaling. From 7.5 g of the starting material could be prepared 20 mg D_3A_2, that means in a yield of 0.23 %. The chromatographic preparation of ChOs has to compete with the synthesis of oligosaccharides starting from glucosamine and *N*-acetylglycosamine. Even though the amounts of homologs prepared by chromatography are still far away from an industrial scale the method offers the advantage to prepare a series of homologs from the same batch of starting material. The method has the potential to prepare libraries of ChOs for various research applications and is in this field superior compared to synthetic methods under economic aspects (cost and time).

Moreover, it was demonstrated that the cation exchange chromatography on monodisperse porous polystyrene / divinyl benzene particles of 10 µm (Mono S™) is useful for the preparation of isomers of high purity (> 98%). Sub-milligram amounts of D_2A_3 and D_3A_3 isomers were prepared. Repeated chromatographic steps would increase the amount of the products into the milligram scale. The chromatogram of the separation of D_3A_4 homologs showed the potential of the material to separate isomers of DP > 6. The amounts of pure isomers isolated so far are precious substances to determine the different biological roles that heterochitoisomers might play in biological processes.

Nomenclature

A, *N*-acetylglucosamine or *N*-acetylglucosaminyl unit in polymers; AMCR, 3-acetylamino-6-aminoacridine; ABS_G, absorption of the glucose standard; ABS_S, absorption of the sample at 540 nm; Ac_2O-d_6, hexadeutero acetic acid anhydride; AMAC, 2-aminoacridone; c, concentration; c_s, sugar content; ChOs, heterochitooligosaccharides; D, glucosamine or glucosaminyl unit in polymers; DHB, 2,5-dihydroxy benzoic acid, DNS, 3,5-Dinitro salicylic acid; DP, degree of polymerization; F_A, molar fraction of A units; FAB MS, fast atom bombardment mass spectrometry; fum., fuming; GPC, gel permeation chromatography; HC gp-39, human cartilage glycoprotein of 39 kDa; HCl aq., hydrochloric acid; HOAc-d_4, tetradeutero acetic acid; HPLC, high performance liquid chromatography; IEC, ion exchange chromatography; M, pseudomolecular ion; M_m, molecular mass; MALDI-TOF MS, matrix-

assisted laser desorption ionisation time-of-flight mass spectrometry; $r_{b,m}$, molar bond refraction; n_r, refractive index; NaCl, sodium chloride; NaOH, sodium hydroxyde; NH_3, ammonia; NMR, nuclear magnetic resonance; ρ, density; R_m, molar refraction; R_s, resolution (of two peaks); RI, refractive index detection; rpm, rotations per minute; r.t. or RT, retention time; t_R, gross retention time; UV, ultraviolet light; w_h, peak width at half of the peak height.

Acknowledgment.

Supporting Information Available

Additional information is available as noted in the text. This material is available free of charge via the Internet at http://pubs.acs.org.

Figures Captions

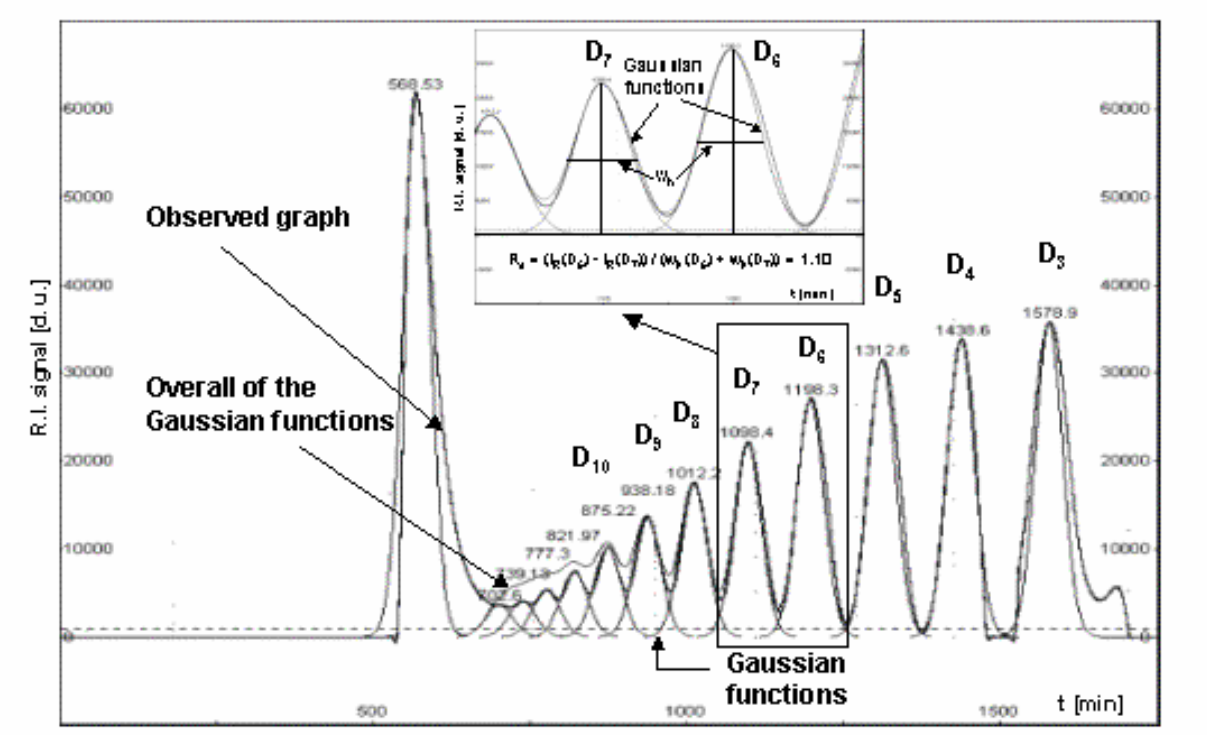

Figure S-1. Gel permeation chromatogram of sample 1 (mixture of chitosan homooligomers). The performance of the Biogel P4 columns (2.5 cm i.d. * 2 * 100 cm length) was tested with a standard mixture containing chitosan homooligomers. The chromatogram shows the separation of oligomers of DP 3 to 15. The peaks are well fitted to singular Gaussian

functions. The figure shows the overlay of the observed graph with the overall of the Gaussian functions indicating a perfect fit for oligomers of DP 3 – 10. Based on the fit the resolution of the peaks for D6 and D7 is calculated using t_R and w_h (inset). The equation for the calculation of R_s is: $R_s = (t_R(D_6) - t_R(D_7)) / (w_h(D_6) + w_h(D_7))$; t_R, gross retention time; w_h, peak width at half of the peak height.

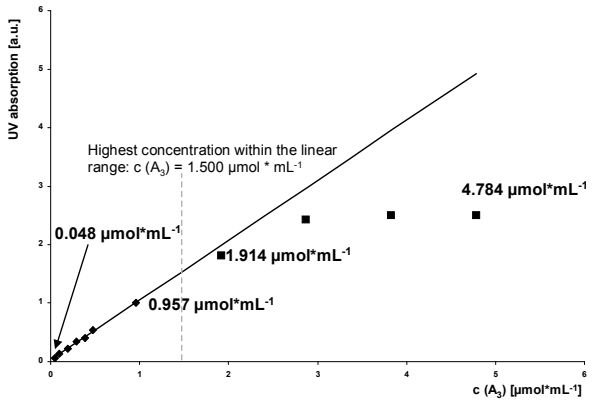

Figure S-2. Plot of the UV absorption of A_3 versus the concentration in the range of 0.048 to 4.784 µmol*mL^{-1}. The fit of the plot to a linear function indicates that the UV absorption is linear in the range of 0.04 to 1.50 µmol*ml^{-1}. As A_3 contains three A units the linear range for equimolar amounts of A_1 is three-fold. Generally, the linear range of UV absorption for a ChO is 0.05 to 4.50 µmol*mL^{-1}*n_A^{-1}, where n_A is the number of A units of the ChO.

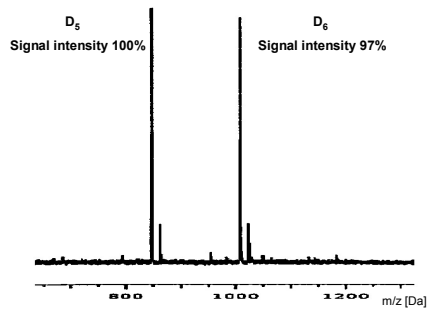

Figure S-3. MALDI-TOF MS of an equimolar mixture of D_5 and D_6. The relative signal intensities differ by 3% (D_5 100%; D_6 97%). The ratio of intensities is equal for sodium and potassium adducts.

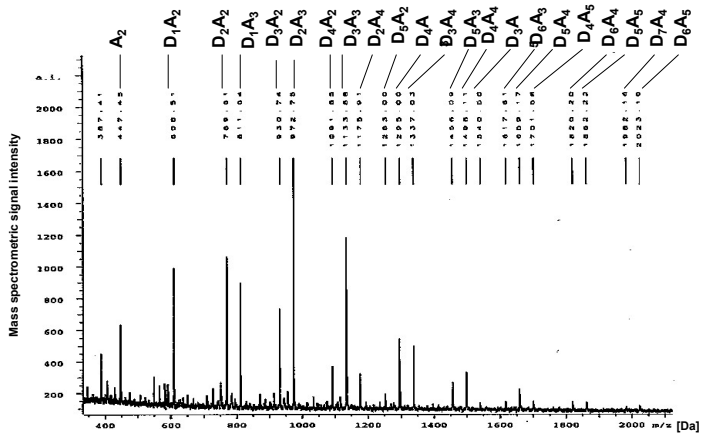

Figure S-4. MALDI-TOF MS of sample 2. Sample 2 is an enzymatic hydrolysate of chitosan which was purified by ultra-filtration to cut out the range of 1000 – 3000 Da. The mass spectrum shows oligomers and homologs from DP2 to DP11.

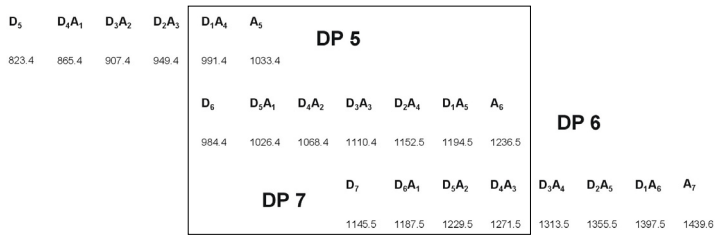

Figure S-5. Overlappings of the molecular masses of all D_5, D_6 and DP7 homologs. Exemplarily for all heterooligosaccharides the overlappings of the DP5 – 7 homologs are displayed. Overlappings are observed for D_1A_4, A_5 (DP5), D_6, D_5A_1, D_4A_2, D_3A_3, D_2A_4,

D_1A_5, A_6 (DP6) and D_7, D_6A_1, D_5A_2, D_4A_3 (DP7). The average distance of the molar masses in the range of 984.4 – 1271.5 Da is 24 Da which is too little for a baseline separation by GPC.

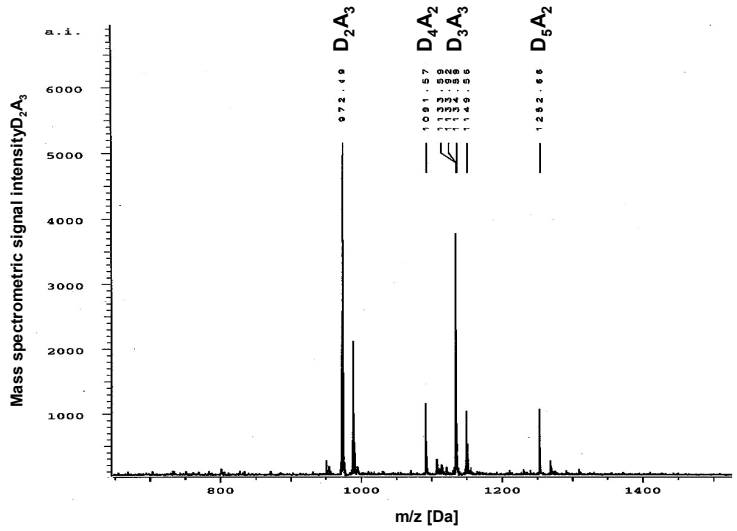

Figure S-6. MALDI-TOF mass spectrum of GPC fraction 5 of sample 2.

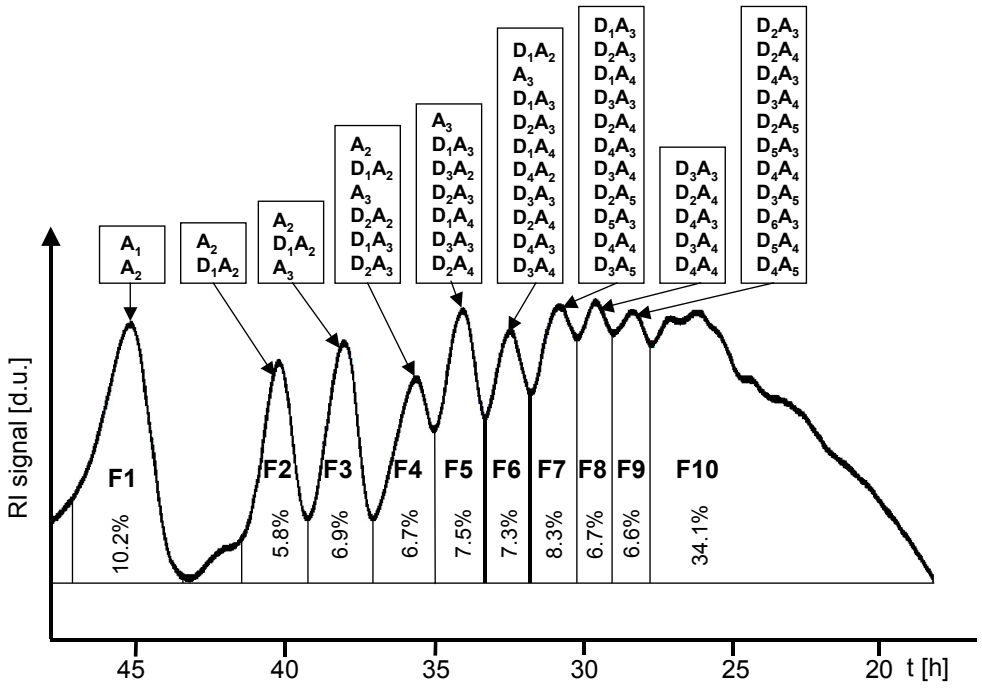

Figure S-7. Gel permeation chromatogram of sample 3. The enzymatic hydrolysate of chitosan was purified by ultrafiltration using a 3 kDa cut-off membrane. Fractions were

collected according to the baseline drops in the chromatogram. The peaks are labeled with the compounds detected in the corresponding fractions by MALDI-TOF MS. The relative peak areas [%] were calculated according to the RI signal intensities basing on baseline drops.

Tables

Table S-1. Results of the GPC of sample 2. The relative masses of fractions 1 – 9 were determined by peak area analysis (RI detection, baseline drop). The compositions of the fractions (oligomers, homologs) were determined by MALDI-TOF MS.

GPC Fraction	Mass [%]	Oligomer	Homolog	GPC Fraction	Mass [%]	Oligomer	Homolog
F1	4.5	DP2	A_2	F6	12.1	DP5	D_4A_1
		DP3	D_1A_2			DP6	D_3A_3
		DP4	D_3A_1				D_2A_4
		DP5	D_5			DP7	D_5A_2
F2	7.5	DP3	D_1A_2				D_4A_3
		DP4	D_3A_1			DP8	D_6A_2
			D_2A_2	F7	10.1	DP6	D_2A_4
		DP5	D_4A_1			DP7	D_4A_3
F3	10.8	DP4	D_2A_2				D_3A_4
		DP5	D_4A1			DP8	D_6A_2
			D_3A_2				D_5A_3
		DP6	D_5A_1	F8	6.5	DP7	D_3A_4
F4	20.2	DP4	D_1A_3				D_2A_5
		DP5	D_3A_2			DP8	D_5A_3
			D_2A_3				D_4A_4
		DP6	D_5A_1			DP9	D_6A_3
			D_4A_2	F9	12.0	DP ≥ 8	
F5	16.3	DP5	D_2A_3				
		DP6	D_4A_2				
			D_3A_3				
		DP7	D_5A_2				

Table S-2. Results of the IEC of sample 2. The compositions of the fractions were determined by MALDI-TOF MS. The table shows the fractions in which each homolog was found.

Oligomer	Homolog	Charge Number	Fractions	Oligomer	Homolog	Charge Number	Fractions
DP2	A_2	0	10 – 17	DP7	D_2A_5	2	42 – 43
	D_1A_1	1	38 – 41		D_3A_4	3	73 – 79
DP3	A_3	0	14 – 18		D_4A_3	4	111 – 121
	D_1A_2	1	19 – 41	DP8	D_4A_4	4	103 – 108
	D_2A_1	2	71 – 79		D_5A_3	5	139 – 149
DP4	D_1A_3	1	19 – 29	DP9	D_4A_5	4	91 – 98
	D_2A_2	2	61 – 70		D_5A_4	5	124 – 134
DP5	D_2A_3	3	52 – 59	DP10	D_4A_6	4	79 – 80
	D_3A_2	3	95 – 98		D_5A_5	5	111 – 123
DP6	D_2A_4	2	46 – 50		D_6A_4	6	145 – 150
	D_3A_3	3	81 – 92	DP11	D_5A_6	5	109 – 110
	D_4A_2	4	123 – 140		D_6A_5	6	135 – 150
				DP12	D_6A_6	6	128 – 129

Table S-3. Results of the preparation of homologs by the sequence IEC – GPC (starting material: sample 2). The masses of the homologs were calculated from the peak areas of the cation exchange and gel permeation chromatograms with respect to the total mass of sample 2 (7.5 g). The purity of the homologs was determined by MALDI-TOF MS with signal quantification.

Oligomer	Homolog	Mass [%] resp. Sample 2 (7.5 g)	Mass [mg]	Purity [%]
DP4	D_3A_1	0.007	0.5	95
	D_1A_3	0.220	16.5	66
DP5	D_3A_2	0.229	17.2	93
	D_2A_3	0.651	48.8	99
DP6	D_3A_3	0.308	23.1	100
	D_2A_4	0.016	1.2	97
DP7	D_4A_3	0.129	13.5	98
	D_3A_4	0.180	9.7	96
DP8	D_5A_3	0.045	3.4	96
	D_4A_4	0.127	16.3	100
	D_3A_5	0.004	0.3	87
DP9	D_4A_5	0.004	0.3	91
DP10	D_6A_4	0.023	1.7	94
	D_5A_5	0.021	1.6	90
DP11	D_6A_5	0.009	0.7	74
	D_5A_6	0.015	1.1	94
DP12	D_7A_6	0.008	0.6	91

References and Notes

1. M. G. Peter in *Biopolymers;* Steinbüchel, A.; Ed.; Polysaccharides II; Wiley-VCH: Weinheim, **2002**; Vol. 6, pp 481-557.
2. Bahrke, S.; Einarsson, J. M.; Gislason, J.; Haebel, S.; Letzel, M. C.; Peter-Katalinić, J.; Peter, M. G. *Biomacromolecules* **2002**, *3*, 696-704.
3. Muzzarelli, R.A.A. *Carbohydr. Polym*. **1993**, *20*, 7-7.
4. Usami, Y.; Minami, S.; Okamoto, Y.; Matsuhashi, A.; Shigemasa, Y. *Carbohydr. Polym*. **1997**, *32*, 115-122.
5. Bakkers, J.; Kijne, J. W.; Spaink, H. P. *EXS (Chitin and Chitinases)* **1999**, *87*, 71-83.
6. Semino, C. E.; Allende, M. L. *Int. J. Dev. Biol*. **2000**, *44*, 183-193.
7. Vander, P.; Vårum, K. M.; Domard, A.; El Gneddari, N. E.; Moerschbacher, B. M. *Plant. Physiol.* **1998**, *118*, 1353-1359
8. Akiyama, K.; Kawazu, K.; Kobayashi, A. Z. *Naturforsch*. **1995**, *50*, 391-397.
9. Ernst, B.; Hart, G. W.; Sinaÿ, P., Eds., *Carbohydrates in Chemistry and Biology*, Part II, Vol. 4: Lectins and Saccharide Biology; Wiley-VCH: Weinheim; **2002**.
10. Cederkvist, F. H.; Zamfir, A. D.; Bahrke, S.; Eijsink, V. G. H.; Sørlie, M.; Peter-Katalinić, J.; Peter, M. G. *Angew. Chem. Int. Ed*. **2006**, *45*, 2429-2434.
11. Fusetti, F.; Pijning, T.; Kalk, K. H.; Bos, E.; Dijkstra, B. W. *J. Biol. Chem*. **2003**, *278*, 37753-37760.

12. Houston, D. R.; Recklies, A. D.; Krupa, J. C.; van Aalten, D. M. F. *J. Biol. Chem*. **2003**, *278*, 30206-30212.
13. Domard, A.; Cartier, N. *Int. J. Biol. Macromol*. **1989**, *11*, 297-302.
14. Aiba, S. *Carbohydr. Res*. **1994**, *265*, 323.
15. Sørbotten, A.; Horn, S. J.; Eijsink, V. G. H.; Vårum, K. M. *FEBS Journal* **2005**, *272*, 538-549.
16. Horn, S. J.; Sørbotten, A.; Synstad, B.; Sikorski, P.; Sørlie, M.; Vårum, K. M.; Eijsink, V. G. H. *FEBS Journal* **2006**, *273*, 491-503.
17. Mitsutomi, M.; Ueda, M.; Arai, M.; Ando, A.; Watanabe, T. *Chitin Enzymology*, **1996**, *2*, 273-284.
18. Mitsutomi, M.; Isono, Uchiyama, A.; Nikaidou, N.; Ikegami, T.; Watanabe, T. *Biosci. Biotechnol. Biochem.*, **1998**, *62*, 2107-2114.
19. Hicks, K. B.; Lim, P. C.; Haas, M. J. *J. Chromatogr*. **1985**, *319*, 159-171.
20. Takahashi, Y. *Adv. Chitin Sci*. **1997**, *2*, 372-379.
21. Schanzenbach, D; Peter M. G. in *Chitin Handbook;* Muzzarelli, R. A. A.; Peter, M. G.; Eds.; Atec: Grottammare, **1997**; pp. 195 -198.
22. Tokuyasu, K.; Ono, H.; Ohnishi-Kameyama, M.; Hayashi, K.; Mori, Y. *Carbohydr. Res.* **1997**, *303*, 353-358.
23. Lopatin, S. A.; Hyin, M. M.; Pustobaev, V. N.; Bezchetnikova, Z.A; Varlamov, V. P.; Davankov, V. A. *Anal. Biochem*. **1995**, *227*, 285-288.
24. Akiyama, K.; Kawazu, K.; Kobayashi, A. *Carbohydr. Res*. **1995**, *279*, 151-160.
25. Bosso, C.; Domard, A. *Org. Mass Spectrom*. **1992**, *27*, 799-806.
26. Letzel, M. C.; Synstad, B; Eijsink, V. G. H.; Peter-Katalinić, P.; Peter, M. G. *Adv. Chitin Sci.* **2000**, *4*, 545-551.
27. Zhang, H; Du, Y. G.; Yu, J. X.; Mitsutomi, M.; Aiba, S. *Carbohydr. Res*. **1999**, *320*, 257-260.
28. Barker, S.A.; Foster, A.B.; Stacey, M.; Webber, J.M. *J. Chem. Soc.* **1958**, *80*, 2218-2227.
29. Ley, J.-P.; Schweikhart, F.; Peter, M.G. in *Chitin Handbook;* Muzzarelli, R. A. A.; Peter, M. G.; Eds.; Atec: Grottammare, **1997**, pp. 313-320.
30. Schanzenbach, D.; Matern, D.; Peter, M.G. in *Chitin Handbook;* Muzzarelli, R. A. A.; Peter, M. G.; Eds.; Atec: Grottammare, **1997**, pp. 171-174.
31. Hirano, S. in *Chitin Handbook;* Muzzarelli, R. A. A.; Peter, M. G.; Eds.; Atec: Grottammare, **1997**, pp. 71-75.
32. Ley, J.P.; Peter, M.G. *Synthesis* **1994**, *8*, 28-30.
33. Sorlier, P.; Denuzière, A.; Viton, C.; Domard, A. *Biomacromolecules*, **2001**, *2*, 765-772.
34. Nudelman, A.; Gottlieb, H.E.; Fischer, B. *J. Org. Chem.* **1986**, *51*, 727-730.
35. Binder, W.H.; Kählig, H.; Schmid, W. *Tetrahedron* **1994**, *50*, 10407-10417.
36. Flitsch, S.L.; Taylor, J.P.; Turner, N.J. J. Chem. Soc., Chem. Commun. **1991**, 380-382.
37. *Physikalische Chemie;* Atkins, P. W., Ed.; Wiley-VCH: Weinheim, **1990**; pp 595-597.
38. Schiene-Fischer, C.; Habazettl, J.; Schmid, F. X.; Fischer, G. *Nature Structural Biology* **2002**, *9*, 419-423.
39. *Physikalische Chemie;* Atkins, P. W., Ed; Wiley-VCH: Weinheim, **1990**; pp 475-476.
40. Note: If not stated otherwise all peaks labelled in the MALDI-TOF mass spectra are sodiated pseudomolecular ions.

Quantitative Sequencing of Complex Mixtures of Heterochitooligosaccharides by vMALDI-Linear Ion Trap Mass Spectrometry

Sophie Haebel,*† Sven Bahrke, ‡ and Martin G. Peter†‡

Center for Mass Spectrometry of Biopolymers, University of Potsdam, Karl-Liebknecht Strasse 24-25, Building 20, 14476 Potsdam, Germany, and Institute for Chemistry, University of Potsdam, Karl-Liebknecht Strasse 24-25, Building 25, 14476 Potsdam, Germany

Received for review November 28, 2006. Accepted May 10, 2007.

Abstract:

Heterochitooligosaccharides possess interesting biological properties. Isobaric mixtures of such linear heterochitooligosaccharides can be obtained by chemical or enzymatic degradation of chitosan. However, the separation of such mixtures is a challenging analytical problem which is so far unresolved. It is shown that these isobaric mixtures can be sequenced and quantified simultaneously using standard derivatization and multistage tandem mass spectrometric techniques. A linear ion trap mass spectrometer equipped with a vacuum matrix-assisted laser desorption ionization (vMALDI) source is used to perform MS^2 as well as MS^3 experiments.

* To whom correspondence should be addressed. E-mail: haebel@unipotsdam.de. Fax: +49 331 977 2512.
† Center for Mass Spectrometry of Biopolymers.
‡ Institute for Chemistry.
(1) Peter, M. G. In *Biopolymers*; Steinbüchel, A., Ed.; Wiley-VCH: Weinheim, Germany, 2002; Vol. 6, pp 481-574.

The article is published in Analytical Chemistry, 79 (2007), 15, pp. 5557-5566
DOI 10.1021/ac062254u

ADVANCES IN CHITIN SCIENCE — Vol. VIII
H. Struszczyk, A. Domard, M. G. Peter, H. Pospieszny, Eds.
Institute of Plant Protection, Poznań, 2005, ISBN 83-89867-25-7

INCORPORATION OF GLUCOSE INTO CHITOSAN BY *ACETOBACTER XYLINUM*

Danuta Ciechańska[1], Sven Bahrke[2], Sofie Haebel[3], Henryk Struszczyk[1]*, Martin G. Peter[2,3]*

[1] Institute of Chemical Fibres, M. Skłodowskiej-Curie 19/27, 90-570 Łódz, Poland
[2] Institut für Chemie, Universität Potsdam, Karl-Liebknecht – Str. 25, D-14476 Potsdam, Germany
[3] Interdisciplinary Research Centre for Biopolymers, Universität Potsdam, Karl-Liebknecht – Str. 25, D-14476 Potsdam, Germany
* iwch@iwch.lodz.pl, peter@chem.uni-potsdam.de

Abstract: Modified bacterial cellulose was biosynthesised by *Acetobacter xylinum* in a liquid medium of 2.0 wt.% glucose, 0.5 wt.% peptone, 0.5 wt.% yeast extract, 0.27 wt.% disodium phosphate, 0.115 wt.% citric acid monohydrate and 0.5 wt.% chitosan acetate (DD=84.1%, $\overline{M}_v$=98 kD) at 30°C for 7 days. The polysaccharide pellicle was digested with cellulase from *Trichoderma reesei*. Fractionation on Biogel P4 afforded, as the main products, low molecular weight oligosaccharide fractions which, as shown by MALDI-TOF mass spectrometry, were oligosaccharides of hexoses (Glc, Man and Fru) of DP ≤ 3 as well as chito-oligomers (DP ≤ 9), composed of GlcNAc and GlcN. Most interestingly, the mass spectra indicated the presence of several minor oligosaccharides containing GlcNAc, GlcN, and hexoses (Hex). Sequence analysis by MALDI-TOF MSMS of the oligosaccharides after reductive amination with 2-aminoacridone revealed, that the hexose containing products were linear hetero-oligosaccharides, where one hexose residue was randomly distributed within the sequences of chito-oligosaccharides. The hexose residue was more often positioned at the reducing end and rarely at the non-reducing end.

INTRODUCTION

Bacterial cellulose is one of the most promising materials in modern technology. It possesses a variety of unique features, such as biocompatibility, biodegradability and chemical purity, and can be easily modified during synthesis. Modified bacterial cellulose (e.g. by polyaminosaccharides) is composed of ultrafine fibrils. Some outstanding mechanical parameters are attributed to this structure, such as a very high Young modulus, tensile strength and sonic velocity [1].

Acetobacter xylinum is unique in its prolific synthesis of cellulose. Rows of pores characteristically secrete mini-crystals of glucan chains, which then coalesce into microfibres. Clusters of microfibrils result in a compound structure known as the ribbon. The ribbon can be observed directly using light microscopy, and the time-lapse studies show *Acetobacter* cells generating cellulose.

In the present study, bacterial cellulose biosynthesised by Acetobacter xylinum was modified with chitosan. The aim of the work was to examine the molecular structure and composition of the modified bacterial cellulose applying different hydrolytic, chromatographic and mass spectrometric techniques. Whereas the mass spectrometric sequence analysis of chito-oligosaccharides is established [3], the sequence analysis of hetero-oligosaccharides of glucosamine, *N*-acetylglucosamine and hexoses is challenging, as the difference of molecular masses between hexose and glucosamine is 1 Da.

MATERIALS AND METHODS

Preparation of modified bacterial cellulose:

The cellulose producing bacterium *Acetobacter xylinum* was cultured in a liquid medium (2.0 wt.% glucose, 0.5 wt.% peptone, 0.5 wt.% yeast extract, 0.27 wt.% disodium phosphate, 0.115 wt.% citric acid monohydrate) containing 0.5 wt.% chitosan acetate (DD = 84.1%, Mv = 98 kD) at 30°C for 7 days. In order to separate acid soluble and insoluble fractions, biosynthesised polysaccharide pellicle was isolated from the culture medium (pH = 4.5) by filtration, washed with distilled water, sterilised in the autoclave at 121°C for 15 min, thoroughly washed with distilled water and dried.

Monosaccharide analysis

The dry polysaccharide pellicle was milled and suspended in 7.6mL of 72% (w/w) H_2SO_4. The mixture was stirred at 40°C for 1h, diluted with distilled water to a final concentration of 5% (w/w) H_2SO_4 and stirred at 120°C for another 1.5h. After neutralisation with barium hydroxide, the solution was filtrated and lyophilised. 150 ng of the total hydrolysate were objected together with 11 monosaccharide standards (each 150 ng) to ion chromatography (HPAEC-PAD DX 600 system equipped with a CarboPac™-PA 1 column, Dionex, Idstein, Germany). For separation, the column was flushed with 200 mM NaOH for 10 min and afterwards equilibrated with 18 mM NaOH for 15 min. Analytes were eluted isocratically with 18 mM NaOH using a flow rate of 1 ml × min^{-1} and detected by pulsed amperometric detection.

MALDI-TOF MS of the cellulase digest

The polysaccharide pellicle was digested with cellulase Econase CE (AB Enzymes Oy, Finland). The lyophilisate was objected in batches of 50 mg to GPC: stationary phase, Biogel P4, fine grade (BioRad, München, Germany), column dimension, 2.5 cm i. d. × 200 cm; mobile phase, 0.05 M ammonium acetate buffer, adjusted with 0.23 M acetic acid to pH 4.2; flow rate, 25 mL × h^{-1}; detector, Shimadzu RID 6A. Fractions of 8 mL were collected, approximately combined and lyophilised. For MALDI-TOF MS of oligosaccharides, 10 μg of each fraction from GPC were redissolved in 50 μL of methanol/water (v/v 1:1). An aliquot of the solution (0.5 μL) was mixed on the target with 0.5 μL of the matrix, a 0.1 M solution of DHB in 30% aqueous ethanol, and the drop was dried under a gentle stream of air. Crystallization of the matrix occurred usually spontaneously. Mass spectra were recorded on a Bruker Reflex II (Bruker Daltonik, Bremen, Germany) in the

positive ion mode. For ionisation, a nitrogen laser (337 nm, 3 ns pulse width, 3 Hz) was used. For optimisation of the mass spectra, the laser was aimed at the outmost edge of the crystal rim. All spectra were measured in the reflector mode using external calibration (2-point calibration with α-cyano-4-hydroxycinnamic acid $[3M+H]^+$, 568.14 amu and angiotensine II $[M+H]^+$, 1046.54 amu.

Sequence analysis of hetero-oligosaccharides

10 μg of each GPC fraction were redissolved in 5 μL of a 0.1 M solution of 2-aminoacridone in acetic acid/DMSO (v/v 3:17) and agitated manually for 30 s, followed by addition of 5 μL of a 1 M solution of sodium cyanoborhydride in water and further agitation for 30 s. The mixture was heated in the dark for 30 min at 90°C. To terminate the reaction, the vessel was cooled to – 20°C followed by lyophilisation. For sequence analysis, MALDI-TOF MSMS of tagged oligosaccharides was applied (sample preparation cf. *MALDI-TOF MS of the cellulase digest*). Mass spectra were recorded on an API QSTAR Pulsar I (Applied Biosystems/MDS Sciex, Toronto, Canada) hybrid mass spectrometer equipped with a MALDI ion source. MSMS spectra were recorded by selecting the ion of interest in the Q1 quadrupole, generating fragments by collision with argon in the collision cell and analysing the fragments in the TOF analyser. All spectra were measured using external calibration.

RESULTS AND DISCUSSION

Total hydrolysis of the polysaccharide biosynthesised by *Acetobacter xylinum* followed by HPAEC/PAD analysis (Figure 1) gave the following monosaccharide composition: 53.0% Glc; 21.2% Man; 13.0% Fru; 12.8% GlcN/GlcNAc.

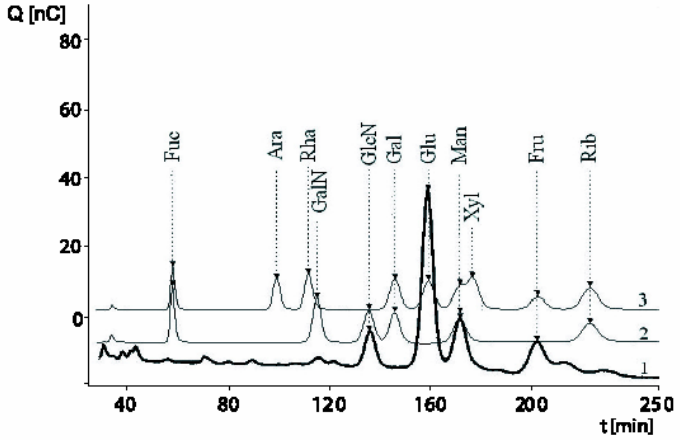

Figure 1. HPAEC/PAD of the polysaccharide total hydrolysate (1), and monosaccharide standards (2, 3)

Partial hydrolysis of the modified bacterial cellulose with cellulase Econase CE afforded a mixture of oligosaccharides of DP ≤ 9, which was fractionated by GPC on Biogel P4

(Figure 2). MALDI-TOF MS analysis of the fractions showed that the main components were oligosaccharides of hexoses (Glc, Man, Fru) of DP ≤ 3 as well as chito-oligosaccharides composed of GlcN and GlcNAc. Most interestingly, the mass spectra indicated the presence of several minor hetero-oligosaccharides of DP ≤ 9 containing GlcN, GlcNAc and one hexose residue.

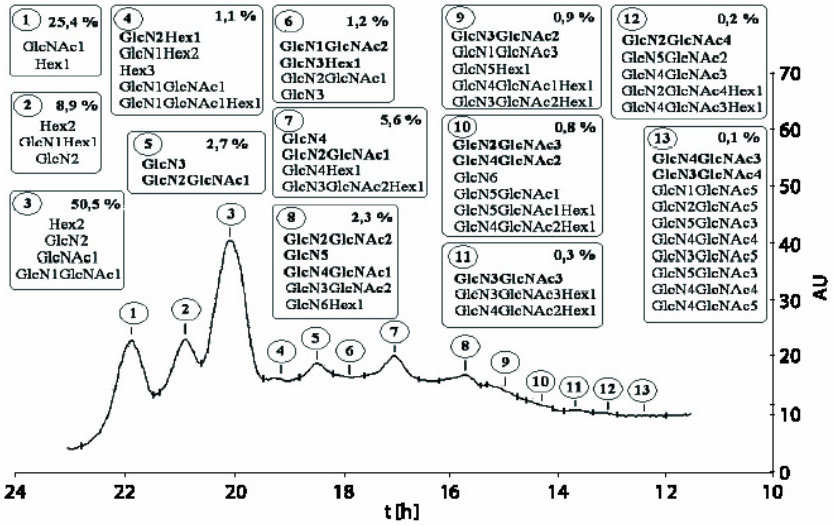

Figure 2. GPC / MALDI-TOF MS results of the cellulase digest of modified bacterial cellulose

Main components are in bold letters.

For sequence analysis of hetero-oligosaccharides, GPC fractions were tagged with 2-aminoacridone (AMAC) at the reducing end. MALDI-TOF MSMS was applied for fragmentation of the ions of the interesting homologue, which were previously selected in the quadrupole of the mass spectrometer. In the case of AMAC derivatives, the mass increment of 194 Da allows for unambiguous identification of Y-type fragment ions and straightforward readout of the oligosaccharide sequence from the reducing end.

Fragment Ion	Peak Assignment	Ratio of Peak Intensities
Y1	$GlcN_1$-amac : Hex_1-amac	0.55 : 1
Y2	$GlcN_2$-amac : $GlcN_1Hex_1$-amac	0.42 : 1
Y3	$GlcN_3$-amac : $GlcN_2Hex_1$-amac	0.25 : 1
Y4	$GlcN_4$-amac : $GlcN_3Hex_1$-amac	0 : 1

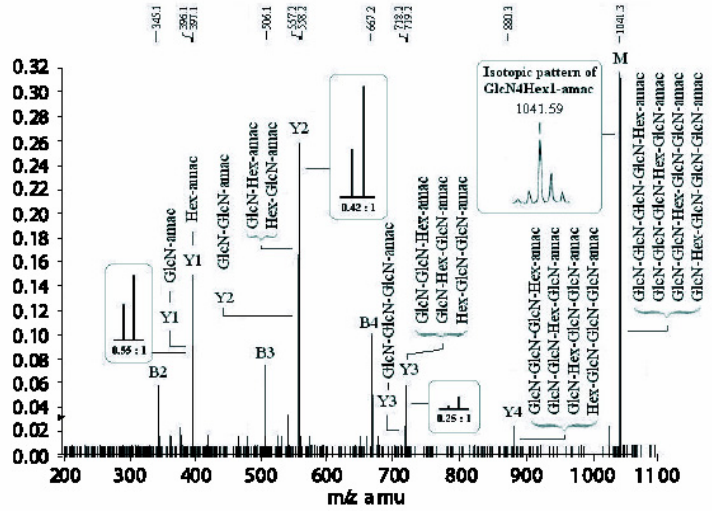

Figure 3. MALDI-TOF MSMS of the AMAC derivative of $GlcN_4Hex_1$. Relative intensities of Y-type fragment ions indicated that the hexose residue was more likely positioned at the reducing end and never at the non-reducing end

CONCLUSIONS

1. Bacterial cellulose from *Acetobacter xylinum*, which was modified with chitosan, is composed of 53.0% Glc, 21.2% Man, 13.0% Fru, and 12.8% GlcN / GlcNAc.
2. Modified bacterial cellulose is a copolymer of hexoses and amino sugars (not a composite of cellulose and chitosan), as hetero-oligosaccharides of GlcN, GlcNAc and one hexose residue were detected by MALDI-TOF MS in the cellulase digest. The distribution of the hexose residue within the sequences of chito-oligosaccharides (cf. Figure 3.) reflects the cleaving specificity of the cellulase. The cleaving rate for different types of glycosidic bonds decreases in the following order (reducing end on the right): Glc-Glc > GlcNAc-Glc > GlcN-Glc > Glc-GlcNAc > Glc-GlcN > GlcNAc-GlcNAc > GlcN-GlcN.
3. Modified bacterial cellulose is a linear polysaccharide as fragmentation mass spectra of oligosaccharides obtained by enzymatic degradation showed only fragment ions of linear oligosaccharides (B- and Y-type ions) but none of branched oligosaccharides.
4. Cellulase partial hydrolysis of the polysaccharide pellicle gave as main products oligosaccharides of hexoses (DP ≤ 3) and chito-oligosaccharides of DP ≤ 9. This fact indicates, that chito-oligosaccharides are building blocks for the biosynthesis of modified bacterial cellulose by *Acetobacter xylinum* [2]. Most probably chitosan is depolymerised to cell wall permeable chito-oligosaccharides, which act as a carbon source. Activated hexose residues (Hex-X) are linked to the initial building blocks by transglycosylation.

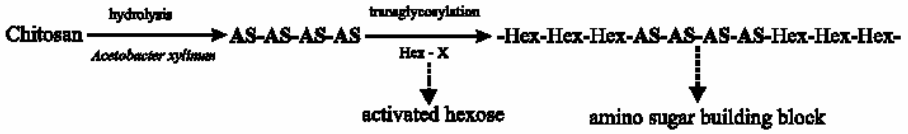

REFERENCES

1. Ciechanska D., Struszczyk H., Guzinska K.: Modification of Bacterial Cellulose. Fibres & Textiles in Eastern Europe 1998, 6, 61–65.
2. Shirai A., Sakairi N., Nishi N., Tokura S.: Preparation of a novel (1,4)-*β*-D-glycan by *Acetobacter xylinum* – a proposed mechanism for incorporation of a *N*-acetyl-glucosamine residue into bacterial cellulose. Carbohydrate Polymers 1997, 32, 223–227.
3. Bahrke S., Einarsson J. M., Gislason J., Haebel S., Letzel M. C., Peter-Katalinić J., Peter M. G.: Sequence Analysis of Chitooligosaccharides by Matrix-Assisted Laser Desorption Ionization Postsource Decay Mass Spectrometry. Biomacromolecules 2002, 3, 696–704.

The Potency of Heterochitooligomers to Inhibit Family 18 Chitinases Depends on DP, F_A and Sequence of D and A Units

Sven Bahrke[1], Jón M. Einarsson[2], Jóhannes Gislason[2] and Martin G. Peter[1]

[1]Institute of Chemistry, University of Potsdam, Karl-Liebknecht-Str. 25, D-14476 Potsdam, Germany
[2]Genis ehf, Myrargata 2, IS- 101 Reykjavik, Iceland

Abbreviations

A, 2-acetamido-2-deoxy-D-glycopyranose; AMCR, 3-(acetyl amino)-6-aminoacridine, ChiA, chitinase A from *Serratia marcescens*; ChiB, chitinase B from *Serratia marcescens*; ChO's, heterochitooligosaccharides; D, 2-amino-2-deoxy-D-glucopyranose; DHB, 2,5-dihydroxy benzoic acid; DP, degree of polymerisation; F_A, mole fraction of A residues; GPC, gel permeation chromatography; HCT, human chitotriosidase; HPCEC, high performance cation exchange chromatography; IC_{50}, inhibitor concentration for 50% inhibition; MS^2, tandem mass spectrometry; MS^n, multiple-stage tandem mass spectrometry; 4-MU, 4-methylumbelliferone; 4-MU-A_2, 4-methylumbelliferyl-beta-D-*N,N′*-diacetylchitobioside; 4-MU-A_3, 4-methylumbelliferyl-beta-D-*N,N′,N″*-triacetylchitotrioside; NRE, non-reducing end; RE, reducing end; RI, refractive index; vMALDI-LTQ, vacuum matrix-assisted laser desorption
ionisation linear quadrupole ion trap.

Abstract

Heterochitooligosaccharides of DP 3 to 15 were analysed with respect to the affinities to chitinase A and B (*Serratia marcescens*). Dependencies of the affinities on the DP, F_A and the sequence of chitooligosaccharides as well as the pH of the solution were investigated. IC_{50} concentrations in the µmolar range were found for both enzymes. For chitinase B the IC_{50} concentrations are in average four times lower than for chitinase A (pH 5.5). At pH 7.4 (physiological conditions) the IC_{50} concentrations are decreased compared to pH 5.5. The affinities of ChO's to chitinase A and B are increasing with DP and F_A. Also the sequence of D and A units influences the affinity of ChO's to ChiA and ChiB as well as the stability against enzymatic hydrolysis. Based on the experimental results a model of ChO binding to family 18 chitinases was developed allowing to predict the order of affinities with respect to the structural details of ChO's as well as the stability against enzymatic hydrolysis.

Keywords

chitinase A, chitinase B, chitooligosaccharides, enzyme inhibition, *Serratia marcescens*

Introduction

Chitin / Chitosan

Chitin is a sugar copolymer composed of *N*-acetylglucosamine (2-acetamido-2-deoxy-D-glycopyranose, A) and glucosamine (2-amino-2-deoxy-D-glucopyranose, D), which is insoluble in diluted acid. Chitin covers F_A values from 0.41 to 1.00.[1] Deacetylation of chitin gives chitosan, which is soluble in diluted acid giving viscous solutions. Homogenous deacetylation leads to chitosans with random distributions of D and A units. In nature we usually find chitin (exceptionally for some fungi) in the α-modification (exceptionally a few maritime organisms).[1] Chitin is the natural substrate of chitinases. The monomer units of both polymers, chitin and chitosan, are connected via *β*-(1,4)-linkages. Crystal structure analyses revealed that adjacent monomers are related by 180° rotation.

Heterochitooligosaccarides (ChO's) or heterochitooligomers are composed of *N*-acetylglucosamine (A) and glucosamine (D). ChO's are prepared by either chemical or enzymatic degradation of chitosan. The degree of polymerisation (DP) varies from 2 to 20 units in a segment, and each segment differs in the mole fraction of A residues (i.e. homologs) and in the sequences of D and A residues (i.e. isomers). Thus, a heterochitooligomer of DP3 includes 4 homologs, D_3, D_2A_1, D_1A_2 and A_3 with 8 sequences of A and D units (Table 1).[2]

Table 1
Summery of all DP3 homologs and isomers.

D_3	D_2A_1	D_1A_2	A_3
DDD	DDA	DAA	AAA
	DAD	ADA	
	ADD	AAD	

The hydrolysis of chitin or chitosan yields a complex mixture of oligomers, homologs and isomers, which is commonly further purified by chromatographic methods.[2, 3, 4]
ChO's are in contrast to the corresponding polymers water-soluble. This property offers a wide range of industrial applications especially in the fields of cosmetics, pharmaceutics and food ingredients (for a review see [1]).
The analysis of the sequences of ChO's is essential previous to biological evaluations. Qualitative sequence analyses of mixtures of isomers were performed employing controlled enzymatic hydrolysis followed by re-acetylation and HPLC analysis of the fragments (DP ≤ 6)[5], NMR spectroscopy (DP ≤ 4)[6,7], and mass spectrometric methods (DP 5-7).[8]
Heterochitooligomers up to DP12 were sequenced employing reducing end tagging in combination with MALDI-TOF PSD MS.[2] Besides qualitative sequence information, quantitative data concerning the composition of an isomeric mixture are important. Quantitative sequence information is obtained employing reducing end tagging in combination with multiple-stage MS techniques as employed in the present study.
Chitinases are divided into two families of glycosyl hydrolases: family 18 and 19.
The classification is based on structural differences of the amino acid sequences. Whilst family 18 chitinases are found in many organisms like bacteria, fungi, viruses, animals and some plants, the presence of family 19 chitinases is strictly coupled to plants.[9] The characteristic of family 18 chitinases is the catalytic mechanism of the hydrolysis of chitinous material.[10, 11, 12] The mechanism depends on the participation of the *N*-acetyl group of the sugar unit bound to subsite -1 (neighbouring group assistance) due to the lack of a second acidic amino acid residue next to the scissile bond. Based on this mechanism of hydrolysis, for family 18 chitinases an A unit bound to subsite -1 is essential for hydrolysis.[13]
Chitinase A (EC 3.2.1.14) from the soil bacterium *Serratia marcescens* is a family 18 chitinase. The structure of ChiA (native or catalytically impaired by mutation) was studied employing crystal structure analysis.[14, 15, 16] The analysis of complexes of ChiA with chitin oligomers revealed 7 subsites of the groove-like catalytic domain, +2 to –5.[16] Besides the catalytic domain a chitin-binding domain was located involving subsites –6 to –13.[16, 17]
Hydrophobic interactions between amino acid residues of ChiA (mostly aromatic residues) and acetamido groups of the chitinous substrate were found mainly for subsites +2, +1, -1, and besides for all odd numbered subsites (-3, -5, …).[15, 16] Hydrophilic interactions (hydrogen bonds) between amino acid residues and hydroxy groups of the sugar rings were mainly found for subsites +2, +1, -1.[15]
For the hydrolysis of chitinous material with ChiA a processive mechanism is discussed[17] where the chitin chain first contacts the protein at the exposed aromatic amino acid residues of the chitin-binding domain. Subsequently the polymer chain is moving on the surface of the protein into the catalytic domain into a position where subsites +1 and +2 are occupied by the

two reducing end sugar units followed by hydrolysis and release of the aglycon hydrolysis product. Consecutively, the chitin chain is moving two positions along the subsites towards the reducing end so that subsites +1 and +2 are occupied again. In conclusion, one (single) contact of the chitin chain with the protein produces several oligomers (single-attack, processive mode of hydrolysis).[18] The proposed mechanism is based on the observation that chitin fibres are sharpened by ChiA at one end exclusively (proved by electron microscopy).[17] A_2 is the main product of the hydrolysis of chitin by ChiA.[16] Crystal structure analyses show that Y418 is positioned at one end of the catalytic cleft, putatively blocking sugar residues to extend beyond subsite +2.[15] Thus, ChiA is classified as an exo-chitinase cleaving chitosan from the reducing end.

Hydrolysis studies on chitin oligomers (A_4 to A_6) revealed that oligosaccharide residues may extend beyond subsite +2 for at least one monomer unit (binding modes of -2 → +3 for A_5 and -3 → +3 for A_6).[16] However, HPLC analysis shows that hydrolysis products related to -2 → +3 and -3 → +3 binding modes are minor compounds indicating that binding modes -3 → +2 for A_5, and -4 → +2 for A_6 are preferred.

Chitinase B (EC 3.2.1.14) from *Serratia marcescens* is a family 18 chitinase. Crystal structure analyses of the native protein as well as mutants show that ChiB possesses a catalytic domain (subsites –3 to +3) aligned with a number of aromatic residues.[10, 18, 19] Subsite -3 is locked by the porch loop, indicating that ChiB is an exo-type enzyme.[19] The catalytic domain is connected through the support loop (Trp^{240}, Tyr^{252}) with the chitin-binding domain (Tyr^{481}, Trp^{479}).[19, 20]

The structures of ChiA and ChiB show some important differences. The catalytic domain of ChiB has the shape of a tunnel with a roof.[19] That means the sugar is bound much stronger to ChiB than to ChiA with its more open, groove-like catalytic cleft. The catalytic domain of ChiA is locked from the reducing end (subsite +2), the catalytic cleft of ChiB is locked from the non-reducing end (subsite -3). Thus, ChiA hydrolyses chitosan from the reducing end while ChiB is cleaving chitosan from the non-reducing end.

A model was developed for the hydrolysis of chitosan by ChiB allowing for a quantitative prediction of the product distribution.[3, 4, 13] The model is based on a single-attack, processive mode of hydrolysis and a cleaving from the non-reducing end. Calculations based on the model show a preference for A units in subsites -2 and -1. Subsites -3, +1 and +3 have no significant preference, subsite +2 shows a little preference for D units.

The calculation of the propagation parameter indicates that a moving of the chitosan chain on the surface of catalytic domain is preferred compared to dissociation.[4]

Materials and methods

Materials

Homochitooligomers D_5, D_6, A_3, A_5, and A_6 were purchased from Seikagaku (Tokyo, Japan). 4-MU-A_2) and 4-MU-A_3 were purchased from Sigma (Munich,Germany). Purified preparations of ChiA and ChiB from *Serratia marcescens* were generous gifts from Prof. M. Sørlie and Prof. V. G. H. Eijsink, Agricultural University of Norway, Ås, Norway. A preparation of ChO's was a generous gift from Genis ehf, Reykjavik, Iceland. All other chemicals were bought from Sigma-Aldrich Chemie GmbH (Munich, Germany).

Table 2
The sequence compositions of the DP3 – 9 homologs were determined by means of vMALDI-TOF LTQ MS sequencing with previous tagging of the reducing end and quantification of the mass spectrometric signal intensity. For the DP12 and 15 homologs the compositions were not determined (n. d.).

Oligomer [DP]	Homolog	Sequences / Composition [mol-%]	Annotations
3	D_1A_2	DAA 100%	
	A_3	AAA 100%	
4	D_2A_2	DADA 3% ADDA 5% DDAA 92%	
5	D_2A_3	ADDAA 17% DADAA 57% DDAAA 26%	
6	D_6	DDDDDD 100%	
	D_3A_3	DDADAA 51% DADDAA 49%	
	D_2A_4	ADADAA 19% DADAAA 43% AADDAA 12% ADDAAA 12% DAADAA 9% DDAAAA 4%	
9	D_9	DDDDDDDDD 100%	
	D_5A_4	DDADDADAA 25% DADDDADAA 25% DDADADDAA 25% DADDADDAA 25%	
12	D_7A_5	DDADDADDADAA DADDDADDADAA DDADADDDADAA DADDADDDADAA DDADDADADDAA DADDDADADDAA DDADADDADDAA DADDADDADDAA	composition n.d.
15	D_9A_6	DDADDADDADDADAA DADDDADDADDADAA DDADADDDADDADAA DADDADDDADDADAA DDADDADADDDADAA DADDDADADDDADAA DDADADDADDDADAA DADDADDADDDADAA DDADDADDADADDAA DADDDADDADADDAA DDADADDDADADDAA DADDADDDADADDAA DDADDADADDADDAA DADDDADADDADDAA DDADADDADDADDAA DADDADDADDADDAA	composition n.d.

Methods

Preparation of Heterochitooligomers and Homologs

Details of the preparation of heterochitooligomers and homologs are described elsewhere.[2] Briefly, a preparation of ChO's was purified by ultrafiltration over 0.5 and 3.0 kDa cut-off

membranes resulting in an oligomer composition of mainly DP3 to DP15. The oligomers were separated employing GPC on Biogel P4 (stationary phase: Biogel P4, fine grade (Bio-Rad, Munich, Germany), column size 2.5 × 200 cm (2 × XK26, Pharmacia, Uppsala, Sweden), sample amount 50 mg; mobile phase: 0.05 M ammonium acetate buffer pH 4.2, flow rate 25 $mL \times h^{-1}$;equipment: peristaltic pump (Pharmacia P1, Uppsala, Sweden), RI detector (Shimadzu RID 6A, Duisburg, Germany), fraction collector (Pharmacia, Uppsala, Sweden)). Further purification of the GPC fractions by HPCEC afforded pure homologs of heterochitooligomers (stationary phase: Resource S (Pharmacia, Uppsala, Sweden), bed volume 1 mL, sample amount 1 mg; mobile phase: hydrochloric acid pH 3.5, sodium chloride gradient 0 – 1 M, flow rate 1 $mL \times min^{-1}$;equipment: HPLC instrument (Jasco, Gross-Umstadt, Germany) with UV detector (detection wavelength 210 nm)). Finally, the HPLC fractions were desalted by dialysis (Floatalyzer®, SpektraPor, Germany).

Separation of Two DP6 Isomers of the Sequences DDADAA and DADDAA

Briefly, 100µg of the pure homolog D_3A_3 was objected to a Tricorn MonoS 5/50 GL column (Pharmacia, Uppsala, Sweden) with 1 mL bed volume. The column was run with 20 mM formic acid and a gradient of 0 – 0.5 M sodium chloride (5 – 60 min) on a Jasco HPLC system (Jasco, Gross-Umstadt, Germany) with UV detector (detection wavelength 210 nm). Fractions were collected manually.

Qualitative and Quantitative Sequence Analysis of Heterochitooligosaccharides

The sequences of ChO's were determined qualitatively as described elsewhere.[2] The relative composition of isomeric mixtures (like DDADAA and DADDAA in the case of D_3A_3) was analysed employing derivatisation and multiple-stage tandem MS techniques. Briefly, the heterochitohomolog (= mixture of isomers) was tagged with AMCR at the reducing end to distinguish Y from B fragments (essentially Y fragments were observed). All free amino groups were derivatized with hexadeuterio acetic acid anhydride to form per-*N*-acetylated compounds (A-d_3 units) with identical mass spectrometric properties. MS^2 and MS^3 experiments employing a Finnigan-LTQ™ vMALDI linear ion trap mass spectrometer (Thermo GmbH, Dreieich, Germany) gave a series of fragments, which allows for an unambiguous readout of the sequences. Peak heights enable for quantification of the components of the isomeric mixture. Table 2 summarizes the relative compositions of isomeric mixtures used for the present study.

Chitinase A Inhibition Assays[18, 21]

First, the kinetics of the hydrolysis of 4-MU-A_3 by ChiA was analysed (Figure 1) to ensure that the assays are performed in the linear range of the 4-MU release.

25 µL of each solution were mixed and incubated at 37°C for different times: 0, 1.5, 5, 10 and 30 minutes. All experiments were done in triplicate and averaged before calculations.

Inhibition Assays at pH 7.4

ChiA was dissolved in 50 mM phosphate buffer pH 7.4 containing 0.1 mg/ml BSA to a final concentration of 0.5 nM (enzyme solution). 4-MU-A_3 was dissolved in 50 mM phosphate buffer pH 7.4 to a final concentration of 40 µM (substrate solution). Different concentrations of homologs (usually 0, 25, 50, 100, 200, 400 and 800 µM) were prepared in the substrate solution. For the assay, 25 µl of the enzyme solution was mixed with 25 µl of the substrate solution, and incubated at 37°C for 10 min. The reaction was stopped with 1.95 ml 0.2 M sodium bicarbonate buffer (Na_2CO_3). The formation of the product, 4-MU, was read for each reaction in a Perkin-Elmer LS 50B fluorescence spectrometer (Perkin-Elmer, Überlingen,Germany). The excitation wavelength was 380 nm (5 nm adjusting slit) and the emission wavelength 460 nm (4 nm adjusting slit). Each reaction was measured in triplicate. Fluorescence values were converted to 4-MU release according to the 4-MU standard curve. The 4-MU release was converted to the specific activity of ChiA for a given inhibitor concentration with respect to the ChiA concentration and the assay running time.

specific activity = 4-MU release [nmol] × sample volume [µL] / assay running time [s] × concentration of ChiA [$mg \times \mu L^{-1}$][19,22]

Specific activities were converted to relative specific activities with 100 % activity for an inhibitor concentration of 0 µM. The relative specific activities were plotted against the inhibitor concentration. The IC_{50} is calculated from non-linear regression based on a four-parameter logistic approach, or in case of low affinities (D_6, D_9, D_1A_2, D_2A_2 and A_3) based on a two-parameter hyperbolic approach.

four-parameter logistic model: specific activity of ChiA = min + (max-min/1+(c(ChO)/IC$_{50}$)^Hillslope)

two-parameter hyperbolic model: specific activity of ChiA = a×b/b+ c(ChO)

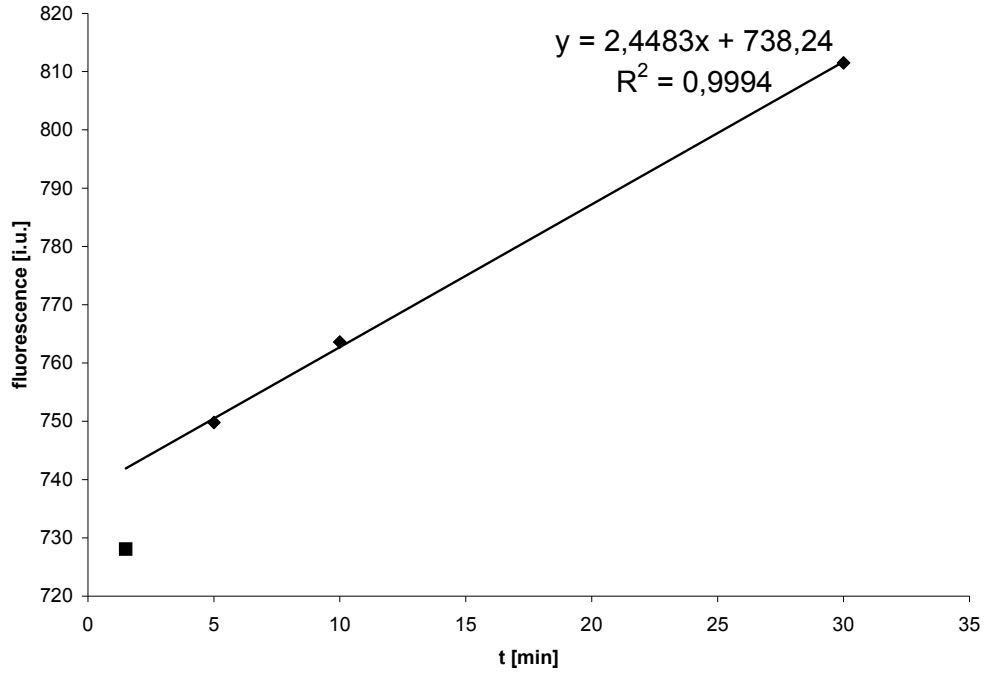

Fig. 1. Hydrolysis of 4-MU-A_3 with ChiA for different times. In the range from 10 to 30 min the graph was fitted to a linear function (fluorescence = 2.4483 × t + 738.24; R^2 = 0.9994). ChiA was dissolved in a 50 mM citrate-phosphate buffer of pH 5.5 containing 0.1 mg/ml BSA to a final concentration of 50 nM. 4-MU-A_3 was dissolved in the same buffer to a final concentration of 20 µM.

Inhibition Assays at pH 5.5

The assays were performed essentially according to the description under *Inhibition Assays at pH 5.5* with the difference that a 50 mM citrate-phosphate buffer of pH 5.5 containing 0.1 mg/ml BSA was used.

Chitinase B Inhibition Assays

Inhibition Assays at pH 5.5

The assays were performed essentially according to the description under *Chitinase A Inhibition Assays*, *Inhibition Assays at pH 7.4* with the difference that a 50 mM citrate-phosphate buffer of pH 5.5 containing 0.1 mg/ml BSA and 4-MU-A_2 as the substrate was used. Like for ChiA the kinetics of the hydrolysis of 4-MU-A_2 by ChiA was analysed to ensure that the assays are performed in the linear range of the 4-MU release.

Hydrolysis Studies

ChiA or ChiB respectively were dissolved in 50 mM phosphate buffer pH 7.4 (ChiA) or 5.5 (ChiB) containing 0.1 mg/ml BSA to a final concentration of 0.5 nM (enzyme solution). The ChO was dissolved in 50 mM phosphate buffer of pH 7.4 (ChiA) or 5.5 (ChiB) to a final concentration of 800 µM (substrate solution). For the hydrolysis assays, 25 µl of the enzyme solution was mixed with 25 µl of the substrate solution, and incubated at 37°C for 10 min, 1h,

6h, 12h. The reaction was stopped by lyophilisation of the reaction mixture. For the analysis of fragments MALDI-TOF MS was employed. The following homologs were used for fragmentation analyses: ChiA: D_3A_3 (DDADAA 51%, DADDAA 49%); ChiB: A_3, A_5, A_6, D_2A_3 (DDAAA 26%, DADAA 57%, ADDAA 17%).

Results

Inhibition Assays of ChO's with Chitinase A

Chitinase A releases 4-MU from 4-MU-A2 and 4-MU-A3 with almost equivalent hydrolysis rates.[23] 4-MU is fluorescent in alkaline solutions. The addition of ChO's causes a decrease of the 4-MU release resulting in a decrease of fluorescence. Figure 2 shows the fluorescence reduction caused by addition of different concentrations of the heterochitohomolog D_3A_3 (DP6) to a mixture of ChiA and 4-MU-A_3 at pH 7.4.

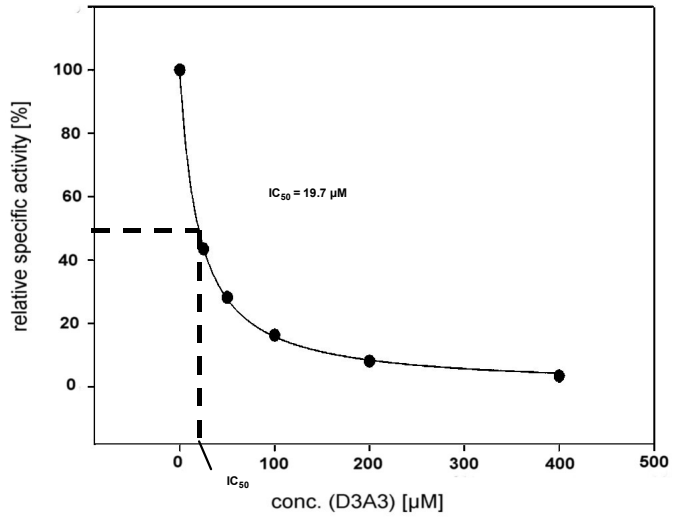

Fig. 2. Chitinase A releases 4-MU (4-methylumbelliferone) from 4-MU-A_3. The 4-methylumbelliferyl anion formed in alkaline solutions is fluorescent. Any inhibition of chitinase A by ChO's is measured as a decrease of fluorescence. Figure 2 shows the plot of the relative specific activity of chitinase A (*Serratia marcescens*) for different concentrations of the inhibitor D_3A_3. Conditions of the assay: 20 mM 4-MU-A_3, pH 7.4, 37°C, incubation time 10 min. The data were fitted to a single site binding model by non-linear regression: *specific activity of ChiA = min + (max-min/1+(c(ChO)/IC$_{50}$)^Hillslope)*.

For calculation of the IC_{50} concentration of D_3A_3, the concentration dependent fluorescence intensities are converted into 4-MU release rates resulting in specific affinities of ChiA for a given concentration of D_3A_3. The data points are fitted to a four-parameter logistic curve (Figure 1), and the IC_{50} concentration is determined according to the equation:

specific activity of ChiA = min + (max-min/1+(c(ChO)/IC$_{50}$)^Hillslope)

The IC_{50} concentrations of low affinity ChO's (D_6, D_9, D_1A_2, D_2A_2 and A_3) are determined fitting the data points to a two-parameter hyperbolic approach. Table 3 summarizes the results of the inhibition assays for ChiA at pH 7.4 and pH 5.5.

The inhibition of the enzymes is expressed as the concentration of the ChO causing 50% inhibition of the enzyme (IC_{50}). Figure 3 shows the IC_{50} concentrations of different ChO's in relation to DP and F_A.

Considering the IC_{50} values of different oligomers and homologs two main principles become evident:

1. The IC_{50} concentrations are decreased as the DP of ChO's is increased.
2. The IC_{50} concentrations are decreased as the F_A of ChO's is increased.

Table 3
Summary of the IC_{50} concentrations determined by the inhibition assays for chitinase A from *Serratia marcescens* with different heterochitooligomers and –homologs. The homologs were in most cases applied as a mixture of isomers, the composition of which was determined previously by means of vMALDI LTQ MS. In the case of D_3A_3, both isomers were additionally applied separately to the inhibition assays.

Chitinase	pH	Oligomer	Homolog	Isomer	IC_{50} [µM]
ChiA	7.4	DP3	D_1A_2		2305.1
			A_3		237.0
		DP4	D_2A_2		1581.2
		DP5	D_2A_3		64.5
		DP6	D_6		2726.4
			D_3A_3		19.7
				DDADAA	21.1
				DADDAA	15.9
			D_2A_4		17.4
		DP9	D_9		1406.5
			D_5A_4		9.9
		DP12	D_7A_5		4.6
		DP15	D_9A_6		5.6
	5.5	DP6	D_3A_3		514.6
		DP9	D_5A_4		132.5
		DP12	D_7A_5		76.9
		DP15	D_9A_6		85.0

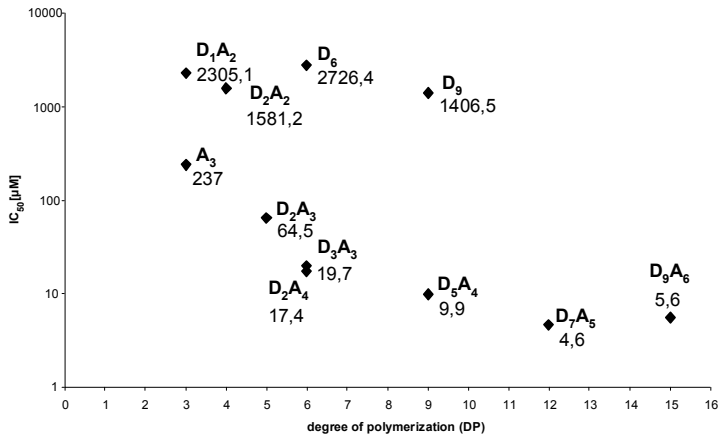

Fig. 3. Summary of the IC_{50} concentrations of ChO's (oligomers and homologs) employed for the inhibition assays with chitinase A at pH 7.4. The IC_{50} concentrations (given as the decadic logarithm) are plotted as a function of DP and F_A.

The chromatographic separation of the heterochitohomolog D_3A_3 gave two fractions, one containing the isomer of the sequence DDADAA, the second containing the isomer of the sequence DADDAA. Both fractions proved to possess different affinities towards ChiA; the IC_{50} concentration for DDADAA is 21.1 µM, the IC_{50} for DADDAA is 15.9 µM, the IC_{50} concentration for the mixture (51% DDADAA, 49% DADDAA) is 19.7 µM.

Besides the specifications of the ChO (DP and F_A), the IC_{50} concentration also depends on the pH of the solution used for incubation. Figure 4 compares the IC_{50} concentrations of ChO's for inhibition assays run at pH 5.5 and 7.4.

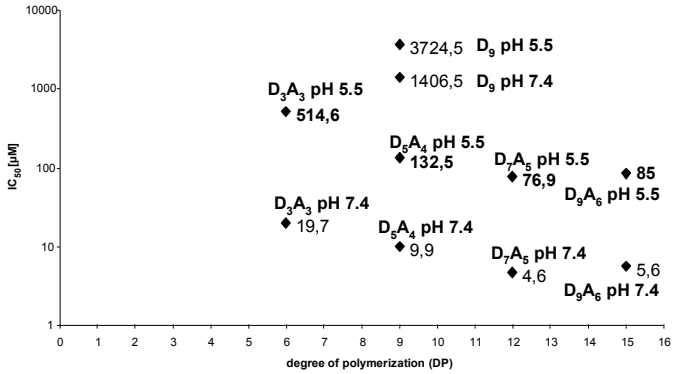

Fig. 4. Comparison of the IC_{50} concentrations for the inhibition of chitinase A with ChO's at pH 5.5 and 7.4.

It is apparent that the IC_{50} concentrations decrease for increasing pH values.

Inhibition Assays of ChO's with Chitinase B

Table 4
Summary of the IC_{50} concentrations determined by the inhibition assays for chitinase B from *Serratia marcescens* with three heterochitooligomers.

Chitinase	pH	Oligomer	Homolog	IC_{50} [µM]
ChiB	5.5	DP6	D_3A_3	105.7
		DP9	D_5A_4	40.4
		DP12	D_7A_5	23.3

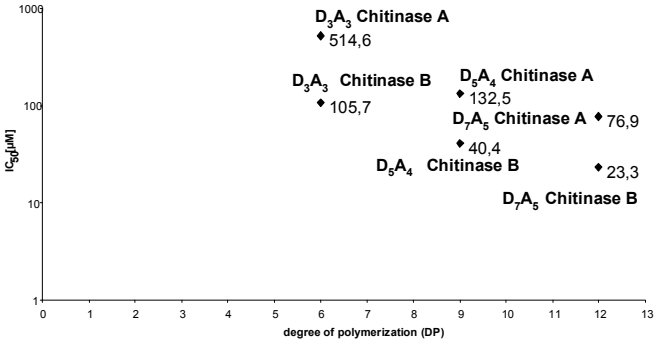

Fig. 5. Comparison of the IC_{50} concentrations for the inhibition of chitinase A or B with ChO's at pH 5.5.

Chitinase A and B from *Serratia marcescens* not only differ not only in the mode of action on chitinious material (ChiA, hydrolysis from the reducing end; ChiB, hydrolysis from the non-reducing end) but also in the architecture of their carbohydrate binding sites: while the binding site of ChiA has an open, groove-like structure, the binding site of ChiB is more

closed at the top resulting in a tunnel-like structure. Table 4 summarises the results of the inhibition assays for ChiB at pH 5.5.
Figure 5 compares the IC_{50} concentrations of three ChO's with respect to the inhibition of ChiA and B.
The IC_{50} concentrations for ChiB are lower compared to ChiA. Like for ChiA, the IC_{50} concentrations decrease with increasing DP and F_A (ChiB: D_3A_3, IC_{50} = 106 μM; D_2A_4, IC_{50} = 20 μM).

Hydrolytic Activity of Chitinase A on ChO's
The IC_{50} concentrations determined for the series of heterochitooligosaccharides reflect on one hand the affinities of the ChO's to ChiA and B. On the other hand the stability of the ChO's against hydrolysis by the active chitinases from *Serratia marcescens* determines the IC_{50} concentration. For the fluorescence based inhibition assays employed presented here, both effects, affinity and stability against hydrolysis, are undistinguishable. Therefore, the hydrolytic activity of chitinase A on ChO's used for the inhibition assays was studied.
D_3A_3 was incubated for 12 h with chitinase A followed by evaluation of the fragments employing MALDI-TOF MS in order to obtain information on the binding modes of D_3A_3 homologs to the carbohydrate binding site of chitinase A. D3A3 consists of only two isomers DDADAA (51%) and DADDAA (49%) so that the fragment mass spectra are unambiguously assigned. Figure 6 shows the MALDI-TOF MS recorded after 12 h of incubation with chitinase A.

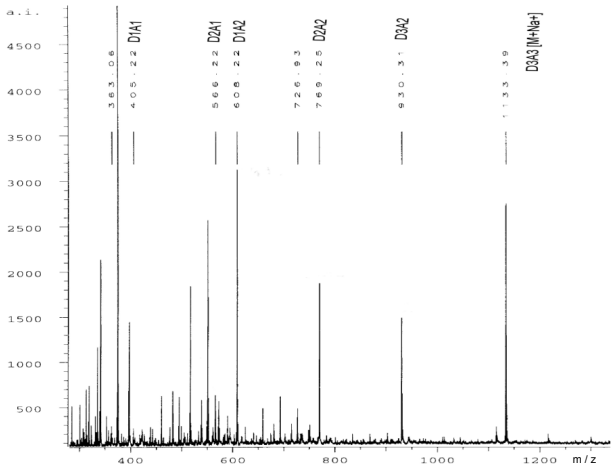

Fig. 6. MALDI-TOF MS of D_3A_3 taken after 12 h of incubation with chitinase A at pH 7.4, 37°C. The sodiated molecular ion peak for D_3A_3 appears at m/z = 1133.57. Sodiated fragment ions appear at m/z = 930.3 (D_3A_2), 769.2 (D_2A_2), 608.2 (D_1A_2), 566.2 (D_2A_1) and 405.2 (D_1A_1).

Table 5 summarizes the fragments expected for the four binding modes -2 → +2, -3 → +2, -4 → +2, -5 → +1 and compares them with the fragments found experimentally. DDADAA is hydrolysed to D_2A_1 and D_1A_2 resulting from the binding mode -3 → +2; DADDAA is cleaved to D_1A_1 and D_2A_2 resulting from the binding mode -2 → +2. Fragments originating from the -4 → +2 binding mode were not detected for any of both isomers. Detection of the D_3A_2 fragment indicates that additionally the -5 → +1 binding mode occurs.
No fragments were detected for ChO's after 10 min of incubation with ChiA (see Supporting Information Figure S-1).

Table 5
Summary of the fragments expected for the four binding modes -2 → +2, -3 → +2, -4 → +2, -5 → +1 and the fragments found by MALDI-TOF MS after 12 h incubation of D_3A_3 (DDADAA (51%) and DADDAA (49%)) with ChiA.

Isomer of D_3A_3	**Binding Mode**	**Scissile Bond**	**Fragments expected**	**Fragments MALDI-TOF MS**
DDADAA	(-2 → +2)	-D-A-	D_2, D_1A_3	-- , --
	(-3 → +2)	-A-D-	D_2A_1, D_1A_2	D_2A_1, D_1A_2
	(-4 → +2)	-D-A-	A_2, D_3A_1	-- , --
	(-5 → +1)	-A-A-	D_3A_2, A_1	D_3A_2
DADDAA	(-2 → +2)	-A-D-	D_1A_1, D_2A_2	D_1A_1, D_2A_2
	(-3 → +2)	-D-D-	D_2A_1, D_1A_2	(D_2A_1, D_1A_2)
	(-4 → +2)	-D-A-	A_2, D_3A_1	-- , --
	(-5 → +1)	-A-A-	D_3A_2, A_1	D_3A_2

Hydrolytic Activity of Chitinase B on ChO's
ChO's employed for the inhibition assays on ChiB were analysed for stability against hydrolysis by ChiB. Additionally, the hydrolysis studies afford information on the binding modes of ChO's to ChiB. Figure 7 shows exemplarily the MALDI-TOF MS of D_2A_3 after incubation with ChiB for 12h at 37°C, pH5.5.

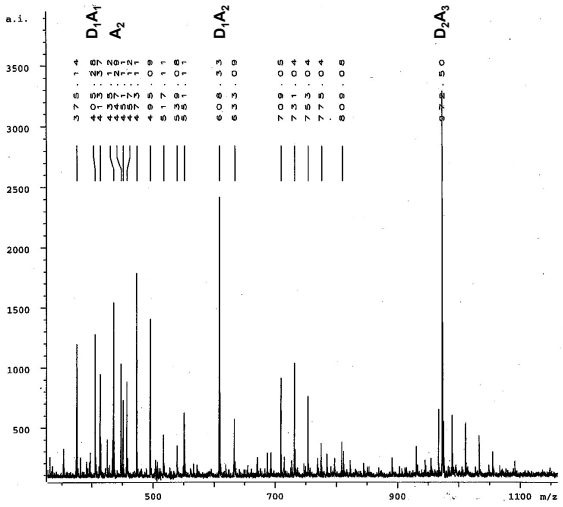

Fig. 7. MALDI-TOF MS of D_2A_3 after incubation with ChiB for 12h at 37°C, pH5.5. Fragment ions are detected at 608.3 (D_1A_2), 447.3 (A_2) and 405.3 (D_1A_1). The peak at 972.5 is attributed to the sodiated molecular ion of D_2A_3.

Table 6 summarizes the fragments expected for the three binding modes -1 → +4, -2 → +3, -3 → +2 and compares them with the fragments found experimentally. ADDAA is not hydrolysed. DADAA is cleaved to D_1A_1 and D_1A_2 resulting from the binding mode -2 → +3; DDAAA is hydrolysed to D_2A_1 and A_2 according to the binding mode –3 → +2.
No fragments were detected for ChO's after 10 min of incubation with ChiB (see Supporting Information Figure S-2).
The carbohydrate binding site of chitinase B is similar to the binding site of human chitotriosidase (HCT).[24] Thus, hydrolysis studies on ChiB reflect the biostability of ChO's in the human body.

Table 6
Summary of the fragments expected for the three binding modes -1 → +4, -2 → +3, -3 → +2 and the fragments found by MALDI-TOF MS after 12 h incubation of D_2A_3 (ADDAA (17%), DADAA (57%) and DDAAA (26%)) with ChiB. Fragments in brackets cannot result from the preset binding mode as the scissile bond would be either -D-D- or -D-A-.

Isomer of D_3A_3	**Binding Mode**	**Scissile Bond**	**Fragments expected**	**Fragments MALDI-TOF MS**
ADDAA	(-1 → +4)	-A-D-	A_1, D_2A_2	-- , --
	(-2 → +3)	-D-D-	D_1A_1, D_1A_2	(D_1A_1, D_1A_2)
	(-3 → +2)	-D-A-	A_2, D_2A_1	(A_2)
DADAA	(-1 → +4)	-D-A-	D_1, D_1A_3	-- , --
	(-2 → +3)	-A-D-	D_1A_1, D_1A_2	D_1A_1, D_1A_2
	(-3 → +2)	-D-A-	A_2, D_2A_1	(A_2)
DDAAA	(-1 → +4)	-D-D-	D_1, D_1A_3	-- , --
	(-2 → +3)	-D-A-	D_2, A_3	-- , --
	(-3 → +2)	-A-A-	A_2, D_2A_1	A_2

Discussion

Inhibition Assays

ChO's inhibit both family 18 chitinases, ChiA and ChiB, with IC_{50} concentrations in the µmolar range. The IC_{50} concentrations determined in the present study are comparable to data published previously for the inhibition of ChiA and ChiB with ChO's and the potent inhibitor allosamidin (Table 7).[18, 25]

Despite the fact that the results obtained by Letzel et al. are in the same range as the results of the present study, Letzel et al. reported a higher IC_{50} concentration for the DP6 oligomer of avarridge F_A 0.5 in the case of ChiA (Letzel et al.: DP6, F_A 0.5, IC_{50} = 1000 µM at pH 5.5; present study: DP6, F_A 0.5, IC_{50} = 515 µM at pH 5.5) whereas in the case of chitinase B Letzel et al. report higher IC_{50} concentration for DP6 oligomer F_A 0.5 compared to the present study (Letzel et al.: DP6, F_A 0.5, IC_{50} = 15 µM at pH 5.5; present studies: DP6, F_A 0.5, IC_{50} = 106 µM at pH 5.5). Recently, Cederkvist et al.[26] reported on the inhibition of ChiB from *Serratia marcescens* at pH 6.1 (enzyme concentration of 2.5 nM) by ChO's of defined DP. A fraction of DP5 showed in apparent IC_{50} concentration of 16 µM, whereas the DP8 fraction gave an IC_{50} concentration of 18 µM. The experiments performed for the present thesis give an IC_{50} concentration of 106µM for the D_3A_3 homolog (DP6) representing a mixture of 51% DDADAA and 49% DADDAA. A possible explanation would be the fact that the fractions of DP5 oligomers contained ChO's of stronger inhibition potency than the well defined isomers DDADAA and DADDAA. Secondly, the IC_{50} concentrations show a strong pH dependency. Therefore, data recorded at pH 6.1 will generally show lower IC_{50} concentrations compared to data recorded at pH 5.5.

Allosamidin inhibits ChiB at pH 5.4 with an IC_{50} concentration of 2.5 µM which is ca. 10-fold lower than the IC_{50} concentration of the strongest ChO inhibitor used for the present study (D_7A_5, DP12, IC_{50} = 23.3 µM at pH 5.5 for ChiB, cf. Table 4).

In conclusion, the results of the present research contribute to establish certain ChO's being strong inhibitors of the family 18 chitinases ChiA and ChiB of *Serratia marcescens*. Considering the IC_{50} concentrations of different oligomers (ChiA and ChiB) and homolog (ChiA) two main rules can be drawn:

1. The IC_{50} concentrations are decreased as the DP of ChO's is increased.
2. The IC_{50} concentrations are decreased as the F_A of ChO's is increased.

That means, the higher the DP and F_A of the heterochitooligomer / homolog the higher its affinity to ChiA. For ChiB, only the DP dependency was proved.
Figure 8 summarizes the DP dependency of IC_{50} concentrations of ChO's of nearly equal F_A for the inhibition of ChiA at pH 7.4.

Table 7
Comparison of the IC_{50} concentrations with results from Letzel et al.[25], Cederkvist et al.[26] and Vaaje-Kolstad et al.[18]

Author	**Enzyme**	**pH**	**Inhibitor**	**Oligomer (homolog)**	**F_A**	**IC_{50} [µM]**
Letzel et al.[25]	ChiA	5.5	ChO	DP4	0.50	3000
				DP5	0.50	500
				DP6	**0.50**	**1000**
	ChiB	5.5	ChO	DP4	0.50	500
				DP5	0.50	15
				DP6	**0.50**	**15**
Cederkvist et al.[26]	ChiB	6.1	ChO	DP5	not defined	16
		6.1	ChO	DP8	not defined	18
Vaaje-Kolstad et al.[18]	ChiB	5.4	Allosamidin			2.5
present studies	ChiA	5.5	ChO	**DP6 (D_3A_3)**	**0.50**	**514.6**
				DP9 (D_5A_4)	0.44	132.5
				DP12 (D_7A_5)	0.42	76.9
				DP15 (D_9A_6)	0.40	85.0
	ChiB	5.5	ChO	**DP6 (D_3A_3)**	**0.50**	**105.7**
				DP9 (D_5A_4)	0.44	40.4
				DP12 (D_7A_5)	0.42	23.3

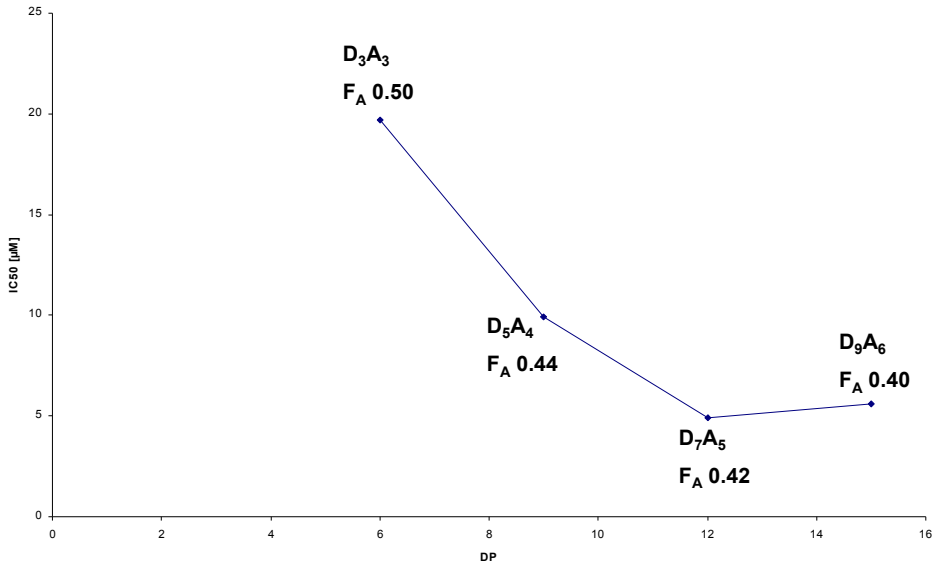

Fig. 8. Correlation between the IC_{50} concentration and the DP of ChO's of a series of DP6, 9, 12, and 15 oligomers (F_A 0.40 to 0.50) for the inhibition of ChiA at pH 7.4.

Figure 9 shows the DP dependency for the inhibition of ChiB at pH 5.5.

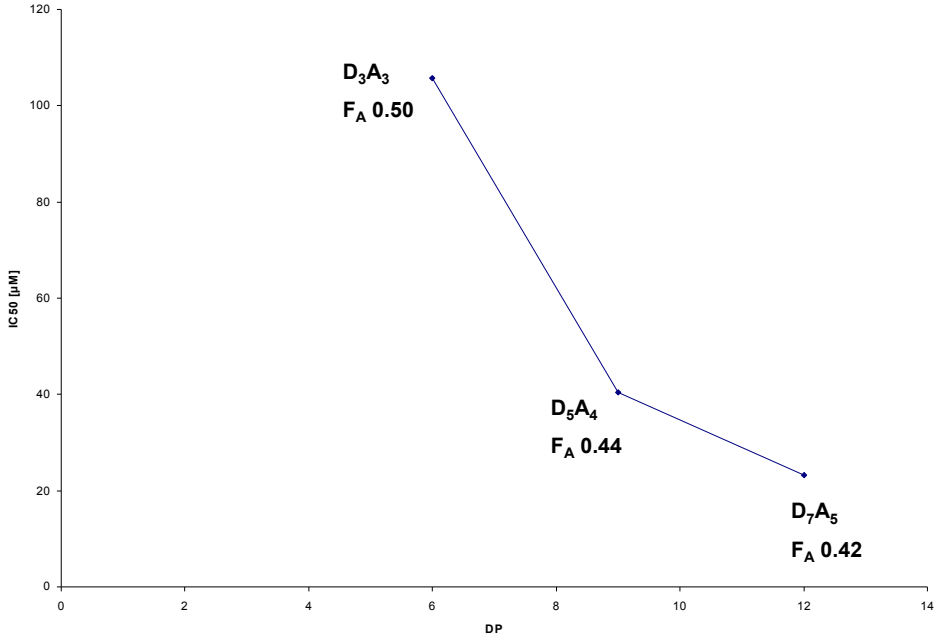

Fig. 9. Correlation between the IC_{50} concentration and the DP of ChO's of a series of DP6, 9, and 12 oligomers (F_A 0.42 to 0.50) for the inhibition of ChiB at pH 5.5.

Figure 10 summarizes the F_A dependency of IC_{50} concentrations of ChO's of equal DP for the inhibition of ChiA at pH 7.4.

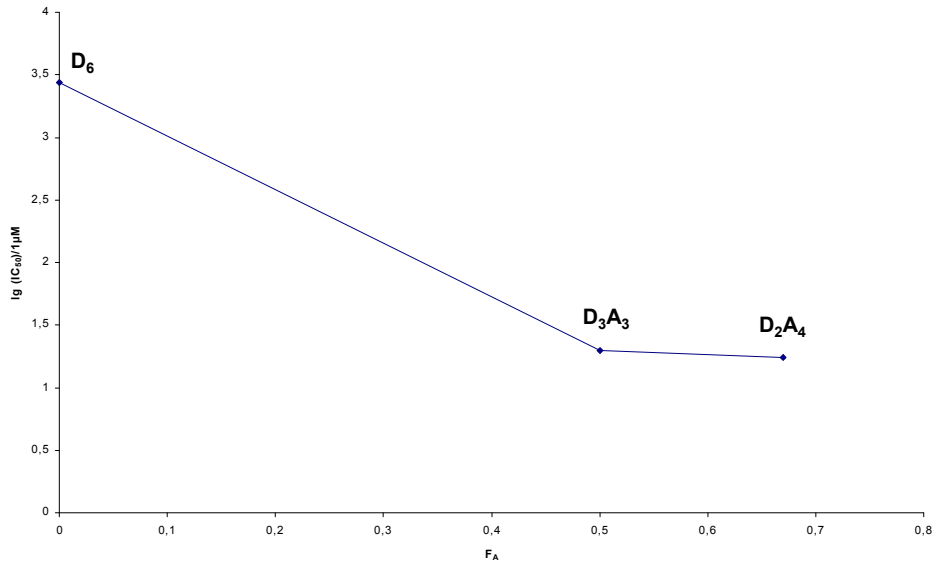

Fig. 10. Correlation between the decadic logarithm of the IC_{50} concentration and the F_A of a series of DP6 homologs for the inhibition of ChiA at pH 7.4.

The inhibitory effect of heterochitooligosaccharides on active family 18 chitinases like ChiA and ChiB from *Serratia marcescens* depends on two limiting factors: the affinity of the ChO to the carbohydrate binding sites of ChiA and ChiB, and secondly the stability of the ChO against hydrolysis by ChiA or ChiB, respectively.

Focussing on affinities, the structures of the carbohydrate binding sites of ChiA and ChiB have to be considered as well as the mode of action of these enzymes on chitinous material to explain the observed DP and F_A dependencies of the IC_{50} concentrations. Figure 11 shows a schematic drawing of the carbohydrate binding site of ChiA.

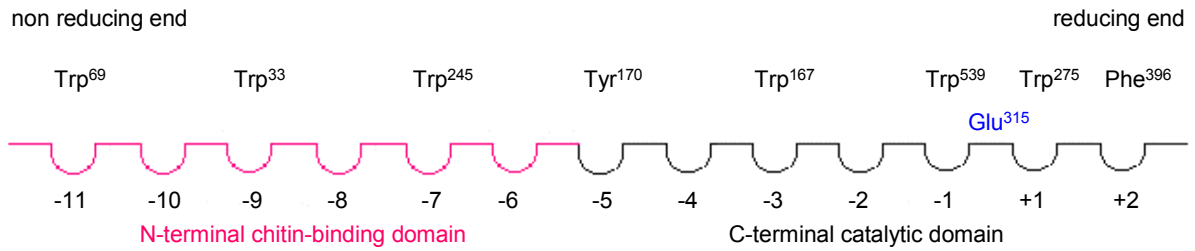

Fig. 11. Schematic drawing of the N-terminal chitin-binding domain (red) and the C-terminal catalytic domain (black) of chitinase A with subsites ranging from –11 (non-reducing end) to +2 (reducing end). The catalytic site (with Glu^{315}) is positioned asymmetrically in the binding cleft between subsites –1 and +1. The catalytic domain is locked beyond subsite +2.

The binding site is subdivided into the catalytic domain (subsites -5 to +2) with core subsites -3 to +2[16], and the N-terminal domain (subsites -6 to -11).[17] Affinity between ChO's and ChiA is predominately based on hydrophobic interactions of A monomer residues with hydrophobic amino acid residues positioned at subsites +2 (Phe^{396}), +1 (Trp^{275}), -1 (Trp^{539}), -3 (Trp^{167}), -5 (Tyr^{170}), -7 (Trp^{245}), -9 (Trp^{33}), and -11 (Trp^{69}).[14, 16, 27, 28] Furthermore, hydrogen bonding contributes to binding unspecifically at all subsites with a maximum for subsites -1 and +1.[14]
The hydrolysis studies on D_3A_3 with ChiA indicate that for DP6 oligomers binding modes -1 → +2, -2 → +2, -3 → +2, and -4 → +2 occur. Also binding mode -5 → +1 has to be considered. Figure 12 summarizes all alignments of the series of DP6 homologs, D_6, D_3A_3, and D_2A_4, to the core subsites of ChiA, -3 to +3. The results of the hydrolysis study on D_3A_3 employing ChiA show that the carbohydrate binding site of ChiA is not (completely) locked at subsite +2 so that ChO's might extend beyond subsite +2.
Hexamers D_3A_3 bind with a higher number of hydrophobic interactions to ChiA than D_6. For isomer DDADAA of hexamer D_3A_3, only alignment 11 results in three hydrophobic interactions, which is consequently favourable over all other alignments. Nevertheless, also alignments resulting in two or even one hydrophobic interaction contribute to the overall affinity of the isomer DDADAA. Moreover, only alignment 12 results in the highest number of hydrogen bondings as all monomer residues are aligned to a subsite of ChiA (-4 to +2). These considerations result in different evaluation methods of the data from the alignment of the isomers. Table 8 compares four different ways of evaluation.

1. All different alignments (-3 → -1 to -1 → +2) of a sequence are regarded. The number of hydrophobic interactions between A units and subsites –3, -1 and +1 are counted, summed up for each isomer, and weighted by the contribution of the isomer to the amount of the homolog. Finally the weighted hydrophobic interactions of the isomers are summed up to the overall number of hydrophobic interactions of the homolog.
2. Only alignment are regarded, for which three or minimum two hydrophobic interactions are obtained.
3. Only alignments are regarded, for which minimum three hydrophobic interactions are obtained.
4. Only one alignment per isomer is regarded. It is the alignment, for which all monomer units of the isomer are aligned to one of the subsites -4 to +2.

A

D_6

01 D – D – D – D – D – D
02 D – D – D – D – D – D
03 D – D – D – D – D – D
04 D – D – D – D – D – D
05 D – D – D – D – D – D

D_3A_3

11 D – D – A – D – A – A
12 D – D – A – D – A – A
13 D – D – A – D – A – A
14 D – D – A – D – A – A
15 D – D – A – D – A – A

21 D – A – D – D – A – A
22 D – A – D – D – A – A
23 D – A – D – D – A – A
24 D – A – D – D – A – A
25 D – A – D – D – A – A

D_2A_4

31 D – D – A – A – A – A
32 D – D – A – A – A – A
33 D – D – A – A – A – A
34 D – D – A – A – A – A
35 D – D – A – A – A – A

41 A – D – D – A – A – A
42 A – D – D – A – A – A
43 A – D – D – A – A – A
44 A – D – D – A – A – A
45 A – D – D – A – A – A

B

D_2A_4

51 D – A – D – A – A – A
52 D – A – D – A – A – A
53 D – A – D – A – A – A
54 D – A – D – A – A – A
55 D – A – D – A – A – A

61 A – A – D – D – A – A
62 A – A – D – D – A – A
63 A – A – D – D – A – A
64 A – A – D – D – A – A
65 A – A – D – D – A – A

71 D – A – A – D – A – A
72 D – A – A – D – A – A
73 D – A – A – D – A – A
74 D – A – A – D – A – A
75 D – A – A – D – A – A

81 A – D – A – D – A – A
82 A – D – A – D – A – A
83 A – D – A – D – A – A
84 A – D – A – D – A – A
85 A – D – A – D – A – A

Fig. 12 A, B. Alignment of the sequences of the hexamers D_6, D_3A_3, and D_2A_4 to the carbohydrate binding domain of ChiA. Only the core subsites -3 to +3 are regarded. It is assumed that subsites < -3 and > +3 do not contribute significantly to binding. Monomer units extending beyond subsites –3 to +3 are coloured red, monomer units aligned to subsites –3, -1 and +1, which mainly contribute to hydrophobic interactions, are coloured blue. Each alignment is signed with a code.

Table 8
Summary of the different evaluation methods 1 – 4 for the alignment of the sequences of DP6 hexamers D_6, D_3A_3 and D_2A_4.

DP6 homolog	$1/IC_{50}$ [μM^{-1}] (inhibition assay)	№ of hydrophobic interactions (evaluation method 1)	№ of hydrophobic interactions (evaluation method 2)	№ of hydrophobic interactions (evaluation method 3)	№ of hydrophobic interactions (evaluation method 4)
D_2A_4	5.8×10^{-2}	8	5.5	2.3	2.2
D_3A_3	5.1×10^{-2}	6	3.5	1.5	1.5
D_6	3.7×10^{-4}	0	0	0	0

All four evaluation methods lead to numbers of hydrophobic interactions between the series of DP6 homologs and ChiA that reflect the observed affinities (expressed as $1/IC_{50}$) qualitatively correctly: $D_2A_4 > D_3A_3 > D_6$. Therefore, the observed IC_{50} concentrations are correlated to the number of hydrophobic interactions of the isomers comprising a homolog. A more detailed look on the influence of the sequence of D and A units allows the example of two D_3A_3 isomers, DDADAA (IC_{50} = 21.1 µM) and DADDAA (IC_{50} = 15.9 µM). Table 9 summarizes the results of evaluation methods 1 - 4 for the alignment of the D_3A_3 sequences DDADAA and DADDAA (Figure 12, alignments 11 to 15 and 21 to 25).

Table 9
Summary of the different evaluation methods 1 – 4 for the alignment of the D_3A_3 isomers DDADAA and DADDAA.

D_3A_3 isomer	**$1/IC_{50}$ [μM^{-1}] (inhibition assay)**	**№ of hydrophobic interactions (evaluation method 1)**	**№ of hydrophobic interactions (evaluation method 2)**	**№ of hydrophobic interactions (evaluation method 3)**	**№ of hydrophobic interactions (evaluation method 4)**
DDADAA	4.8×10^{-2}	6	3	3	1
DADDAA	6.3×10^{-2}	6	4	0	2

Only evaluation methods 2 and 4 lead to numbers of hydrophobic interactions between the two D_3A_3 isomers and ChiA that reflect the observed affinities (expressed as $1/IC_{50}$) qualitatively correctly: DADDAA > DDADAA. Consequently, two times a double hydrophobic interaction (alignments **21** and **22**) is favourable over one time a triple hydrophobic interaction (alignment **11**). And alignments involving subsite +2 as **12** or **22** are favourable over alignments involving subsite –5 instead as **11** or **21**.
Apparently, the affinity of ChO's increases with DP if the number of A units increases, like for $D_3\mathbf{A_3}$ (DP6) and $D_7\mathbf{A_5}$ (DP12). However, there are several examples of increasing affinity for increasing number of D units, like $\mathbf{D_1}A_2$ (IC_{50} = 2305.1 µM) and $\mathbf{D_2}A_2$ (IC_{50} = 1581.2 µM) or A_3 (IC_{50} = 237.0 µM), $\mathbf{D_2}A_3$ (IC_{50} = 64.5 µM) and $\mathbf{D_3}A_3$ (IC_{50} = 19.7 µM) or $\mathbf{D_2}A_4$ (IC_{50} = 17.4 µM) and $\mathbf{D_5}A_4$ (IC_{50} = 9.9 µM). (Figure 13)

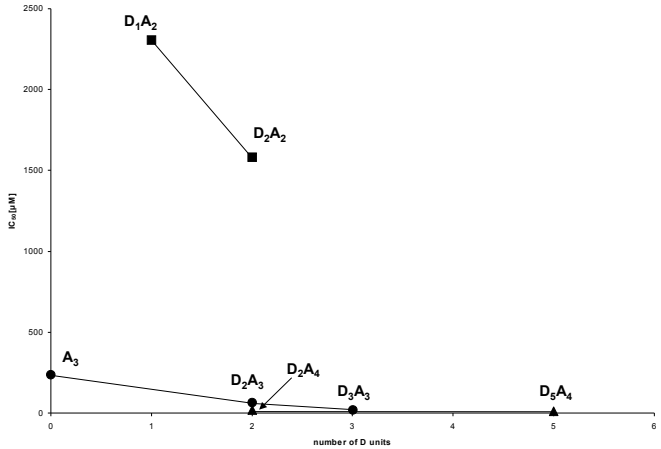

Fig. 13. Comparison of the IC_{50} concentrations of ChO's with constant number of A units but different numbers of D units (D_nA_2, D_nA_3, and D_nA_4).

Three factors cause this effect: First, an increasing number of D units increases the stability of ChO's against hydrolysis. ChO's are mechanism-based inhibitors of ChiA, ChiB and family 18 chitinases in general. In order to cleave a glycosidic bond, a family 18 chitinase requires binding of an A residue at subsite -1. Binding of a D residue at subsite -1 is non-productive

and actually results in competitive inhibition of the enzyme. E.g. A_3 = AAA is hydrolysed to A_2 and A_1, DADAA and ADDAA (D_2A_3) are not or very slowly hydrolysed whereas only DDAAA is hydrolysed to D_2A_1 and A_1. DADDAA and DDADAA are both hydrolysed rather slowly by ChiA and ChiB. The second factor is the fact that D units contribute to affinity through hydrogen bonding. The third factor is the fact that the number of alignments increases with increasing DP. This entropic effect contributes to the affinity. E.g. for A_3 two high-affinity alignments -2 → +1 and -1 → +2 are possible whereas for each D_3A_3 isomer five alignments (**11** – **15** and **21** to **25**) are possible (Figure 12). The binding of ChO's with DP > 6 to ChiA involves subsites beyond the core subsites of the chitin binding domain. Although the IC_{50} concentration of D_5A_4 is lower than for D_3A_3, the decrease is significantly less than from A_3 to D_3A_3 (Table 3). In conclusion, binding sites beyond -4 are more shallow than the core subsites. The DP15 oligomer shows a slightly higher IC_{50} concentration than the DP12 oligomer. Consequently, binding of monosaccharide residues beyond subsite –10 is so weak that no more subsites are observed.
IC_{50} concentrations decrease from pH 5.5 (pH optimum for the hydrolysis of ChO's with ChiA or ChiB) to 7.4 (physiological conditions). At pH 5.5 most amino groups of ChO's are protonated. The charge of the ammonium groups results in a stronger repulsion of D units with hydrophobic amino acid residues of the carbohydrate binding site.
The IC_{50} concentrations of the series of oligomers binding to ChiB can be explained by the same model developed for the binding to ChiA. The carbohydrate binding site of ChiB is similar to that of ChiA (Figure 14).

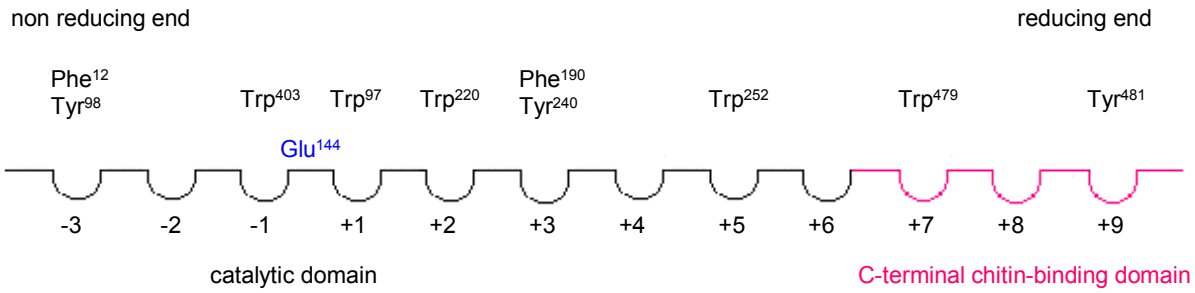

Fig. 14. Schematic drawing of the C-terminal chitin-binding domain (red) and the N-terminal catalytic domain (black) of chitinase B with subsites ranging from -3 (non-reducing end) to +9 (reducing end). The catalytic site (with Glu^{144}) is positioned asymmetrically in the binding cleft between subsites –1 and +1. The catalytic domain is locked beyond subsite -3.

The number of A units continuously increases from D_3A_3 over D_5A_4 to D_7A_5 resulting in an increase in the number of hydrophobic interactions. The total number of monomer units increases equally resulting in an increased number of hydrogen bondings. Again, the IC_{50} concentration increases from D_7A_5 to D_9A_6 indicating that binding beyond subsite +9 is so weak that further subsites do not contribute to affinity. Generally, the IC_{50} concentrations for ChiB are lower than for ChiA for the reason that ChiB has a more closed, tunnel-like architecture of the carbohydrate binding site than ChiA resulting in a tighter binding of any ligands.
Besides affinity, the stability of ChO's against enzymatic hydrolysis determines the IC_{50} concentration. For the present studies, the molar ratio of sugar vs. enzyme is 50,000 to 1,600,000 : 1. Therefore, hydrolysis of the sugars, which are potential substrates of ChiA and ChiB, might occur during the assay running time of 10 min but only to such little extend that the measured IC_{50} concentrations reflect predominately affinities rather than stability against hydrolysis. MALDI-TOF mass spectra recorded on ChiA and ChiB after 10 min of incubation with D_3A_3 or D_2A_3 confirm this assumption as no signals of fragment ions are observed. Nevertheless hydrolysis studies afford information on the binding modes of ChO's to ChiA or ChiB (cf. Figures 6, 7; Tables 5, 6) on one hand and biostabilities on the other hand. Under

this aspect especially ChiB is interesting as its carbohydrate binding domain shows a high homology with the binding domain of human chitotriosidase. ChiB binds longer ChO's with the non-reducing end preferably located at subsite –2 but also at subsites –3 and –1, as the fragments of the hydrolysis of A_6 with ChiB indicate (see Supporting Information Figure S-3). Furthermore, in order to cleave a glycosidic bond, ChiB requires binding of an A residue at subsite –1, while the preferences at subsites –2 and –3 are less pronounced.[3] Binding of a D residue at subsite -1 is non-productive and actually results in competitive inhibition of the enzyme.[29] Hydrolysis occurs processivly at every second glycosidic bond, provided that an A residue is positioned at subsite -1.[3] Glycosidic bonds are cleaved with relative rates AA-X : DA-X : YD-X ca. 3 : 1 : 0, and bonds of the type YYA-X (Y = D or A) are cleaved slowly.[3] Figure 15 shows the alignments of the three D_2A_3 isomers employed for affinity studies to the carbohydrate binding site of ChiB.

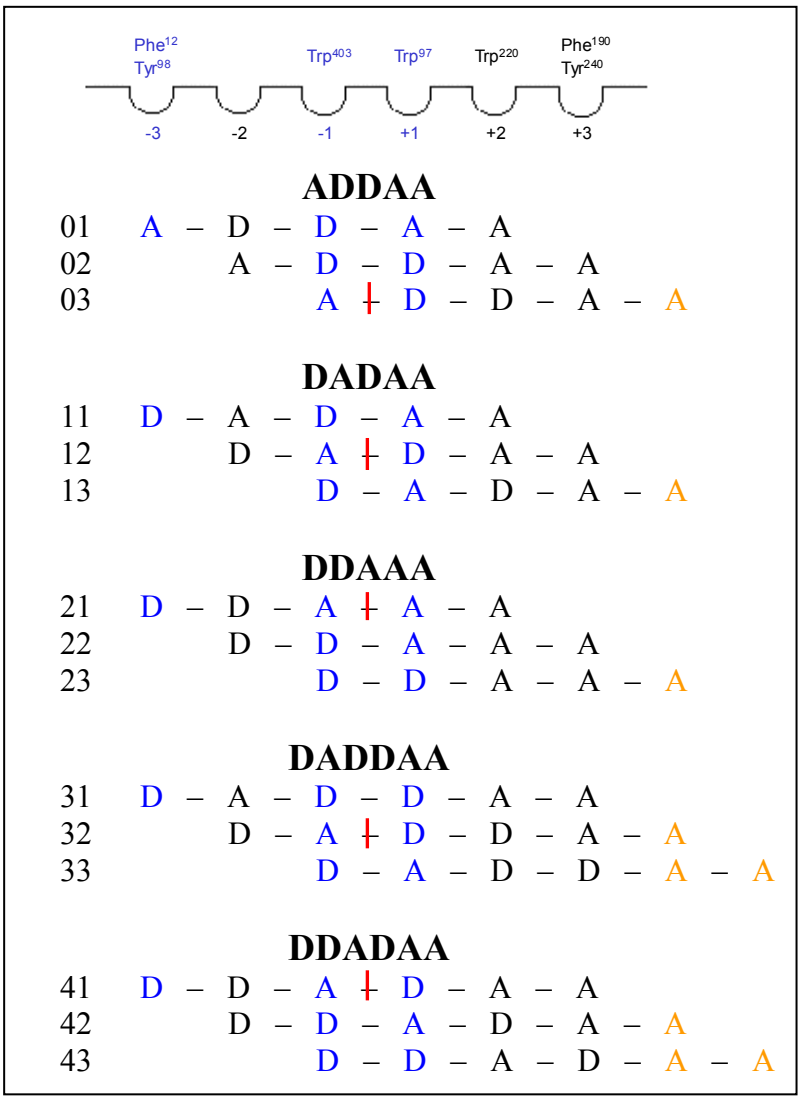

Fig. 15. Hydrolysis of the isomers of D_2A_3 (ADDAA, DADAA, DDAAA) and D_3A_3 (DADADD, DDADAA) with chitinase B. Monosaccharide residues complexed with core subsites –3, -1, and +1 are in blue colour, red lines mark scissile bonds. Monosaccharide units that extend beyond subsite +3 are in red colour.

ADDAA is only slowly hydrolysed in the disfavoured binding mode –1 → +4. Therefore, ADDAA is identified to be the most biostable isomer of D_2A_3, which is confirmed by experimental results (Figure 7, Table 6).
Figure 12 (alignments 11 to 15 and 21 to 25) shows the binding of two isomers of D_3A_3 to ChiA. The IC_{50} concentration of DADDAA is lower than for DDADAA. Unlike ChiB, ChiA

binds longer ChO's with the reducing end preferably located at subsite +2.[16] Less preferably the reducing end can be bound to subsite +1 or extend beyond subsite +2, as the hydrolysis of two D_3A_3 isomers indicates (Figure 6, Table 5). Like for ChiB, ChiA requires binding of an A residue at subsite –1 in order to cleave a glycosidic bond. Binding of a D residue at subsite -1 is non-productive and actually results in competitive inhibition of the enzyme.[16] Hydrolysis occurs processivly at every second glycosidic bond, provided that an A residue is positioned at subsite -1.[17] Glycosidic bonds are cleaved with relative rates XA-AY > XA-DY, whereas bonds of the sequence XD-Y are not cleaved (X, non-reducing end; Y, reducing end). Bonds of the type XA-A or XA-D (binding modes -x → +1) are cleaved slowly.[16] Figure 16 summarizes the hydrolysis of both isomers, DDADAA and DADDAA.

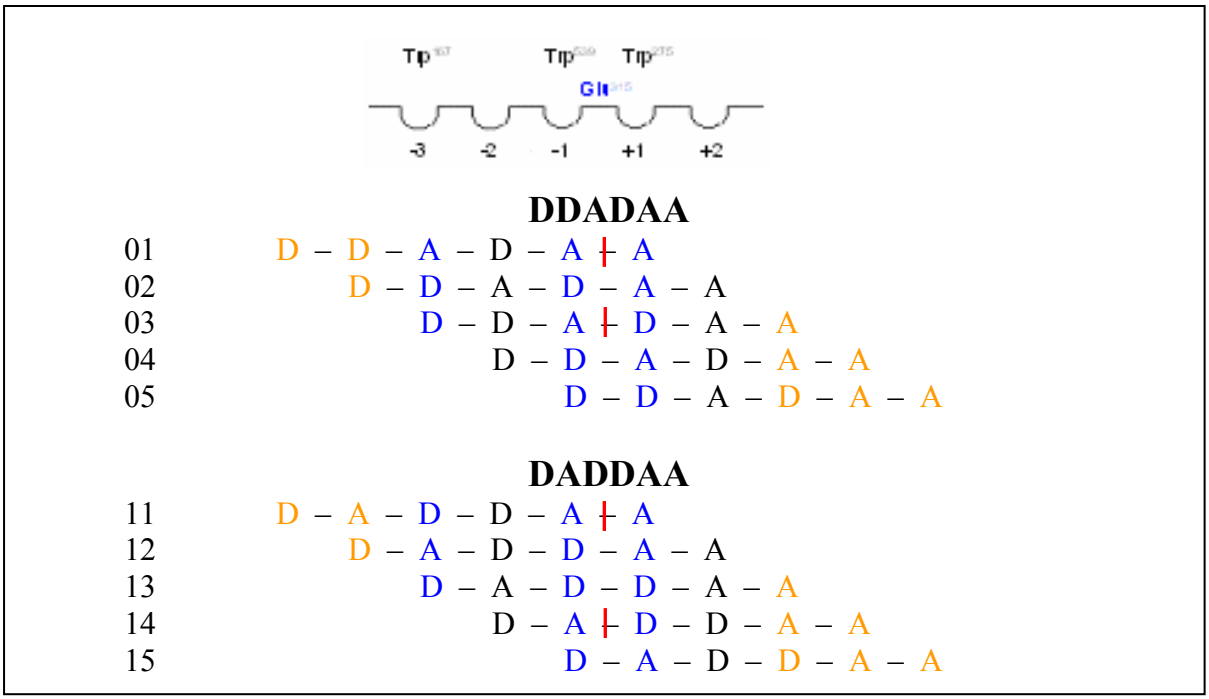

Fig. 16. Hydrolysis of the isomers of D_3A_3 (DADADD, DDADAA) with chitinase A. Monosaccharide residues complexed with core subsites –3, -1, and +1 are in blue colour, red lines mark scissile bonds. Monosaccharide units that extend beyond subsites -3 or +2 are in red colour.

The fragments of the hydrolysis of D_3A_3 identified by MALDI-TOF mass spectrometry (Figure 6, Table 5) confirm the theoretical considerations. Accordingly, both isomers are hydrolysed in the -5 → +1 binding mode (XA-A). More preferably the XA-DY bond of DDADAA is hydrolysed resulting from either the -3 → +2 binding mode or hydrolysis of DDADA in the -3 → +2 binding mode consecutively to the hydrolysis of the XA-A bond. For DADDAA, preferably hydrolysis of the XA-DY bond occurs resulting from binding mode -2 → +2. In conclusion, both D_3A_3 isomers are slowly hydrolysed by ChiA. ChiB will hydrolyse DADDAA preferably according to the order of hydrolysis rates DA-X > DDA-X. Therefore, DDADAA could be identified as the isomer of higher biostability (with respect to hydrolysis by ChiB) even though slightly lower affinity to ChiA compared to DADDAA.
In conclusion, heterochitooligomers are strong inhibitors of ChiA and ChiB from *Serratia marcescens*. This allows for the conclusion that in general the products of the hydrolysis of ChO's with chitinases are mechanism-based competitive inhibitors. Therefore, a reactor for the production of ChO's has to be designed in a way that the products of the hydrolysis are conducted off continuously. Inhibitors of family 18 chitinases are under investigation as agents against insects[30], fungi[31], nematodes[32, 33] or even protozoa (e.g. malarial parasites)[34] as these organisms require chitinases for reproduction. Therefore, ChO's could play a future role

in the development of inhibitors of chitinases for pharmaceutical purpose. Chitinase A from *Serratia marcescens* has a similar architecture of the carbohydrate binding domain as the human chito-lectin HC gp39[35], which plays a significant role in rheumatoid arthritis.[36] Therefore, inhibition experiments on catalytically inactive ChiA mutants could replace affinity studies employing the hardly available HC gp39 to investigate the role that ChO's could play in the fight against rheumatoid arthritis. The architecture of the carbohydrate binding domain of ChiB is similar to the binding domain of human chitotriosidase. Therefore, hydrolysis studies employing ChiB allow to estimate the biostability of ChO's in the human body.

Heterochitooligosaccharides are drastically more biostable than homochitooligosaccharides through the introduction of D units into the oligosaccharide chain, whereas the loss of affinity is tolerable. Oligomers of DP6 –12 with F_A of 0.50 to 0.75 have proven to be the optimal compromise between affinity on one hand and biostability on the other hand. In any case the affinity and biostability of singular sequences have to be experimentally proved or at least theoretically estimated on base of the models introduced by the present work, as affinity and biostability finally depend on the sequence of D and A units.

References

1. Peter M G (2002) Chitin and chitosan from animal sources. In *Biopolymers, Vol. 6: Polysaccharides II* (Steinbüchel A, ed), pp. 481-557. Wiley-VCH, Weinheim.
2. Bahrke S, Einarsson J M, Gislason J, Haebel S, Letzel M C, Peter-Katalinić J, Peter M G (2002) Sequence analysis of chitooligosaccharides by matrix-assisted laser desorption ionization postsource decay mass spectrometry. *Biomacromolecules* **3**, 696 - 704.
3. Sørbotten A, Horn S J, Eijsink V G H, Vårum K M (2005) Degradation of chitosans with chitinase B from *Serratia marcescens*. Production of chito-oligosaccharides and insight into enzyme processivity. *FEBS Journal* **272**, 538-549.
4. Horn S J, Sørbotten A, Synstad B, Sikorski P, Sørlie M, Vårum K M, Eijsink V G H (2006) Endo/exo mechanism and processivity of family 18 chitinases produced by *Serratia marcescens*. *FEBS Journal* **273**, 491-503.
5. Mitsutomi M, Isono M, Uchiyama A, Nikaidou N, Ikegami T, Watanabe T (1998) Chitosanase activity of the enzyme previously reported as β-1,3-1,4-glucanase from *Bacillus circulans* WL-12. *Biosci. Biotechnol. Biochem.* **62**, 2107-2114.
6. K. M. Vårum K M, M. W. Anthonsen M W, H. Grasdalen H, O. Smidsrød O (1991) Determination of the degree of *N*-acatylation and the distribution of *N*-acetyl groups in partially N-deacetylated chitins (chitosans) by high-field n.m.r. spectroscopy. *Carbohydr. Res.* **217**, 17-23.
7. Fukamizo T, Othakara A, Mitsutomi M, Goto S (1991) NMR spectra of partially deacetylated chitotrisaccharides. *Agric. Biol. Chem.* **55**, 2653-2655.
8. Akiyama K, Kawazo K, Kobayashi A Z (1995) Partially N-deacetylated chitin oligomers (pentamer to heptamer) are potential elicitors for (+)-pisatin induction in pea epicotyls. *Z. Naturforsch.,C J. biosci.* **50**, 391-397.
9. Henrissat B (1999) Classification of chitinases modules. *EXS* **87**, 137-156.
10. van Aalten D M F, Komander D, Synstad B, Gåseidnes S, Peter M G, Eijsink V G H (2001) Structural insights into the catalytic mechanism of a family 18 exo-chitinase. *Proc. Natl. Acad. Sci. USA* **98**, 8979-8984.
11. Brameld K A, Shrader W D, Imperiali B, Goddard III W A (1998) Substrate assistance in the mechanism of family 18 chitinases: theoretical studies of potential intermediates and inhibitors. *J. Mol. Biol.* **280**, 913-923.
12. Synstad B, Gåseidnes S, van Aalten D M F, Vriend G, Nielsen J E, Eijsink V G H (2004) Mutational and computational analysis of the role of conserved residues in the active site of a family 18 chitinase. *Eur. J. Biochem*. **271**, 253-262.

13. Sikorski P, Stokke B T, Sørbotten A, Vårum K M, Horn S J, Eijsink V G H (2005) Development and application of a model for chitosan hydrolysis by a family 18 chitinase. *Biopolymers* **77**, 273-285.
14. Perrakis A, Tews I, Dauter Z, Oppenheim A B, Chet I, Wilson K S, Vorgias C E (1994) Crystal structure of a bacterial chitinase at 2.3 Å resolution. *Structure* **12**, 1169-1180.
15. Papanikolau Y, Prag G, Tavlas G, Vorgias C E, Oppenheim A B, Petratos K (2001) High resolution structural analyses of matant chitinase A complexes with substrates provide new insight into the machanism of catalyses. *Biochem.* **40***, 11338-11343.*
16. Aronson Jr. N N, Halloran B A, Alexyev M F, Amable L, Madura J D, Pasupulati L, Worth C, van Roey P (2003) Family 18 chitinase-oligosaccharide substrate interection: subsite preference and anomer selectivity of *Serratia marcescens* chitinase A. *Biochem. J.* **376**, 87-95.
17. Uchiyama T, Katouno F, Nikaidou N, Nonaka T, Sugiyama J, Watanabe T (2001) Roles of the exposed aromatic residues in crystalline chitin hydrolysis by chitinase A from *Serratia marcescens* 2170. *J. Biol. Chem.* **44**, 41343-41349.
18. Vaaje-Kolstad G, Houston D R, Rao F V, Peter M G, Synstad B, van Aalten D M F, Eijsink V G H (2004) Structure of the D142N mutant of the family 18 chitinase ChiB from *Serratia marcescens* and its complex with allosamidin. *BBA* **1696**, 103-111.
19. van Aalten D M F, Synstad B, Brurberg M B, Hough E, Riise B W, Eijsink V G H, Wierenga R K (2000) Structure of a two-domain chitotriosidase from *Serratia marcescens* at 1.9-Å resolution. *Proc. Natl. Acad. Sci. USA* **97**, 5842-5847.
20. Katouno F, Taguchi M, Sakurai K, Uchiyama T, Mikaidou N, Nonaka T, Sugiyama J, Watanabe T (2004) Importance of exposed aromatic residues in chitinase B from *Serratia marcescens* 2170 for crystalline chitin hydrolysis. *J. Biochem.* **136**, 163-168.
21. Fukamizo T, Ohkawa T, Ikeda Y, Torikata T, Goto S (1995) Binding mode of N, N', N'', N'''-tetraacetylchitotetraitol to hen egg white lysozyme. *Carbohydr. Res.* **267**, 135-142.
22. Hollis T, Honda Y, Fukamizo T, Marcotte E, Day P J, Robertus J D (1997) Kinetic analysis of barley chitinase. *Archives of Biochemistry and Biophysics* **344**, 335-342.
23. M. B. Brurberg, I. F. Nes, V. G. H. Eijsink, *Microbiol.* (1996) **142**, 1581.
24. Fusetti F, von Moeller H, Houston D, Rozeboom H J, Dijkstra B W, Boot R G, Aerts J M, van Aalten D M F (2002) Structure of human chitotriosidase – implications for specific inhibitor design and function of mammalian chitinase-like lectins. *J. Biol. Chem.* **277**, 25537-25544.
25. Letzel M C, Synstad B, Eijsink V G H, Peter-Katalinić J, Peter M G (2000) Libraries of chito-oligosaccharides of mixed acetylation patterns and their interactions with chitinases. *Advan. Chitin Sci.* **4**, 545-551.
26. Cederkvist F H, Parmer M P, Vårum K M, Eijsink V G H, Sørlie M (2008) Inhibition of a family 18 chitinase by chitooligosaccharides. *Carbohydrate Polymers*, Article in press.
27. Fukamizo T, Sasaki C, Schelp E, Bortone K, Robertus J D (2001) Kinetic properties of chitinase-1 from the fungal pathogen *Coccidioides immitis*. *Biochem.* **40**, 2448-2454.
28. Chipman D M, Grisaro V, Sharon N (1967) The binding of oligosaccharides containing N-acetylglucosamine and N-acetylmuramic acid to lysozyme. *J. Biol. Chem.* **242**, 4388-4394.
29. Cederkvist F H, Zamfir A D, Bahrke S, Eijsink V G H, Sørlie M, Peter-Katalinić J, Peter M G (2006) Identification of a high-affinity-binding oligosaccharide by (+) nanoelectrospray quadrupole time-of-flight tandem mass spectrometry of a noncovalent enzyme-ligand complex. *Angew. Chem. Int. Ed*. **45**, 2429-2434.
30. Bade M L, Wyatt D R, (1962) Metabolic conversion during pupation of the cecropia silkworm. 1. Deposition and utilisation of nutrient reserves. *Biochem. J.* **83**, 470-478.
31. Gooday G W, Zhu W Y, O'Donnell R W (1992) What are the roles of chitinases in the growing fungus? *FEMS Microbiol. Lett.* **100**, 387-391.
32. Boot R G, Renkema G H, Verhoek M, Strijland A, Bliek J,

Meulemeester T M A M O, Mannens M M A M, Aerts J M F G (1998) *J. Biol. Chem.* **273**, 25680.
33. Hollak C E M, van Weely S, van Oers M H J, J. Aerts J M F G (1994) *J. Clin. Invest.* **93**, 1288
34. Huba M, Cabib E, Miller L H (1991) Malaria parasite chitinase and penetration of the mosquito peritrophic membrane. *Proc. Natel. Acad. Sci. USA* **88**, 2807-2810.
35. Fusetti F, Pijning T, Kalk K H, Bos E, Dijkstra B W (2003) *J. Biol. Chem.* **278**, 37753.
36. Johansen J S, Hvolris J, Hansen M, Backer V, Lorenzen L, Price P A (1996) *Br. J. Rheumatol.* **35**, 553.

Supporting Information

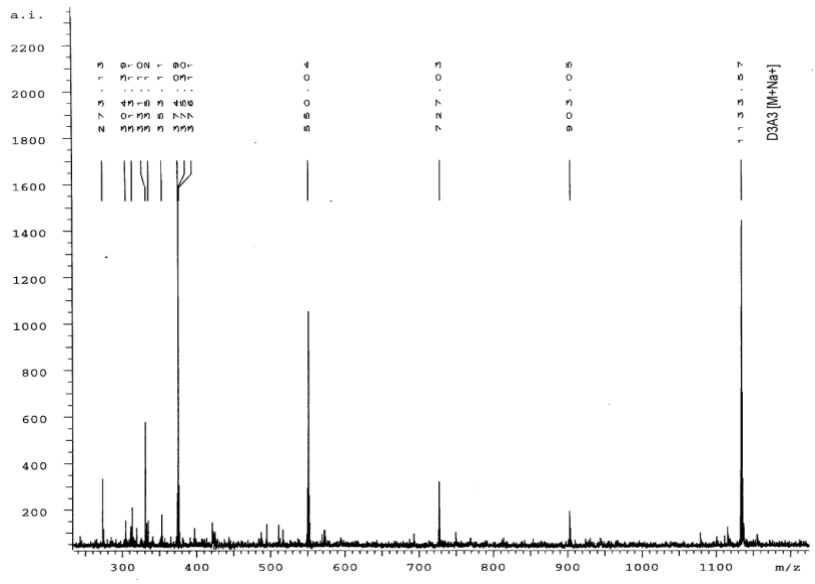

Fig. S-1. MALDI-TOF MS of D_3A_3 taken after 10 min of incubation with chitinase A at pH 7.4, 37°C. The sodiated molecular ion peak for D_3A_3 appears at m/z = 1133.57. The mass spectrum shows no signals caused by fragments of D_3A_3. The other peaks observed in the mass spectrum are either caused by protein fragments or the matrix.

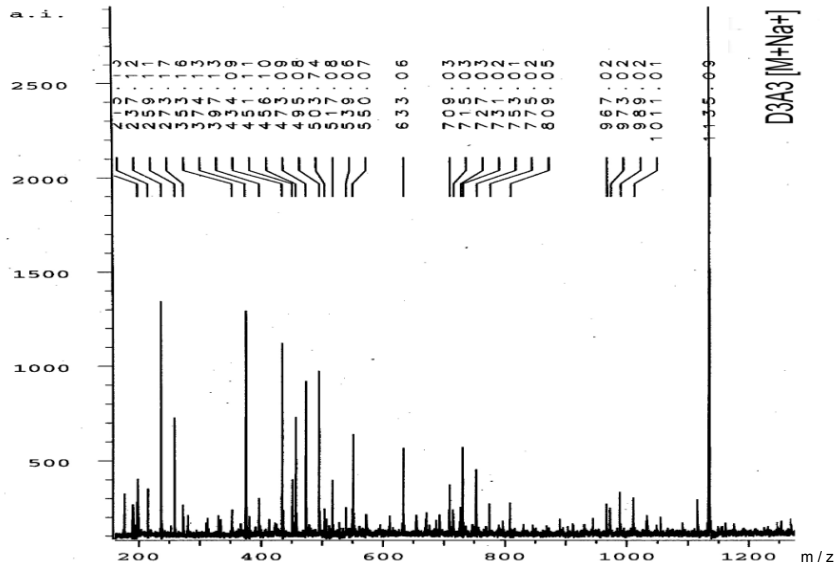

Fig. S-2. MALDI-TOF MS of D_3A_3 taken after 10 min of incubation with chitinase B at pH 5.5. The sodiated molecular ion peak for D_3A_3 labelled at m/z = 1135.09 is expected to appear at m/z = 1133.44. The difference of 1.65 Da is caused by the imprecise automatic labelling routine of the software for the analysis of the mass spectra. The mass spectrum shows no signals caused by fragments of D_3A_3. The other peaks observed in the mass spectrum are either caused by protein fragments or the matrix.

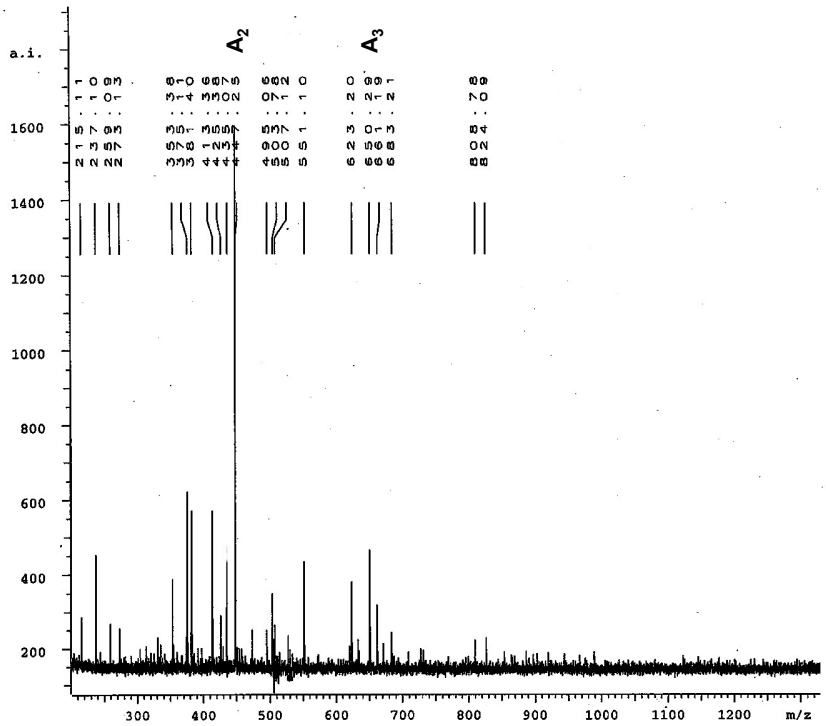

Fig. S-3. MALDI-TOF MS of A_6 after incubation with ChiB for 10 min at 37°C, pH5.5. Fragment ions are detected at 650.3 (A_3) and 447.3 (A_2).

Partially Acetylated Chitooligosaccharides Bind with High-affinity to the 39-kDa Human Cartilage Glycoprotein (HC gp-39)

Sven Bahrke[1], Jón M. Einarsson[2], Jóhannes Gislason and Martin G. Peter[*1]

[1] *Institute of Chemistry, University of Potsdam, Karl-Liebknecht-Str. 25, D-14476 Potsdam, Germany*

[2] *Genis ehf, Myrargata 2, IS-101 Reykjavik, Iceland*

---

* Corresponding Author: Fax: +49-331-977-5300, e-mail address: Martin.Peter@uni-potsdam.de

Abbreviations

A: 2-acetamido-2-deoxy-D-glucopyranosyl unit; AMCR: 3-acetylamino-6-aminoacridine, as well as the tag unit derived by reductive amination of sugars with AMCR; ChO: chitooligosaccharide; D: 2-amino-2-deoxy-D-glucopyranosyl unit; DP: degree of polymerisation; F: fluorescence intensity; F_A: mole fraction of A units; GPC: gel permeation chromatography; HPCEC: high performance cation exchange chromatography; i.u.: intensity units; K_d: equilibrium dissociation constant; MS^2: tandem mass spectrometry; vMALDI-LQT: vacuum matrix-assisted laser desorption ionisation linear quadrupole ion trap.

Abstract

Aminoglucan oligosaccharides (i.e. chitooligosaccharides, ChO's) bind with high affinity to the chitolectin HC gp-39. based on changes of the intrinsic tryptophan fluorescence of the protein, it was found that, for a series of DP6 homologs, the affinity increased with increasing F_A (mole fraction of GlcNAc units): the K_d values were 13.7 µM for $(GlcNAc)_6$ (= A_6), 40.6 µM for $(GlcN)_2(GlcNAc)_4$ (= D_2A_4), 51.1 µM for $(GlcN)_3(GlcNAc)_3$ (= D_3A_3), and 420 µM for $(GlcN)_6$. The results are consistent with a model describing hydrophobic and hydrogen bond interactions contributed by the subsites of the carbohydrate-binding domain.

Keywords: affinity binding, chitin, HC gp-39, oligosaccharides, YKL-40

1. Introduction

The human chondrocyte glycoprotein 39 (HC gp-39, also named YKL-40) is a member of the recently discovered chitolections.[1,2] The protein is over expressed in several severe diseases like rheumatoid and osteo-arthritis1, fibrotic liver[3], and some types of cancer.[4] Recently, it was demonstrated that HC gp-39 as well as a homologous protein isolated from molluscs[5] regulate the synthesis of extra cellular matrix in mammalian chondrocytes.[6] HC gp-39 is a potent growth factor, inducing cell proliferation through activation of protein kinase mediated signalling pathways.[7] It possesses 53% sequence homology with human chitotriosidase. The crystal structure of HC gp-39 shows a $(\beta\alpha)_8$ TIM barrel[8,9], which is typically also found in family 18 chitinases. The catalytic site of these enzymes contains the highly conserved motif DxxDxDxE.[10] A similar motif occurs also in HC gp-39, where Glu is replaced by Leu, and Asp by Ala to give the catalytically inactive assembly DxxDxAxL. Indeed, HC gp-39 shows high affinity binding chitooligosaccharides, with K_d = 331 μM for A_4 and 6.7 μM for A_6.[9] Binding of $(GlcNAc)_8$ to HC gp-39 induces a conformational change in the protein, suggesting that ChO's may be involved in regulatory signal transduction cascades.[9]

The natural ligands and mechanism of action of HC gp-39 are still unknown. The protein could interact with heparin sulfate, hyaluronan, chitooligomers that synthesized as primers for hyaluronan biosynthesis, an/or the chitobiose-cores of *N*-glycans (for a review, see [11]). It was reported recently that partially acetylated aminoglucan oligosaccharides, i.e. hetero-chitooligosaccharides, composed of GlcN (= D) and GlcNAc (= A) possess a therapeutic potential in patients suffering from inflammatory polyarthritis.[12] Furthermore, certain partially acetylated ChO's are strong competitive, mechanism based inhibitors of chitinase A[13,14] and B[15,16] from *Serratia marcescens* (see also Chapter 2, Offprint *Heterochitooligomers as Inhibitors of Chitinase A and B from Serratia marcescens*). Thus, it was of interest to investigate the mode of binding of hetero-ChO's to the chitinase-homologous, but catalytically inactive HC gp-39 and to compare the data with the binding of ChO's to chitinase A and B.

2. Materials and Methods

2.1. Chemicals:

Chitohexaose (D_6) and hexa-*N*-acetylchitohexaose (A_6) were from Seikagaku (Tokyo, Japan). HC gp-39 from articular chondrocytes was from Quidel (San Diego, CA, USA). All other chemicals were from Sigma-Aldrich (Munich, Germany).

2.2 Chromatography:

GPC: Biogel P4 (fine grade; Bio-Rad, Munich, Germany), column size 2.5 cm i.d. × 200 cm, sample loading 50 mg; mobile phase: 0.05 M ammonium acetate buffer pH 4.2, flow rate 25 mL × h^{-1}; detector RID 6A (Shimadzu, Duisburg, Germany). HPCEC: HPLC instrument with UV detector (Jasco, Gross-Umstadt, Germany), Resource S column (Pharmacia, Uppsala, Sweden), bed volume 1 mL, sample loading 1 mg; mobile phase: hydrochloric acid pH 3.5, sodium chloride gradient 0 – 1 M, flow rate 1 mL × min-1, detection at 210 nm.

2.3 Preparation of Heterochitooligosaccharides:

Enzymatic digestion of chitosan with a chitinolytic enzyme from *Penicillium sp.* afforded a crude mixture of chitooligosaccharides.[17] Ultra filtration over 0.5 and 3.0 kDa cut-off membranes resulted in a fraction containing mainly oligomers of DP3 to DP15. Separation by GPC was followed by HPCEC of selected GPC fractions to give homologs of heterochitooligomers, which were desalted by dialysis (Floatalyzer, SpektraPor, Germany).

2.4. Mass spectrometry:

Oligosaccharides were derivatized by reductive amination with 3-acetylamino-6-aminoacridine[18] and *N*-deuterioacetylation of the GlcN (= D) units with d_6-deuterioacetic anhydryde as described previously.[19] For mass spectrometry, a solution of the sample in acetonitrile / water (0.5 µL) was mixed on the target with 0.5 µL of the matrix solution (15 mg × mL^{-1} of 2,5-dihydroxybenzoic acid in 30 % aqueous methanol) and the drop was dried under a gentle stream of air. Qualitative analysis of the oligosaccharides and derivatives was carried out in the positive ion mode on a Reflex II mass spectrometer (Bruker Daltonik, Bremen, Germany). All spectra were measured in the reflector mode using external calibration (Angiotensin II).[17] MALDI ion trap mass spectra were recorded on a Finnigan vMALDI-LQT Mass Spectrometer (Thermo GmbH, Dreieich, Germany). The experiments were performed by selection of the monoisotopic peak of an AMCR-tagged

chitooligosaccharide, using a window width of 1.5 mass units. The centre of the window was carefully adjusted to allow for exclusion of ions of ^{13}C isotopic as well as of dideuterioacetylated molecules. MS^2 spectra were recorded at high resolution in the normal as well as in the zoom mode. Due to higher sensitivity, the normal mode was preferred for MS^3 spectra.[19]

2.5 Determination of binding affinity[9]:

HC gp39 was dissolved in 25 mM Tris-HCl buffer, pH 7.4, containing 1 mM dithiothreitol, to give a final protein concentration of 1.00 µM. The oligosaccharides were dissolved in amounts corresponding to the desired final concentration in the same buffer. For binding assays, protein and sugar solutions were brought to 25°C for 15 min in a shaking water bath. After mixing 50 µL of protein and 50 µL of the sugar solution, the mixtures were incubated for 7 min at 25°C. The fluorescence (excitation 295 nm, emission 340 nm) was read in a Perkin-Elmer LS 50B fluorescence spectrometer (Perkin-Elmer, Überlingen, Germany). All data were calculated as the means of triplicate experiments. $F - F_0$ was plotted versus the concentration of the oligosaccharide and the data were fitted by non-linear regression to a one-site saturation model employing SigmaPlot® software to obtain binding isotherms. The affinity was calculated from the equation:

$$F - F_0 = B_{max} \times c / (K_d + c)$$

where B_{max} is the fluorescence intensity of HC gp39 under saturation conditions and K_d is the equilibrium dissociation constant. For correlation of K_d and F_A, the K_d values found with a series of DP6 homologs (D_6, D_3A_3, D_2A_4 and A_6) were plotted against the number of A units and the data were fitted by non-linear regression (software SigmaPlot®) to a two-parameter hyperbolic decay:

$$K_d = a \times b / (b + n)$$

where n is the number of GlcNAc residues.

3. Results

The MALDI-TOF mass spectrum of commercial A_6 (Fig. 1) shows a major peak at m/z = 1259.35 $[M+Na]^+$. The ions at m/z = 1241.31 and 1275.30 are assigned to $[M-H_2O+Na]^+$ and $[M+K]^+$, respectively. Traces of sodiated ions of homologs are detected at m/z = 853.22 (A_4), 1056.29 (A_5), and 1462.35 (A_7). The sample contains also some unidentified impurities which are not considered further.

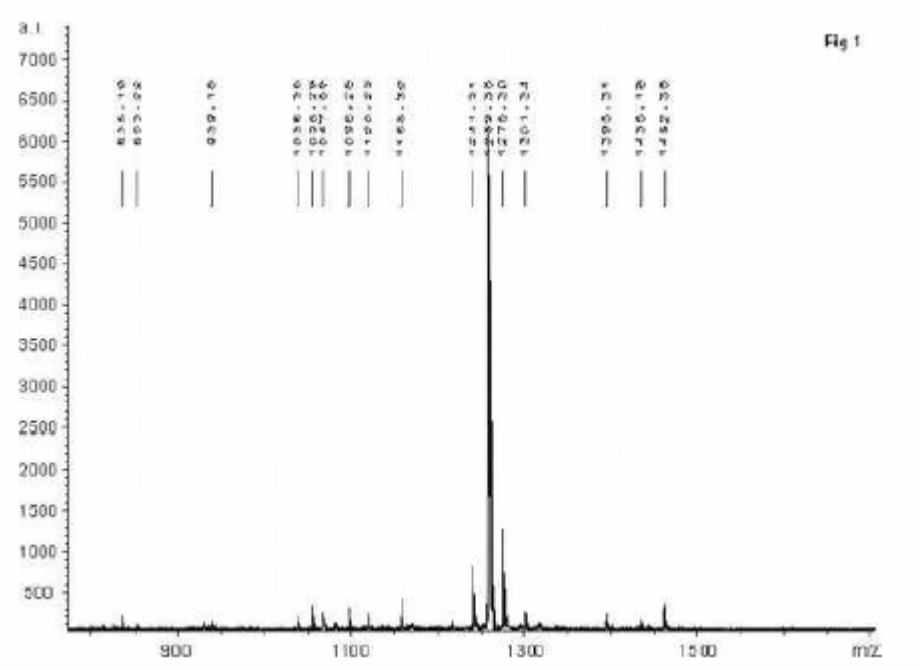

Fig. 1. MALDI-TOF mass spectrum of commercial A_6.

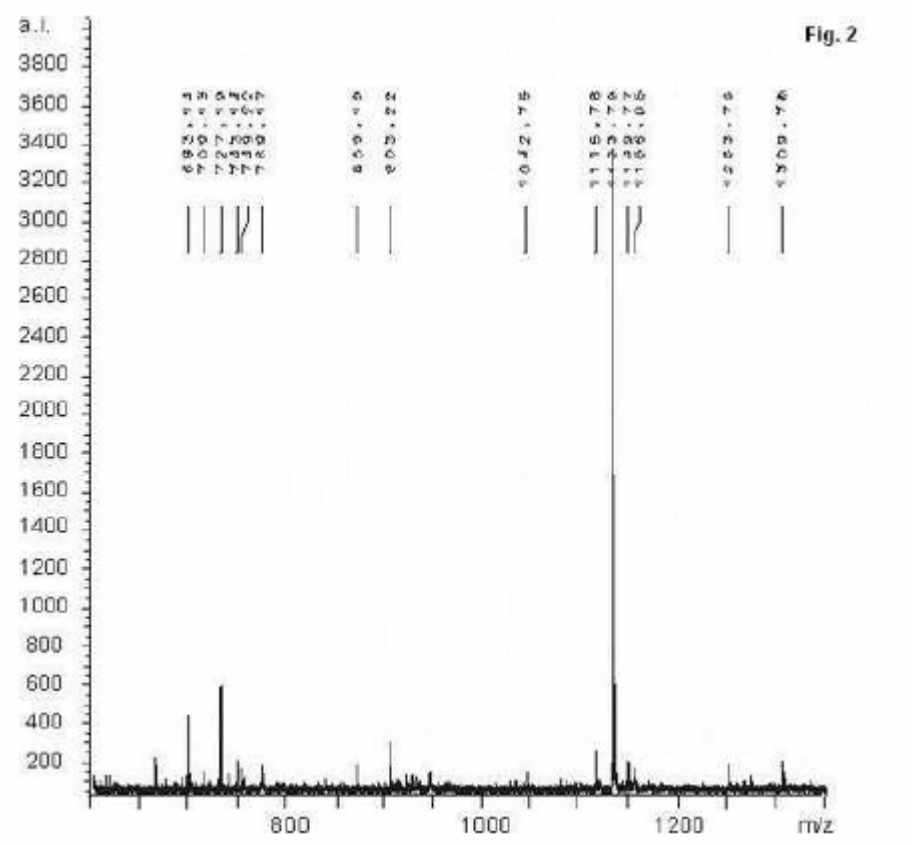

Fig. 2. MALDI-TOF mass spectrum of chitoheterooligomer D_3A_3.

Heterochitooligosaccharides were isolated from an enzymatic digest of chitosan by a sequence of ultrafiltration, GPC, and HPCEC.[19] The composition was determined by MALDI-TOF MS, as shown for the hexamer D_3A_3 fraction in Fig. 2. The main component, appears at m/z = 1133.79 $[M+Na]^+$, together with the corresponding peaks of the dehydrated and potassiated ions. Besides unidentified impurities, low intensity peaks of other oligomers are also detected at m/z = 656.67 (A_3) $[M+K]^+$, 727.19 (D_3A_1) $[M+Na]^+$, 769.17 (D_2A_2) $[M+Na]^+$, 869.19 (D_4) $[M+K]^+$.

Reductive amination with AMCR introduces the reducing-end tag. Fragmentation produces predominantly tag-bearing Y-ions[20], thus allowing easy oligosaccharide sequencing.[17] Furthermore, per-*N*-deuterioacetylation introduces an increment of 45.03 a.m.u. for each GlcN (= D) residue, thus allowing quantitative determination of the isomer composition.[19] Besides D_3A_3, hexamer D_2A_4 was isolated and the sequences of isomers were determined by mass spectrometry (Table 1). A fraction containing undecamer D_5A_6 was not analysed with respect to the composition of isomers. The results shown in Table 1 reveal that D_3A_3 is composed of two isomers in nearly equal amounts while the lower homolog D_2A_4 contains six isomers with DADAAA as the main component.

Table 1

Composition of hexamers

Homolog	**F_A**	**Composition**
D_6	0.00	DDDDDD
D_3A_3	0.50	DDADAA (51%); DADDAA (49%)
D_2A_4	0.67	DDAAAA (4%); ADDAAA (12%)
		DADAAA (43%); AADDAA (12%)
		DAADAA (9%); ADADAA (19%)
A_6	1.00	AAAAAA

The affinities of non-covalent complexes between ChO's and HC gp-39 were analysed by measuring the difference of the intrinsic tryptophan fluorescence of the protein in the absence resp. presence of a ligand.[9,21] Fitting of the data to a one-binding-site model by non-linear regression yields saturation curves shown in Fig. 3. Transformation of the data yields the equilibrium dissociation constants listed in Table 2. Within the series of hexamers, the values for the dissociation constants decrease with increasing F_A. The undecamer homolog D_5A_6 showed higher affinity than the hexamer of the same number of A units, A_6.

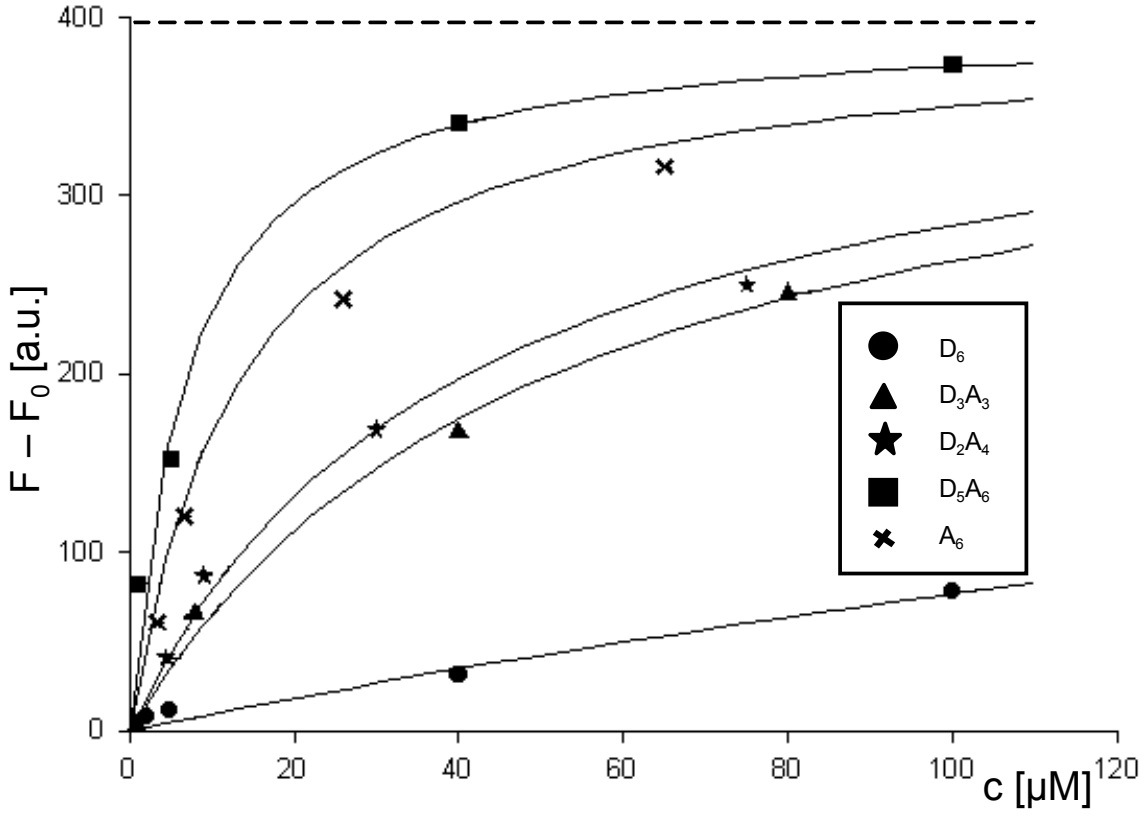

Fig. 3 Plot of fluorescence versus concentration for ChO hexamers.

Table 2

K_d concentrations of homologous hexamers.

Homolog	**K_d [µM]**
D_6	419.9
D_3A_3	51.1
D_2A_4	40.6
A_6	13.7
D_5A_6	6.9

Correlation of K_d concentrations with the number of A residues yields a hyperbolic function:

$$K_d = a \times b / (b + n)$$

Where a = 419.932; b = 0.3839; n = number of A residues (Fig. 4).

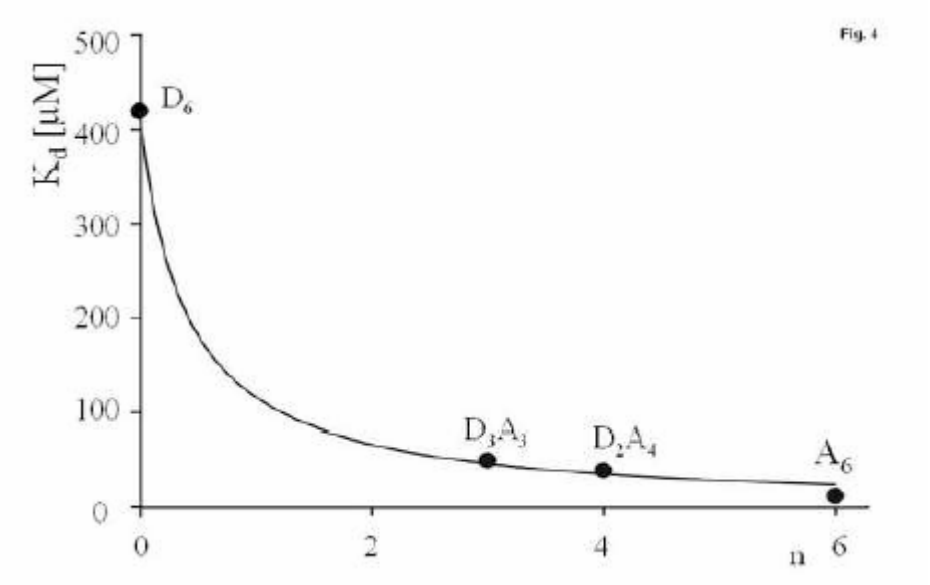

Fig. 4. Correlation of K_d with the number of A residues (n) in hexamers: $K_d = 419.932 \times 0.3839 / (0.3839 + n)$ (R^2: 0.9986).

4. Discussion

Houston et al. reported for HC gp-39 K_d concentrations of 6.7 µM for A_6 and 331 µM for A_4.[9] We found similar K_d for A_6 (13.7 µM) while the affinity of D_6 (K_d = 420 µM) is even lower than for the tetramer A_4. Partially acetylated hexamers containing four resp. three GlcNAc residues show much higher affinity than the tetramer A_4 and only slightly lower affinity than the hexamer A_6.

For the explanation of these findings one have to take a detailed look on the subsites of HC gp-39 on one hand and on the isomer composition of the homologs employed for the affinity studies on the other hand (Table 1). According to Fusetti et al.[8] and Houston et al.[9], the binding site of HC gp-39 is divided into subsites –6 to +3 (based on crystallographic data obtained from complexes of HC gp-39 with A_4, A_6, and A_8). Alternatively, two distinct binding sites (-6 to –5 and –3 to +3) with a distance of 10 Å are discussed in the literature.[22] In this case chitin homooligomers of DP > 3 occupy the binding site containing subsites –3 to +3, whereas dimers and trimers occupy the distal binding site containing subsites –6 to –5. The present results show a two times higher affinity of D_5A_6 than for the homooligomers of equal number of A residues, A_6. This finding indicates that chitooligomers of DP > 6 extend beyond subsite –3 occupying both binding sites at the same time.

A

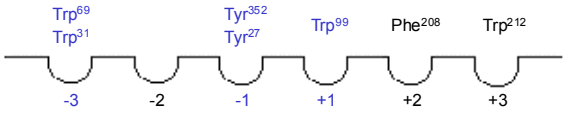

D_6

01 D – D – D – D – D – D
02 D – D – D – D – D – D
03 D – D – D – D – D – D
04 D – D – D – D – D – D
05 D – D – D – D – D – D
06 D – D – D – D – D – D

D_3A_3

11 D – D – A – D – A – A
12 D – D – A – D – A – A
13 D – D – A – D – A – A
14 D – D – A – D – A – A
15 D – D – A – D – A – A
16 D – D – A – D – A – A

21 D – A – D – D – A – A
22 D – A – D – D – A – A
23 D – A – D – D – A – A
24 D – A – D – D – A – A
25 D – A – D – D – A – A
26 D – A – D – D – A – A

D_2A_4

31 D – D – A – A – A – A
32 D – D – A – A – A – A
33 D – D – A – A – A – A
34 D – D – A – A – A – A
35 D – D – A – A – A – A
36 D – D – A – A – A – A

41 A – D – D – A – A – A
42 A – D – D – A – A – A
43 A – D – D – A – A – A
44 A – D – D – A – A – A
45 A – D – D – A – A – A
46 A – D – D – A – A – A

B

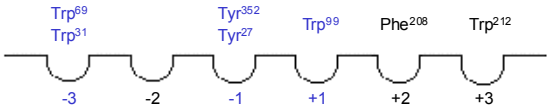

D_2A_4

51 D – A – D – A – A – A
52 D – A – D – A – A – A
53 D – A – D – A – A – A
54 D – A – D – A – A – A
55 D – A – D – A – A – A
56 D – A – D – A – A – A

61 A – A – D – D – A – A
62 A – A – D – D – A – A
63 A – A – D – D – A – A
64 A – A – D – D – A – A
65 A – A – D – D – A – A
66 A – A – D – D – A – A

71 D – A – A – D – A – A
72 D – A – A – D – A – A
73 D – A – A – D – A – A
74 D – A – A – D – A – A
75 D – A – A – D – A – A
76 D – A – A – D – A – A

81 A – D – A – D – A – A
82 A – D – A – D – A – A
83 A – D – A – D – A – A
84 A – D – A – D – A – A
85 A – D – A – D – A – A
86 A – D – A – D – A – A

A_6

91 A – A – A – A – A – A
92 A – A – A – A – A – A
93 A – A – A – A – A – A
94 A – A – A – A – A – A
95 A – A – A – A – A – A
96 A – A – A – A – A – A

Fig. 5 A, B Alignment of the sequences of the hexamers D_6, D_3A_3, D_2A_4, and A_6 to the carbohydrate binding domain of HC gp-39. Only the core subsites (-3 to +3) are regarded. It is

assumed that subsites < -3 and > +3 do not contribute significantly to binding. Monomer units extending beyond subsites –3 to +3 are coloured red, monomer units aligned to subsites –3, -1 and +1, which mainly contribute to hydrophobic interactions, are coloured blue. Each alignment is signed with a code. Alignments resulting in two hydrophobic interactions are signed with an underlined code, alignments resulting in three hydrophobic interactions are signed with a double underlined code. Alignments -3→ +3 are signed with a blue code number.

The K_d concentrations observed for the series of DP 6 homologs (D_6, D_3A_3, D_2A_4, andA_6) are consistent with a model of the carbohydrate binding site of HC gp-39 which contains 6 core subsites (-3 to +3), with hydrophobic amino acid residues positioned at subsites –3 (Trp^{31}), -1 (Trp^{352}), and +1 (Trp^{99}). Minor hydrophobic interactions are measured for subsites +2
(Phe^{208}) and +3 (Trp^{212}). Furthermore, hydrogen bonding contributes to binding at all subsites, but predominately at the –1 subsite (for a detailed discussion, see [9]).
The model which had been developed originally for chitinases can also be applied to HC gp-39.
Figure 5 summarizes all alignments -3 → -1 to -1 → +3 of the isomers of the DP6 homologs D_6, D_3A_3, D_2A_4, and A_6.
Hexamer A_6 binds with a maximum of hydrophobic and hydrogen bonding interactions while the protein complex with D_6 will be the least favoured. For isomer DDADAA of hexamer D_3A_3, only alignment **12** results in three hydrophobic interactions, which is consequently favourable over all other alignments. Nevertheless, also alignments resulting in two or even one hydrophobic interaction contribute to the overall affinity of the isomer DDADAA. Moreover, only alignment **14** results in the highest number of hydrogen bondings as all monomer residues are aligned to a subsite of HC gp-39. These considerations result in different evaluation methods of the data from the alignment of the isomers. Table 3 compares four different ways of evaluation.

1. All different alignments (-3 → -1 to -1 → +3) of a sequence are regarded. The number of hydrophobic interactions between A units and subsites –3, -1 and +1 are counted, summed up for each isomer, and weighted by the contribution of the isomer to the amount of the homolog. Finally the weighted hydrophobic interactions of the isomers are summed up to the overall number of hydrophobic interactions of the homolog.

2. Only alignment are regarded, for which three or minimum two hydrophobic interactions are obtained.
3. Only alignments are regarded, for which minimum three hydrophobic interactions are obtained.
4. Only one alignment per isomer is regarded. It is the alignment, for which all monomer units of the isomer are aligned to one of the subsites -3 to +3.

Table 3
Summary of the different evaluation methods 1 – 4 for the alignment of the sequences of DP6 hexamers D_6, D_3A_3, D_2A_4 and A_6.

DP6 homolog	**rel. affinity [%] (fluorescence assay)**	**rel. affinity [%] (evaluation method 1)**	**rel. affinity [%] (evaluation method 2)**	**rel. affinity [%] (evaluation method 3)**	**rel. affinity [%] (evaluation method 4)**
A_6	100	100	100	100	100
D_2A_4	34	45	70	25	51
D_3A_3	27	17	46	17	27
D_6	3	0	0	0	0

Table 3 shows that all four evaluation methods result in the correct order of affinities $D_6 < D_3A_3 < D_2A_4 < A_6$. Methods 3 (only alignments are regarded, for which minimum three hydrophobic interactions are obtained) and 4 (only one alignment per isomer is regarded; it is the alignment, for which all monomer units of the isomer are aligned to one of the subsites -3 to +3) reflect the results of the fluorescence assays best: Method 3 gives a deviation of 27 % for D_2A_4 and 37 % for D_3A_3. Method 4 gives a deviation of 50 % for D_2A_4 and 0 % for D_3A_3. Methods 1 and 2 show higher deviations especially for D_2A_4.
In conclusion, for isomer DDADAA of hexamer D_3A_3, only alignment **12** results in three hydrophobic interactions and is therefore favourable over all other alignments according to evaluation method 3. As no alignment of DADDAA results in three hydrophobic interactions, this isomer does not significantly contribute to the affinity of D_3A_3 to HC gp-39.
Evaluation method 4 gives the same result regarding alignments **14** and **24**. With respect to hexamer D_2A_4, three hydrophobic interactions are possible with alignments **32**, **53**, **72** and **82**. The corresponding isomers account for 75 % of the total amount of this mixture of hexamers (Table 1). Evaluation method 4 gives two hydrophobic interactions for alignment **34**, two for alignment **44**, one for alignment **54**, one for alignment **64**, one for alignment **74**, and two for alignment **84**.

The observed K_d concentrations of the hexamers (Table 2) correspond well with the binding model developed for HC gp-39 in analogy to family 18 chitinases.

The increased affinity of the undecamer D_5A_6 compared to the affinity of the hexamer A_6, which contains the same number of A residues, can be only explained by the fact that D_5A_6 covers additional subsites of HC gp-39 beyond subsite –3.

Under the aspect of possibly replacing expensive affinity studies on HC gp-39 by affinity studies on chitinase A from *Serratia marcescens*, we now compare HC gp-39 with chitinase A as HC gp-39 is highly homologous to human family 18 chitinases.[9] Figure 6 shows that the carbohydrate binding sites of HC gp-39 and ChiA are similar.

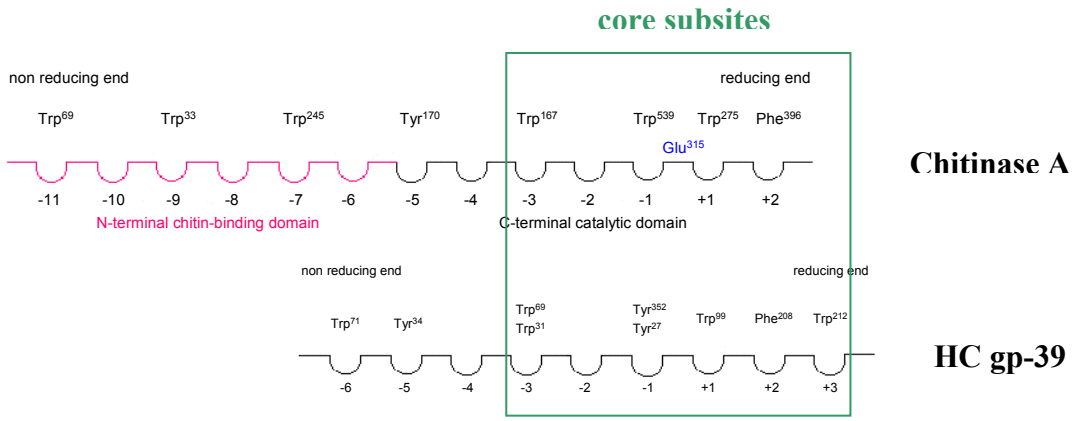

Fig. 6 Comparison of the binding sites of chitinase A and HC gp-39. Subsites –3 to +3 are the core subsites for HC gp-39 whereas for chitinase A the core subsites are –3 to +2.

Subsites –3 to +2 form the core of the carbohydrate binding site of ChiA with predominating hydrophobic amino acid residues positioned at subsites –3 (Trp^{167}), -1 (Trp^{539}), and +1 (Trp^{275}). An additional hydrophobic amino acid residue is positioned at subsite +2 (Phe^{396}). Subsites beyond –3 are shallow. As for HC gp-39, the carbohydrate binding site of ChiA is an open groove so that ChO chains might extend beyond subsite +2. Therefore, the alignments shown for HC gp-39 in Figure 5 are equally valid for ChiA giving the same qualitative results employing evaluation method 3. For evaluation method 4, the results differ slightly as most stable alignments require the –4 → +2 binding mode for DP6 oligomers resulting in a favourable affinity of DADDAA over DDADAA (for a detailed discussion see Chapter 2, Offprint *Heterochitooligomers as Inhibitors of Chitinase A and B from Serratia marcescens*).

However, the overall order of affinities of DP6 oligomers is unaffected by these minor differences.

In case that affinity studies on chitolectins like HC gp-39 are replaced by affinity studies on ChiA, inactive mutants have to be employed as otherwise affinity patterns are overlaid by stabilities against hydrolysis. Nevertheless inhibition of active ChiA with a series of DP6 homologs gave a first proof of these theoretical thoughts: IC_{50} of D_6 = 2726.4 µM; IC_{50} of D_3A_3 = 19.7 µM; IC_{50} of D_2A_4 = 17.4 µM. The isomeric composition of the heterochitohomologs employed for the blocking of ChiA was the same as for the heterochitohomologs employed for the affinity studies on HC gp-39. A low IC_{50} concentration means a strong inhibitory effect and thus high affinity if hydrolysis is neglected. Therefore reciprocal IC_{50} concentrations allow to estimate the affinities of ChO's to ChiA. The same order of affinities is obtained as for HC gp-39: $D_6 < D_3A_3 < D_2A_4$. In conclusion, inactive ChiA mutants promise to become an excellent model for affinity studies on chitolectins like HC gp-39, which are hardly assessable and therefore expensive.
Under the aspect of possible therapeutic uses of ChO's, the stability of isomers with high affinity to HC gp-39 against hydrolysis in the human body is important. Human chitinases degrade chitinous material in the human body. Up to now HCT[23] and AMCase[24] are described in the literature with HCT being found in the blood stream. Hydrolysis studies on chitinase B from *Serratia marcescens* have model character for the biostability of ChO's in the human body as ChiB and HCT show a high sequence homology of the carbohydrate binding sites (Figure 7).

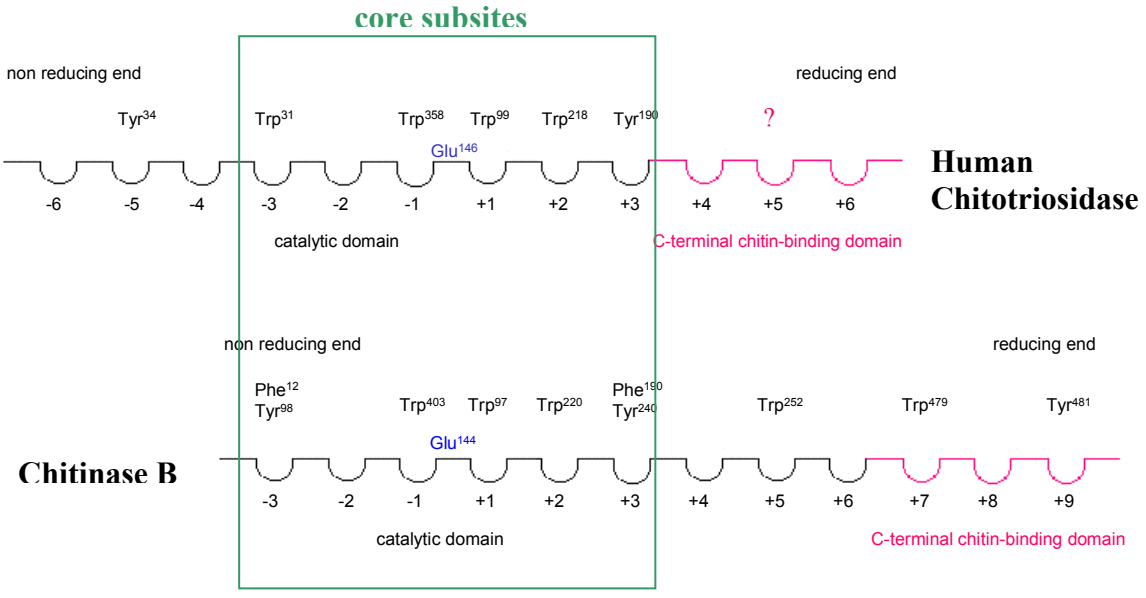

Fig. 7 Comparison of the binding sites of human chitotriosidase and chitinase B. Subsites

–3 to +3 are the core subsites for both, human chitotriosidase and chitinase B.

Calculation of the binding parameters for each subsite of ChiB supports the assumption that the occurrence of a D residue at subsites –2 and –1 is unfavourable, while occurrence of an A residue at subsites –3, -1 and +1 is favourable for stabilisation of the enzyme-ligand complex.[25] ChiB binds chitooligomers with the non-reducing end preferentially located at the –2 subsite. The carbohydrate binding site is locked beyond subsite –3. In order to cleave a glycosidic bond, chitinase B requires binding of an A residue at subsite –1, while the preference at subsite -2 is less pronounced.[26] Binding of a D residue at subsite –1 is non-productive and actually results in competitive inhibition of the enzyme.[16] Hydrolysis occurs processively at every second glycosidic bond, provided that an A residue is positioned at subsite –1.[26] The possibilities for hydrolysing the hexamers are shown in Figure 8.

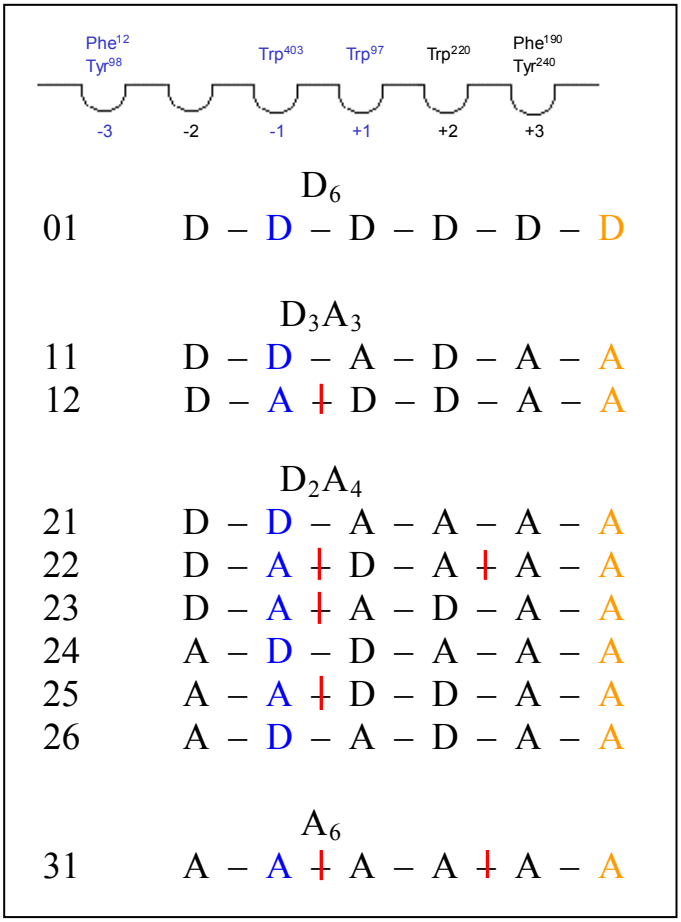

Fig. 8 Hydrolysis of the isomers of the DP6 homologs D_6, D_3A_3, D_2A_4 and A_6 with chitinase B. Monosaccharide residues complexed with subsite –1 are in blue colour, red lines mark scissile bonds. Two red lines in the same sequence indicate that processive hydrolysis occurs. Monosaccharide units that extend beyond subsite +3 are in red colour.

Glycosidic bonds are cleaved with relative rates AA-X : DA-X : YD-X ca. 3 : 1 : 0 whereas bonds of the type YYA-X are cleaved very slowly (Y = D or A).[26] It appears, that the most stable hexamer of D_3A_3 will be DDADAA, whereas the most stable isomers of D_2A_4 will be DDAAAA, ADDAAA, and ADADAA. Table 4 summarizes the relative amounts and the number of hydrophobic interactions with HC gp-39 of the isomers that are stable against hydrolysis with ChiB.

Table 4
Summary of the relative amounts and the number of hydrophobic interactions with HC gp-39 of the isomers that are stable against hydrolysis with chitinase B.

Homolog	**Sequence of the isomer**	**Relative share of the homolog**	**Number of hydrophobic interactions with HC gp-39**	**Alignment (binding mode)**
D_6	DDDDDD	100%	0	any
D_3A_3	DDADAA	51%	3	-3 → +1
D_2A_4	DDAAAA	4%	3	-3 → +1
	ADDAAA	12%	2	-3 → -1 -3 → +1 -3 → +2 -3 → +3
	ADADAA	19%	3	-3 → +1

In conclusion, quantitative analysis of oligosaccharide sequences present in mixtures of isomers, determination of binding affinities, and application to knowledge on the properties of carbohydrate binding proteins allows a prediction of the isomer which will be most useful for further biochemical and pharmacological studies. It can be concluded from Table 6 that in the case of DP6 isomers one isomer is a promising candidate: ADADAA. This D_2A_4 isomer shows three hydrophobic interactions with HC gp-39, is stable against hydrolysis with ChiB / HCT, and is obtained in a yield of 19 % from a mixture of D_2A_4 isomers prepared by enzymatic hydrolysis of chitosan. Generally, D_2A_4 isomers are favoured over D_3A_3 isomers as they show higher affinities / lower K_d concentrations.

Acknowledgements: This work was founded in part, by the Deutsche Forschungsgemeinschaft, grant no. Pe 264/18-1 and 2.

References

1. B. E. Hakala, C. White, A. D. Reklies, *J. Biol. Chem.* **1993**, *268*, 25803 – 25810.
2. G. Bleau, F. Massicotte, Y. Merlen, C. Boisvert, *EXS* **1999**, *87*, 211 – 221.
3. J. S. Johansen, P. Christoffersen, S. Moller, P. A. Price, J. H. Henriksen, C. Garbarsch, F. Bendtsen, *J. Hepatol.* **2000**, *32*, 911 – 920.
4. J. S. Johansen, B. V. Jensen, A. Roslind, D. Nielsen, P. A. Price, *Cancer Epidem. Biomarkers & Prevention* **2006**, *15*, 194 – 202.
5. F. Badariotti, M. Kypriotou, C. Lelong, M. P. Dubos, E. Renard, P. Galera, P. Favrel, *J. Biol. Chem.* **2006**, *281*, 29583 – 29596.
6. F. De Ceuninck, S. Gaufillier, A. Bonnaud, M. Sabatini, C. Lesur, P. Pastoureau, *Biochem. Biophys. Res. Commun.* **2001**, *285*, 926 – 931.
7. A. D. Recklies, C. White, H. Link, *Biochem. J.* **2002**, *365*, 119 – 126.
8. F. Fusetti, T. Pijning, K. H. Kalk, E.Boss, B. W. Dijkstra, *J. Biol. Chem.* **2003**, *278*, 37753 – 37760.
9. D. R. Houston, A. D. Recklies, J. C. Krupa, D. M. F. van Aalten, *J. Biol. Chem.* **2003**, *278*, 30206 – 30212.
10. D. M. F. van Aalten, D. Komander, B. Synstad, S. Gaseidnes, M. G. Peter, V. G. H. Eijsink, *Proc. Natl. Acad. Sci. USA* **2001**, *98*, 8979 – 8984.
11. J. S. Johansen, *Dan. Med. Bull.* **2006**, *53*, 172 – 209.
12. J. M. Einarsson, J. Gislason, M. G. Peter, S. Bahrke, (**2003**) PCT Int. Appl., pp. 30 (Primex ehf, Iceland), WO 03/026677 A1.
13. N. N. J. Aronson, B. A. Halloran, M. F. Alexyev, L. Amable, J. D. Madura, L. Pasupulati, C. Worth, P. van Roey, *Biochem. J.* **2003**, *376*, 87.
14. N. N. J. Aronson, B. A. Halloran, M. F. Alexyev, X. E. Zhou, Y. Wang, E. J. Meehan, L. Chen, *Biosci. Biotechnol. Biochem.* **2006**, *70*, 243.
15. M. C. Letzel, B. Synstad, V. G. H. Eijsink, J. Peter-Katalinić, M. G. Peter, *Advan. Chitin Sci.* **2000**, *4*, 545 – 552.
16. F. Cederkvist, A. D. Zamfir, S. Bahrke, V. G. H. Eijsink, M. Sørlie, J. Peter-Katalinić, M. G. Peter, *Angew. Chem. Int. Edn.* **2006**, *45*, 2429 – 2434.
17. S. Bahrke, J. M. Einarsson, J. Gislason, S. Haebel, M. C. Letzel, J. Peter-Katalinić, M. G. Peter, *Biomacromol.* **2002**, *3*, 696 – 704.

18. J. Charlwood, H. Birrell, A. Gribble, V. Burdes, D. Tolson, P. Camilleri, *Anal. Chem.* **2000**, *72*, 1453 – 1461.
19. S. Haebel, S. Bahrke, M. G. Peter, *Anal. Chem.* **2007**, *79*, 5557.
20. B. Domon, C. E. Costello, *Glycoconj. J.* **1988**, *5*, 397 – 409.
21. M. R. Efting, *Meth. Enzymol.* **1997**, *278*, 221 – 257.
22. Zaheer-ul-Haq, P. Dalal, N. N. Aronson Jr., J. D. Madura, *Biochem. Biophys. Res. Comun.* **2007**, Article in Press.
23. F. Fusetti, H. von Moeller, D. Houston, H. J. Rozeboom, B. W. Dijkstra, R. G. Boot, J. M. F. G. Aerts, D. M. F. van Aalten, *J. Biol. Chem.* **2002**, *277*, 25537.
24. R. G. Boot, E. F. C. Blommaart, E. Swart, K. Ghauharali-van der Vlugt, N. Bijl, C. Moe, A. Place, J. M. F. G. Aerts, *J. Biol. Chem.* **2001,** 276*,* 6770.
25. P. Sikorski, B. T. Stokke, A. Sørbotten, K. M. Vårum, S. J. Horn, V. G. H. Eijsink, *Biopolym.* **2005**, *77*, 273 – 285.
26. A. Sørbotten, S. J. Horn, V. G. H. Eijsink, K. M. Vårum, *FEBS J.* **2005**, *272*, 538 – 549.

Identification of a High-Affinity Binding Oligosaccharide by (+) Nanoelectrospray Quadrupole Time-of-Flight Tandem Mass Spectrometry of a Non-Covalent Enzyme-Ligand Complex **

F. Henning Cederkvist, Alina D. Zamfir, Sven Bahrke, Vincent G.H. Eijsink, Morten Sørlie, Jasna Peter-Katalinić, and Martin G. Peter*

---

* Dipl.-Chem. S. Bahrke, Prof. Dr. M.G. Peter
Institut für Chemie
Universität Potsdam
P.O. Box 60 15 53
D – 14415 Potsdam
Germany
E-mail: peter@chem.uni-potsdam.de

M.Sc – Biochem. F. Henning Cederkvist***, Prof. Dr. Vincent G.H. Eijsink, Dr. Morten Sørlie
Department of Chemistry,
Biotechnology and Food Science
Norwegian University of Life Sciences
P.O. Box 5003
N - 1432 Ås, Norway

Dr. Alina D. Zamfir***, Prof. Dr. Jasna Peter-Katalinić
Universität Münster
Institut für Medizinische Physik und Biophysik
Robert-Koch-Str. 31
D - 48149 Münster
Germany

** **Abbreviations**: A: 2-acetamido-2-deoxy-D-glucopyranosyl monosaccharide unit, D: 2-amino-2-deoxy D-glucopyranosyl monosaccharide unit in chitooligosaccharides; CID: collision induced dissociation; DP: degree of polymerization; F_A: mole fraction of A units in A_nD_m chitooligosaccharides; nanoESI: nanoelectrospray ionization; QTOF MS: quadrupole time-of-flight mass spectrometer/spectrometry; MS/MS: tandem mass spectrometry; TIC: total ion current

This work was supported by the Deutsche Forschungsgemeinschaft, Sonderforschungsbereich 492, project Z2 to JPK, and grant Pe 264/18-1 to MGP and by the Norwegian Research Council, grant 140497/420 to MS and VGHE.

*** equal contribution

Oligosaccharides are of current interest as targets for the development of novel pharmaceuticals and plant growth regulators[1]. Recently, it was discovered that so called "heterochitooligosaccharides", which are composed of *N*-acetylglucosamine (GlcNAc, or A) and glucosamine (GlcN, or D), possess various biological activities, such as promotion of chondrocyte growth in cell culture and morphogenetic activity in vertebrates, or elicitor action in plants (for a review, see[2]). The entities used for biological studies are usually prepared by enzymatic hydrolysis of the aminoglucan chitosan, obviously yielding intractable, complex mixtures of aminoglucan oligomers which differ in DP, as well as in the mole fraction of A residues (i.e. homologs) and in the sequences of D and A residues (i.e. isomers).

Despite the fact that several protein-ligand complexes containing GlcNAc homooligomers or enzyme inhibitors have been investigated by protein crystallography[3] (see also[2]) and ^{1}H NMR spectroscopy[4], the molecular mechanisms of the biological actions of heterochitooligosaccharides remain essentially unknown. This is due to a lack of structural information and to the fact that pure ligands are not available. One option for obtaining more information is the use of mass spectrometry, which may be employed for detection and chemical/structural analysis of non-covalent protein-carbohydrate complexes. In principle MS-based techniques could provide information on binding stoichiometry and identification of the ligand by fragmentation [5, 6].

We have observed earlier that mixtures of heterochitooligosaccharides of F_A 0.5 and DP 5 and 6 contain inhibitory compounds with high affinity for the chitinolytic enzyme chitinase B (ChiB) from the soil bacterium *Serratia marcescens* [5]. The apparent IC_{50} was ca. 15 μM, using $(GlcNAc)_2$-4-methylumbelliferone as the substrate (K_m of A_2-MU = 30 μM[7]). Assuming that not all components are inhibitors, the IC_{50} of

the active component must, indeed, be lower, possibly in the sub-μM range. The challenge was now to identify a high-affinity binding ligand from a complex oligosaccharide mixture.

We report on the specificity and stoichiometry of enzyme-ligand recognition, using (+) nanoESI MS for analysis of the non-covalent protein-ligand complex formation. A novel methodology based on nanoESI QTOF CID MS/MS was employed for *top-down* sequencing of the complex generating fragment ions of the bound ligand. The MS-based method provides an excellent tool for the study of biological complexes[6, 8-9], especially when protein crystallography or NMR spectroscopy cannot be applied.

The choice for nano ESI QTOF MS was guided by the advantage of using low flow rates for sample infusion[10] in a hybrid system which combines the simplicity of a quadrupole for precursor ion selection with the ultrahigh efficiency of an orthogonal acceleration TOF mass analyzer. This system is capable to achieve simultaneous detection of all analyte (MS mode) and fragment ions (MS/MS mode) across the full mass range with a resolution above 5000 (FWHM). Unlike scanning instruments, the TOF performs parallel detection of all masses within a spectrum at high sensitivity and acquisition rates. This characteristic is important for following the kinetics of noncovalent interactions since each spectrum is representative for the infused sample composition at that point of time.

A fraction of heterochitooligosaccharides was separated by gel permeation chromatography from an enzymatic hydrolyzate of chitosan, as described previously [11]. Analysis by (+) nanoESI MS revealed a mixture of nine components, oligomers and homologs (Figure 1 and Table 1). Major components were D_1A_3 and D_2A_3 while the

remaining were present in minor amounts (< 10%). In fact, the mixture is even more complex, as any of the heterooligomers could contain different isomers.

(Insert Fig. 1 and Table 1)

The (+) nanoESI-QTOF mass spectrum of ChiB (Figure 2) revealed the presence of four pseudomolecular ions at charges 13-16, confirming, after deconvolution, the molecular weight[12] of 55,338.36 ± 2.07 Da. Oligomerization of the protein was not observed in the nanoESI MS.

(Insert Fig. 2)

A mass spectrum recorded after incubation of ChiB with the chitooligosaccharide mixture for 5 min revealed, besides ChiB, two additional molecular species at charge states 13-16, shifted to masses of 56,288.05 Da (major) and 56,124.25 Da (minor) (Fig. 3a) indicating complexation of ChiB with the oligomers D_2A_3 and D_1A_3, respectively. In Fig. 3b depicting a spectrum of the complex measured after 90 min incubation, a third peak appeared at 55,923.23 Da corresponding to the ChiB-D_1A_2 complex. The mass spectrum recorded after incubation of ChiB with the chitooligosaccharide mixture for 180 min revealed that the relative ion abundance of the complexes did not change, documenting a kinetic equilibrium of the species in the solution. The binding of the trisaccharide D_1A_2 to ChiB is interesting since this compound was present at low levels (≤ 5%) in the original mixture (Fig. 1 and Table 1).

a)

(Insert Fig. 3a and 3b)

A top-down CID experiment was carried out on the ChiB-D_2A_3 complex, using the B^{14+}molecular ion at *m/z* 4021.51 as a precursor. Two events, namely the breakdown of the protein-sugar complex and fragmentation of the released D_2A_3 pentasaccharide ligand took place (Fig. 4a).

Permutation of the monosaccharide units in the D_2A_3 pentamer shows that 10 isomeric sequences exist (Table 3). The CID MS/MS provided diagnostic fragment ions (Table 2) that can be used to deduce the sequence of the pentameric ligand that was stably bound to ChiB. According to the fragmentation pattern obtained in the top-down experiment, sequence **1** and **3** must be excluded, since no A_3 triad fragment ions were obtained in the top-down spectrum. In contrast, the A_3 fragment ion and its dehydrated counterpart are present in the MS/MS of the D_2A_3 in the heterosaccharide mixture (Fig. 4b and Table 2). This strongly suggests that the enzyme selectively binds from the mixture a D_2A_3 isomer which does not contain A-A-A sequence. Sequence **2** is excluded since D_2A_1 and D_2A_2 fragment ions cannot arise from this isomer. The presence of the highly abundant fragment ion at *m/z* 526.23 corresponding to D_2A_1 excludes the sequences **5** and **7**. Furthermore, D_1A_3 cannot be formed from the sequences **6**, **8** and **9**.

The ion at *m/z* 323.25 could principally be formed as a diad D_2 from sequences **1**, **3** and **9**. Comparison between Fig. 4 a and b shows, however, that in the top-down spectrum this ion is low abundant and unlike the pentamer sequenced from the mixture it is not accompanied by further loss of H_2O. This feature along with the clear-cut exclusion of the sequences **1**, **3** and **9**, demonstrates that the D_2 fragment is generated in the top-down experiment either via the loss of an acetyl group from other fragment ions, e.g. from the abundant D_1A_1 ion or by 0, 4 ring cleavage of the DA fragment in either of the monosaccharides. The sequences **4** and **10** are indistinguishable by tandem MS as no diagnostic fragment ion supporting one or the other can be obtained. However detailed studies of the degradation of chitosans by ChiB have shown that isomer **4** is an excellent substrate for ChiB (cleavage between A-A and D-A-D)[13], leading to the conclusion that the pentamer that is stably bound to ChiB must be the pentasaccharide **10,** D-A-D-A-A.

(Insert Fig. 4a, 4b, Table 2 and Table 3)

The first investigation of an enzyme-oligosaccharide non-covalent complex by ESI-MS was reported by Ganem for lysozyme and the GlcNAc homohexamer [14]. In the present study, complex mixtures of chitooligosaccharides were analyzed with respect to their binding to the chitinolytic enzyme ChiB. The structure and mechanism of catalysis of this chitinase are known in much detail. The enzyme is a family 18 *exo*-glycosidase, possessing three sugar binding sites, numbered –1 to –3, at the glycon side[3a,15]. Hydrolysis of GlcNAc homooligomers yields A_2 (substrate DP = 4) and A_3 (substrate DP ≥ 4), the latter being cleaved further into A_1 and A_2 [7,16]. Catalysis proceeds *via* anchimeric nucleophilic assistance of the acetyl group to give an oxazolinium ion as the crucial intermediate. Therefore, the presence of an A residue at the glycon (– 1) subsite of the fissile bond was shown to be required for an efficient hydrolysis[3a,13,16]. No exclusive structural requirement is to be posed for the first aglycon subsite (+1), whereas the –2 glycon subsite has a strong, but not absolute preference for an A residue[13].

K_m values of chitinases have been determined with A_n homooligomers in few cases. They are generally in the low μM range for the hexamer of GlcNAc and roughly one order of magnitude higher for the lower oligomers[17]. The K_m of heterochitooligosaccharides in not known for any of chitinases. In our study, we have found that ChiB binds particular components out of a complex mixture of chitooligosaccharides. The results allow conclusions with respect to specificity of ligand selection from complex mixtures and stoichiometry of binding. Formation of non-covalent complexes occurs fast with the penta- and tetramers, D_1A_3 and D_2A_3, while binding of the trimer D_1A_2 is observed only after prolonged incubation. This, *a priori*, is expected as, in general, the affinity of polysaccharide cleaving enzymes for

oligosaccharides increases with the chain length [18]. On the other hand, detection of the D_1A_2 complex is surprising, as the trimer would bind with lower affinity than the higher oligomers. Most likely, the concentration of D_1A_2 could be increased during the incubation because of productive binding of other oligomers and even of D-A-D-A-A (**10**) which could be cleaved very slowly at the fissile -A-D- glycosidic bond (Fig. 5). On the other hand, high-affinity, non-productive binding of sequence **10** (occupying subsites –3 to +2, i.e. with a D position in the crucial –1 subsite and a highly favorable A in the subsite –2) would result in the observed[5]. competitive enzyme inhibition because the crucial oxazolinium ion intermediate cannot be formed.

(Insert Fig. 5)

In summary, we have shown that 1) a carbohydrate binding enzyme selects high affinity binding ligands from a complex mixture of closely related oligosaccharides, 2) identification of a heterooligosaccharide in a non-covalent protein-ligand complex is feasible by top-down sequencing in combination with sequence analysis of components present in the original complex mixture, 3) the mechanism of enzyme inhibition is conclusively deduced by combination of knowledge on the mechanism of catalysis and structure identification of a high-affinity binding oligosaccharide ligand. NanoESI-MS and fragmentation of the specific sequence of the bound ligand by CID MS/MS is presented as a powerful tool of general applicability in functional proteomics and glycomics.

Experimental Section

For preparation of the chitooligosaccharides, the lyophilized product (F_A 0.63; 2.16 g) of an enzymatic hydrolyzate of chitosan[11] was dissolved in 180 mL of a 0.05 M ammonium acetate buffer, pH 4.2. The solution was filtered sequentially through a 0.8

μm, and a 0.2 μm cellulose acetate membrane (Schleicher & Schuell), and a 3000 Da cut-off membrane (Amicon), and the filtrate was lyophilized. The residue was subjected to gel permeation chromatography (GPC) on a 5 cm i. d. x 200 cm Biogel P4 column (fine grade; BioRad), mobile phase 0.05 M ammonium acetate buffer, adjusted with 0.23 M acetic acid to pH 4.2; flow rate 60 mL × h^{-1}; detector: Shimadzu RID 6A. Fractions of 20 mL were collected, appropriately combined, then concentrated to a small volume by rotary evaporation, and finally lyophylized.

Wild-type chitinase B (ChiB) from *Serratia marcescens* was overexpressed in *Escherichia coli* and purified as described elsewhere [7].The protein was > 95 % pure, as determined by SDS- PAGE. Stock solutions of ChiB and heterochitooligosaccharides were mixed and diluted while stirring at 800 rpm, 37°C to a final concentration of 3.0 pmol × μL^{-1} of protein and 60 pmol × μL^{-1} of oligosacharide in 10 mM ammonium acetate, pH 6.0. Oligosaccharide concentrations were calculated using an average molecular mass of 1000 Da. Aliquots were collected after 5, 30, 90, and 180 min and kept on ice prior to MS analysis. Calibration of mass spectra was achieved with a mixture of dextran oligomers, obtained from the Department of Physical Chemistry, University of Wageningen, Netherlands. The reference sample provided ions over a broad *m/z* range, as required for MS and CID MS/MS *top-down* analysis.

MS experiments were conducted in the positive ion mode on an orthogonal hybrid quadrupole time-of-flight mass spectrometer (QTOF Micromass, Manchester, U.K.) equipped with a nanoelectrospray (nanoESI) ion source positioned in the Micromass Z-spray geometry. The QTOF mass spectrometer was interfaced to a PC computer, running the MassLynx software to control the instrument, and to acquire, process and deconvolute the mass spectra. ESI capillary, sampling cone potentials, and the desolvation gas were optimized to promote an efficient ionization, hinder the *in*

source fragmentation, and ensure a maximal ion transfer into the MS quadrupole analyzer. For all experiments the ion source temperature was set at 80 °C and the desolvation gas was used at a 50 l/h flow-rate. The ESI-QTOF-MS system was programmed to record the MS and MS/MS signal at a scan speed of one scan per 2.1 s.

Top-down analysis of the protein-ligand complex was performed by CID at low energy, using argon as a collision gas. The top-down experiment started by tuning the instrument for assessing the possibility to isolate the precursor ion: LM and HM of the quadrupole for isolation set to 6 and 8 respectively, ion acceleration voltage and collision gas pressure set to 0. Ten MS/MS scans were acquired under these conditions, and the ion at *m/z* 4021.51 was detected isolated as a single peak in the tandem mass spectrum. For fragmentation by top-down sequencing, the gas pressure was set to 10 p.s.i. and the ion acceleration energy was stepwise increased during continuous signal acquisition. The spectra combined across the TIC recorded for different energies below 7-8 eV show that no complex dissociation occurred. At 8eV collision energy in the product ion spectrum the abundant $[M+14H]^{14+}$ precursor ion at *m/z* 4021.51, the low abundant $[M+13H]^{13+}$ protein ion at *m/z* 4257.59 and peaks at low *m/z* values corresponding to the detached intact D_2A_3, its sodiated and dehydrated forms were detected. The sequencing of the ligand was obtained by adjusting the gas pressure to 12 p.s.i (P_{lab}) and long (2850 scans) signal acquisition at 9-10 eV for generating large (tetramer) and medium size (trimer) fragment ions and 15 eV (approximately 50 scans) respectively to induce severe fragmentation for generating dimer fragments. In Figure 4a by summing all 2850 scans acquired at collision energies between 8 and 15 eV and 10-12 p.s.i. Ar pressure all fragment ions generated by the succession of the induced dissociation events are displayed in a single spectrum.

[1] B. Ernst, G. W. Hart, P. Sinaÿ, P., Eds., *Carbohydrates in Chemistry and Biology*, Part II, Vol. 4: Lectins and Saccharide Biology. Weinheim: Wiley-VCH, **2002**.

[2] M. G. Peter, in: *Biopolymers, Vol. 6: Polysaccharides II* (A. Steinbüchel, Ed.), Weinheim: Wiley-VCH, **2002**, pp. 481 – 574.

[3] a) D. M. F. van Aalten, D. Komander, B. Synstad, S. Gaseides, M. G. Peter, V. G. H. Eijsink, *Proc. Natl. Acad. Sci. U.S.A*., **2001**, *98*, 8979-8984; b) Y. Papanikolau, G. Prag, G. Tavlas, C. E. Vorgias, A. B. Oppenheim, K. Petratos, *Biochemistry.* **2001**, *40***,** 11338-11343; c) D. R. Houston, K. Shiomi, N. Arai, S. Omura, M. G. Peter, A. Turberg, B. Synstad, V. G. H. Eijsink, D. M. F. van Aalten, *Proc. Natl. Acad. Sci., U.S.A.,* **2002**, *99***,** 9127-9132; d) E. Bokma, H. J. Rozeboom, M. Sibbald, B. W. Dijkstra, J. J. Beintema, *Eur. J. Biochem*., **2002**, *269*, 893-901; e) F. V. Rao, D. R. Houston, R. G. Boot, J. Aerts, S. Sakuda, D. M. F. van Aalten, *J. Biol. Chem.*, **2003**, *278*, 20110-20116; f) D. R. Houston, A. D. Recklies, J. C. Krupa, and D. M. F. van Aalten, *J. Biol. Chem*., **2003**, *278*, 30206–30212; g) G. Vaaje-Kolstad, A. Vasella, M. G. Peter, C. Netter, D. R. Houston, B. Westereng, B. Synstad, V. G. H. Eijsink, D. M. F. van Aalten, *J. Biol. Chem.*, **2004**, *279*, 3612-3619.

[4] a) T. Ikegami, T. Okada, M. Hashimoto, S. Seino, T. Watanabe, M. Shirakawa, *J. Biol. Chem.,* **2000**, *275*, 13654-13661; b) A. Germer, C. Mügge, M. G. Peter, Antje Rottmann, E. Kleinpeter, *Chem. Eur. J.,* **2003**, *9*, 1964 - 1973.

[5] M. C. Letzel, B. Synstad, V. G. H. Eijsink, J. Peter-Katalinić, M. G. Peter, *Advan. Chitin Sci.*, **2000**, *4*, 545-552.

[6] W. Wang, E. N. Kitova, J. S. Klassen, *Anal. Chem*., **2003**, *75*, 4945-4955.

[7] M. B. Brurberg, I. F. Nes, and V. G. H. Eijsink,

[8] S. A. Hofstadler, R. H. Griffey, *Chem. Rev*., **2001**, *101*, 377-390.

[9] A.J.R. Heck, R.H.H. van der Heuvel, *Mass Spectrom. Rev*., **2004**, *23*, 368-389.

[10] K. Benkestock, G. Sundqvist, P.O. Edlund, J.J. Roeraade, *J. Mass Spectrom.,* **2004**, *39*, 1059-1067.

[11] S. Bahrke, J. M. Einarsson, J. Gislason, S. Haebel, M. C. Letzel, J. Peter-Katalinić, M. G. Peter, *Biomacromolecules*, **2002**, *3*, 696-704.

[12] M. B. Brurberg, V. G. H. Eijsink, A. J. Haandrikman, G. Venema, I. F. Nes. *Microbiology*, **1995**, *141*, 123-131.

[13] A. Sørbotten, S. J. Horn, V. G. H. Eijsink, K. M. Vårum, *FEBS J*., **2005**, *272*, 538–549.

[14] B. Ganem, *J. Am. Chem. Soc.* **1991**, *113*, 7818-7819.

[15] D. M. F. van Aalten, B. Synstad, M. B. Brurberg, E. Hough, B. W. Riise, V. G. H. Eijsink, R. K. Wierenga, *Proc. Natl. Acad. Sc. USA,* **2000**, *97*, 5842-5847.

[16] K. Suzuki, N. Sugawara, M. Suzuki, T. Uchiyama, F. Katouno, N. Nikaidou, T. Watanabe, *Biosci. Biotechnol. Biochem*., **2002**, *66*, 1075-1083.

[17] a) E. Bokma, T. Barends, A. C. Terwisscha van Scheltinga, B. W. Dijkstra, J. J. Beintema, *FEBS Lett.,* **2000**, *478*, 119-122; b) T. Hollis, Y. Honda, T. Fukamizo, E. Marcotte, P. J. Day, J. D. Robertus, *Arch. Biochem. Biophys,.* **1997**, *344*, 335-342.

[18] E. W. Thomas, J. F. McKelvy, N. Sharon, *Nature*, **1969**, *222*, 485-486.

Legends for Figures

F.H. Cederkvist, A.D. Zamfir, S. Bahrke, V. G.H. Eijsink, M. Sørlie, J. Peter-Katalinić, M. G. Peter*

Identification of a High-Affinity Binding Oligosaccharide by (+) Nanoelectrospray Quadrupole Time-of-Flight Tandem Mass Spectrometry of a Non-Covalent Enzyme-Ligand Complex

Figure 1. (+) NanoESI QTOF MS of the chitooligosaccharide fraction used for incubation with ChiB. Solvent: 10 mM ammonium acetate/formic acid pH 6.0; average sample concentration 2 pmol/µl; capillary nanoESI voltage 900 V; sampling cone potential 30-40 V.

Figure 2. (+) NanoESI QTOF MS of ChiB. Solvent: 10 mM ammonium acetate/formic acid pH 6.0; concentration 3 pmol/µl; capillary nanoESI voltage 1kV; sampling cone potential 80-100 V; A_n: $[M+nH]^{n+}$ ion of ChiB.

Figure 3. (+) NanoESI QTOF MS of the ChiB /chitooligosaccharide incubation mixture. Solvent 10 mM ammonium acetate/formic acid pH 6.0; capillary ESI voltage 1.0 kV; sampling cone potential 100 V; incubation at 37°C. A) after 5 min incubation; B) after 90 min incubation; A_n = $[M+nH]^{n+}$ ion of ChiB (calculated: 55,338.1); B_n = $[M+nH]^{n+}$ ion of ChiB-D_2A_3 (calculated: 56,287.5); C_n = $[M+nH]^{n+}$ ion of ChiB-D_1A_3 (calculated: 56,128.6); D_n = $[M+nH]^{n+}$ ion of ChiB-D_1A_2 (calculated: 55,923.3).

Figure 4. a) *Top-down* analysis by CID MS/MS of the ChiB-D_2A_3 non-covalent complex detected as $[M+14H]^{14+}$ ion at *m/z* 4021.51. Solvent 10 mM ammonium acetate/ammonia pH 6.0; incubation 90 min at 37°C; capillary nanoESI voltage 1.0 kV; sampling cone potential 100 V; signal acquisition 100 min, 2850 scans over collision energies within 8-15 eV; collision gas pressure P_{lab}=10-12 p.s.i.; Inset: zoomed out of the (350-975) *m/z* range. b) CID MS/MS of the singly charged ion at *m/z* 950.71 of D_2A_3 present in the original heterooligosaccharide mixture; solvent: 10 mM ammonium acetate/formic acid pH 6.0; concentration 2 pmol/μl; capillary nanoESI voltage 900 V; sampling cone potential 30 V; collision energy 30-50 eV. Collision gas pressure: P_{lab}=15 p.s.i.

Figure 5. Structure of D-A-D-A-A (**10**), mechanism of glycoside bond hydrolysis by family 18 chitinases, and competitive inhibition by nonproductive binding of **10**.

Tables

F.H. Cederkvist, A.D. Zamfir, S. Bahrke, V. G.H. Eijsink, M. Sørlie, J. Peter-Katalinić, M. G. Peter*

Identification of a High-Affinity Binding Oligosaccharide by (+) Nanoelectrospray Quadrupole Time-of-Flight Tandem Mass Spectrometry of a Non-Covalent Enzyme-Ligand Complex

Table 1. Oligomers and homologs present in the heterochitooligosaccharide fraction

m/z	**assignment**
407.22 $[M\text{-}H_2O+2H]^{2+}$	A_4
526.32 $[M\text{-}H_2O+2H]^{2+}$	D_4A_2
586.37 $[M+H]^+$; 608.46 $[M+Na]^+$	D_1A_2
628.39 $[M+H]^+$; 650.37 $[M+Na]^+$	A_3
747.50 $[M+H]^+$; 729.47 $[M\text{-}H_2O+H]^+$	D_2A_2
789.48 $[M+H]^+$; 811.49 $[M+Na]^+$	**D_1A_3**
908.62 $[M+H]^+$; 890.73 $[M\text{-}H_2O+H]^+$	D_3A_2
950.59 $[M+H]^+$; 972.60 $[M+Na]^+$; 475.79 $[M+2H]^{2+}$; 466.77 $[M\text{-}H_2O+2H]^{2+}$	**D_2A_3**
1111.73 $[M+H]^+$; 556.36 $[M+2H]^{2+}$	D_3A_3

Table 2. Assignment of peaks detected in *top-down* CID MS/MS of the ChiB-D_2A_3 complex and of the original D_2A_3 fraction, shown in Fig. 4a and Fig. 4b, respectively.

fragment	in *top-down* CID MS/MS, *m/z*	in CID MS/MS of original D_2A_3, *m/z*
D	not considered	162.10 $[D\text{-}H_2O+H]^+$; 180.12 $[D+H]^+$
A	not considered	204.12 $[A\text{-}H_2O+H]^+$; 222.14 $[A+H]^+$
D_2	323.25	323.25 $[D_2\text{-}H_2O+H]^+$; 305.48 $[D_2\text{-}2H_2O+H]^+$
D_1A_1	365.28; 383.29	347.25 $[D_1A_1\text{-}2H_2O+H]^+$; 365.28 $[D_1A_1\text{-}H_2O+H]^+$; 383.29 $[D_1A_1+H]^+$
A_2	407.32; 447.83 $[A_2+Na]^+$	407.32 $[A_2\text{-}H_2O+H]^+$; 425.33 $[A_2+H]^+$
D_2A_1	508.34; 526.43;	508.42 $[D_2A_1\text{-}2H_2O+H]^+$; 526.43 $[D_2A_1\text{-}H_2O+H]^+$; 544.46 $[D_2A_1+H]^+$
D_1A_2	586.47; 586.48; 608.49 $[D_1A_2+Na]^+$	568.47 $[D_1A_2\text{-}H_2O+H]^+$; 586.48 $[D_1A_2+H]^+$
A_3	absent	628.50 $[A_3+H]^+$;610.46 $[A_3\text{-}2H_2O+H]^+$
D_2A_2	688.49 $[D_2A_2\text{-}HOAc+H]^+$; 729.59; 747.63; 769.64 $[D_2A_2+Na]^+$	687.59 $[D_2A_2\text{-}HOAc+H]^+$; 729.59 $[D_2A_2\text{-}H_2O+H]^+$; 747.63 $[D_2A_2+H]^+$
D_1A_3	789.65; 811.65 $[D_1A_3+Na]^+$;	789.68 $[D_1A_3+H]^+$
D_2A_3	908.76 $[M\text{-}HOAc+H]^+$; 932.76; 950.81; 972.82 $[M+Na]^+$	890.73 $[M\text{-}H_2O\text{-}HOAc+H]^+$; 932.76 $[M\text{-}H_2O+H]^+$; 950.71 $[M+H]^+$

Table 3. The ten possible sequences of D_2A_3

Sequence I.D. Number	Sequence
1	A-A-A-D-D
2	D-A-A-A-D
3	D-D-A-A-A
4	A-A-D-A-D
5	A-D-A-A-D
6	A-A-D-D-A
7	D-A-A-D-A
8	A-D-A-D-A
9	A-D-D-A-A
10	**D-A-D-A-A**

Table of Contents:

F.H. Cederkvist, A.D. Zamfir, S. Bahrke, V. G.H. Eijsink, M. Sørlie, J. Peter-Katalinić, M. G. Peter*

Identification of a High-Affinity Binding Oligosaccharide by (+) Nanoelectrospray Quadrupole Time-of-Flight Tandem Mass Spectrometry of a Non-Covalent Enzyme-Ligand Complex

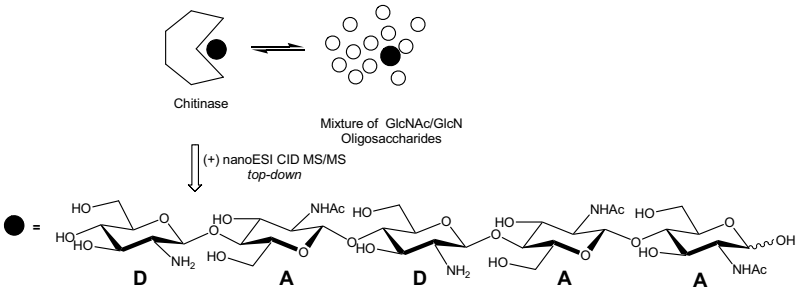

Protein-Ligand Recognition

*F.H. Cederkvist, A.D. Zamfir, S. Bahrke, V. G.H. Eijsink, M. Sørlie, J. Peter-Katalinić, M. G. Peter**

NanoESI CID MS/MS *top-down* analysis of a non-covalent enzyme-ligand complex present in a complex mixture of closely related amino-glucan heterooligo-saccharides and a chitinase revealed that the enzyme binds selectively a unique pentasaccharide composed of three *N*-acetyl-glucosamine and two glucosamine units. The technique employed is of general value for identifications of high-affinity binding ligands in non-covalent enzyme- and receptor-complexes.

F.H. Cederkvist, A.D. Zamfir, S. Bahrke, V. G.H. Eijsink, M. Sørlie, J. Peter-Katalinić, M. G. Peter*

Identification of a High-Affinity Binding Oligosaccharide by (+) Nanoelectrospray Quadrupole Time-of-Flight Tandem Mass Spectrometry of a Non-Covalent Enzyme-Ligand Complex

Keywords:

Enzymes, Hydrolases, Electrospray Ionization Mass Spectrometry, Oligosaccharides, Sequence Determination

Graphical Material

F.H. Cederkvist, A.D. Zamfir, S. Bahrke, V. G.H. Eijsink, M. Sørlie, J. Peter-Katalinić, M. G. Peter*

Identification of a High-Affinity Binding Oligosaccharide by (+) Nanoelectrospray Quadrupole Time-of-Flight Tandem Mass Spectrometry of a Non-Covalent Enzyme-Ligand Complex

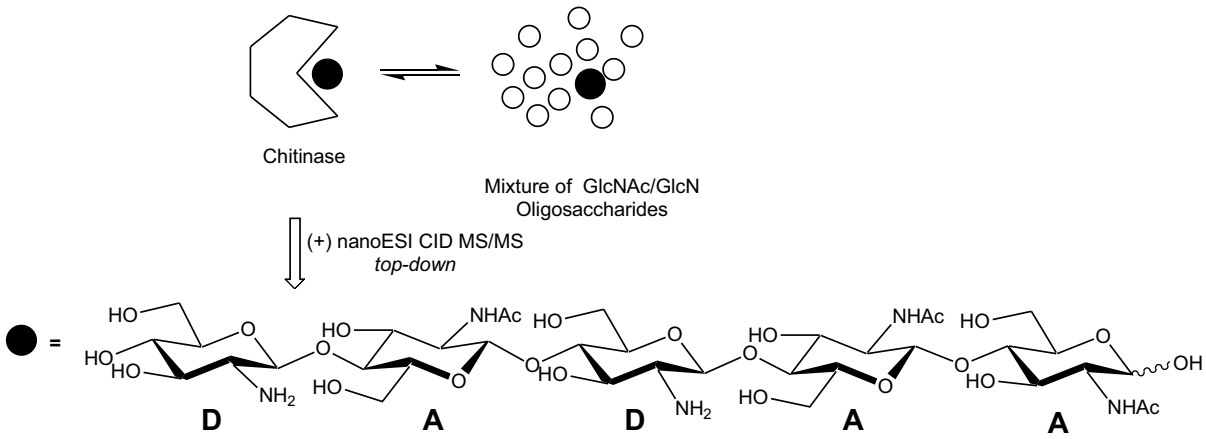

Table of Contents

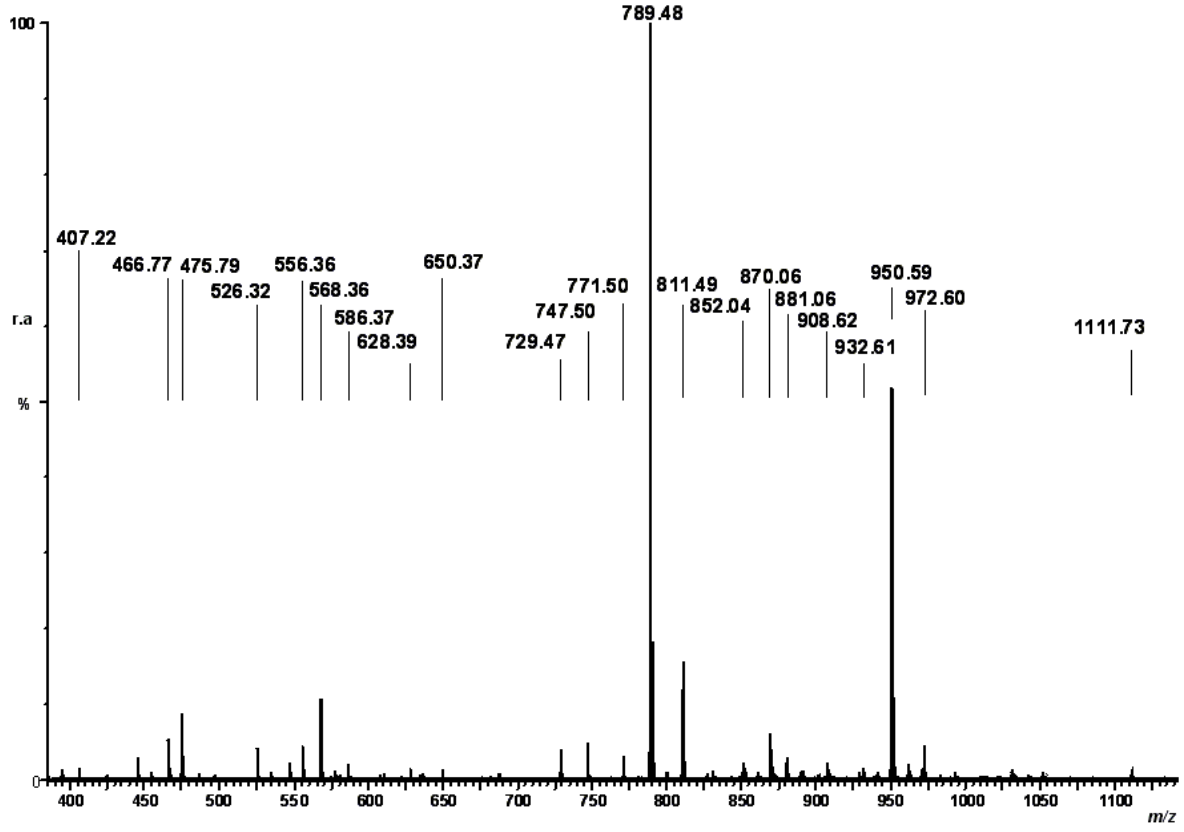

Fig. 1

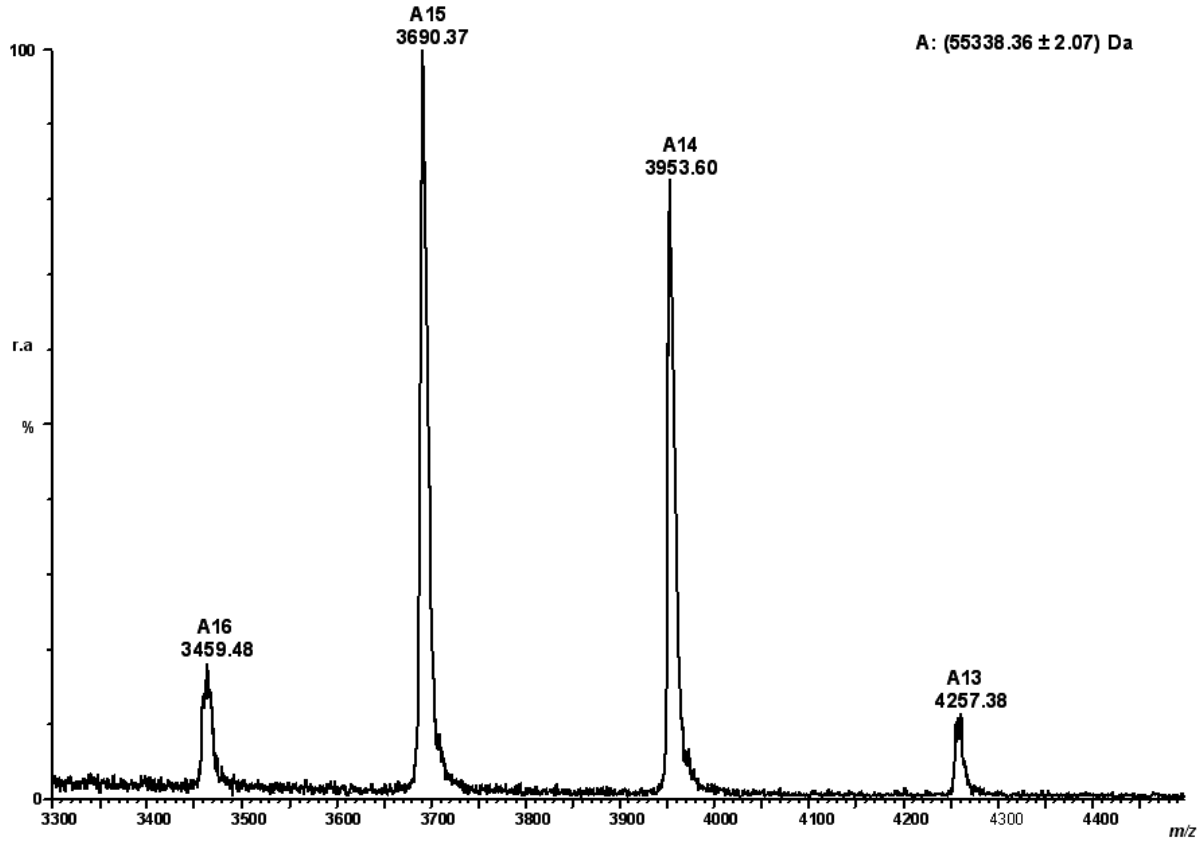
A15
3690.37
A: (55338.36 ± 2.07) Da
A14
3953.60
A16
3459.48
A13
4257.38
100
r.a
%
0
3300
3400
3500
3600
3700
3800
3900
4000
4100
4200
4300
4400
m/z

Fig. 2

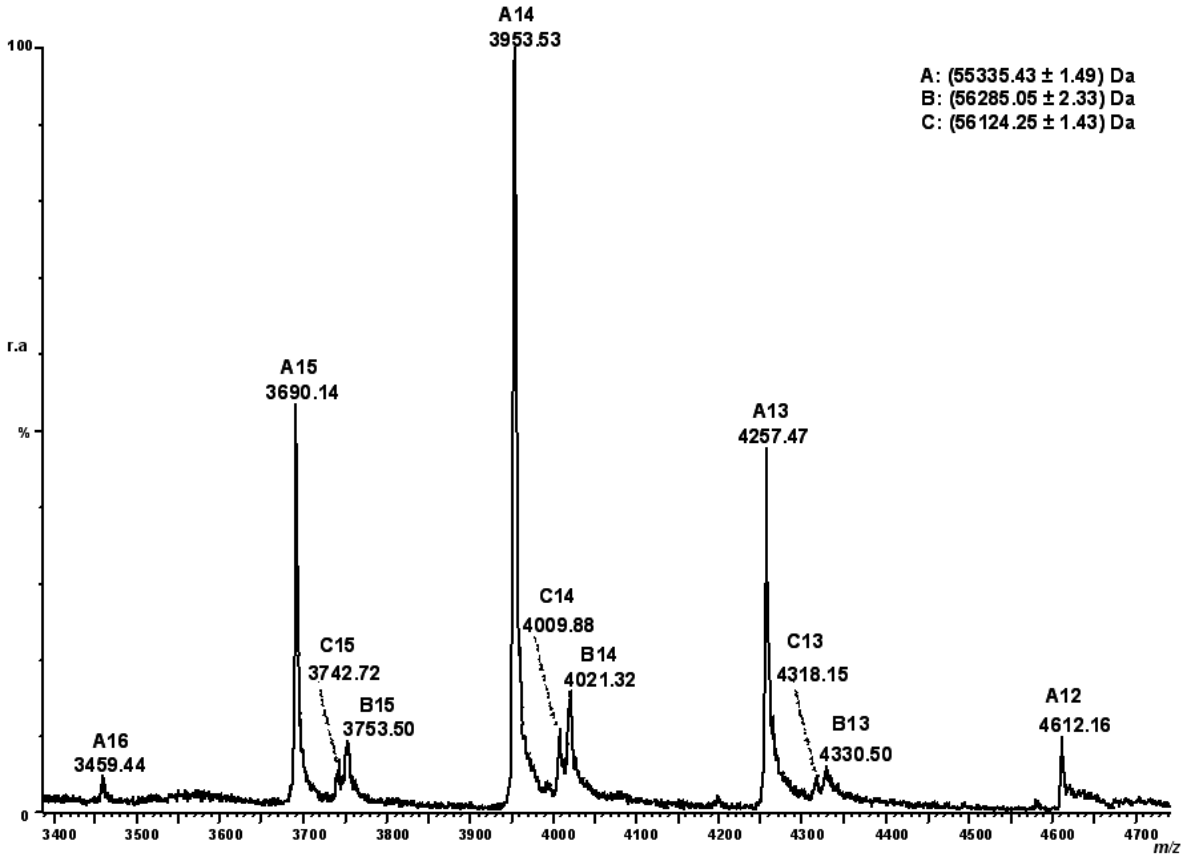
A14
3953.53
A: (55335.43 ± 1.49) Da
B: (56285.05 ± 2.33) Da
C: (56124.25 ± 1.43) Da
A15
3690.14
A13
4257.47
C14
4009.88
C15
3742.72
B14
4021.32
C13
4318.15
B15
3753.50
A12
4612.16
B13
4330.50
A16
3459.44
100
r.a
%
0
3400
3500
3600
3700
3800
3900
4000
4100
4200
4300
4400
4500
4600
4700
m/z

Fig. 3a

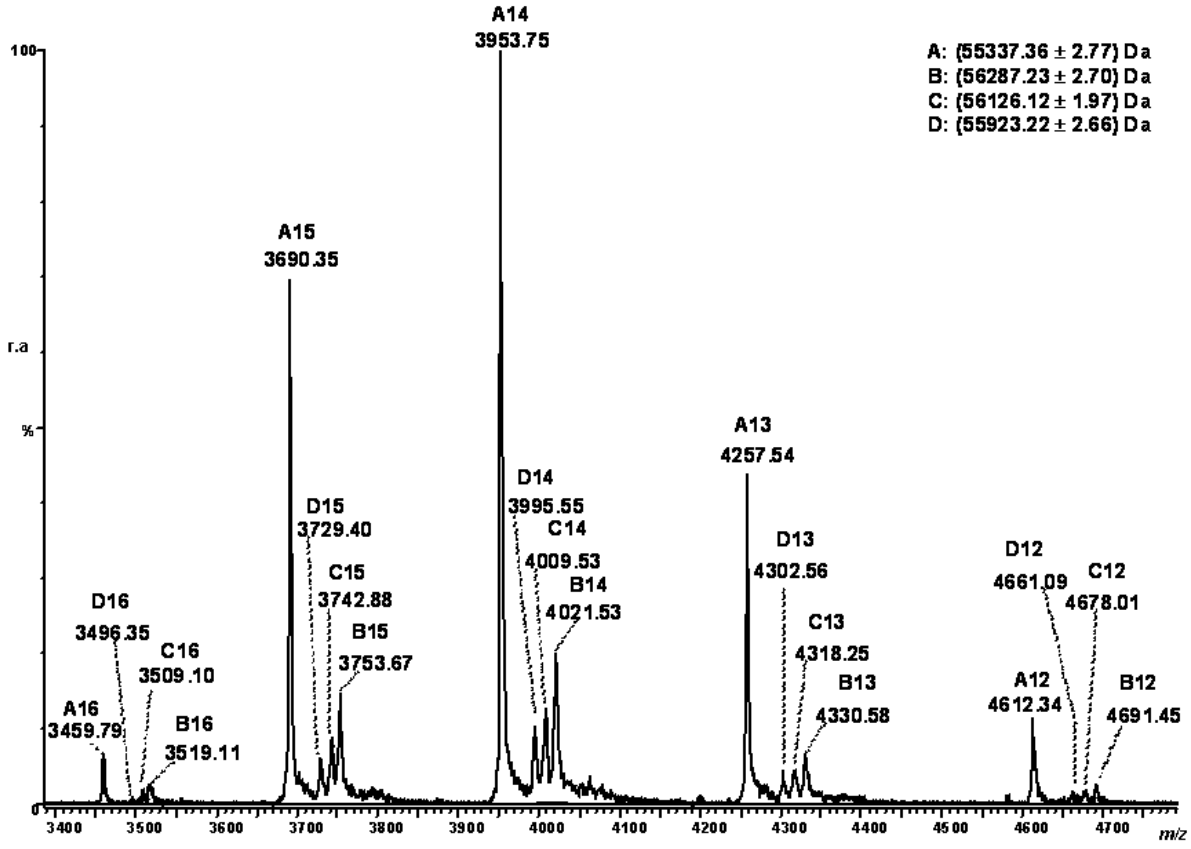
A14
3953.75
A: (55337.36 ± 2.77) Da
B: (56287.23 ± 2.70) Da
C: (56126.12 ± 1.97) Da
D: (55923.22 ± 2.66) Da
A15
3690.35
A13
4257.54
D14
3995.55
D15
3729.40
C14
4009.53
D13
4302.56
D12
4661.09
C12
4678.01
C15
3742.88
B14
4021.53
D16
3496.35
C13
4318.25
C16
3509.10
B15
3753.67
B13
4330.58
A12
4612.34
B12
4691.45
A16
3459.79
B16
3519.11
100
r.a
%
0
3400
3500
3600
3700
3800
3900
4000
4100
4200
4300
4400
4500
4600
4700
m/z

Fig. 3b

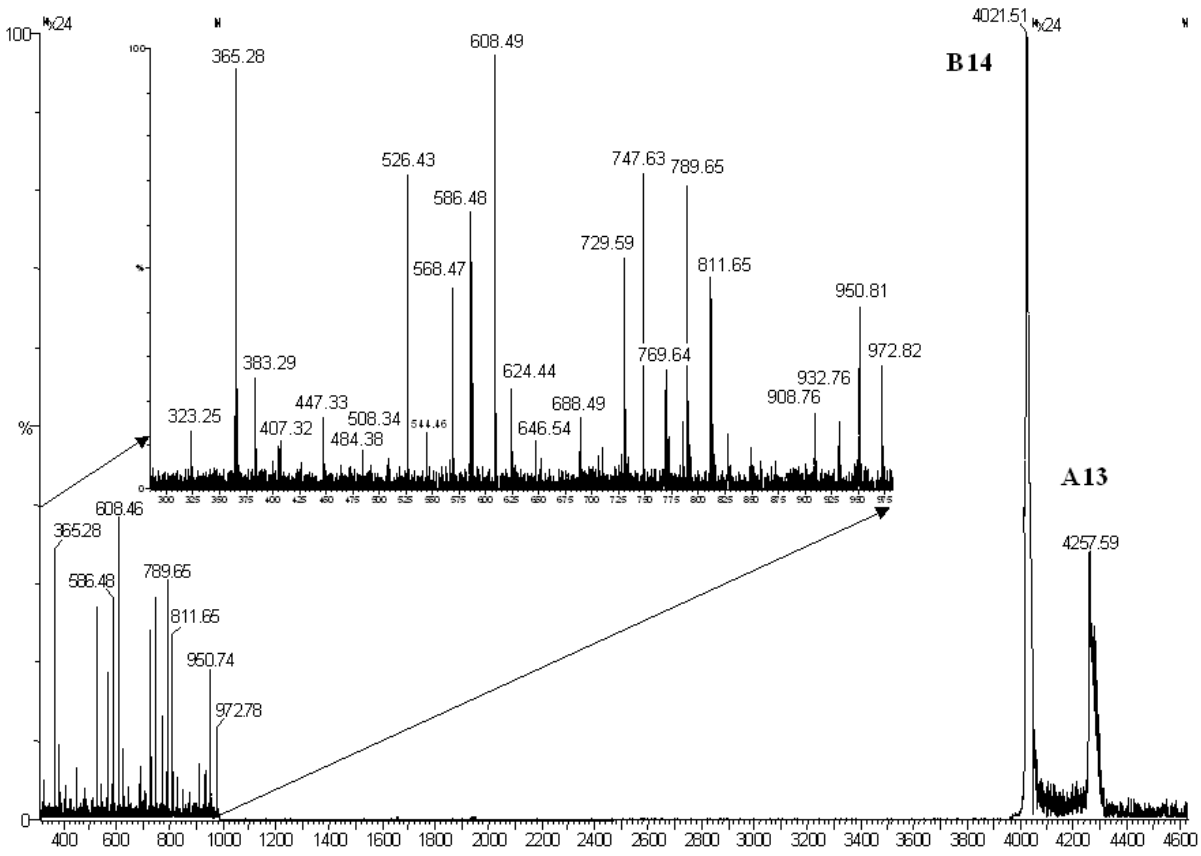
%x24
100
%
0
365.28
608.49
526.43
747.63
789.65
586.48
729.59
568.47
811.65
950.81
383.29
769.64
624.44
972.82
932.76
908.76
447.33
323.25
508.34
688.49
407.32
646.54
484.38
608.46
365.28
586.48
789.65
811.65
950.74
972.78
4021.51
B14
A13
4257.59
400
600
800
1000
1200
1400
1600
1800
2000
2200
2400
2600
2800
3000
3200
3400
3600
3800
4000
4200
4400
4600

Fig. 4a

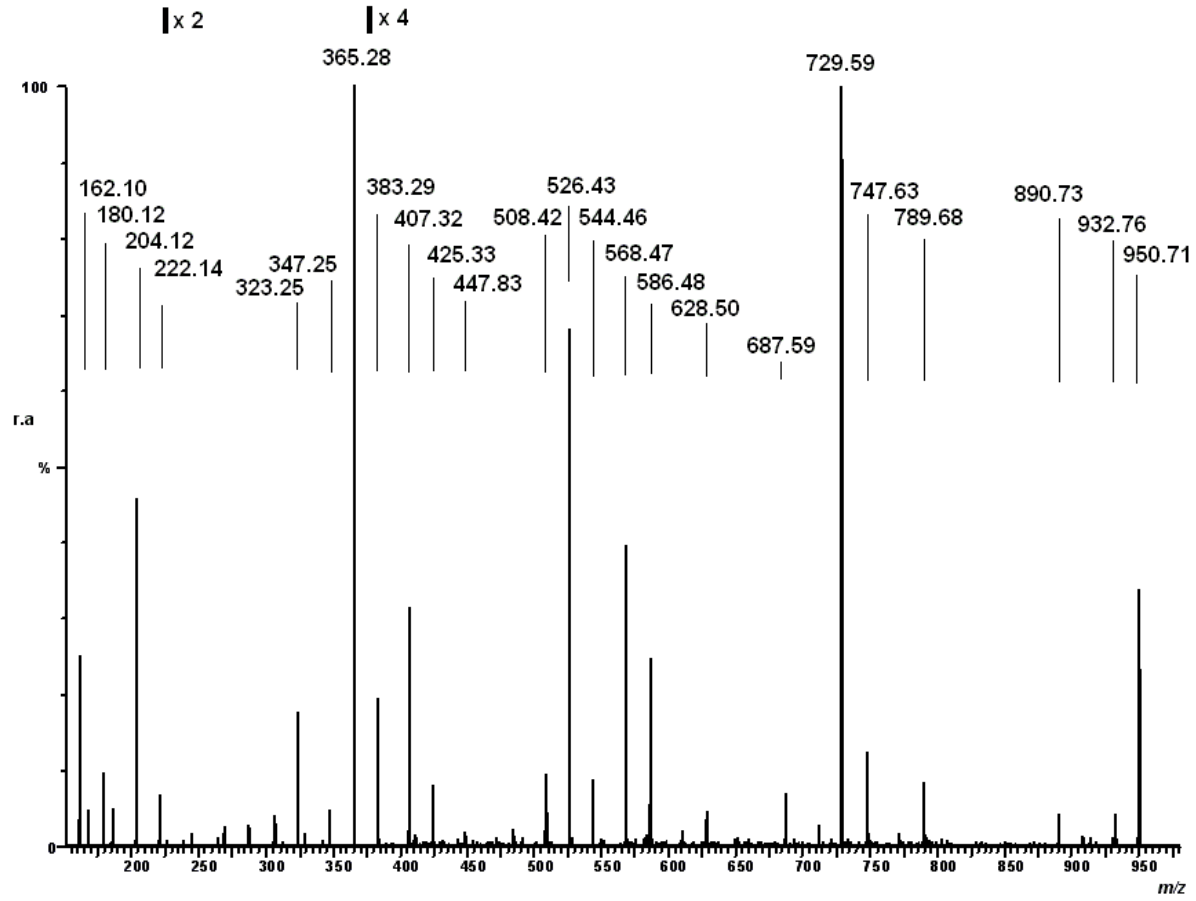
x 2
x 4
365.28
729.59
100
162.10
180.12
204.12
222.14
347.25
323.25
383.29
407.32
425.33
447.83
526.43
508.42
544.46
568.47
586.48
628.50
687.59
747.63
789.68
890.73
932.76
950.71
r.a
%
0
200
250
300
350
400
450
500
550
600
650
700
750
800
850
900
950
m/z

Fig. 4b

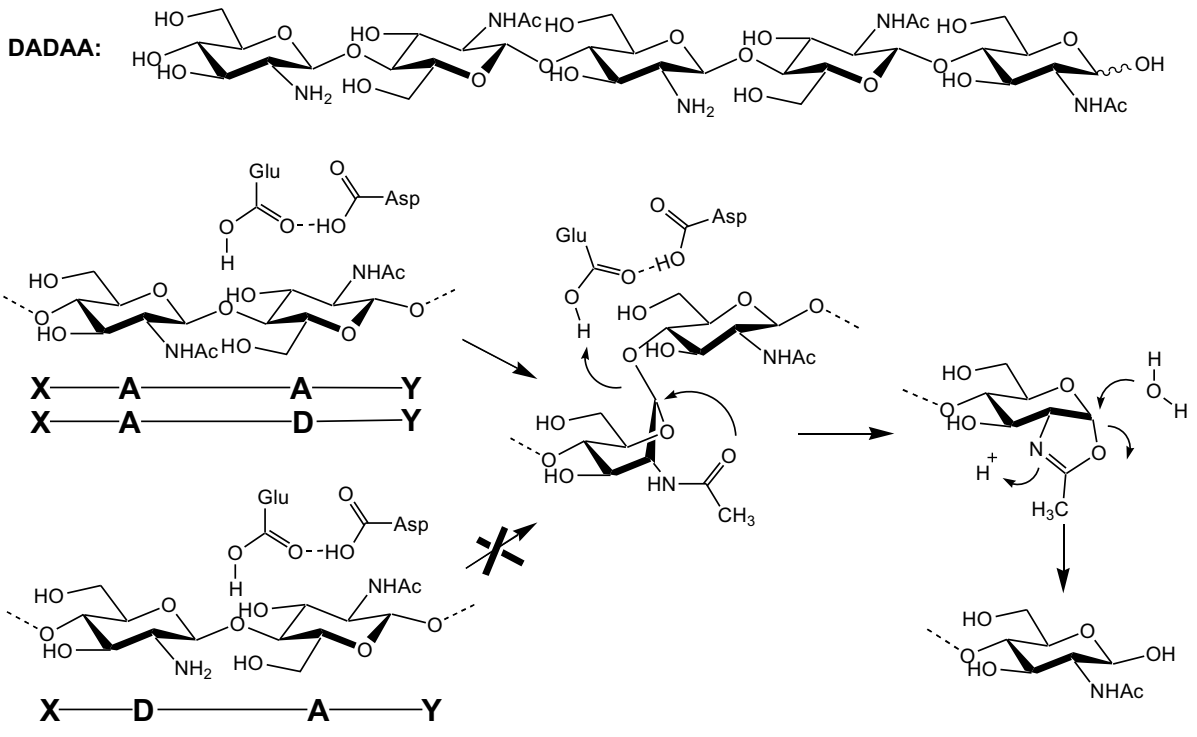
DADAA:
Glu
Asp
X—A—A—Y
X—A—D—Y
X—D—A—Y

Fig. 5

GROWTH PROMOTING EFFECT OF CHITO-OLIGOSACCHARIDES ON CHONDROCYTES IN CULTURE.

Thormodsson, F.R.[1*], Einarsson, J.M.[2], Gislason, J.[2], Bahrke, S.[3] og Peter, M.P.[3]

1) University of Iceland, Faculty of Medicine, Vatnsmyrarvegur 16, 101 Reykjavik, Iceland.
2) Primex ehf, R&D Division, Myrargötu 2, 101 Reykjavík, Iceland.
3) Universität Potsdam, Institut für Chemie und Strukturanalytik, Karl-Liebknecht-Str. 24-25, D-14476 Golm, Germany.
* finnbogi@hi.is

Introduction:

Chito-oligosaccharides are oligosaccharides made from chitin through hydrolysis. Chitin forms a large family of oligosaccharides composed from of two different monosaccharides, N-acetyl glucosamine (GlcNAc) and glucosamine (GlcN). The bioactivity of chito-oligosaccharides on chondrocytes, among other cells, has been studied and indicates growth promotional effect. The material used in these studies are crude mixtures of chito-oligosaccharides thus no information exist on which fractions of the chito-oligosaccharides do carry the bioactivity. Primex ehf (formerly Genis ehf) is developing a method of preparing water soluble oligosaccharides from shrimp chitin using chitinolytic enzymes. Fractionation of different oligosaccharides and in depth analysis of their structure will enable a thorough characterisation of their bioactive properties. This poster presents the first results in this project.

Material and methods

The chito-oligosaccharides were manufactured by Primex. Water-soluble chito-oligosaccharides were prepared from chitin by enzymatic hydrolysis. The oligosaccharides where spray-dried and their properties determined. A more precise analyses of there composition (size and GlcN-GlcNAc sequence) was made by MALDI-TOF mass spectrometry at the University of Potsdam. Human chondrocytes (Cell-Lining GmbH, Germany) where cultured in 96 well microplates, supplemented with different concentrations of chito-oligosaccharides (0, 10, 50, 100, 500 and 1000 µg/ml). After four weeks of incubation the cells were fixed in –20° C methanol and HE stained. Finally, we photographed the cells in each well through a microscope and used the photographs to count the cells and evaluate there appearance.

Results

Number of cells per well (cell density) was increased in proportion to an increase in chito-oligosaccharide concentration, (50 - 500 µg/ml) with high degree of statistical significance. However, at 1000 µg/ml there was a profound reduction in cell density compared to the control. The cells in the most condense wells took on a typical cartilage appearance.

Conclusions

These results show clearly that chito-oligosaccharides have a growth promoting effect on chondrocytes in culture. The observed change in appearance of the more rapidly growing cells could be due to the direct effect of chito-oligosaccharides on the cell phenotype or alternatively just a response to increased confluence of the rapidly growing cells. At 1000 µg/ml the chito-oligosaccharides hamper for an unknown reason. Further studies will evaluate the growth promoting effect of different fractions of chito-oligosaccharides.

[Supported by af RANNÍS]

Protein-Ligand Interactions of Chitooligosaccharides with the Chitolectin HC gp39 and with Chitinases

Sven Bahrke[1], Jón M. Einarsson[2], Jóhannes Gislason[2], Martin G. Peter[1]

[1] Institute of Chemistry, University of Potsdam, P.O. Box 60 15 53
D-14415 Potsdam, Germany
e-mail: Martin.Peter@uni-potsdam.de
[2] Genis ehf, Myrargata 2, IS- 101 Reykjavik, Iceland

Aminoglucan oligosaccharides (i.e. chitooligosaccharides) bind with high affinity to the chitolectin HC gp39. Based on changes of the intrinsic tryptophan fluorescence of the protein, it was found that, for a series of DP6 homologues, the affinity increased with increasing F_A (mole fraction of GlcNAc units): the K_d values were 13.7 µM for $(GlcNAc)_6$ (= A_6), 40.6 µM for $(GlcN)_2(GlcNAc)_4$ (= D_2A_4), 51.1 µM for $(GlcN)_3(GlcNAc)_3$ (= D_3A_3), and 420 µM for $(GlcN)_6$ (= D_6). The undecamer D_5A_6 shows high binding affinity with K_d = 6.9 µM.
Chitooligosaccharides apparently inhibit chitinases when methylumbelliferyl chitobioside or trioside is used as the substrate. At pH 5.5, ChiB, the IC_{50} values are 3 to 5 times lower than for ChiA from *Serratia marcescens*. The inhibitory potency increases with increasing DP and F_A. Sequence analysis of the oligosaccharides revealed that, under the assay conditions, productive binding results in competitive substrate inhibition while non-productive binding effects competitive enzyme inhibition.
The results are consistent the mechanism of chitinases as well as with a model describing hydrophobic and hydrogen bond interactions contributed by the subsites of the carbohydrate-binding domains.

Acknowledgements: Partial funding by the Deutsche Forschungsgemeinschaft (Pe 264/18-1) is gratefully acknowledged. We thank Prof. Vincent Eijsink, Ås, Norway, for generously providing a sample of chitinase B.

Keywords: affinity binding, chitinases, chitolectins, inhibitors, oligosaccharides

3.0 General Reflection and Discussion of the Results

3.1 Analytics of Heterochitooligomers, Homologs and Isomers

Chromatographic Methods

The thesis presents chromatographic methods for the quantitative analysis of complex mixtures of heterochitooligomers. Previous to chromatographic analysis, the crude depolymerisate is purified by means of filtration over membranes with pore sizes of 0.2 and 0.8 µm to remove all material, which is insoluble in acidic aqueous solution at pH 4.2. The first purification step is followed by ultrafiltration over a membrane with a cut-off of 3 kDa resulting in a solution containing chitooligomers of DP1 to approximately DP15 as corresponding MALDI-TOF mass spectra prove. Occasionally, additional ultra filtration steps employing 0.5 and 1 kDa cut-off membranes follow the first ultrafiltration step to remove oligomers of low DP, mainly DP1.

The first step of the chromatographic separation is the GPC on Biogel P4™. The relative masses of the fractions were calculated from peak areas of RI signals according to baseline drops. Fractions obtained from GPC contain homologs and oligomers to some extend as well. The second step of the analysis is the IEC employing the strong cation exchange material Resource S™. Compounds are separated by charge number, which equals the number of D units (ammonium groups) in the case of chitooligosaccharides. Homologs differ in the number of D units resulting in different charge numbers. These compounds are baseline separated on strong cation exchangers. The relative masses of fractions were calculated from peak areas of UV signals including a division by the number of A units and the conversion of molar amounts into masses. The combination of the data from the GPC separation with that of the IEC separation allows for a comprising of the oligomers and homologs of complex mixtures of heterochitooligosaccharides.

Figure 6 in off-print 1 shows the GP chromatogram of a mixture of heterooligosaccharides. Figure 2 in off-print 1 shows the IE chromatogram of one of the GPC fractions. The relative mass of D_2A_3 with respect to the IEC run of GPC fraction 5 is 49 %. As the relative mass of GPC fraction 5 is 16, 3 %, the relative mass of D_2A_3 with respect to the total amount of

sample is 8.0 %. (see Figures 2 and 6 in off-print 1) According to this example, the masses of all homologs of DP2 to 8 were determined (Figure 22).

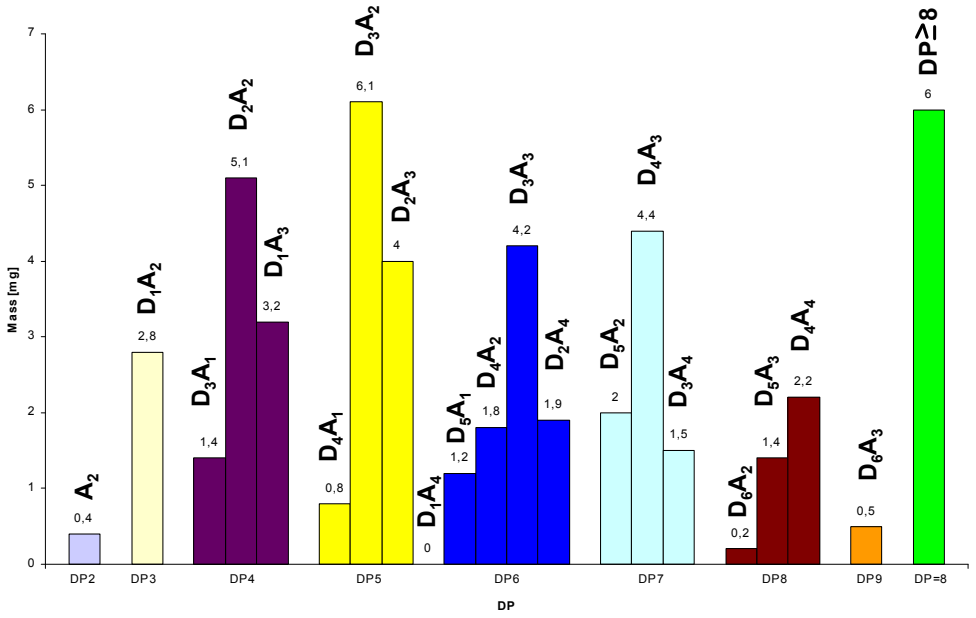

Figure 22. Mass distribution of the homologs of DP2 to 8 (sample 2) as determined by the combination of GPC and IEC. Homologs of identical DP (oligomers) are represented by bars of same colour.

Limitations of the method are overlapping charge numbers of oligomeric compounds occurring in some of the GPC fractions. Compounds of identical charge numbers are not separated by IEC. Secondly, a significant peak broadening is observed for compounds of charge numbers equalling five or more, resulting in a complication of the precise determination of the masses of minor compounds.

Each homolog represents a mixture of isomers.[2] The theoretical number of isomers increases exponentially with the DP and shows a Gaussian distribution with respect to F_A. The maximum is observed for $F_A = 0.5$. The analysis of several samples of mixtures of heterochitooligosaccharides obtained by enzymatic hydrolysis of partially deacetylated chitin showed that some isomers are preferably produced by the enzymatic hydrolysis. Consequently, the number of *main* isomers is limited to five in average for homologs of DP ≤ 10. Employing cation exchange chromatography on a Mono S™ stationary phase, it was possible to separate a mixture of mainly three D_2A_3 isomers and a mixture of two D_3A_3 isomers obtained by enzymatic hydrolysis of chitosan with a chitinase.

The masses of isomers are quantified according to peak areas of UV signals. As the peaks are usually not baseline separated, peak fitting methods are applied for peak deconvolution and determination of peak areas.

Figure 9 in off-print 2 shows exemplarily the cation exchange chromatogram of the three D_2A_3 isomers ADDAA, DADAA, DDAAA as well as a model for the principle of the separation. The sequence of retention times of the D_2A_3 and D_3A_3 isomers (ADDAA < DADAA < DDAAA and DADDAA < DDADAA) indicates that the interactions causing the separation are of ionic nature like for the separation of homologs. But in the case of isomers, which possess identical numbers of D units, the number of exposed D units at the reducing or non-reducing end, respectively, is decisive for the retention time. E.g. ADDAA has none exposed D unit at the reducing end, DADAA has one and DDAAA has two. For the stationary phase it is assumed that the cation exchange sulfonic acid groups are unequally distributed over the resin surface and inside the pores so that in some cases the distance of neighbouring sulfonic acid groups fits the distance of two neighbouring D units of the heterochitooligosaccharide resulting in a double ionic interaction (Figure 7 in off-print 1).

Mass Spectrometric Methods

For the quantitative analysis of homologs and oligomers, fractions from GPC are per-*N*-acetylated with Ac_2O-d_6. Each former glucosamine unit becomes a trideuterio-*N*- acetyl glucosamine unit providing distinguishable molar masses for homologs. E.g. D_3A_2 becomes $A^*_3A_2$ (M = 1042.4 Da), and D_2A_3 becomes $A^*_2A_3$ (M = 1039.4 Da) with A* being a trideuterio-*N*-acetyl glucosamine unit. The mass spectrometric properties (especially desorption properties) of the per-*N*-acetylated compounds are identical, as they just differ in the number of deuterium atoms, but the exchange of a hydrogen atom by a deuterium atom has no influence on the mass spectrometric properties. The number of deuterium atoms allows to conclude the number of D units of the native heterochitooligosaccharide. The peak areas are proportional to the relative molar amounts. It was demonstrated that calculations based on peak heights give results of equal precision.

The MALDI-TOF mass spectra of equimolar amounts of chitin oligomers or chitosan oligomers, respectively, showed that the method is as well feasible for the quantitative determination of oligomers as long as Δ DP ≤ 3. Consequently, the mass spectrometric method is a universal tool for the rapid quantitative analysis of GPC fractions of complex mixtures of chitooligomers. Figures 5 and 9 in off-print 1 show the sequence of analytical steps leading to the quantification of a mixture of homologs (and oligomers), GPC fraction 5 (sample 2). The sample is derivatised with Ac_2O-d_6.

Figures 5 and 9 in off-print 1 show exemplarily the per-*N*-deuterioacetylation of D_2A_2 followed by selective deacetylation of by-products with NH_3. The quantification of peak areas

or peak heights allows for the calculation of the relative masses of homologs. In case of overlapping isotopic patterns (e. g. A_6-d_9 and A_6-d_{12}), the subtraction of the calculated isotopic pattern from the observed isotopic pattern allows for the determination of peak areas of homologs (inset 1, and inset 2). According to this example, the masses of all homologs of DP2 to 8 were determined (Figure 23).

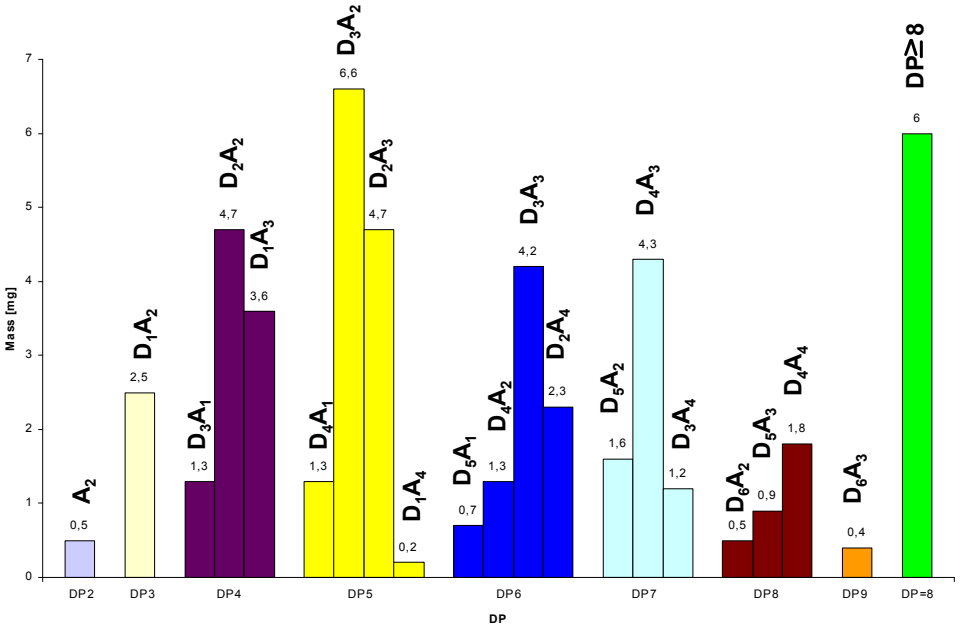

Figure 23. Mass distribution of the homologs of DP2 to 8 (sample 2) as determined by the combination of GPC and MALDI-TOF MS. Homologs of identical DP (oligomers) are represented by bars of same colour.

The quantitative analysis of mixtures of ChO's employing a combination of GPC and MALDI-TOF MS is advantageous compared to the combination of GPC and IEC: the analysis is more rapid, no overlapping of identical charge numbers occurs and the sensitivity for oligomers of DP > 6 is higher.

Mass spectrometric methods were successfully applied for the analysis of mixtures of isomers.

Each homolog represents a mixture of isomers. The number of isomers comprising one homolog depends on the F_A and DP. For a constant F_A, the number of isomers is increasing exponentially with DP. E.g. for D_3A_3 (DP 6, F_A 0.5) (6!) / (3!)² = 20 isomers exist.

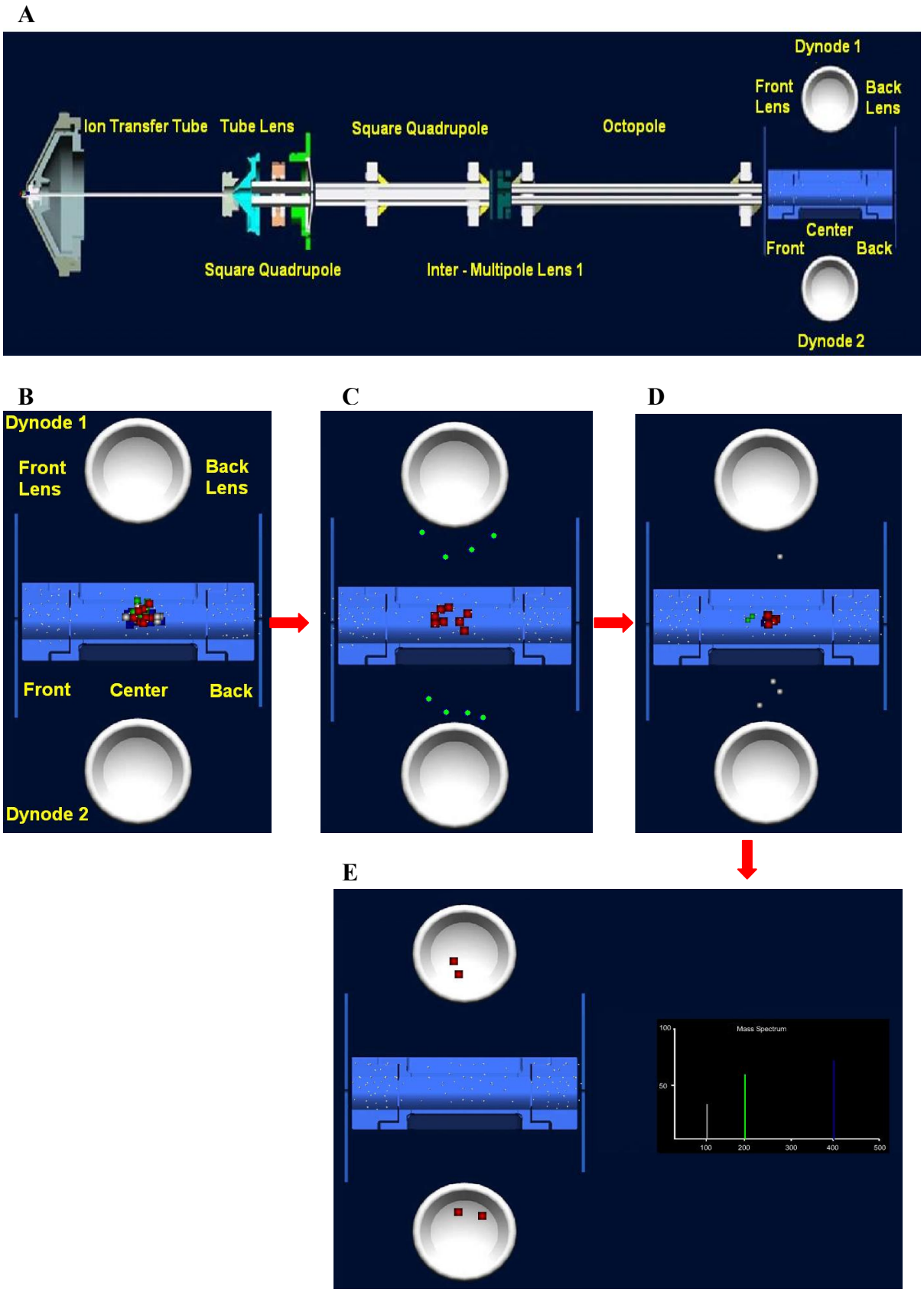

Figure 24.[213]
A. Overview of 2D Linear Ion Trap Mass Spectrometer.
B. Ion trapping. Ions are either injected into or created within the interior of the ion trap. They are confined by application of appropriate RF and DC voltages with their final position maintained within the centre section of the ion trap. Ions of different m/z ratio are represented by coloured circles and squares.

C. Precursor Ion Isolation. The RF voltage is adjusted and multi-frequency resonance ejection waveforms are applied to the trap to eliminate all but the desired ion(s) in preparation for subsequent fragmentation and mass analysis. The desired precursor ions are represented by red coloured squares whereas eliminated ions are represented by green circles.
D. Precursor ion excitation. The energy of the selected ions is increased by application of a supplemental resonance excitation voltage applied to all segments of the two rods located on the X-axis. This increase of energy causes dissociation of the selected ions due to collisions with the damping gas. The product ions formed are retained in the trapping field. Product ion ejection. Scanning the contents of the trap to produce a mass spectrum is accomplished by linearly increasing the RF voltage applied to all sections of the trap and utilizing a supplemental resonance ejection voltage. These changes sequentially move ions from within the stability diagram to a position where they become unstable in the X-direction and leave the trapping field for detection. Precursor ions are represented by red coloured squares. Fragment ions are represented by white coloured circles (ejected) and green circles (non ejected).
E. Product ion detection. Ions are accelerated into the two high voltage dynodes where ions produce secondary electrons. This signal is subsequently amplified by two electron multipliers, and the analogue signals are then integrated together and digitised.

Any quantitative evaluation of mass spectrometric signals requires compounds that show equivalent mass spectrometric behaviours, including desorption, ionisation, and fragmentation. For the present studies the compounds of the mixture of isomers were sequenced applying controlled fragmentation requiring equivalent energies for the fragmentation of –D-D-, -D-A-, -A-D- and –A-A- bonds, which is unfortunately not the case for native compounds. Thus, the free amino groups of D units are derivatised with Ac_2O-d_6 affording -A*-A*-, -A*-A-, -A-A*- and -A-A- bonds, which show unique fragmentation properties because the exchange of a hydrogen atom by a deuterium atom has no influence on the fragmentation of the glycosidic bond or the anchimeric assistance of the *N*-acetyl group. Previous to the sequence analysis the compounds of the sample are tagged at the reducing end with AMCR, which provides a distinction between ions produced by fragmentation from the reducing and ions produced by fragmentation from the non-reducing end. Moreover, the reducing end derivatisation supports the fragmentation from the non-reducing end.
For fragmentation experiments, a vMALDI-Linear Ion Trap mass spectrometer was applied. Figure 24 shows the principal assembly of such type of mass spectrometer.[213]
The 2D linear ion trap in the LTQ is comprised of four parallel hyperbolic shaped rods, segmented into three sections. Ions are trapped radially in a radio frequency electric field and axially in a static electric field using DC voltages. Application of appropriate voltages to all three segments generates a homogenous field throughout the trapping region. Mass analysis involves ejecting the trapped ions in the radial direction through the two parallel slots in the centre section of the linear ion trap where two detectors are placed. multiple-stage

experiments are performed as follows: The parent ion of interest is selected in a step that involves ejecting all other ions from the trap which is achieved by variation of the radio frequency. The parent ion is the translationally excited applying a supplementary radio frequency voltage. The product ions result from collision-induced dissociation of these excited ions with the helium buffer gas (1 mTorr), which generally functions to lower the energies of trapped ions. The product ions are either recorded by scanning the radio frequency voltage resulting in MS/MS experiments, or the process of selection / fragmentation is repeated resulting in MS^n experiments.

MS^n experiments have to be performed, since the m/z values of fragment ions comprising different sequences may overlap. E.g. D_1A_1 is a fragment of D_3A_3 comprising two sequences, DA and AD, of equivalent m/z ratios and consequently overlapping signals. An additional MS^2 experiment resulting in the fragmentation of D_1A_1 affords A_1 in the case of DA, and D_1 in the case of AD. In conclusion, the MS^2 allows to distinguish between DA and AD and thus to distinguish between D_3A_3 isomers like DDAA**DA** and DDAA**AD**. In the case of per-*N*-acetylated compounds, A*A*AAA* and A*A*AA*A (A*, trideuterio *N*-acetylglucosamine), of identical fragmentation properties the quantification of mass spectrometric signals allows to calculate the relative amounts of A^*_1 and A_1 (Δ m/z = 3) leading to the relative amounts of DA and AD, which are equivalent to the relative amounts of DDAADA and DDAAAD. From the relative amounts the mass of each isomer can be calculated.

Figure 3 in off-print 2 shows the pre-analytical derivatisation procedure of the mixtures of heterochitoisomers. Figures 4 and 5 in off-print 2 illustrate the mass spectrometric sequencing inclusive quantification for the example of a mixture of D_3A_4 heterochitoisomers. The MS^2 fragment spectrum gives the following information: Y1 and Y2 appear as single peaks indicating 100% A-T and AA-T. The isotopic pattern of Y3 reveals a doublet indicating the presence of both, AAA-T (4.4%) and A*AA-T / DAA-T (95.6%). The Y4 fragment appears as a doublet of $A^*_1A_3$-T (81.0 %) and $A^*_2A_2$-T (19.0 %). The $A^*_2A_2$-T fragment is stringently derived from the A*AA-T / DAA-T sequence. Consequently, exclusively the A*A*AA-T / DDAA-T sequence can be attributed to the $A^*_2A_2$-T fragment. The $A^*_1A_3$-T fragment is composed of 4.4% A*AAA-T / DAAA-T and 81.0 % - 4.4% = 76.6% AA*AA-T / ADAA-T. For the Y5 fragment a singulet ($A^*_2A_3$-T) is observed, which stringently results from the sequences A*A*AAA-T / DDAAA-T (4.4%), A*AA*AA-T / DADAA-T (76.6%), and AA*A*AA-T / ADDAA-T (19.0%). For the deduction of the Y6 sequences the information of at least one MS^3 spectrum is demanded. The Y6 fragment appears as a doublet

composed of $A^*_3A_3$-T (50.7%) and $A^*_2A_4$-T (49.3%). $A^*_3A_3$-T is composed of A*A*A*AAA-T / DDDAAA-T, A*A*AA*AA-T / DDADAA-T, and A*AA*A*AAT / DADDAA-T. The MS^3 of the $A^*_3A_3$-T precursor shows a doublet for the Y3 fragment resulting from A_3-T (5.7%) and $A^*_1A_2$-T (94.3%). The A_3-T fragment exclusively arises from A*A*A*AAA-T / DDDAAA-T, the amount of which is consequently calculated to 5.7% of 50.7% = 2.9%. The Y4 fragment shows a doublet of $A^*_1A_3$-T (65.3%) and $A^*_2A_2$-T (34.7%). The $A^*_2A_2$-T fragment exclusively arises from A*AA*A*AA-T / DADDAA-T, the amount of which is consequently calculated to 34.7% of 50.7% = 17.6%. The amount of A*A*AA*AA-T / DDADAA-T is calculated to 50.7% - 2.9% - 17.6% =33.1%. In analogy, the MS^3 fragment spectrum of $A^*_2A_4$-T allows to calculate the relative amounts of AA*A*AAA-T / ADDAAA-T (1.5%), AA*AA*AA-T / ADADAA-T (46.4%), and AAA*A*AA-T / AADDAA-T (1.4%). From the Y6 fragments automatically are concluded to be A*AA*A*AAA-T / DADDAAA-T (1.5%), AA*A*A*AAA-T / ADDDAAA-T (2.9%), A*AA*AA*AA-T / DADADAA-T (46.4%), AA*A*AA*AA-T / ADDADAA-T (30.2%), A*AAA*A*AA-T / DAADDAA-T (1,4%), and AA*AA*A*AA-T 7 ADADDAA-T (17.6%). The example shows that despite the fact that MS^n (n>2) experiments are necessary for the conclusion of the amounts of all sequences, the number of MS^n experiments can be drastically reduced employing an appropriate calculation of unknown quantities of fragment ions due to the quantitative evaluation of the MS data. Thus, for the quantitative determination of the compositions of mixtures of isomers up to DP 9 (with maximally 8 main compounds) only MS^3 experiments were necessary (Table 1 in off-print 2).

Figure 25 summarizes the different procedures for the quantitative analysis of heterochitooligomers, -homologs, and isomers.

The quantitative determination of the compositions of mixtures of isomers employing MS techniques is superior compared to chromatographic methods as it is faster, requires less amount of sample (in the range of nanomols) and offers a wider range of applications concerning the DP and complexity of the mixtures.

However, a comparison of the results obtained by mass spectrometry and chromatography shows that they are at least in the same range indicating that both methods give trustworthy results with a higher accuracy for the mass spectrometric results.

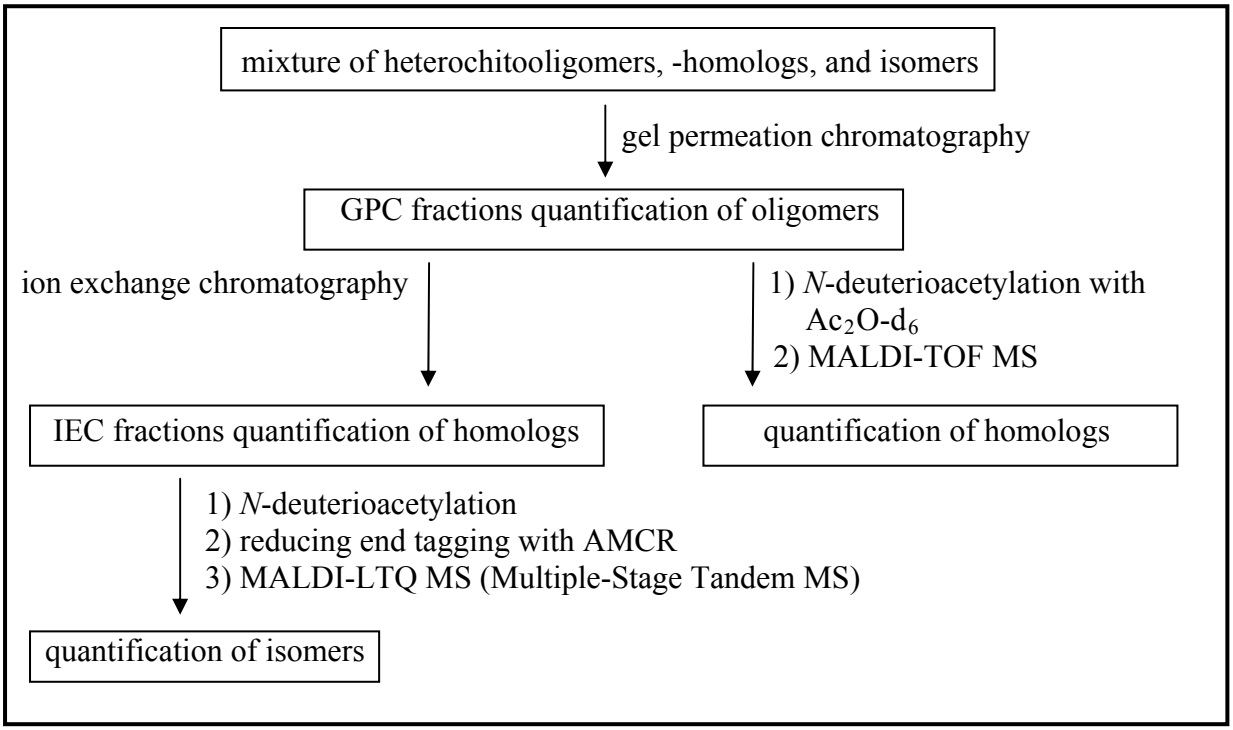

Figure 25. Summary of the different techniques employed for the quantitative analysis of mixtures containing heterochitooligomers, -homologs, and isomers. The first step in any case is GPC (on Biogel P4™) resulting in the quantification of oligomers. IEC (on Resource S™) of the GPC fractions allows for the quantification of homologs. Alternatively MALDI-TOF MS of the GPC fractions after N-deuterioacetylation allows for the quantification of homologs. For the quantification of isomers MALDI-LTQ MS^n after derivatisation of the desalted IEC fractions with Ac_2O-d_6 (free amino groups) and AMCR (reducing end) is employed.

In conclusion, the present work delivers novel analytical tools for the quantitative analysis of mixtures of heterochitooligomers, -homologs and -isomers. Herein, mass spectrometric methods have proved to possess an outstanding performance, especially with respect to the analysis time, the sample amount and the sensitivity, so that the chromatographic methods are rather used for reference. With the present work for the first time it has become possible to completely comprise these complex mixtures typically consisting of hundreds to thousands of compounds within a few days.

As complex mixtures of ChO's are obtained from the chemical or enzymatic degradation of chitosan and as they are or will in the near future be used for pharmaceutical products or food additives, the analytics presented here will be used for quality control or development of improved active compounds as well as the research upon biological functions of ChO's.

3.2 Analytics of Chitin, Chitosan, and a Copolymer of Chitosan and Cellulose

Another application of the quantitative analysis of complex mixtures of ChO's is the sequence analysis of polymers like chitin or chitosan. The distribution of D and A units is one important factor that influences the properties of chitin and chitosan. This matters on one hand to naturally occurring polymers like chitin in insect cuticles or chitosan in fungi. On the other hand, the reaction conditions of the deacetylation process that transforms chitin into chitosan influences the distribution of D and A units resulting either in a random or blockwise distribution.[214, 215] An even more complex and thus interesting example is presented with this thesis.

Acetobacter xylinum is a soil bacterium, which produces cellulose. The addition of chitosan to the nutrient medium results in the production of chitosan modified bacterial cellulose. The nutrient medium is 2.000 % (w/w) glucose, 0.500 % (w/w) peptone, 0.500 % (w/w) yeast extract, 0.270 % (w/w) disodium phosphate, 0.115 % (w/w) citric acid monohydrate, and 0.500 % (w/w) chitosan acetate (F_A 0.16; M_V 98 kDa). The modification results in a material with outstanding properties: The elasticity of bacterial cellulose is increased, which manifests in mechanical properties like maximal breaking load or braking stress.[216] (Figure S1 Appendix) The modification results in a material with bacteriostatic properties. Moreover, the modification of bacterial cellulose with chitosan increases its biodegradability. E.g. chitosan modified bacterial cellulose is degradable with endogenous lysozyme.[217, 218] The outstanding properties of the material are used in loudspeaker membranes,[219] functionalised clothes (sportswear, baby-wear)[220] or wound dressings[221]. The material is degraded with time, and some of the degradation products (chitooligosaccharides) stimulate the growth of new tissue so that the artificial tissue is replaced by the natural tissue (tissue regeneration).

The chitosan modified bacterial cellulose was applied to a partial hydrolysis with Econase CE (a commercial cellulolytic complex prepared from *Trichoderma reesei* and characterized by the following specific activities: endo-β-1,4-glucanase 2330 U/mL; β-glucosidase 22 U/mL) affording a mixture of oligosaccharides with DP < 10 (MALDI-TOF MS). The IR spectrum (Figures S2, S3, Table S1, Appendix) of the partial hydrolysate shows bands of functional groups that are characteristic for chitosan besides the bands for cellulose (3350 – 2000 cm^{-1} amine; 800 cm^{-1} $\delta(NH_2)$ amine; 1650 cm^{-1} υ(C=O) amide; 1550 cm^{-1} υ(C-N) + δ(C-N-H) amide). Also the ^{1}H- and ^{13}C-NMR spectra of the partial digest of chitosan modified bacterial cellulose (D_2O / DCl; room temperature; 300 MHz; Figures S4, S5, Table S2 and Figures S6,

S7, Table S3 Appendix) show characteristic peaks for chitosan besides peaks for cellulose (^{1}H-NMR: 4.528 ppm, doublet, H-1 β-glucose, ^{3}J(H-1, H-2) = 8.1; 4.818 ppm, doublet, H-1 β-glucosamine / *N*-acetylglucosamine, ^{3}J(H-1, H-2) = 8.0; ^{13}C-NMR: 23.6 ppm, methyl group connected with the carbonyl function *N*-acetylglucosamine; 61.9 ppm, C-6 glucosamine / *N*-acetylglucosamine; 62.4 ppm, C-6 glucose; 95.7 ppm, C-1 glucosamine / *N*-acetylglucosamine; 99.4 ppm, C-1 glucose; 162.7 ppm, carbonyl function *N*-acetylglucosamine).

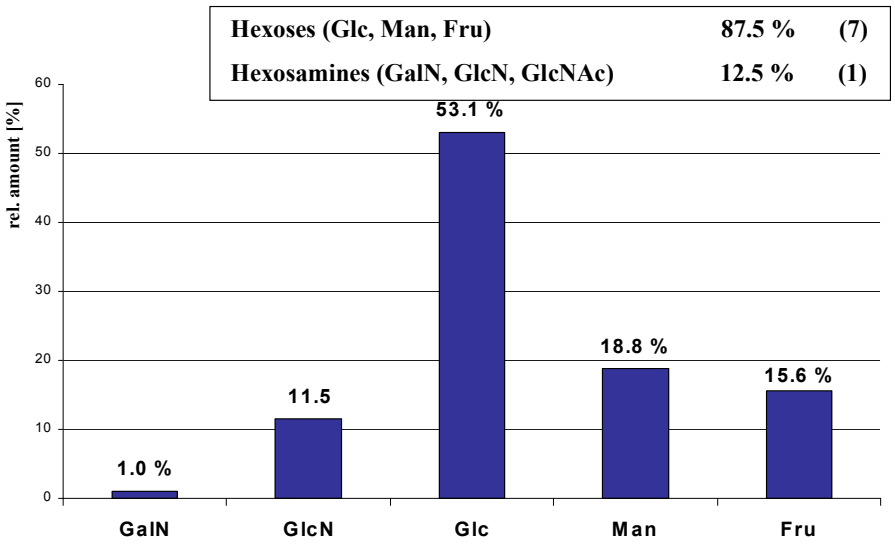

Figure 26. Relative amounts of the monosaccharides comprising chitosan modified bacterial cellulose (HPAEC-PAD). The non-significant amount of N-acetylglucosamine was not further regarded.

Detailed information about the monosaccharide units forming the polymer is obtained from a monosaccharide analysis. The chitosan modified bacterial cellulose was applied to a total hydrolysis with sulfuric acid followed HPAEC-PAD of the monomer units. The following monosaccharide composition was found: 53% glucose, 21% mannose, 13% fructose and 13% glucosamine / *N*-acetylglucosamine (Figure 1 in off-print 3 and Figure 26). It is remarkable that besides the hexose glucose also mannose and fructose were found in significant amounts. Structural information on the polymer is obtained from sequence analysis. The partial hydrolysis of chitosan modified bacterial cellulose with Econase CE™ afforded a mixture of oligosaccharides with DP < 10 (MALDI-TOF MS). The oligosaccharides mixture was fractionated by GPC on Biogel P4™. The fractions were analysed by MALDI-TOF MS indicating that the main components were oligosaccharides of hexoses (Glc, Man, Fru) with DP < 4 as well as chitooligosaccharides D_xA_y. The detection of oligosaccharides composed of

glucosamine, *N*-acetylglucosamine and hexose $D_xA_yH_z$ (z = 1 or 2) indicates that the chitosan modified bacterial cellulose produced by *Acetobacter xylinum* is a copolymer and not just a mixture of cellulose and chitosan (Figure 27).

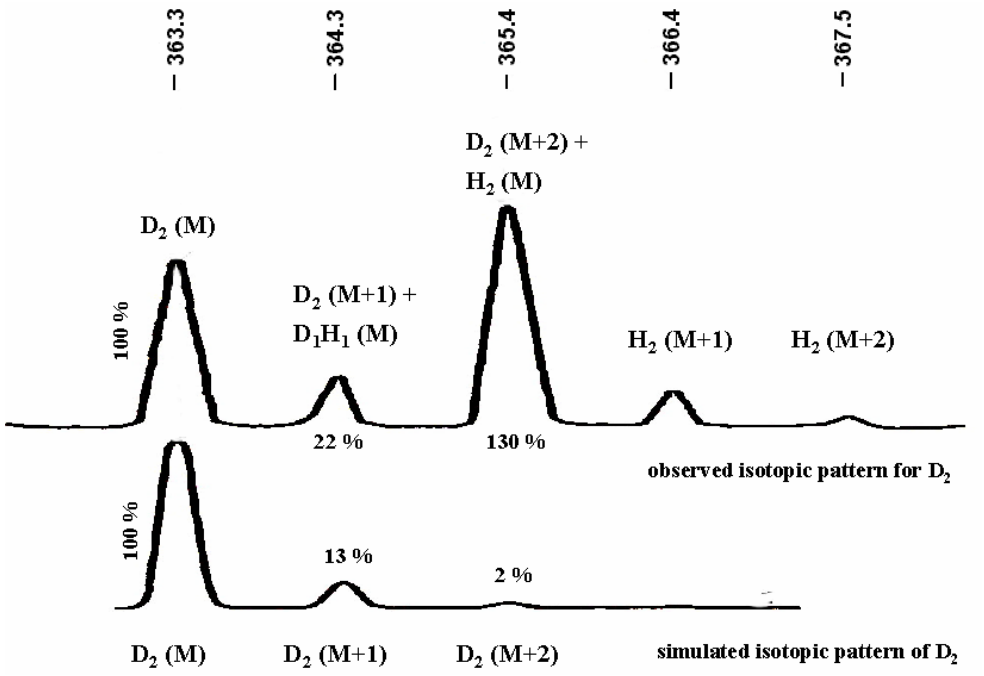

Figure 27. The comparison of the observed isotopic pattern (MALDI-TOF MS) of D_2 (upper part) with the simulated isotopic pattern of D_2 (lower part) proofs the presence of H_2 and a little amount of D_1H_1 . The relative peak areas are depicted in the figure. Monoisotopic molecular ions (M) as well as M + 1 and M + 2 isomers are labelled.

Additionally, cation exchange chromatography proves the presence of hexose containing oligosaccharides besides pure chitooligosaccharides (Figure 28).

The components of the GPC fractions were derivatised with AMAC at the reducing end and sequenced applying MALDI-TOF Tandem MS. The sequence analysis of oligosaccharides composed of glucosamine, *N*-acetylglucosamine and hexose shows Y-type and B-type fragment ions. The mass differences of the series of Y-type ions reflect the sequence of D, A, and H units. A mass difference of 161 amu represents a D unit, 203 amu an A unit and 162 amu a H unit. Especially challenging is the mass spectrometric differentiation of D and H units (Δ m/z = 1 amu). The isotopic patterns of the fragment ions have to be applied in this case.

The sequence analysis of oligosaccharides containing glucosamine, *N*-acetylglucosamine and hexose clearly indicates that chitosan modified bacterial cellulose is a copolymer with covalent linkages between hexosamine and hexose units (Figure 3 in off-print 3).

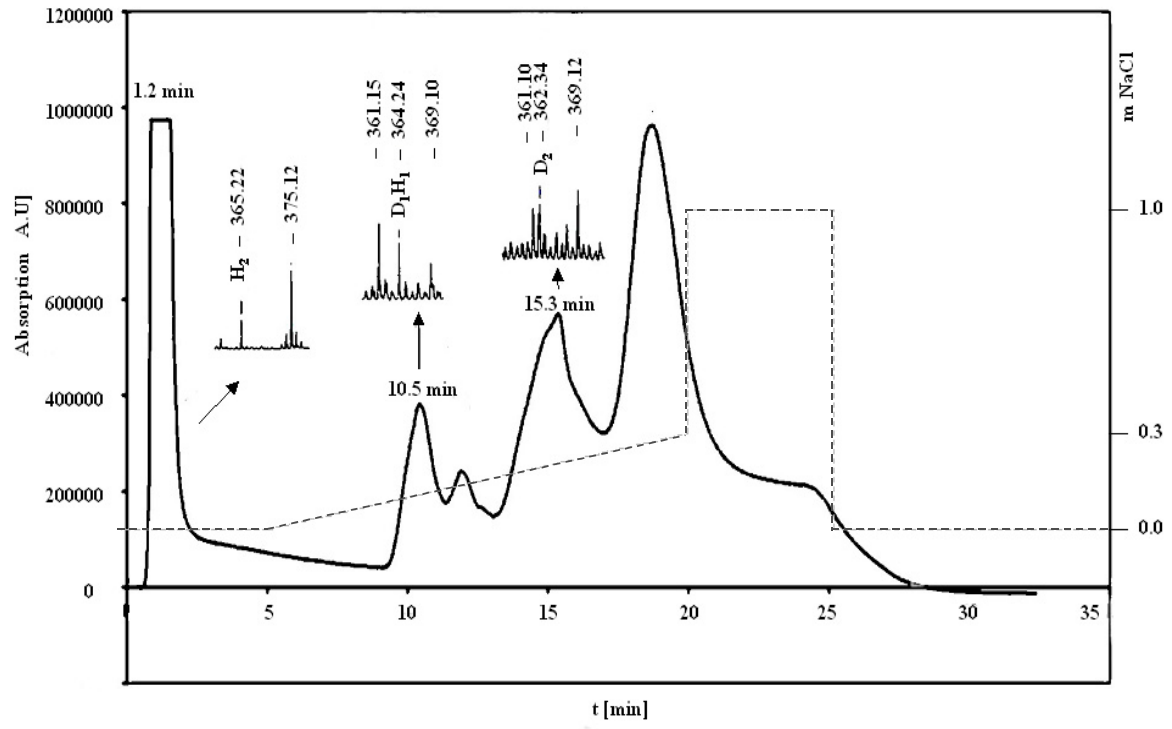

Figure 28. Cation exchange chromatogram of a mixture of D_2, D_1H_1 and H_2. The inset MALDI-TOF mass spectra verify the peak assignments. The retention times increase with the overall charge of the oligosaccharides in acidic solution. The NaCl gradient is depicted as a dashed line (right hand scale).

The quantitative evaluation of the GPC profile of the partial hydrolysate of chitosan modified bacterial cellulose in combination with the quantitative evaluation of the sequence data allows to retrieve information on the total composition of the copolymer. The GPC profile in combination with the MALDI-TOF MS data of the fractions shows high amounts of hexose monomers and dimers as well as significant amounts of heterochitooligomers of DP2 to 8, whereas oligomers composed of both, hexose and hexosamine units are minor compounds (Figure 2 in off-print 3).

The quantitative evaluation of the sequence data of the chitooligosaccharides allows to conclude the relative amounts of the main sequences (Figure 29).

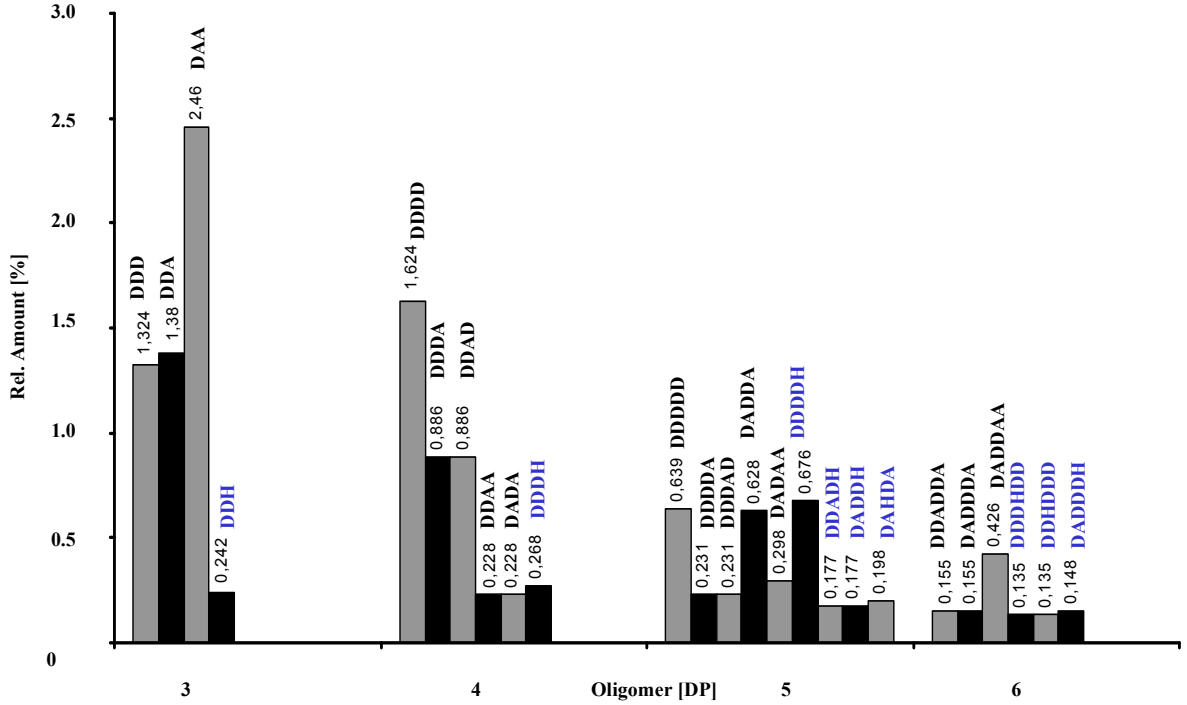

Figure 29. Relative amounts of the main chitosan sequence fragments contributing to the structure of the polymer. Hexose containing chitooligomers are displayed in blue colour. The results were obtained by the quantitative evaluation of the gel permeation chromatogram (oligomers), MALDI-TOF mass spectra of the GPC fractions (homologs), and MALDI-TOF Tandem mass spectra of homologs (isomers). The molar amounts of the sequences are calculated with respect to the total amount of sequences. Hexose oligomers are not displayed in this figure.

Additionally, the quantitative evaluation of the sequence data of hexose containing chitooligomers gave the information that the hexose units are preferably found in terminal positions.

It should be noted at this point that the mass spectrometric quantification of chitooligosaccharides that are not per-*N*-deuterioacetylated is an estimation. The experiments on modified bacterial cellulose were done before the method for the quantitative sequence analysis of chitooligosaccharides was established. However, the general methodology for the sequence analysis of chitin or chitosan containing polymers, which will be explained in the following, is not influenced by this fact.

1. The sequences and relative amounts of hexose oligomers, chitooligomers and hexose containing chitooligomers are obtained from GPC and MS (Table 2).

Table 2. Relative amounts of the main chitosan sequence fragments. Oligomers containing only hexose are not displayed in the table. The molar amounts are calculated with respect to the total amount of hexosamine containing oligomers (The amount of hexose oligomers was not regarded).

Oligomer	Homolog	Sequence	Relative Amount	Oligomer	Homolog	Sequence	Relative Amount
DP 3	D_3	DDD	9.44 %	DP 5	D_3A_2	DADDA	4.51 %
	D_3A_1	DDA	9.87 %		D_2A_3	DADAA	2.15 %
	D_1A_2	DAA	17.60 %		D_4H_1	DDDDH	4.86 %
	D_2H_1	DDH	1.72 %		$D_3A_1H_1$	DDADH	1.29 %
DP4	D_4	DDDD	11.59 %			DADDH	1.29 %
	D_4A_1	DDDA	6.37 %		$D_2A_2H_1$	DAHDA	1.43 %
		DDAD	6.37 %	DP6	D_4A_2	DDADDA	1.15 %
	D_2A_2	DDAA	1.65 %			DADDDA	1.15 %
		DADA	1.65 %		D_3A_3	DADDAA	3.08 %
	D_3H_1	DDDH	1.93 %		D_5H_1	DDDHDD	1.00 %
DP5	D_5	DDDDD	4.58 %			DDHDDD	1.00 %
	D_4A_1	DDDDA	1.65 %		$D_4A_1H_1$	DADDDH	1.07 %
		DDDAD	1.65 %				

2. The number of data is reduced. More extended sequences are virtually split to smaller units of the same sequence so that the diversity of oligomers is reduced.

Table 3. Virtual splitting of the main sequences of hexosamine containing sequences for the purpose of data reduction. Hexose units are split off and not further regarded. Mono- and disaccharide units were appropriately virtually recombined to trisaccharide units.

Oligomer	Homolog	Sequence	Splitting	Oligomer	Homolog	Sequence	Splitting
DP 3	D_3	DDD	-. -	DP 5	D_3A_2	DADDA	DAD + DA
	D_3A_1	DDA	-. -		D_2A_3	DADAA	DAD + AA
	D_1A_2	DAA	-. -		D_4H_1	DDDDH	DDD + D
	D_2H_1	DDH	DD		$D_3A_1H_1$	DDADH	DDA + D
DP4	D_4	DDDD	DDD + D			DADDH	DAD + D
	D_4A_1	DDDA	DDD + A		$D_2A_2H_1$	DAHDA	DA + DA
		DDAD	DDA + D	DP6	D_4A_2	DDADDA	DDA + DDA
	D_2A_2	DDAA	DDA + A			DADDDA	DAD + DDA
		DADA	DAD + A		D_3A_3	DADDAA	DAD + DAA
	D_3H_1	DDDH	DDD		D_5H_1	DDDHDD	DDD + DD
DP5	D_5	DDDDD	DDD + DD			DDHDDD	DD + DDD
	D_4A_1	DDDDA	DDD + DA		$D_4A_1H_1$	DADDDH	DAD + DD
		DDDAD	DDD + AD				

3. Knowledge on the cleaving specificity of the enzyme employed for hydrolysis of the copolymer allows concluding to connectivity of the sequence segments. The Econase

CE™ enzyme mixture shows endo-β-1,4-glucanase and β-glucosidase activity. Consequently, Glc-Glc bonds were cut predominately, to less extend Glc-GlcN/GlcNAc or GlcN/GlcNAc-Glc bonds were cleaved, and GlcN-GlcNAc or GlcNAc-GlcN bonds were not cleaved.

In conclusion, Econase CE™ did not cleave sequences of chitooligosaccharides whereas sequences of hexoses were cleaved. Chitooligosaccharides containing one hexose unit at the reducing end represent linkers between the well-cut hexose segments and the non-cut chitooligosaccharide segments. One hexose unit is left at the reducing end as GlcN/GlcNAc-Glc bonds are cleft very slowly. Since Econase CE™ cleaves Glc-GlcN/GlcNAc bonds faster, a hexose unit is rarely found at the non-reducing end. Consequently, the polymer is composed of building blocks of chitooligosaccharides and building blocks of cellooligosaccharides. The monosaccharide analysis gives the ratio of hexose units to glucosamine / *N*-acetylglucosamine units, it is 87.5% vs. 12.5%. That means, one D or A unit corresponds to seven hexose units. The quantitative sequence analysis of chitooligosaccharides including data reduction gives 43% DDD, 36% D(DA), and 21% (DA)A. A possible average repetition unit of the chitooligosaccharide blocks is given in Figure 30.

- DDD D(DA) (DA)A DDD D(DA) DDD DAA DDA DDD -

Figure 30. Smallest repetition unit that represents the sequence of D and A units of the chitooligosaccharides segments of chitosan modified bacterial cellulose. As the chitosan fragments of modified bacterial cellulose mainly contain chitotri- to hexasaccharides, only fragments (DP 3 – 6) of the calculated smallest repetition unit are observed.

1 to 5 D units changing with one or two A units characterize the sequence.
However, the average repetition unit does not respect the DP of the chitooligosaccharides, which is mainly 3, 4, and 5. Thus, typical sequences of chitooligomers that occur in the copolymer are DDD, DDA, DAA; DDDD, DD(DA), D(DA)A; DDDDD, DDD(DA), DADDA, and DADAA. These chitooligosaccharides are linked to blocks of in average 21 to 35 hexose units.
The experimental data allow for the conclusion that *Acetobacter xylinum* degrades chitosan with exogenous enzymes to chitooligosaccharides, which are able to penetrate the bacterial cell membrane. Putatively, the copolymer is biosynthesized by transglycosylation of activated

enzyme-bound intermediates of chitooligosaccharides. These intermediates are reported for the biosynthesis of glucans that are part of the cell wall of fungi.[222]

Besides glucose also mannose and fructose were detected as compounds of the hydrolysate of modified bacterial cellulose. Probably, these hexoses are contaminations of the copolymer caused by either extracellular bacterial polysaccharides or compounds of the culture medium. The present research results in the detailed knowledge of the molecular structure of chitosan modified bacterial cellulose and allows to establish a model for the biochemical details of the incorporation of chitosan into bacterial cellulose. Moreover the analytical methodology for the structure elucidation of this copolymer of chitosan and cellulose can be applied to any chitosan polymer or copolymer. Thus, the analysis of chitosan modified bacterial cellulose is an example for the practical use of the quantitative sequencing analysis of chitooligosaccharides.

Figure 31 summarizes the general steps that allow concluding the sequence of a chitosan polymer (or copolymer) based on quantitative GPC and MS data.

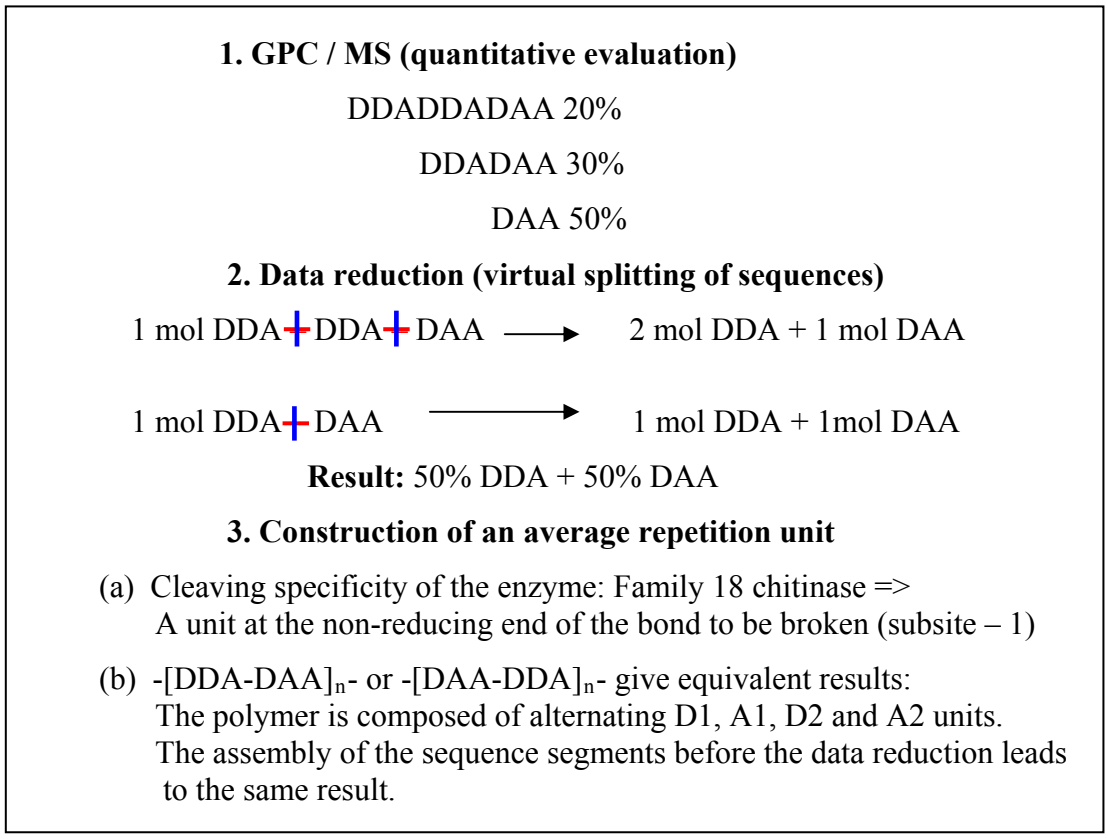

Figure 31. Summary of the general steps that are necessary to conclude the sequence of chitosan polymers (or copolymers) based on quantitative GPC and MS data. The given example corresponds to a chitosan sample from Genis ehf, Reykjavik, Iceland.

3.3 Preparation of a Library of Heterochitooligomers, Homologs and Isomers

Whereas the IEC proved less powerful for the analytics of ChOs compared to mass spectrometric methods, it was an important tool for the preparation of a library of pure homologs and isomers used for biological tests. Figure 32 summarizes the different combinations of GPC and IEC methods that were used for the preparation of pure homologs. The most effective combination proved to be IEC on SP Sepharose™ of the crude enzymatic hydrolysate of chitosan affording fractions, which contain molecules of identical charge numbers but different DP. The IEC fractions were further purified by GPC on Biogel P4™ resulting in pure homologs.

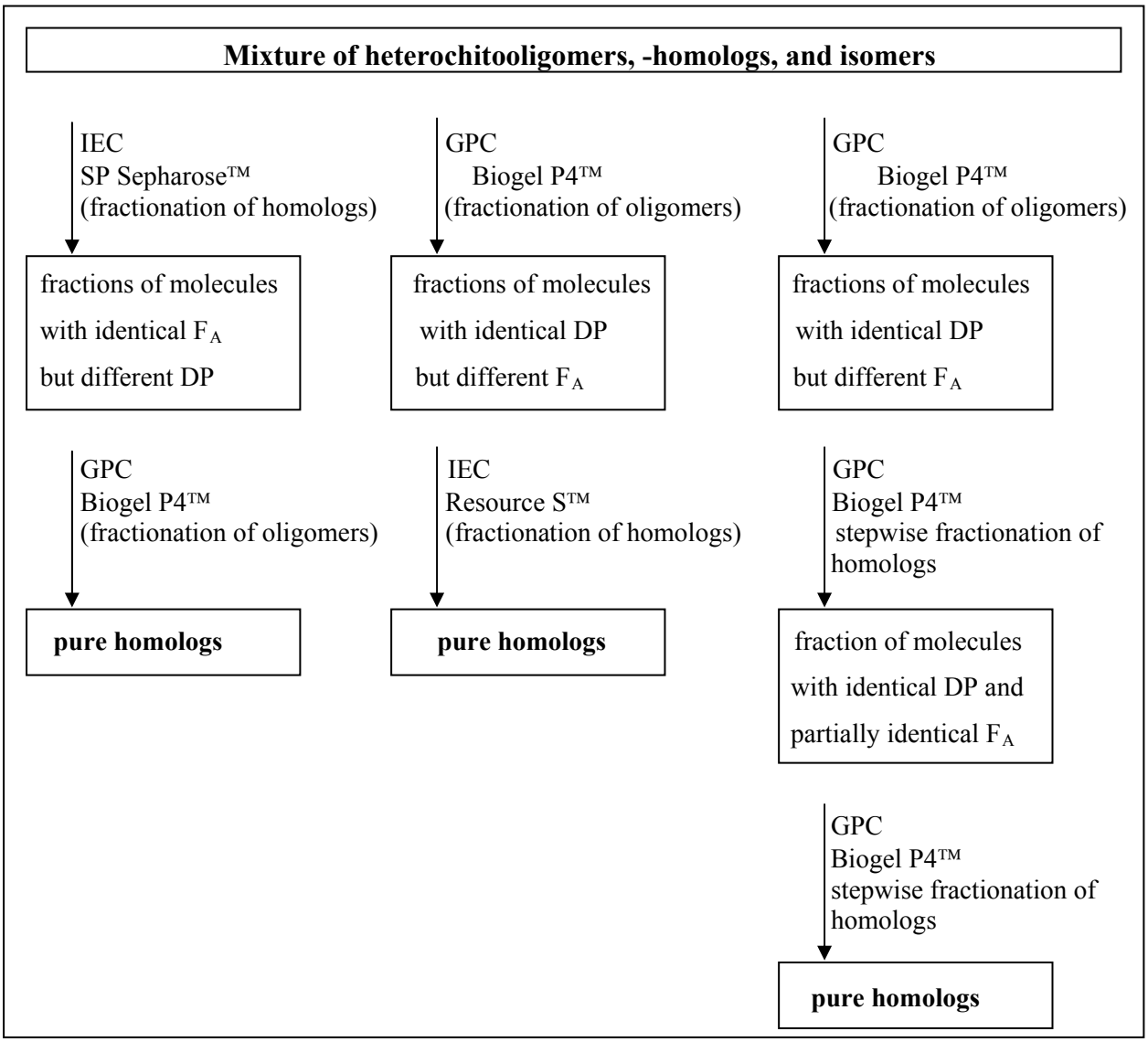

Figure 32. Scheme of the different combinations of GPC and IEC that were employed for the preparation of pure homologs in a milligram scale.

Additionally, GPC followed by IEC on Resource S™ material (a strong cation exchanger based on sulfonic acid groups), and GPC followed by two re-chromatographic steps on Biogel P4™ were applied for the preparation of pure homologs in a milligram scale (Figures 11 and S-7 in off-print 1). The cation exchange chromatography on SP Sepharose™ or Resource S™ separates molecules of different charge numbers (chitooligosaccharides by the number of D units). The gel permeation chromatography on Biogel P4™ separates molecules of different sizes, chitooligosaccharides mainly by DP. Therefore stepwise separations on Biogel P4™ afford pure homologs.

The purity of the homologs was in any case higher than 90%, typically 97+%. The isomeric composition was mainly determined by vMALDI-LTQ MS^n (and in a few cases by MALDI-QTOF Tandem MS or MALDI-TOF PSD MS). The combination IEC-GPC proved to be superior compared to GPC-IEC. The reason is that GPC fractions occasionally contain molecules of different DP but identical F_A as impurities (e.g. D_2A_3 and D_2A_4). These molecules are not separated by IEC resulting in overlapping or impurities, respectively. Table 4 summarizes the homologs (mass [%], purity [%]), which were prepared with the combination IEC-GPC.

Table 4. Results of the preparation of homologs employing the combination IEC-GPC. The purity was determined by MALDI-TOF MS (signal quantification). The masses of the homologs were calculated from the peak areas of IE and GP chromatograms with respect to the total mass of the starting material (chitosan hydrolysed, 7.5 g).

Oligomer	Homolog	Mass [%] resp. sample 2 (7.5 g)	Mass [mg]	Purity [%]
DP4	D_3A_1	0.007	0.5	95
	D_1A_3	0.220	16.5	66
DP5	D_3A_2	0.229	17.2	93
	D_2A_3	0.651	48.8	99
DP6	D_3A_3	0.308	23.1	100
	D_2A_4	0.016	1.2	97
DP7	D_4A_3	0.129	13.5	98
	D_3A_4	0.180	9.7	96
DP8	D_5A_3	0.045	3.4	96
	D_4A_4	0.127	16.3	100
DP9	D_3A_5	0.004	0.3	87
	D_4A_5	0.004	0.3	91
DP10	D_6A_4	0.023	1.7	94
	D_5A_5	0.021	1.6	90
DP11	D_6A_5	0.009	0.7	74
	D_5A_6	0.015	1.1	94
DP12	D_7A_6	0.008	0.6	91

Besides for homologs, IEC on Mono S™ was used for the preparation of pure isomers. Mixtures of isomers containing two or three components were partially separated, fractions were collected giving homologs with purities of ca. 91 – 100 % as determined by vMALDI-

LTQ MS^n or MALDI-QTOF Tandem MS. Repeated separations allowed to obtain pure DP 5 and 6 homologs in the scale of 0.5 mg. Table 5 summarizes the results.

Table 5. Results of the preparation of heterochitoisomers employing IEC on Mono S™ stationary phases. The chromatography was repeated with 200 µg of the starting material. The purity was determined by MALDI-TOF MS.

Oligomer	Homolog	Isomer	Mass [mg]	Purity [m%]
DP5	D_2A_3	ADDAA	0.4	100
		DADAA	0.5	100
DP6	D_3A_3	DADDAA	0.4	99
		DDADAA	0.4	91

Figure 9 in off-print 2 shows exemplarily the IE chromatogram of the separation of three D_2A_3 isomers. The sequences of elution of the isomers indicate that definite distances between the cation exchange groups (matching the distance of the ammonium groups of neighbouring D units) are the cause for the separation. That means, the general separation principle is the fractionation by charge number, which is identical for homologs and isomers. But for the separation of isomers, in addition, the distances of the cation exchange groups is crucial for the separation.

In conclusion, the model offers interesting perspectives for the development of new, specific materials for the separation of heterochitoisomers. Side chains of the backbone material bearing two cation exchange groups with definite spatial distance are a first step into this direction. Another promising perspective is the use of imprinting techniques for the preparation of a template, which is highly specific for a definite sequence of D and A units. On the other hand, the present studies give an insight into the interactions between chitinous material and putative receptors based on ionic forces (hydrogen bonds).

3.4 Interactions of Heterochitooligomers, Homologs and Isomers with Proteins

Inhibition of Chitinase A and B *Serratia marcescens*

The homologs and isomers prepared by chromatographic methods were employed for inhibition assays with chitinase A and B from *Serratia marcescens*, which is a soil bacterium. For the assay, a substrate analogue of the chitinase is added. For the inhibition assays on

chitinase A, 4-MU-A_3 (an analogue of A_4) was used. For chitinase B, 4-MU-A_2 (an analogue of A_3) was employed. Figure 33 summarises the hydrolysis reactions. Chitinase A releases 4-MU from 4-MU-A2 and 4-MU-A3 with almost equivalent hydrolysis rates.[223] Chitinase B, a chitotriosidase, releases 4-MU from 4-MU-A2. [223] The hydrolysis of the substrates is accompanied by the release of 4-MU, which is fluorescent in alkaline solutions (Figure 34).

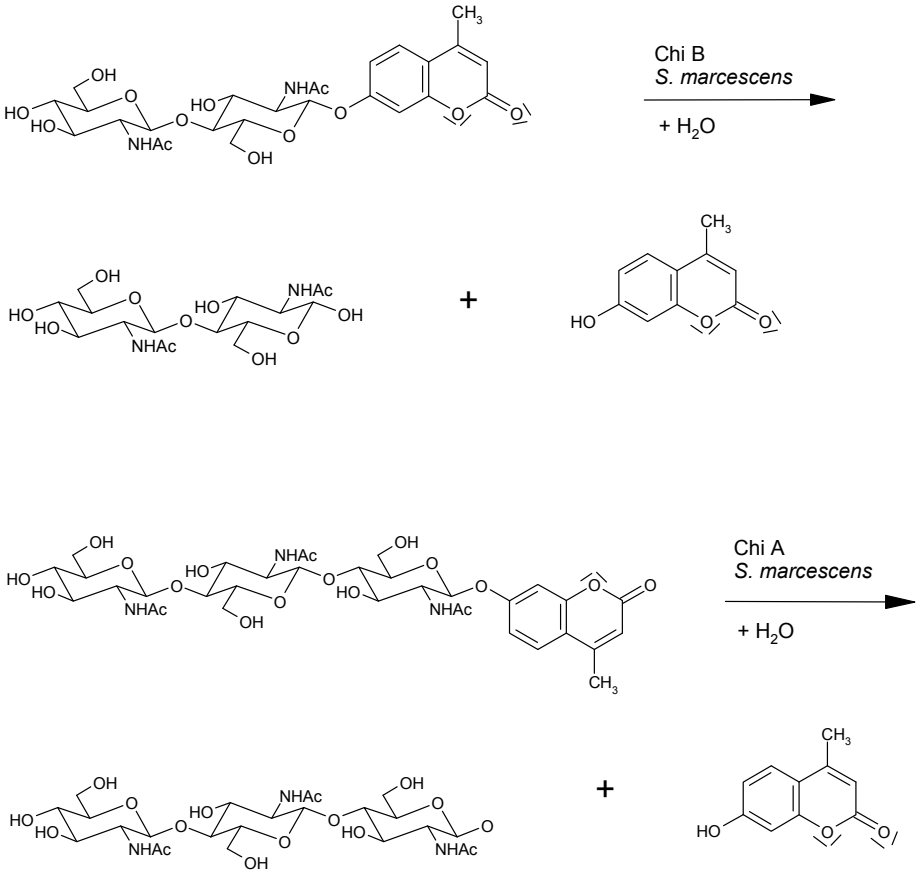

Figure 33. The hydrolyses of 4-MU-A_2 with chitinase B from Serratia marcescens affords A_2 and 4-MU. 4-MU-A_2 is an analogue of A_3. Chitinase B cleaves A_3 from the non-reducing end yielding A_2 + A_1. The hydrolyses of 4-MU-A_3 with chitinase A from Serratia marcescens affords 4-MU and a mixture of A3, A2 and A1. 4-MU-A_3 is an analogue of A_4. Chitinase A cleaves A_4 from the reducing end yielding A3 + A_2 + A_1.

Family 18 chitinases require stringently an A unit bound to subsite –1 for successful hydrolysis as the hydrolytic mechanism demands anchimeric assistance of the acetamido group of the A unit bound to subsite –1 (Figure 2).[86, 87, 88, 224] Any heterochitooligosaccharide that binds with a D unit to subsite – 1 is not hydrolysed by family 18 chitinases. It is an inhibitor as it prevents further binding and hydrolysis of the substrate (4-MU-A_2 or 4-MU-A_3). For the assay, the inhibition of the family 18 chitinase is notable by a decrease of the fluorescence intensity as less 4-MU is released. Heterochitooligosaccharides and 4-MU-A_2 /

4-MU-A_3 compete for the same binding site of chitinase A or chitinase B, respectively. Figure 35 summarises the basic steps of the fluorescence inhibition assay. Heterochitooligosaccharides are inhibitors that bind reversibly to the enzyme.

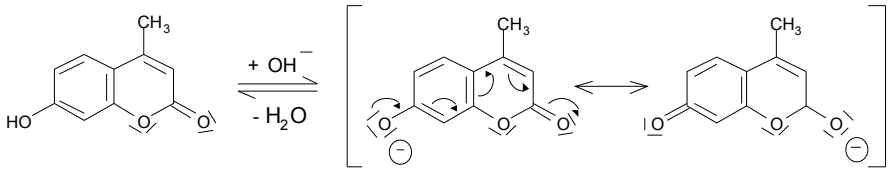

Figure 34. 4-MU is fluorescent in alkaline solutions. The hydroxy function is deprotonated, followed by a shift of electron pairs according to the arrows depicted in the structure giving a second resonance structure, which together form the resonance hybrid. The molecule is excited at 380 nm. Stokes with solvent molecules result in a partial loss of vibration energy of the excited 4-MU. The remaining vibration energy is spontaneously emitted in form of radiation if the life cycle of the excited state is long enough. The emission wavelength is consequently longer (460 nm representing less energy, respectively) than the excitation wavelength (380 nm).

The inhibition assays were run for 10 min to ensure that an equilibrium between the enzyme, the inhibitor and the substrate was established. The substrate was added in 80,000 fold molar excess to the enzyme, the inhibitor up to 1,600,000 fold molar excess. That means, the assay was performed under saturation of the binding site of the enzyme. In order to prevent substrate inhibition the substrate concentration was in the same range as the K_m of the substrate.

The inhibitor was added at different concentrations (0.25, 50, 100, 200, 400, and 800 µM) to the substrate (40 µM). The fluorescence signal is correlated to the concentration of 4-MU via a standard curve (Figure S8, Appendix). The concentration of 4-MU is used for the calculation of the specific activity of the enzyme (specific activity specific activity = 4-MU release [nmol] × sample volume [µL] / assay running time [s] × concentration of ChiA [mg × μL^{-1}]). A plot of the specific activity vs. the concentration of the inhibitor allows for the calculation of the IC_{50} concentration. The IC_{50} concentration is the concentration of the inhibitor, which causes a 50 % decrease of the activity of the enzyme. Tables 3 and 4 in off-print 4 summarise the IC_{50} concentrations for different oligomers and homologs inhibiting chitinase A and B at pH 5.5 (pH optimum of chitinase A and B) or 7.4 (physiological conditions), respectively.

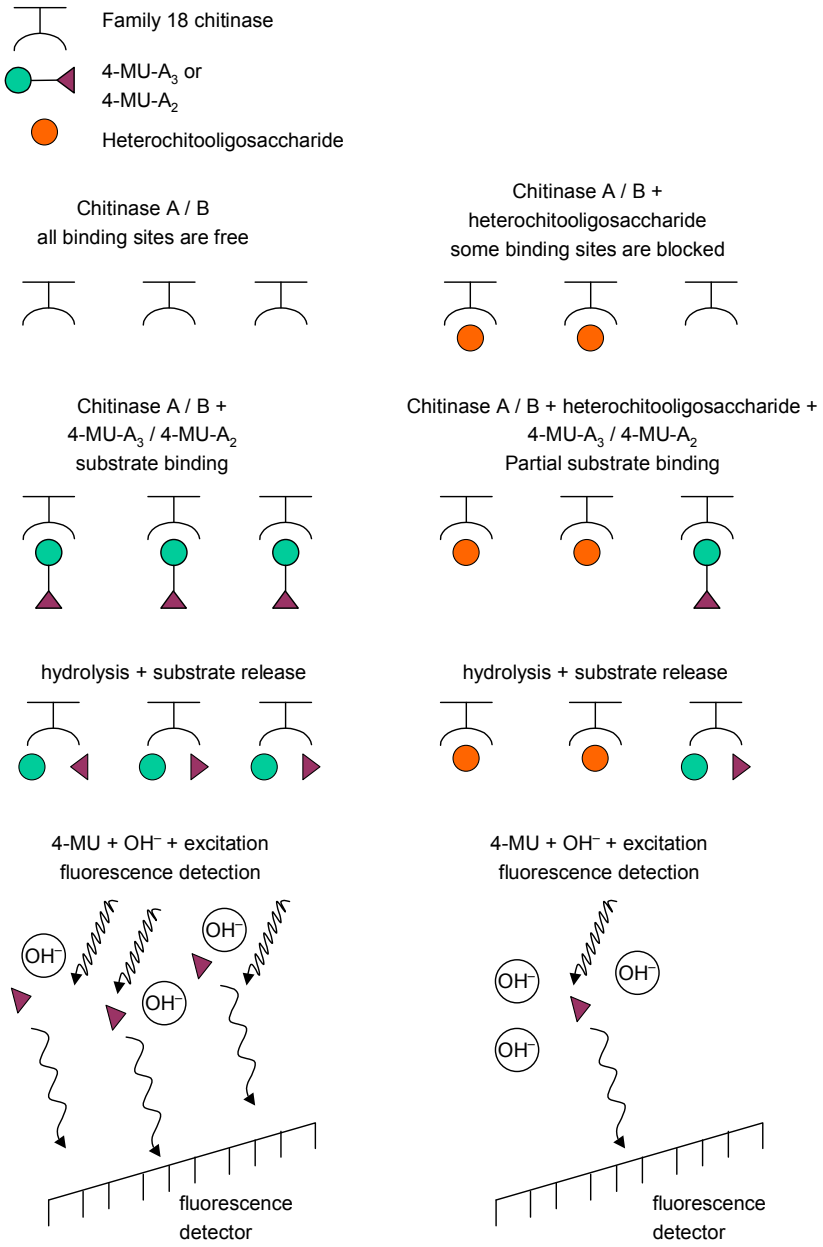

Figure 35. Fluorescence reduction assay. Chitinase A / B is incubated with the substrate (4-MU-A_2 / 4-MU-A_3). Hydrolysis of the substrate is accompanied with the release of 4-MU, which is fluorescent in alkaline solution. If chitinase A / B is incubated with a substrate under addition of heterochitooligosaccharides some of the binding sites of the enzyme are blocked by heterochitooligosaccharides that are not hydrolysed. Consequently, less substrate molecules are able to bind to the enzyme resulting in a reduced rate of hydrolysis leading to a smaller amount of 4-MU and reduced fluorescence.

A small IC_{50} concentration means that the heterochitooligosaccharide is a strong inhibitor. The IC_{50} concentration decreases with increasing DP of the heterochitooligomers. At DP 12 a plateau is reached, which means that above DP 12 no significant decrease of the IC_{50} concentration is observed. The IC_{50} concentration decreases with increasing F_A of the homolog, and depends on the sequence of the isomer (the IC_{50} concentration of DADDAA is

25% lower than that of DDADAA). However, the sequence dependency of the IC_{50} concentration is less significant than the dependency on F_A or DP. The IC_{50} concentration decreases with increasing pH, and the IC_{50} concentrations for chitinase B are lower than for chitinase A. Table 6 summarises the results.

Table 6. Summary of the dependency of the IC_{50} concentrations of heterochitooligosaccharides.

№	Effect	IC_{50}	Limit
1	DP ↑	↓	DP 12
2	F_A ↑	↓	F_A 1.00
3	pH ↑	↓	?
4	sequence	dependency	-. -
5	chitinase A or B	dependency	-. -

The present results can be compared to previous experiments of Letzel et al. and Cederkvist et al. (Table 7 in off-print 4).[225, 226]

The direct comparison of the results obtained for the DP 6 oligomers shows that in the present studies a lower IC_{50} concentration is obtained for chitinase A (÷ 2) whereas for chitinase B a higher IC_{50} concentration is obtained (× 7). Letzel et al. used mixtures of homologs with an average F_A of 0.50 whereas for the present studies a pure homolog (D_3A_3) of F_A 0.50 was used. Recently, Cederkvist et al.[226] reported on the inhibition of ChiB from *Serratia marcescens* at pH 6.1 (enzyme concentration of 2.5 nM) by ChO's of defined DP. A fraction of DP5 showed in apparent IC_{50} concentration of 16 µM, whereas the DP8 fraction gave an IC_{50} concentration of 18 µM. Comparible data were produced by Letzel et al.[225] for a fraction of DP5 oligomers giving an IC_{50} concentration of 15 µM for ChiB at pH 5.5. The experiments performed for the present thesis give an IC_{50} concentration of 106µM for the D_3A_3 homolog (DP6) representing a mixture of 51% DDADAA and 49% DADDAA. A possible explanation would be the fact that the fractions of DP5 oligomers contained ChO's of stronger inhibition potency than the well defined isomers DDADAA and DADDAA. Secondly, the IC_{50} concentrations show a strong pH dependency. Therefore, data recorded at pH 6.1 will generally show lower IC_{50} concentrations compared to data recorded at pH 5.5.

The IC_{50} concentration is the concentration of the inhibitor that causes 50% decrease of the activity of the enzyme.[227] A second constant is frequently used to describe the potency of an inhibitor. It is K_d, the concentration of ligand at which the binding site on a particular protein is 50% occupied ($K_d = [P] \times [L] / [C]$; [P]: concentration of protein with no ligand bound; [L]: concentration of ligand which is not bound; [C]: concentration of protein with ligand bound).[228] Even though both constants are obtained from different measurements. They are

closely related as 50% blocking of the binding sites will nearly result in 50% decrease of the enzyme activity. However, K_d takes into account that in the equilibrium not 100% of the binding sites are occupied. Both constants have the dimension of a concentration, and K_d values may be estimated from IC_{50} values. Thus, it makes sense to compare the measured IC_{50} concentrations to the K_d concentrations determined by other working groups (Table 7), which are at least in the same order of magnitude.

Table 7. K_d concentrations of chitin oligomers (DP3 – 6) inhibiting chitinase B (S. marcescens) at various pH values.

Authors	Enzyme	pH	Oligomer (homolog)	K_d [µM]
Hollis et al.[116]	Barley chitinase	7.0	DP3 (A_3)	19
			DP4 (A_4)	6
Fukamizo et al.[31, 115]	Chitinase I Coccidioidis immitis	8.4	DP4 (A_4)	50
	Lysozyme	5.0	DP3 (A_3)	9
Chipman et al.[117]	Lysozyme	5.4	DP3 (A_3)	9
Dalal et al.[229]	Chitinase A E315L *Serratia marcescens*	5.0	DP3 (A_3)	22
			DP4 (A_4)	3
			DP5 (A_5)	0.06
			DP6 (A_6)	0.07

Another obstacle against the proper comparison of experimental data is the fact that different authors used different chitinases and experimental conditions (e.g. pH). Generally the IC_{50} or K_d concentrations of chitooligosaccharides are in the range of µM. (It should be mentioned at this point that Dalal et al. found K_d concentrations of 60 / 70 nM for A_5 / A_6 with respect to Chitinase A E315L (*S. marcescens*) employing fluorometric titration at pH 5.0.[229] These exceptional experimental results could neither be confirmed by other authors nor by the results presented in this thesis.) Allosamidin is the classical inhibitor of chitinases. The structure of allosamidin is depicted in Figure 36.

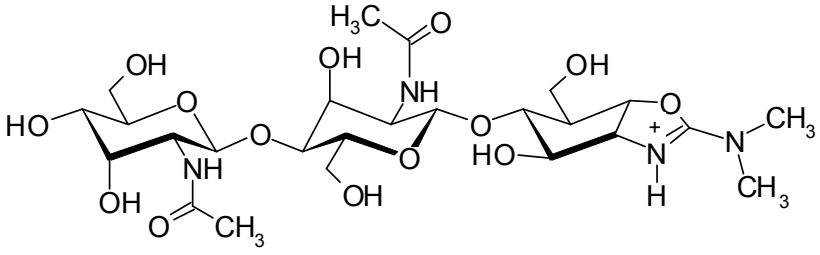

Figure 36. Structure of the chitinase inhibitor allosamidin. Allosamidin mimics the transition state of the hydrolysis of ChO's.

Table 8 summarizes the IC_{50} and K_i concentrations that were determined for the inhibition of chitinase B with allosamidin. Allosamidin inhibits chitinase B at pH 5.4 with an IC_{50}

concentration of 2.5 µM.[99] D_7A_5 inhibits chitinase B at pH 5.5 with an IC_{50} concentration of 23.3 µM, which is roughly tenfold.

Table 8. Inhibition of chitinase B with allosamidin.[99]

pH	IC_{50} [µM]	K_i [µM]
5.4	2.5	1.4
6.1	0.4	0.2
7.2	0.2	0.1
8.0	0.07	0.04

The observation that chitooligosaccharides with DP > 12 show no significant increase in inhibition potency allows for the conclusion that the IC_{50} / K_d concentrations even of the polymeric chitosan will not be significantly lower.

The inhibitory effect of heterochitooligosaccharides depends on two limiting factors: first the affinity to the binding sites of chitinase A / B, and secondly the stability against hydrolysis. Both effects are opposite. The affinity of heterochitooligosaccharides to the binding sites of chitinase A and B (and chitinases in general) is correlated to the number of A units. Chitin oligomers of DP ≥ 12 or polymeric chitin show the strongest affinities to chitinases. (This would be expected, as chitin is the natural substrate of chitinases.) On the other hand, chitin of F_A 1.00 consists exclusively of A units and is therefore cleaved with the highest rate of hydrolysis. The IC_{50} concentrations of the series of DP6 homologs (D_6, D_3A_3, D_2A_4) shows that the IC_{50} concentration significantly decreases for homologs up to F_A 0.50.

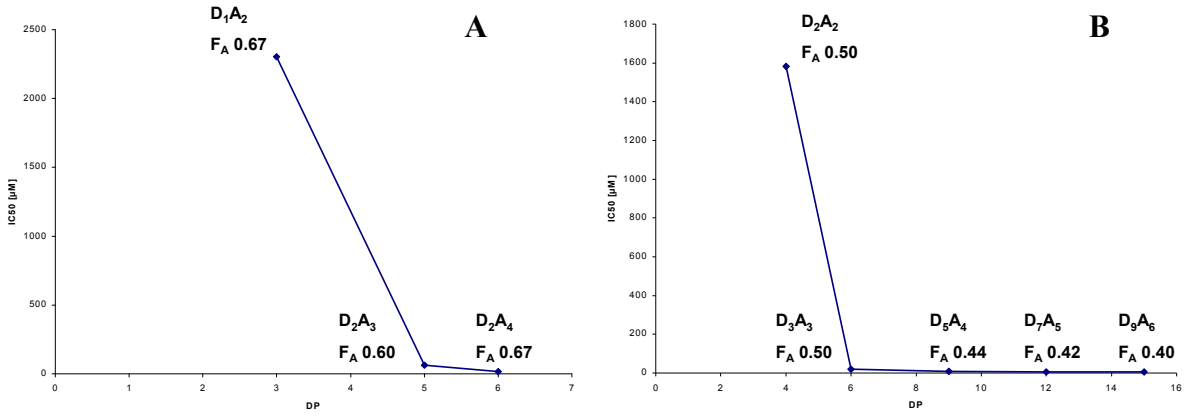

Figure 37. A. Correlation of the IC_{50} concentration with the DP of ChO's with an F_A of 0.60 – 0.67. B. Correlation of the IC_{50} concentration with the DP of ChO's with an F_A of 0.40 – 0.50.

Heterochitooligosaccharides of F_A 0.50 – 0.67 reflect the optimal compromise between affinity on one hand and stability against hydrolysis on the other hand so that heterochitooligosaccharides of an F_A around 0.50 are the strongest inhibitors of chitinase A

and B with the lowest IC_{50} concentrations. Figure 37 summarizes the IC_{50} concentrations of heterochitooligomers of (nearly) constant F_A. The IC_{50} concentrations most significantly decrease from DP3 to DP9.

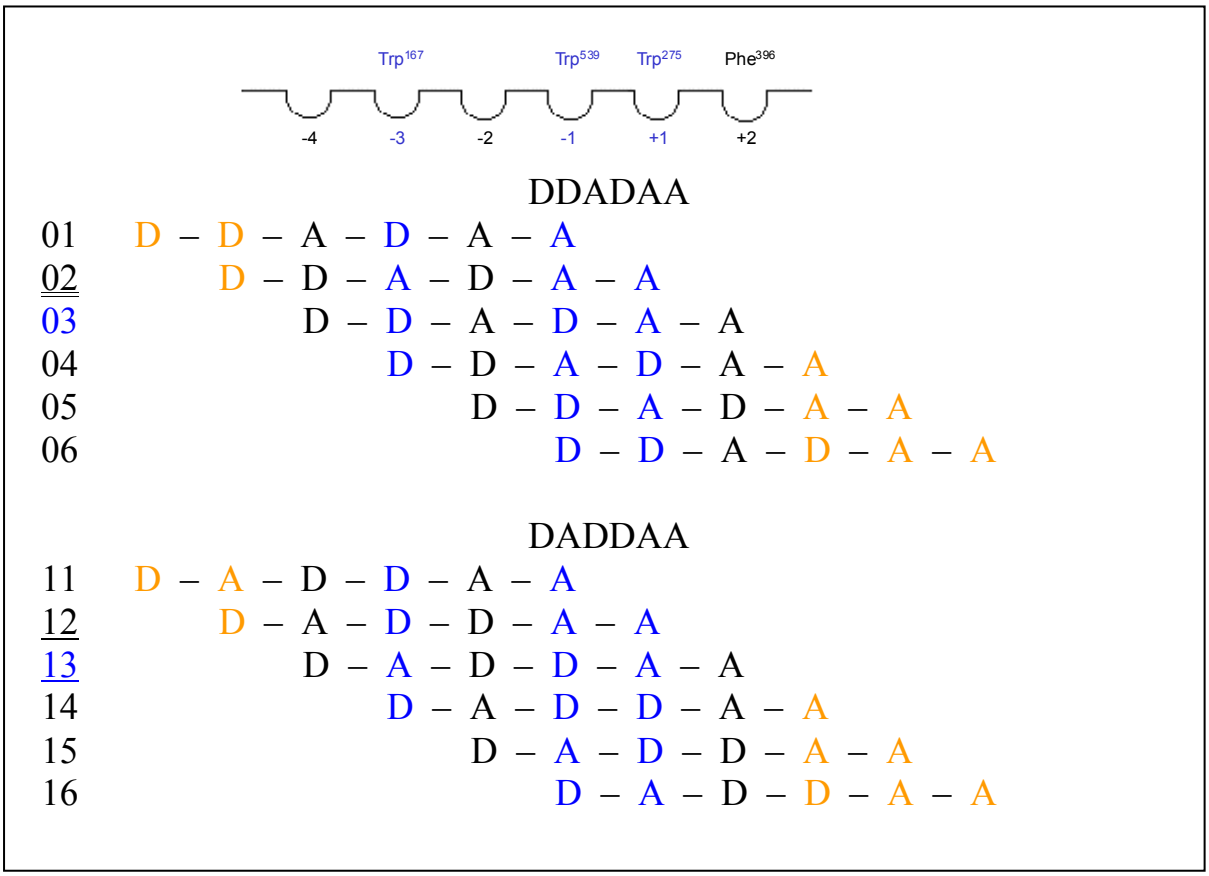

Figure 38. Alignment of the isomers DADDAA and DDADAA to the carbohydrate binding domain of chitinase A. Only the core subsites (-4 to +2) are regarded. It is assumed that subsites < -4 and > +2 do not contribute significantly to binding. Monomer units extending beyond subsites –4 to +2 are coloured red, monomer units aligned to subsites –3, -1 and +1, which mainly contribute to hydrophobic interactions, are coloured blue. Each alignment is signed with a code. Alignments resulting in two hydrophobic interactions are signed with an underlined code, alignments resulting in three hydrophobic interactions are signed with a double underlined code. Alignments -4⟶ +2 are signed with a blue code number.

Each homolog employed for the determination of the IC_{50} concentrations represents a mixture of isomers. Isomers differ in the sequences of A and D units. The most detailed look on the affinity of ChO's to chitinase A / B and their stability against hydrolysis is based on the sequences of isomers. A mixture of two isomers (51 % DDADAA and 49 % DADDAA, IC_{50} 19.7 µM at pH 7.4) was separated by chromatography. DDADAA shows an IC_{50} of 21.1 µM, DADDAA shows an IC_{50} of 15.9 µM. The difference is not high but significant. The exemplary analysis of the binding modes of both isomers to chitinase A should answer the question whether the difference results from different affinities or different stabilities against hydrolysis. The affinity of ChO's to chitinase A / B is on one hand the result of hydrophobic

interactions between the hydrophobic sites of A units and hydrophobic amino acid residues of definite subsites of the binding bag of chitinase A. Secondly hydrogen bonds between amino acids of the binding bag and -OH or -NH groups of A or D units contribute to the overall affinity.[90, 91, 92, 100] Hydrogen bonds are formed unspecific with any subsite of the enzyme. Decisive for differences in affinities are mainly hydrophobic interactions. The core subsites of chitinase A (-4 to +2) bear three hydrophobic amino acid residues, which significantly contribute to the hydrophobic interactions with chitooligosaccharides. These are positioned at subsite –3 (Trp^{167}), -1 (Trp^{539}), and +1 (Trp^{275}). A minor hydrophobic interaction is measured with the hydrophobic amino acid residue positioned at subsite +2 (Phe^{396}).[90] Figure 38 shows all alignments (binding modes) -3 → -1 to -1 → +2 of the isomers DADDAA and DDADAA. There are four different ways for the evaluation of the data from the alignment of the sequences.

1. All different alignments of a sequence are regarded. The number of hydrophobic interactions between A units and subsites –3, -1, and +1 are counted and summed up for each isomer.
2. Only alignments are regarded, for which three or minimum two hydrophobic interactions are obtained.
3. Only alignments are regarded, for which minimum three hydrophobic interactions are obtained.
4. Only one alignment per isomer is regarded. It is the alignment, for which all monomer units of the isomer are aligned to one of the subsites –4 to +2.

Table 9 summarises the results of the different evaluation methods 1 – 4.

Table 9. Summary of the different evaluation methods 1 – 4 for the alignment of the D_3A_3 isomers DDADAA and DADDAA.

D_3A_3 isomer	IC_{50} [µM] (fluorescence assay)	Number of hydrophobic interactions (evaluation method 1)	Number of hydrophobic interactions (evaluation method 2)	Number of hydrophobic interactions (evaluation method 3)	Number of hydrophobic interactions (evaluation method 4)
DDADAA	21.1	7	3	3	1
DADDAA	15.9	7	4	0	2

DADDAA has a lower IC_{50} concentration compared to DDADAA. That means DADDAA has a higher affinity to chitinase A than DDADAA assuming that hydrolysis during the assay running time is not decisive for the IC_{50} concentration. Only evaluation methods 2 and 4 reflect the experimental results correctly. That means the prediction of affinities of isomers (and ChO's in general) has to be based either on alignments with two and three hydrophobic

interactions or has to be based on alignments for which all monomer units of the isomer are aligned to one of the core subsites (-4 to +2 for chitinase A, -3 to +3 for chitinase B and HC gp-39). For both evaluation methods DADDAA has more hydrophobic interactions than DDADAA.

Hydrolysis takes place between subsites –1 and +1. For the -4 → +2 binding mode hydrolysis neither occurs on DADDAA nor DDADAA. DADDAA can be only hydrolysed in the –2 → +2 binding mode, whereas DDADAA can be hydrolysed in the -3 → +2 binding mode. The study of the hydrolysis of D_3A_3 with chitinase A for 12 h (37°C, pH 7.4) confirms these theoretical considerations (Table 5 in off-print 4).

Moreover, the hydrolysis study on D_3A_3 with chitinase A for 10 min (assay running time, 37°C, pH 7.4) reveals only minor degradation (molar ratio of the enzyme to the inhibitor 1:1,600,000). This result is in accordance with the fact that -A-D- bonds are cleaved with a low hydrolysis rate (in contrary to -A-A- bonds), and with the fact that the hydrolysis takes place only for disfavoured binding modes (–2 → +2 or –3 → +2, respectively). Moreover, the molar ratio of the enzyme to the inhibitor is 1:1,600,000 so that the binding site of chitinase A is even after 10 min still saturated with the inhibitor.

In conclusion, the IC_{50} concentrations measured for DADDAA and DDADAA reflect differences in affinities rather than differences in stabilities against hydrolysis.

The IC_{50} concentrations for chitinase B are lower than for chitinase A with respect to identical homologs and assay conditions (Tables 3 and 4 in off-print 4, pH 5.5). The reason for this observation are higher affinities between ChO's and chitinase B due to the more closed structure of this enzyme (chitinase B: tunnel-like structure; chitinase A: groove-like structure; Figures 3 B; 8 C, D).[100]

The affinities of ChO's to chitinase A / B increase with higher pH as the non protonated amino functions of D units are more non-polar (hydrophobic), and consequently less interfere with the hydrophobic binding sites of the protein.

The affinities of DP 1 and 2 oligomers to chitinase A and B are low.[90, 100] This is an important fact as A_2 is the main product of the enzymatic hydrolysis of the natural substrate chitin. If A_2 would strongly bind to chitinase A or B it would inhibit these enzymes with unfavourable biological effects on plants, insects and other organisms. Above DP12 no significant increase of affinities is observed as the chitin binding domain possesses only a limited number of subsites. For all subsites that are not aligned with aromatic amino acid residues the A unit could be replaced by a D unit with no significant decrease in affinity. The fact that ChO's bind in different modes to chitinase A and B complicates the identification and preparation of

inhibitors on base of heterochitooligosaccharides. However, the present work could demonstrate that a potent chitinase A or B inhibitor should on one hand not be cleaved (requiring D units), and on the other hand should bind strongly to the hydrophobic amino acid residues (requiring A units). A strong binding requires as well that no monomer unit extends subsite +2 in the case of chitinase A or subsite -3 in the case of chitinase B. E.g. a heterochitohexamer binding in the -3 → +2 mode to chitinase A will show an affinity equivalent to heterochitopentamers as one monomer unit takes not part in the binding to the enzyme. Secondly a strong binding requires that subsites +1 and +2 of chitinase A or -1 and -2 of chitinase B are involved in substrate binding as otherwise monomer units are cleaved off, which are less favoured products compared to dimers. Thus, only the well-defined binding modes -X → +2 in the case of chitinase A or -2 → +X in the case of chitinase B significantly contribute to the affinities. In conclusion, any ChO with a D unit in subsite -1 in the -X → +2 binding mode (chitinase A) or -2 → +X binding mode (chitinase B) and additionally as many A units as possible in the other subsites will be a good inhibitor of these enzymes e.g. AAADAA: D unit in subsite -1 of chitinase A in the -4 → +2 binding mode or DADDAA: D unit in subsite -1 and D units in the even numbered subsites (-2 and -4).
A model explaining the affinities to chitinase A regarding only binding modes -X → +2 was feasible to explain the results of the present studies thus justifying this approach.
Chitosan (partially deacetylated chitin) is not a natural substrate of chitinases. Thus, chitinase A / B are not optimised for the hydrolysis of chitosan. Whereas chitin of F_A 1.00 would be completely hydrolysed mainly to dimers and none of the hydrolysis would block the enzyme and slow down its activity, the reaction products of the artificial substrate chitosan partially block the enzyme and slow down its activity.
Nevertheless chitinases are used in many technical processes although they are not optimised for the hydrolysis of chitosan. Thus, the results of the present studies are important for an optimal reactor design. As the hydrolysis products inhibit family 18 chitinases, the results of the present studies demand for a continuous flow reactor where the products of the reaction products are deducted from the enzyme (Figure 39).
Moreover, the results contribute to the prediction of the products of the partial hydrolysis of chitosan employing family 18 chitinases. Chitinase A and B are processive enzymes. In an idealistic scenario a chitin chain consisting only of A units once binds to the chitin binding domain and is never desorbed from the surface of the protein before it is completely hydrolysed to dimers and a low amount of trimers / monomers). In case that the chain contains D units the rate of desorption is increased and processing is not always productive

resulting in the release of ChO's that are resistant against further hydrolysis. Figure 40 shows exemplarily that a polymer consisting of repetitive DDADAA units will give mainly DDADAA (D_3A_3) oligomers when it is hydrolysed with a processive family 18 chitinase. Hydrolysis of the reaction products will occur only slowly as the affinity of DDADAA in the -3 → +2 binding mode required for hydrolysis is slow.

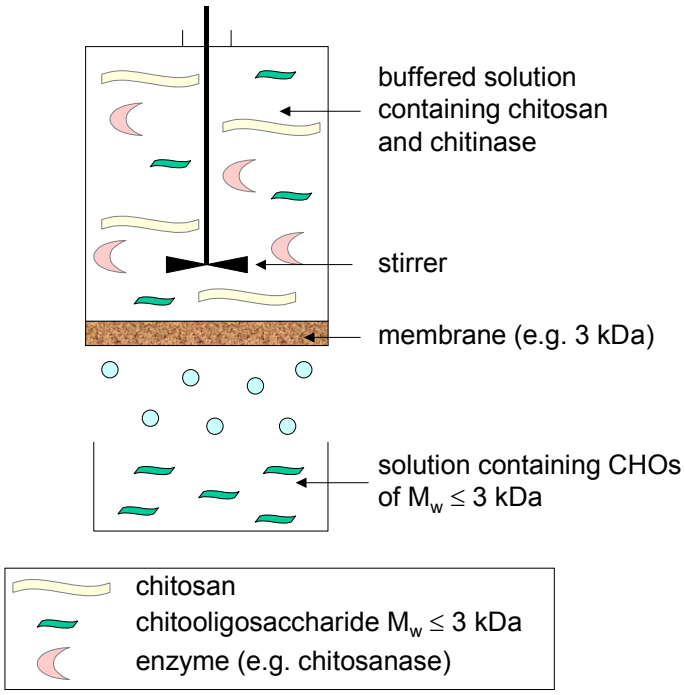

Figure 39. Continuous flow reactor. Chitosan is degraded with chitinase to ChO's. ChO's with $M_w \leq 3$ kDa pass through the membrane. Chitosan remains in the reactor (as well as the enzyme).

Figure 40. Hydrolysis of a chitosan with the sequence $[DDADAA]_n$ with a family 18 chitinase. Even though the processive hydrolysis of chitin yields dimers, D units in the sequence have the effect that the binding is not productive whenever a D unit is bound to subsite -1. Red letters symbolise D units bond to subsite -1 resulting in non-productive binding, green letters symbolise A units in subsite -1 resulting in productive binding. Vertical lines mark scissile bonds (red = no hydrolysis, green = hydrolysis).

A vital function of chitinases is essential for many human parasites like fungi, nematodes or plasmodia. Also insects use chitinases in their life cycle (ref. chapter 1.4.1). Therefore chitinase inhibitors are potential drugs to fight against human parasites and pathogens. Further studies on promising ChO's (e.g. isomers like DADDAA) have to prove whether their

affinities to family 18 chitinases and their stabilities against hydrolysis under physiological conditions in vivo are strong enough to be used as drugs.

A potent inhibitor is not only characterised by a strong inhibitory effect on the targeted protein but also characterised by little side effects that means low affinities to other proteins. For applications of ChO's in humans has to be regarded that family 18 chitinases were also found in the human body (up to now HCT and AMCase, ref. Chapters 1.4.9, 1.4.10). Human chitinases are part of the defence mechanism against chitin containing pathogens.[74, 75] The blocking of human chitinases could therefore lead to an impaired immune system.

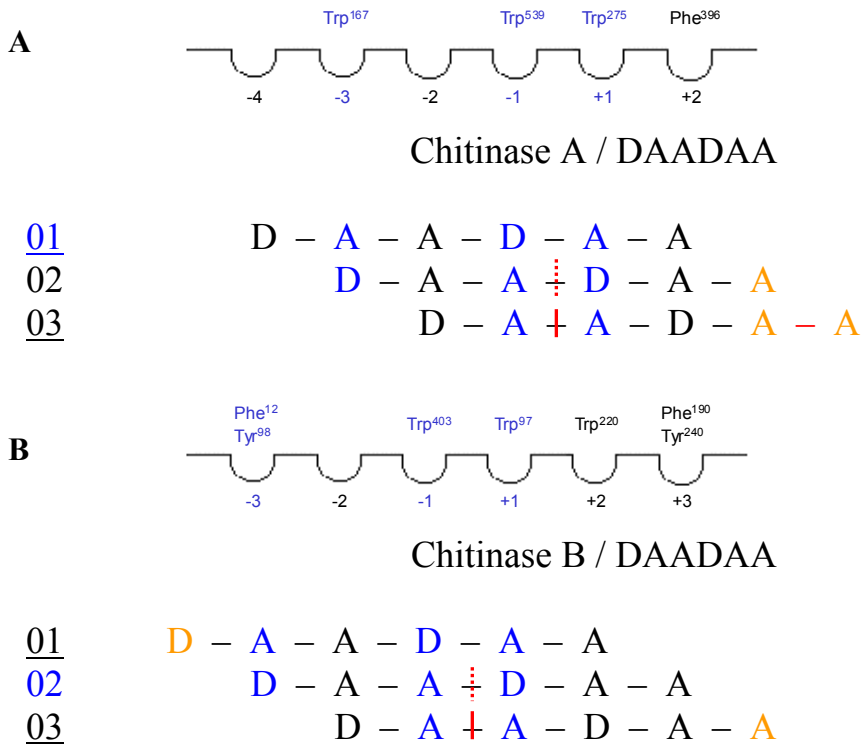

Figure 41 A, B. Comparison of the binding of DAADAA (D_2A_4) to chitinase A or chitinase B, respectively. In the case of chitinase A, two hydrophobic interactions are found for alignment A01, which represents the most stable complex as all core subsites of chitinase A are aligned with monosaccharide units and two hydrophobic interactions are formed. Hydrolysis does not occur in this alignment as a D unit is positioned in subsite –1. Alignment A03, which allows for a fast hydrolysis, is very unfavourable, as two monomer units extend beyond subsite +2. In the case of chitinase B alignment B01 does not occur in reality as the binding site of chitinase B is locked beyond subsite -3. Alignment 03 becomes most favourable as two hydrophobic interactions are formed. Hydrolysis is fast in this alignment as an A unit is positioned in subsite -1 and – A – A – is the scissile bond. Monomer units extending beyond the core subsites are coloured red, monomer units aligned to subsites -3, -1 and +1, which mainly contribute to hydrophobic interactions, are coloured blue. Each alignment is signed with a code. Alignments resulting in two hydrophobic interactions are signed with an underlined code. Alignments -4→ +2 and -3 → +3 are signed with a blue code number. Red lines mark bonds that are fast hydrolysed, red dashed lines mark bonds that are slowly hydrolysed.

Consequently, research is under progress to develop chitinase inhibitors that are specific in their inhibitory effect on chitinases of pathogens and have less or no inhibitory effect on human chitinases.[76] The binding site of HCT has a similar structure as the binding site of chitinase B. An inhibitor based on ChO's that inhibits chitinase A but not chitinase B could be DAADAA (Figure 41).

The experiments presented in this thesis allow studying the chitin binding domains and the catalytic domains of chitinase A and B. E. g. the affinities of ChO's up to DP15 demonstrate that the number of subsites of the chitin binding domain and the catalytic domain is limited to 12. Heterochitooligosaccharides that differ in only one D unit in the sequence indicate subsites of the enzyme that significantly contribute to the hydrophobic interactions. The present results show that the subsites of chitinase A become more shallow with increasing distance from the core of the catalytic cleft (subsites -3 to +2); this gradient of increasing interactions (mainly hydrophilic interactions) is an important part of the processive action of chitinase A.

Affinities of Heterochitooligomers, Homologs, and Isomers to the Human Cartilage Glycoprotein of M_w 39 kDa

Finally, the affinity experiments on chitinase A and B have model character for the affinities of ChO's towards catalytically inactive chitolectins, which are evolved from family 18 chitinases. In general, lectins are receptors for oligosaccharide structures (glycans). Membrane bound lectins mediate interactions between cells. Unbound lectins participate in various signalling pathways. Besides other organisms, lectins were identified in the human body. Among the group of human lectins, human chitolectins are of special interest as they putatively involve ChO's in human signalling cascades (ref. Chapters 1.5, 1.6). HC gp-39 (YKL-40) is a human chitolectin as it was reported that chitin fragments (chitin oligosaccharides) bind to HC gp-39 with K_d concentrations in the range of μM (or reciprocal affinity constants in the range of 10^6 M) resulting in a conformational change of the protein.[187] However, the natural ligands and mechanism of action of HC gp-39 are still unknown. The protein could interact with heparin sulfate, hyaluronan, chitooligomers that synthesized as primers for hyaluronan biosynthesis, and/or the chitobiose-cores of *N*-glycans.[173]

HC gp-39 is a potent growth factor, inducing cell proliferation through activation of protein kinase B and extracellular signal-regulated kinase 1 / 2 mitogen-activated protein kinase signalling pathways.[174] HC gp-39 is over expressed in several severe diseases like rheumatoid

and osteoarthritis,[230] fibrotic liver[231] and some types of cancer.[159] HC gp-39 participates in the regulation of the synthesis of the extracellular matrix in human chondrocytes.[232] Heterochitooligosaccharides are of special interest as it was reported that they possess a therapeutic potential in patients suffering from inflammatory polyarthritis.[181] Furthermore, certain partially acetylated ChO's are strong competitive, mechanism-based inhibitors of the family 18 chitinase B from *S. marcescens*.[225] The binding site of this enzyme has a striking similarity to the binding site of HCT, a human family 18 chitinase. It is reasonable to assume that inhibitors of chitinase B based on the introduction of D units into chitin homooligomers are not or slowly hydrolysed by HCT resulting in an increased biostability in the human body. Therefore it was of interest to investigate the mode of binding of a series of DP6 homologs with differing F_A to HC gp-39. As well the binding of a DP11 oligomer was studied in order to analyse the influence of the DP on the strength of interaction.

The affinities of non-covalent complexes between ChO's and HC gp-39 were analysed by measuring the difference of the intrinsic tryptophane fluorescence of the protein in the absence resp. presence of a ligand. The change of the fluorescence intensity is caused by ligand-induced changes of the solvent layer covering the tryptophan residues of the binding site. The fluorescence of the tryptophan residues is proportional to the formation of the ligand-protein complex. A plot of the relative fluorescence intensity vs. the concentration of the inhibitor gives a binding isotherm (saturation curve) for each ChO. For $c(ChO) \rightarrow \infty$ the fluorescence signal equals the fluorescence intensity for all protein molecules (binding sites) in the state of complexation, which is a constant (B_{max}). The general form of the binding isotherm is the following: $F\text{-}F_0 = B_{max} \times c / (K_d + c)$ (linear regression, one-binding-site model). $F\text{-}F_0$ is the relative intensity of the fluorescence signal. c is the concentration of the inhibitor. K_d is the concentration at which 50% of the binding sites of the protein molecules are occupied. At the same time K_d is the constant of the protein-ligand complex dissociation equilibrium. $K_d = [P] \times [L] / [C]$ ([P], [L] and [C] represent the concentrations of the protein, ligand and complex). Figure 3 in off-print 5 summarises the binding isotherms of the DP6 homologs and a DP11 oligomer, Table 2 in off-print 5 shows the resulting dissociation constant (K_d).

Within the series of DP6 homologs the values for the dissociation constant decrease with increasing F_A (Figure 4 in off-print 5). The DP11 homolog D_5A_6 showed a higher affinity than the hexamer A_6.

Table 10. Summary of the equilibrium association constants K_a (reciprocal dissociation constants) for DP6 homologs with respect to HC gp39. Additionally, the relative affinities of the series of DP6 homologs are given with respect to A_6 (100%).

Homolog	K_a [μM^{-1}]	rel. affinity [%]
D_6	0.002	3
D_3A_3	0.020	27
D_2A_4	0.025	34
A_6	0.073	100
D_5A_6	0.145	-.-

The relative affinities given in Table 10 indicate that the D_3A_3 DP6 homolog (F_A 0.50) recovers ca. 1/3 of the affinity of A_6 (F_A 1.00). A_6 marks the homolog of highest affinity among the DP6 homologs. A_6 shows 1/2 (50 %) of the affinity of D_5A_6.

Houston et al. reported for HC gp-39 K_d values of 6.7 µM for A_6 and 331 µM for A_4.[187] We found a similar K_d for A_6 (13.7µM) while the affinity of D_6 (K_d = 420 µM) is even lower than for the tetramer A_4. D_3A_3 and D_2A_4 show much higher affinity then the tetramer A_4.

For the explanation of these findings one has to take a detailed look on the subsites of HC gp-39 on one hand, and on the isomer composition of the homologs employed for the affinity studies on the other hand. Table 1 in off-print 5 summarises the composition of the isomers comprising the DP6 homologs employed for affinity studies.

The binding site of HC gp-39 is divided into subsites –6 to +3 according to Houston et al. (based on crystallographic data obtained from complexes of HC gp-39 with A_4, A_6, and A_8).[187] Alternatively, two distinct binding sites with a distance of 10 Å are discussed in the literature.[189] In this case chitin homooligomers of DP > 3 occupy a binding site, which is divided into subsites –3 to +3 whereas dimers and trimers occupy the distal binding site, which is divided into two subsites.

The present results show that D_5A_6 shows two times the affinity to HC gp-39 than A_6. Both molecules bear the same number of A units (6) so that D_5A_6 obviously occupies additional subsites compared to A_6, which occupies subsites -3 to +3. Therefore, it is reasonable to assume that chitooligomers of DP > 6 extend beyond subsite -3 and occupy both binding sites at the same time.

This discussion is not reasonable for the explanation of the differences of the affinities of DP6 homologs. The core subsites of HC gp-39 (-3 to +3) bear three hydrophobic amino acid residues, which significantly contribute to the hydrophobic interactions with chitooligosaccharides. These are positioned at subsite –3 (Trp^{31}), -1 (Trp^{352}), and +1 (Trp^{99}). Minor hydrophobic interactions are measured with the hydrophobic amino acid residues positioned at subsites +2 (Phe^{208}) and +3 (Trp^{212}).[187, 188]

Figure 5 in off-print 5 shows all alignments (binding modes) -3 → -1 to -1 → +3 of the sequences of the DP6 homologs D_6, D_3A_3, D_2A_4 and A_6. There are four different ways for the evaluation of the data from the alignment of the sequences.

1. All different alignments of a sequence are regarded. The number of hydrophobic interactions between A units and subsites -3, -1, and +1 are counted and summed up for each isomer and weighted by the contribution of the isomer to the amount of the homolog. Finally the weighted hydrophobic interactions of the isomers are summed up to the overall number of hydrophobic interactions of the homolog.
2. Only alignments are regarded, for which three or minimum two hydrophobic interactions are obtained.
3. Only alignments are regarded, for which minimum three hydrophobic interactions are obtained.
4. Only one alignment per isomer is regarded. It is the alignment, for which all monomer units of the isomer are alignment to one of the subsites -3 to +3.

Table 3 in off-print 5 summarises the results of the different evaluation methods 1 – 4.
All four methods result in the correct order of affinities $D_6 < D_3A_3 < D_2A_4 < A_6$. Method 4 overestimates the affinity of the D_2A_4 (+50 %), whereas method 3 reflects the differences of affinities of D_3A_3 and D_2A_4 well but under estimates the absolute affinities of these two homologs (D_2A_4 –26 %, D_3A_3 –37 %). Nevertheless the comparison of the evaluation methods allows concluding that methods three and four reflect the results of the fluorescence assays best (method 3: only three hydrophobic interactions per alignment are regarded; method 4: only one alignment per isomer is regarded (all core subsites -3 to +3 are aligned with monosaccharide units)).
Figure 42 compares the binding sites of chitinase A, chitinase B and HC gp-39. Regarding only the core subsites, all three family 18 proteins (two chitinases and one chitolectin) reveal a high homology. Involving all subsites described in the literature differences become evident. HC gp-39 like chitinase A show an extension of the binding site towards negative subsites (non-reducing end) whereas chitinase B shows an extension of its binding site towards positive subsites (reducing end, ref. chapter 1.4.8). The reason for this difference is to find in the different modes of hydrolysis for chitinase A and B: Chitinase A hydrolyses chitin from the reducing end whereas chitinase B hydrolyses chitin from the non-reducing end.

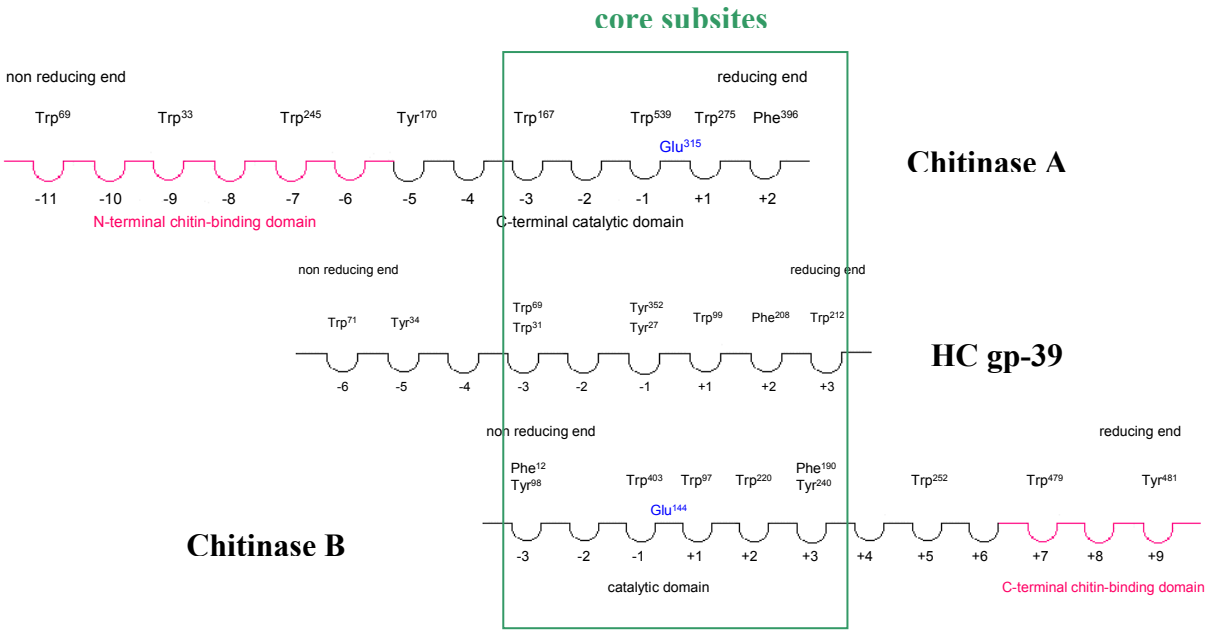

Figure 42. Comparison of the binding sites of chitinase A, chitinase B and HC gp-39. Subsites -3 to +3 are the core subsites for chitinase B and HC gp-39 whereas for chitinase A the core subsites A -3 (-4) to +2.

Consequently, affinity studies on HC gp-39 can be replaced by affinity studies on chitinase A. Either on active chitinase A (as for the present studies) if affinity data should involve stability against hydrolysis or on inactive mutants of chitinase A if affinities should be studied singularly.

Under the aspect of possible therapeutic uses, ChO's showing high affinities to HC gp-39 in vitro under physiological conditions have to show high biostability under these conditions as well. Human chitinases (HCT and AMCase) mainly contribute to the hydrolysis of chitinous material in the human body. Chitinase B shows a high sequence homology of the binding site to HCT. Therefore hydrolysis studies on ChO's employing chitinase B allows to estimate the biostability of ChO's in the human body. Chitinase B binds oligomers with the non-reducing end positioned at subsite -3 or preferentially located at subsite -2. In order to cleave the glycosidic bond, chitinase B requires binding of an A residue at subsite -1 whereas binding of a D residue at this subsite is non-productive and actually results in competitive inhibition of the enzyme.[104] Hydrolysis occurs processively at every second glycosidic bond if an A unit is positioned at subsite -1.[22] Glycosidic bonds are cleaved with relative rates AA-X : DA-X : YD-X ca. 3:1:0 whereas bonds of the type Y YA-X are cleaved very slowly (Y = D or A).[22] Figure 8 in off-print 5 summarises the possibilities for hydrolysing the DP6 homologs D_6, D_3A_3, D_2A_4, and A_6.

Table 4 in off-print 5 summarizes the relative amounts and the number of hydrophobic interactions with HC gp-39 of the isomers that are stable against hydrolysis with chitinase B. The quantitative analysis of oligosaccharides sequences present in mixture of isomers, determination of binding affinities and application to knowledge on the properties of carbohydrate binding proteins allows for the prediction of the isomer, which will be most useful for further biochemical and pharmacological studies. In the case of DP6 isomers, can be concluded from Table 4 in off-print 5 that four candidates are promising with respect to high affinity and biostability on the other hand: ADADAA, DDAAAA, ADDAAA, and DDADAA. DDAAAA is found only in low amounts (4% of D_2A_4), ADDAAA has only two hydrophobic interactions with HC gp-39, and DDADAA is a D_3A_3 isomer, which shows lower affinity to HC gp-39 than D_2A_4 isomers. Consequently, ADADAA (19% of D_2A_4, three hydrophobic interactions with HC gp-39) is the most promising candidate for further biochemical and pharmaceutical studies.

In conclusion, singular sequences of ChO's are available that bind with high affinities to HC gp-39 and show on the other hand high biostabilities like the D_3A_3 isomer DDADAA or the D_2A_4 isomer ADADAA. In this connection it is important to know the effects of ChO's binding to HC gp-39 on the biological functions of this protein. HC gp-39 is secreted by articular chondrocytes[230] and synovial fibroblasts[174]. It is over expressed in patients suffering from rheumatoid arthritis.[170] The synovial tissue of patients suffering from rheumatoid arthritis shows an invasive growing resulting in the destruction of neighbouring tissues like cartilage and bone. Characteristic for the invasive growing is the occurrence of morphogenetically transformed synovial fibroblasts at the invasion border.[233] The downregulation of HC gp-39 should stop or at least reduce the invasive growing of morphogenetically transformed synovial fibroblasts. Putatively the binding of ChO's to HC gp-39 induces the down regulation cascade. One step of this cascade could be a conformational change of the HC gp-39 structure induced by the binding of ChO's.

The results of the present studies show that the strongest binding but less biostable chitin homooligomers can be replaced by heterochitooligosaccharides still recovering affinity. In this sense, D_2A_4 and D_3A_3 isomers should cause the same conformational change as A_6. van Aalten et al. proved that A_6 causes a conformational change. As the affinity decreases with decreasing F_A but increases with increasing DP, it should be interesting and useful to further investigate the affinity of DP11 isomers of $F_A < 0.50$ in order to prove whether they show affinities comparable to ADADAA or DDADAA.

Growth Stimulating Effect of ChO's on Chondrocytes

Whereas the invasive growth of synovial fibroblasts as observed under rheumatoid arthritic conditions should be stopped, a stimulation of the growth of chondrocytes is desired. Chondrocytes are cartilage cells that produce collagen and proteoglycans, which are basic components of cartilage.[234, 235] Thus, a stimulation of the growth and general activity of chondrocytes means an accelerated regeneration of joints that suffer from rheumatoid arthritis or osteoarthritis. In order to study the effect of ChOs on chondrocytes, human chondrocytes were cultured in 96 well microplates, supplemented with different concentrations of water-soluble ChO's (0, 10, 50, 100, 500 and 1000 $\mu g \times mL^{-1}$). After four weeks of incubation the cells were fixed in -20°C methanol and HE stained. Finally the cells in each well were photographed through a microscope. The photos were used to count the cells and to evaluate their appearance. In result, the number of cells per well was increased in proportion to the increase of the ChO concentration in the range of 50 – 500 $\mu g \times mL$ with a high degree of statistical significance. However, at 1000 $\mu g \times mL^{-1}$ there was a profound reduction in cell density compared to the control. The cells in the most condense wells took on a typical cartilage appearance. In conclusion, the results show clearly that ChO's have a growth promoting effect on chondrocytes in vitro. The observed change in appearance of the more rapidly growing cells could be due to the direct effect of ChO's on the cell phenotype or alternatively just a response to increased confluence of the rapidly growing cells. At 1000 $\mu g \times mL^{-1}$ the ChO's hamper for an unknown reason. Further studies will evaluate the growth promoting effect of different fractions of ChO's.

Identification of High-Affinity Non-Covalent Complexes Between Proteins and Heterochitoisomers Employing (+)nanoESI QTOF Top-Down CID MS/MS

The entities used for biological studies are usually prepared by enzymatic hydrolysis of chitosan, yielding complex mixtures of chitooligosaccharides that differ in DP, F_A and the sequence of D and A units. The previous chapters showed that the preparation of definite isomers (with definite sequences) takes a lot of effort. Although several protein-ligand complexes containing *N*-acetylglucosamine or enzyme inhibitors have been investigated by crystallographic methods[100, 107, 187, 236, 237] and ^{1}H-NMR spectroscopy[238, 239], the molecular mechanisms of the biological actions of ChO's (e.g. in the human body) remain essentially unknown. This is due to a lack of structural information resulting from the fact that pure ligands are hardly available. Mass spectrometric methods can be employed for detection and structural analysis of non-covalent carbohydrate-protein complexes. The first investigation of

an enzyme-oligosaccharide non-covalent complex by ESI-MS was reported for lysozyme and GlcNAc.[240] Information on the binding stoichiometry can be obtained, and the ligand can be identified by fragmentation.[225, 241]

A direct, qualitative approach to investigate the interactions between defined sequences of heterochitooligomers and proteins like chitinases was made by the use of (+) nanoelectrospray ionisation quadrupole time-of flight tandem mass spectrometry ((+) nanoESI-QTOF MS).[242] The nanoESI source offers the advantage of using low flow rates for sample infusion[243] whereas the TOF mass analyser performs parallel detection of all masses within a spectrum at high sensitivity and high acquisition rates. The resolution across the full mass range is above 5000 FWHM.

Figure 43 shows the principle construction of a nanoESI QTOF mass spectrometer. The sample is infused into the mass spectrometer employing the nanoESI source. Applying electric forces to the drops of the spray results on one hand in a desolvatisation of the sample molecules and secondly in the ionisation of the analytes. The nanoESI source is equipped with a capillary allowing for flow rates in the range of nL × min^{-1}. The sample ions are separated in quadrupole 1 (selector) resulting in a selection of the precursor of the MS^2 experiment. The precursor is fragmented in the collision cell (CID = collision induced dissociation) and the fragments are separated in quadrupole 2 (analysator). Applying an AC voltage of definite frequency to quadrupole 2 lets only pass ions of definite m/z through the analysator towards the detector whereas all ions of different m/z will collide with the rods of quadrupole 2.

A

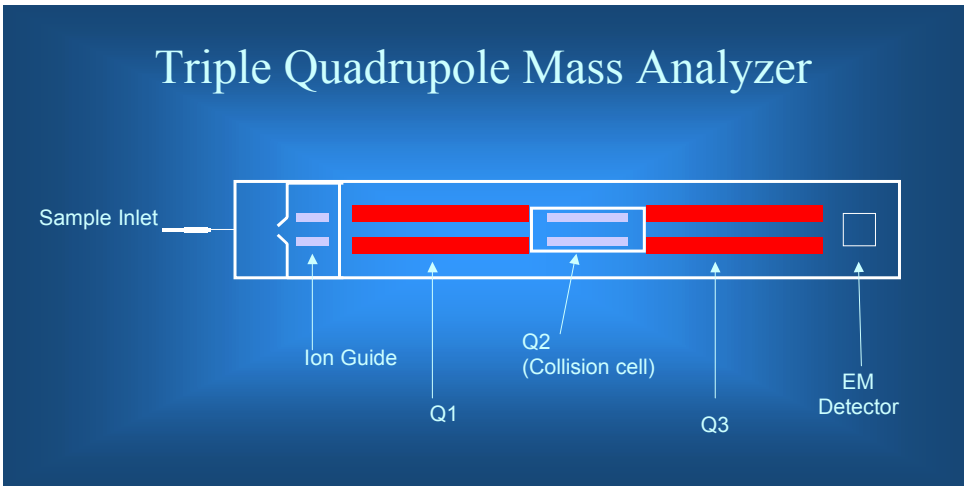

B

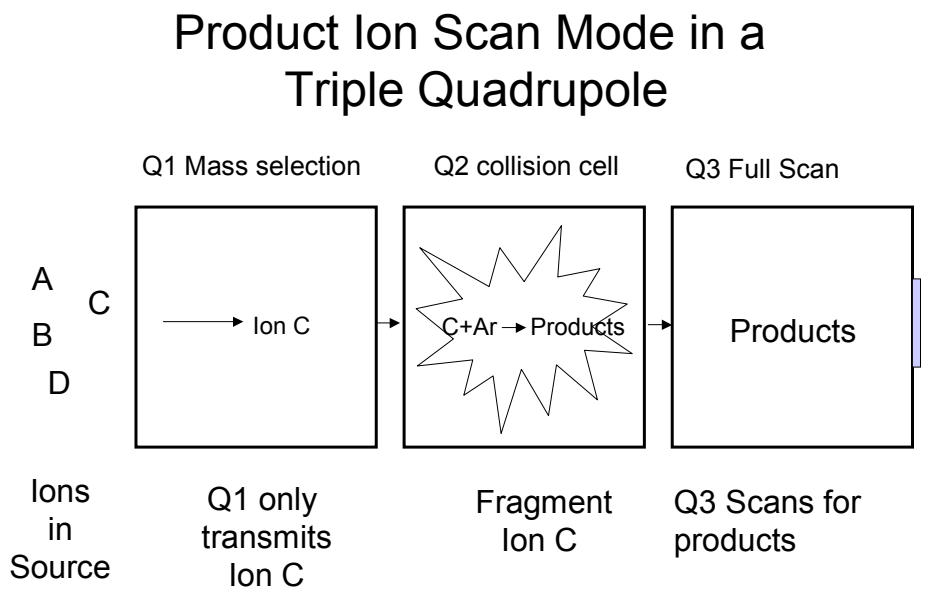

C

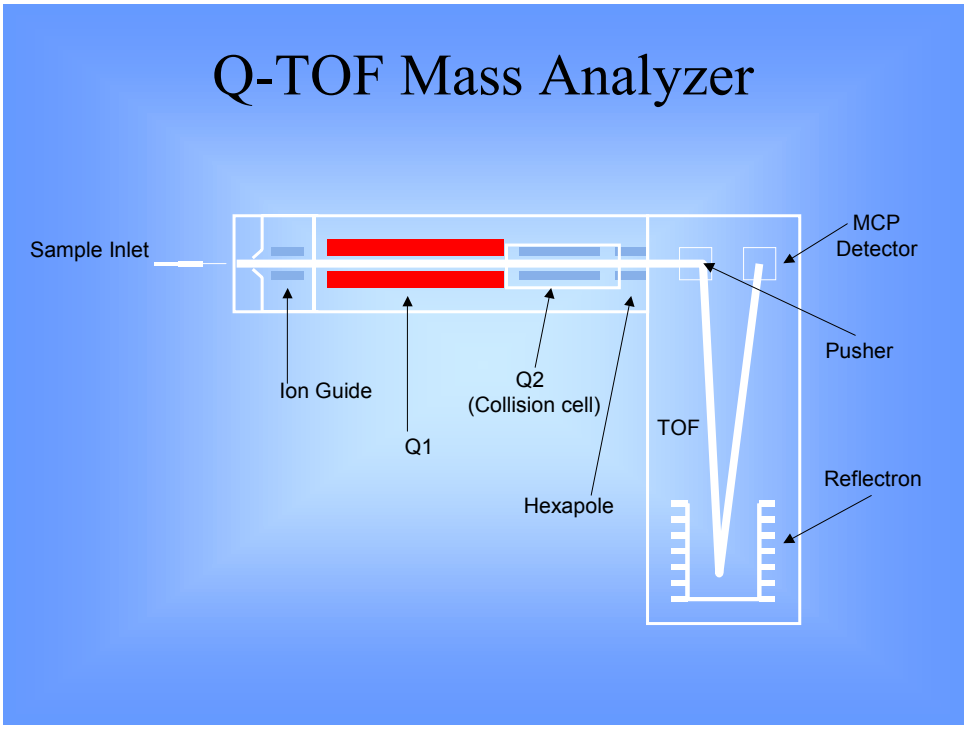

Figure 43. Schematic construction plan of an ESI QTOF mass spectrometer. A and B. In the case that the collision cell is constructed in form of a quadrupole we have a triplequad mass spectrometer. The precursor is selected in quadrupole 1 (selector), fragmented in quadrupole 2 (collision cell), and the fragments are separated (analysed) in quadrupole 3. Collision is performed with accelerated argon atoms. C. QTOF mass analyser. Quadrupole 1: selection of precursor ions, quadrupole 2: collision cell, hexapole + TOF compartment in the reflector mode: analysis of m/z by time of flight. Figures 59 A – C base on modified product information, which is found on the homepage of Thermo-Finnigan (URL: http://www.thermo.com).

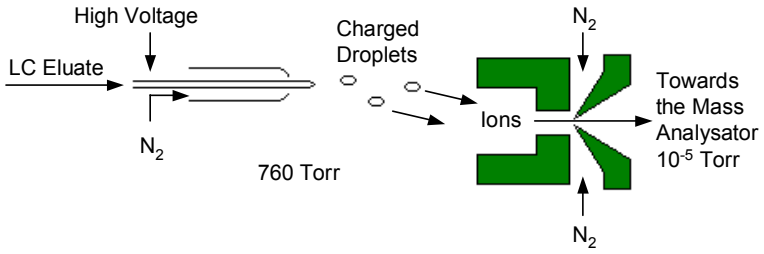

Figure 44. Schematic construction plan of an ion-spray source.[244]

The protein, chitinase B from *S. marcescens*, was incubated with a mixture of chitooligosaccharides of DP3 to 6 (D_1A_2, A_3, D_2A_2, D_1A_3, A_4, D_3A_2, D_2A_3, D_4A_2, D_3A_3). The (+) nanoESI-QTOF MS of the chitooligosaccharide fraction used for incubation with ChiB is shown in the appendix (Figure S9, Table S4, Appendix). According to the MALDI-TOF MS of the mixture, D_1A_3 and D_2A_3 are the main components. The resulting non-covalent enzyme-ligand complexes were identified by (+) nanoESI-QTOF MS. Table 11 summarises the complexes that were identified.

Table 11. Complexes between chitinase B and heterochitohomologs identified after different incubation times with (+) nanoESI-QTOF MS.

Incubation time	Complex type
5 min	D_1A_3-ChiB
	D_2A_3-ChiB
90 min	D_1A_2-ChiB
	D_1A_3-ChiB
	D_2A_3-ChiB
180 min	D_1A_2-ChiB
	D_1A_3-ChiB
	D_2A_3-ChiB

Figures 1, 2, and 3 in off-print 6 show the (+) nanoESI-QTOF mass spectra recorded for the identification of the complexes between chitinase B and heterochitohomologs. The three complexes, ChiB-D_1A_3, ChiB-D_2A_3 and ChiB-D_1A_2, are in a kinetic equilibrium after 90 min as the mass spectra taken after 90 min and 180 min (mass spectrum not depicted) show no change. The initial concentration of D_1A_2 is low ($\leq$ 5% estimated from the MALDI-TOF MS of the mixture). Thus, the identification of the ChiB-D_1A_2 complex after 90 min indicates a partial hydrolysis of D_1A_3 and D_2A_3 yielding D_1A_2 as the hydrolysis product.
For the ChiB-D_2A_3 complex an additional top-down experiment was performed. The ChiB-D_2A_3 complex was isolated in the quadrupole followed by application to a CID experiment resulting in a dissociation of the complex and the fragmentation of D_2A_3. The CID-MS/MS spectrum is shown in Figure 3 in off-print 6. Table 2 in off-print 6 summarises the assignments of peaks detected in the top-down CID MS/MS of the ChiB-D_2A_3 complex.

Permutation of the D and A units of D_2A_3 shows that ten isomeric sequences exist. The fragment ions provided by CID MS/MS (fragmentation from reducing and non-reducing end) are used to deduce the sequence of the D_2A_3 ligand that was most stable bound to ChiB (Table 12).

Table 21. Deduction of the sequences of D_2A_3 that most stable bind to ChiB. The column "CID MS/MS" shows clashes of the expected fragments of the D_2A_3 sequences with the fragments of the top-down CID MS/MS of the ChiB-D_2A_3 complex.

Sequence	CID MS/MS
A-A-A-D-D	A_3 not observed
D-A-A-A-D	D_2A_1 and D_2A_2 observed
D-D-A-A-A	A_3 not observed
A-A-D-A-D	
A-D-A-A-D	D_2A_1 observed
A-A-D-D-A	D_1A_3 observed
D-A-A-D-A	D_2A_1 observed
A-D-A-D-A	D_1A_3 observed
A-D-D-A-A	D_1A_3 observed
D-A-D-A-A	

Only for AADAD and DADAA the expected fragments show no clashes with the fragments of the top-down CID MS/MS of the ChiB-D_2A_3 complex. Therefore only one of these two sequences is the candidate that is most stable bound to ChiB.

Additionally, the D_2A_3 used for affinity studies was analysed by MALDI-LTQ MS to deduce the sequence composition quantitatively.[245] According to this analysis, D_2A_3 consists of mainly three isomers with the following compositions: DADAA 57%, DDAAA 26%, ADDAA 15%.

As AADAD is not a compound of the mixture of D_2A_3 isomers, only DADAA is left to be the sequence most stable bound to chitinase B from *S. marcescens*.

Why is DADAA most stable bound to ChiB and not DDAAA or ADDAA?

Crystallographic data on ChiB-A_5 complexes indicate that pentamers are equally bound in alignments –2 → +3 or –3 → +2.[101] Figure 45 summarises the alignments of DADAA, DDAAA and ADDAA with chitinase B and shows scissile bonds.

Figure 45 shows that DDAAA is rapidly hydrolysed as alignment 12 allows for the hydrolysis of an -A-A- bond with an A unit bound to subsite –1. Additionally, the hydrolysis products DDA and AA have a low affinity to chitinase B. DADAA could be cleaved in alignment 01. Even though hydrolysis of the -A-D- bond occurs slowly, after 90 minutes of incubation one of the hydrolysis products -D_1A_2- forms a complex with chitinase B (a second source of DAA is D_1A_3). ADDAA is not hydrolysed by chitinase B. Never the less, a complex between this sequence and chitinase B is not observed. The only explanation is that ADDAA has a lower

affinity to chitinase B than DADAA. Secondly, the amount of ADDAA is only 26 % of the amount of DADAA.

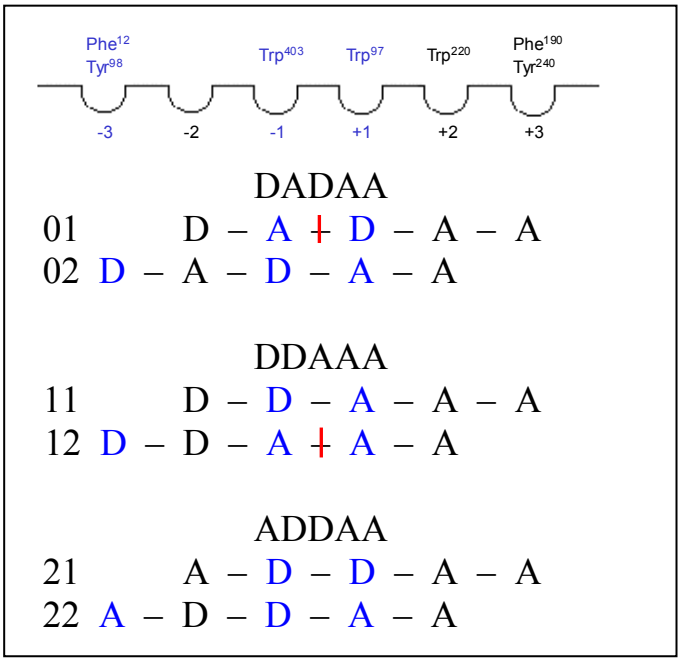

Figure 45. Alignments of DADAA, DDAAA, and ADDAA with chitinase B. Blue coloured monomer units indicate alignments with significantly hydrophobic subsites. Red lines indicate scissile bonds.

The present study demonstrates that ChiB binds particular components (heterochitoisomers) out of a complex mixture of chitooligosaccharides. The results allow conclusions on the specificity of ligand selection from complex mixtures and on the stoichiometry of binding. The mechanism of enzyme inhibition can be conclusively deduced by combination of knowledge on the mechanism of catalysis and structure identification of an oligosaccharide ligand binding with high affinity. In case that DADAA occupies subsites -3 to +2, a D unit is positioned in subsite -1 and a highly favourable A unit in subsite -2 resulting in the observed competitive enzyme inhibition, because the crucial oxazolinium ion intermediate cannot be formed (Figure 5 in off-print 6).[22, 225, 246]

Figure 46 summarises the steps of the identification of the strongest binding ligand out of a mixture of oligomeric, homologous and isomeric glycans employing (+) nanoESI-QTOF top-down CID MS/MS.

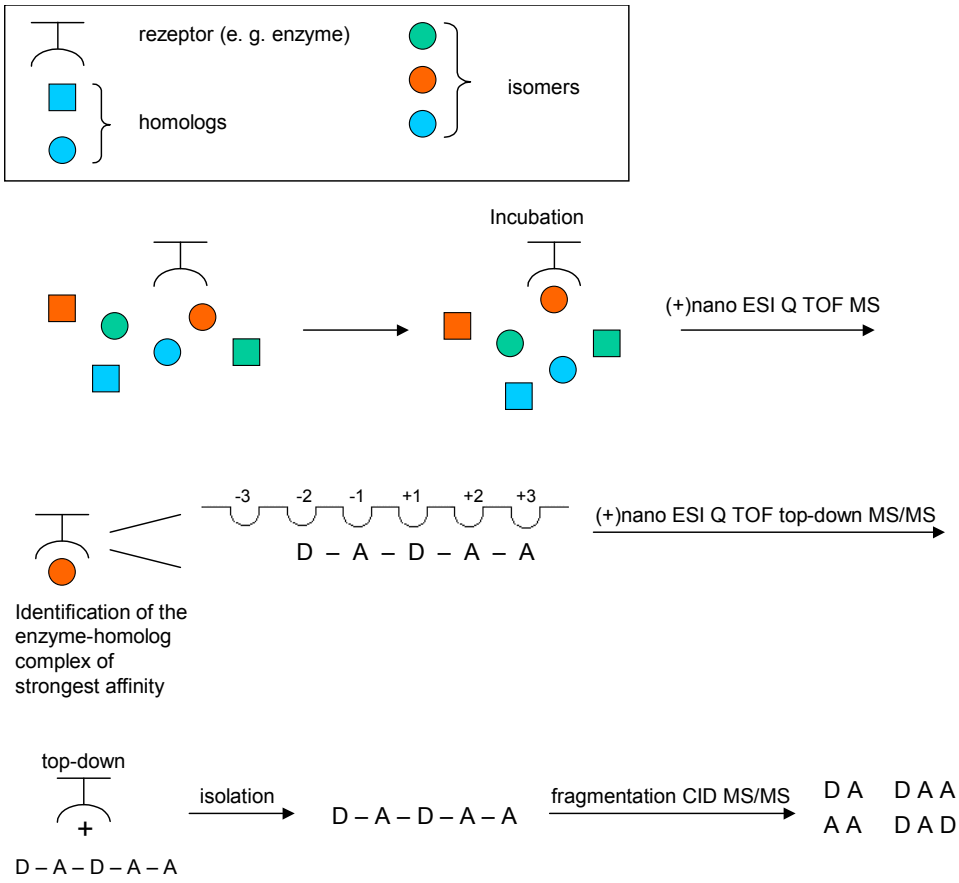

Figure 46. Summary of the analytical steps that lead to the identification of the strongest binding ligand out of a mixture of oligomeric, homologous and isomeric glycans employing (+) nanoESI-QTOF top-down CID MS/MS.

4.0 Summary

Introduction

Chitin is a biopolymer consisting of β-1,4-linked *N*-acetylglucosamine (A) and glucosamine (D) units. Chitin is insoluble in diluted acids and other common solvent systems. Its deacetylation gives chitosan, which is soluble in diluted acids. Heterochitooligosaccharides are the water-soluble form of chitin or chitosan, respectively. Heterochitooligosaccharides differ in the degree of polymerisation (DP), the molar fraction of A units (F_A) and the sequence of A and D units. Thus, we have to divide between oligomers, homologs and isomers.

Heterochitooligosaccharides are of special interest for the pharmaceutical and food industries due to their unique solubility and ability to penetrate cellular membranes resulting in high resorption in contrast to polymeric chitin or chitosan. Heterochitooligosaccharides possess intriguing biological activities in bacteria, fungi, plants and animals. In humans, heterochitooligosaccharides act as growth promoters of osteoblasts. They are primers of the hyaluronan biosynthesis, a polysaccharide that plays important roles in cartilage, synovial fluid and skin tissue. Heterochitooligosaccharides are active in immune stimulation through activation of macrophages. In wound healing they inhibit the production of nitric oxide by activated macrophages under inflammatory conditions resulting in a decreased cytotoxicity.

Closely related to the occurrence of chitinous material is the occurrence of enzymes, which are able to modify chitin, like glycosyl hydrolases (chitinases, chitosanases, chitobiosidases or *N*-acetylglucosaminidases) that degrade chitin, or chitin deacetylases that deacetylate chitin to chitosan. Glycosyl hydrolases occur in fungi for growth purpose, in bacteria for nutrition purpose and in higher organisms like plants and animals as part of the immune system for defence against chitin containing pathogens. Also humans possess chitinases (HCT, AMCase) for defence purpose (e.g. against nematodes) and secondly to digest foodstuff.

In insects chitinases take an important function with respect to moulting. Malarial parasites use insects as vectors. They need chitinases to escape the peritrophic membrane formed by mosquitoes against infection. Chitin and chitin homooligomers are perfect substrates for chitinases. The introduction of D units as present in heterochitooligosaccharides results in a lower chitinase activity up to a blocking of these enzymes, predestinating heterochitooligosaccharides as potential chitinase inhibitors and thus as insecticides, fungicides or anti-malarial agents.

Biologically evolved from active chitinases are catalytically inactive chilectins. Lectins are natural ligands of oligosaccharide structures in plants and vertebrates. These proteins take part

in signalling pathways. Partly they are bound to membranes (e.g. cell surfaces) and thus play important roles in cell-cell recognitions. Non-membrane bound lectins possess hormone-like activities.

Among the well-characterized human chitolectins is HC gp-39 (also named YKL 40). This protein is discussed as a biomarker for diseases like rheumatoid arthritis, asthma or different types of cancer. Details of the signalling pathways involving HC gp-39 are still unknown. HC gp-39 is a potent growth factor inducing cell proliferation. In this case, HC gp-39 activates the protein kinase B signalling pathway (AKT) as well the mitogen-activated protein kinase signalling pathway (kinase 1/2, ERK) through initiating MAP kinase and PI-3K signalling cascades in human connective-tissue cells, leading to the phosphorylation of ERK1 and 2 as well as AKT. Chitin oligomers bind to HC gp-39 with dissociation constants in the range of μM. The binding of chitin oligomers to HC gp-39 induces a conformational change of this protein putatively causing a modulation of signalling pathways. A down regulation of HC gp-39 would have a positive effect on inflammatory diseases like rheumatoid arthritis where aggressive phenotypes of synovial fibroblasts destroy joints.

The scope of the present thesis is the development of a set of analytical methods, which allow determining quantitatively the compositions of complex mixtures of heterochitooligomers, -homologs and –isomers employing chromatographic and mass spectrometric methods. The preparation of heterochitooligosaccharides by partial hydrolysis of chitin or chitosan gives complex mixtures of heterochitooligosaccharides. As biological functions of heterochitooligosaccharides depend on DP, F_A and the sequence of A and D units, a detailed characterization of chitin / chitosan depolymerisates is an obligatory step previous to biological tests.

Additionally, the characterization of chitin / chitosan depolymerisates is necessary for quality control and the determination of the composition of chitin or chitosan polymers.

For biological tests it is desirable to work with a library of pure heterochitooligomers. Thus, the second scope of the present thesis is the development of chromatographic methods for the preparation of a library of pure heterochitooligomers, -homologs and –isomers.

The library of heterochitooligosaccharides is used to investigate the interactions between heterochitooligosaccharides and proteins with respect to DP, F_A and sequence of A and D units. A combination of affinity and hydrolysis studies on the active family 18 chitinases A and B from the soil bacterium *Serratia marcescens* should indicate, which heterochitooligosaccharides are potent inhibitors of family 18 chitinases. This study is important for the finding or design of anti-fungal and anti-malarial agents as well as

biodegradable insecticides. Chitinase B shows a striking sequence homology to human chitotriosidase, a family 18 chitinase found in the human blood and intestine. Thus, the hydrolysis studies on heterochitooligosaccharides employing chitinase B should give an overview how the introduction of D units into a chitin oligomer increases its biostability. Human chitolectins like YKL-39 and YKL-40 are evolved from catalytically active family 18 chitinases and show striking similarities with respect to the architecture of the binding sites. Thus, the affinities of heterochitooligosaccharides to chitinase A and B have a model character for the affinities of heterochitooligosaccharides to human chitolectins like YKL-39 or YKL-40.

It is desirable in this connection to determine the sequence of the most hydrolysis-stable isomer of highest affinity to a protein out of a complex mixture of oligomers, homologs and isomers in one experiment. This is performed by (+)nanoESI QTOF MS using a top-down experiment (MS/MS).

A further scope of the present thesis is the direct determination of the affinities between heterochitooligosaccharides and the human chitolectin HC gp-39 (YKL-40). The affinities between HC gp-39 and chitin homooligomers was determined already by van Aalten et al. The aim of the present study is to investigate how the affinity changes with DP, F_A and sequence.

Based on these observations a theoretical model was developed to explain the results and allowing predicting affinities of heterochitooligosaccharides to HC gp-39.

The investigation of the dependency of the affinities from the F_A is of special importance as a decrease of F_A increases the biostability of ChO's in the human body.

Quantitative Analysis and Preparation of Heterochitooligomers, Homologs and Isomers

The present work provides a series of chromatographic and mass spectrometric methods, which enable the researcher to analyse quickly complex mixtures of heterochitooligomers, homologs and isomers.

For the analysis based on chromatography, an enzymatic chitin hydrolysate (DP2 to 12) is separated by gel permeation chromatography on Biogel P4™ with RI detection. The separation according to molecular size gives mainly oligomers. As the peaks of the chromatogram are overlapping, baseline drops allow for the calculation of relative peak areas. Fractions are collected according to the baseline drops and applied to a further separation by cation exchange chromatography on a MonoS™ stationary phase (strong cation exchange material based on sulfonyl groups) with UV detection. The separation in acidic medium according to charge numbers (i.e. the number of D units) gives mainly homologs. Relative

peak areas, which are calculated from the baseline separated UV signals, give relative molar amounts and the relative masses of the homologs. The combination of the results obtained from GPC and IEC allowed calculating the masses of the DP2 to 7 oligomers and homologs. The mass distribution of oligomers and main homologs is the following: DP2, 1% (A_2 0.7%); DP3, 6% (D_1A_2 5.6%); DP4, 19% (D_2A_2 10.1%, D_1A_3 6.3%); DP5, 22% (D_3A_2 12.1%, D_2A_3 8.0%); DP6, 18% (D_3A_3 8.4%); DP7, 16% (D_4A_3 8.8%); DP ≥ 8, 12%.

Alternatively to the combination of GPC and IEC the combination of GPC and MALDI-TOF MS with signal quantification is successfully used for the quantitative determination of complex mixtures of heterochitooligomers, -homologs and -isomers. The sample is separated by gel permeation chromatography on Biogel P4™ with RI detection. The separation according to molecular size gives mainly oligomers. Previous to the analysis by MALDI-TOF MS each fraction is derivatised with hexadeuterio acetic anhydride transforming all free amino groups into trideuterio acetamido groups, which have the same mass spectrometric properties as acetamido groups but show a mass shift of 3 Da. The mass spectrometric signals are quantified. The combination of the results obtained from GPC and MALDI-TOF MS allowed calculating the masses of DP2 to 7 oligomers and homologs. The mass distribution of oligomers and main homologs according to GPC-MS is the following: DP2, 1% (A_2 0.9%); DP3, 5% (D_1A_2 5.0%); DP4, 19% (D_2A_2 9.4%, D_1A_3 7.1%); DP5, 25% (D_3A_2 13.1%, D_2A_3 9.3%); DP6, 17% (D_3A_3 8.3%); DP7, 14% (D_4A_3 8.6%); DP ≥ 8, 12%. The results are closely related to the results obtained by GPC-IEC. The method GPC-MS is applicable over a wide range of DP with the same precision, it affords less amount of sample and analysis time.

The separation of heterochitoisomers is performed on a MonoS™ cation exchange stationary phase (strong cation exchange material based on sulfonyl groups). A mixture of three DP5 isomers and secondly a mixture of two DP6 isomers were separated. The peaks are successfully fitted to Gaussian or Pulse Peak functions for quantification purpose affording the relative amounts and relative masses of isomers.

For the preparation of heterochitohomologs, the combination of IEC and GPC proved to be optimal. The separation on a SP Sepharose™ column (5 × 24 cm) yielded fractions of identical charge numbers, which are subsequently separated on Biogel P4™ (2.5 × 200 cm) into fractions of pure homologs. A library of homologs up to DP 12 in the scale of 1 - 50 mg and a purity of 96 – 98 % was established. Additionally, separations employing GPC followed by IEC, or separations employing three GPC steps contributed to the library of homologs.

The separation of heterochitoisomers for preparative purpose is performed on a MonoS™ cation exchange stationary phase (1 mL bed volume). A mixture of three DP5 isomers and a

second mixture of two DP6 isomers yielded 0.4 mg ADDAA, 0.5 mg DADAA, 0.4 mg DADDAA, and 0.4 mg DDADAA of 91 to 100% purity.

Quantitative Sequencing of Complex Mixtures of Heterochitooligosaccharides by vMALDI-Linear Ion Trap Mass Spectrometry

The quantitative sequencing yields information concerning the sequence of D and A units of heterochitoisomers. The same experiment gives quantitative information concerning a mixture of heterochitoisomers. The pure homolog (= mixture of isomers) is derivatised with hexadeuterio acetic anhydride, which transducts all free amino groups into trideuterio acetamido groups that have equivalent mass spectrometric properties compared to acetamido groups – especially with respect to the fragmentation energies of glycosidic bonds. Additionally, the reducing end of the isomers is tagged with 3-(acetylamino)-6-aminoacridine to support exclusive fragmentation from the non-reducing end. The derivatised mixture of heterochitoisomers is analysed by vMALDI-linear Ion Trap MS^n performing MS^2 and MS^3 experiments. The signals arising from Y-type fragment ions are quantified. In case of overlapping masses of fragment ions, MS^2 or MS^3 experiments are performed making use of the linear ion trap. The masses of the fragment ions allow deducing the sequence of D and A units from the reducing end. The quantification of signal intensities allows calculating the relative molar amounts or masses of isomers. Appropriate calculations of unknown masses support the deduction of the isomeric composition. It was possible to determine the quantitative composition of isomeric mixtures up to DP9 and up to eight components with a precision of 1-5%. The analysis of a mixture of DP5 isomers gave 57% DADAA, 26% DDAAA and 15% ADDAA. The comparison with the chromatographic analysis (55% DADAA, 26% DDAAA and 19% ADDAA) shows a good agreement. The mass spectrometric method is gives a rapid analysis, little consume of sample in combination with a high precision.

Analysis of a Chitosan-Cellulose Copolymer Produced by *Acetobacter xylinum*

The soil bacterium *Acetobacter xylinum* produces cellulose. If the nutrient medium contains chitosan (F_A 0.16; M_v 98 kDa) the secreted biopolymer contains additionally chitooligosaccharides. The monosaccharide analysis performed by total hydrolysis of the polymer followed by HPAEC-PAD revealed a composition of 53% glucose, 21% mannose, 13% fructose and 13% glucosamine / *N*-acetylglucosamine. The partial hydrolysis of the polymer with a cellulase from *Trichoderma reesei* yields oligomeric fragments, which were separated by GPC on Biogel P4™ followed by analysis of the fractions employing mass spectrometric methods. The quantitative evaluation of the chromatographic peaks indicates

that up to 85% of the mass is contributed by hexose oligomers of DP ≤ 3, 15% are heterochitooligosaccharides of DP ≤ 9. Most interestingly, the mass spectra indicate the presence of several minor oligosaccharides containing hexose units besides chitooligosaccharides. The presence of these oligosaccharides composed of glucosamine, *N*-acetylglucosamine and hexose units clearly indicates that *Acetobacter xylinum* is able to form a copolymer of cellulose and chitosan. The sequence analysis of the hexose-hexosamine oligosaccharides shows that one or two hexose units are randomly distributed within the oligosaccharide chain with a preference for positions at the reducing end. The hexose unit was rarely positioned at the non-reducing end. In conclusion, chitooligosaccharides are building blocks for the biosynthesis of modified bacterial cellulose by *Acetobacter xylinum*. Most probably chitosan is depolymerised to permeable chitooligosaccharides by *Acetobacter xylinum* during the incubation period. These chitooligosaccharides are utilized as a carbon source, and activated hexose residues are linked to the initial building blocks by transglycosylation. As well activated ChO's are linked to the growing polymer chain. The quantitative evaluation of the oligosaccharide fragments by GPC in combination with a mass spectrometric sequence analysis including signal quantification allows to deduce the composition of the copolymer: it consists of blocks of cellooligomers which are interrupted by chitooligomers in a ratio of ca. 6:1. The chitooligosaccharides are very slowly cleaved by the cellulase. Thus, an average DP of 5 for chitooligomers indicates an average DP of 30 for the cellooligomers.

In general, the quantitative sequence analysis of oligosaccharide fragments obtained by hydrolysis with specific enzymes is a powerful tool to conclude the sequence composition of a polymer – as in the present example chitosan modified bacterial cellulose. The combination of both polymers, cellulose and chitosan, to a unique biopolymer gives a graft material with outstanding properties combining the stability of cellulose with the elasticity and bacteriostatic properties of chitosan for use in loudspeaker membranes, wound dressings or even artificial blood vessels.

Inhibition of Chitinase A and B from *Serratia marcescens* by Heterochitooligosaccharides

Chitinase A and B from *Serratia marcescens* are both family 18 chitinases. They require an A unit in subsite –1 for hydrolysis. Chitinase A cleaves chitin from the reducing end whereas chitinase B cleaves chitin from the non-reducing end. Chitinase A possesses a catalytic domain and a chitin-binding domain with subsites from +2 to –11. Subsites –4 to +2, form the

core of the catalytic domain. The overall structure is described as a grove, which is locked beyond subsite +2.

Chitinase B possesses as well a catalytic domain and a chitin-binding domain with subsites from –3 to +9. Subsites –3 to +3, form the core of the catalytic domain. The overall structure is closer than that of chitinase A and described as a tunnel, which is locked beyond subsite -3.

The present studies show that chitooligosaccharides inhibit chitinase A and B with IC_{50} concentrations in the range of μM making use of the fluorescence inhibition of a 4-methylumbelliferyl-beta-D-*N,N'*-diacetylchitobioside or –beta-D-*N,N',N''*-triacetylchitotrioside substrate. The inhibitory effect increases with increasing DP and F_A of the chitooligosaccharide. A maximum DP of 12 is observed above which the inhibitory effect is rather constant due to the limited number of subsites. The inhibitory effect also depends on the sequence of the chitooligosaccharide although the inhibitory effects of two DP6 isomers (DDADAA and DADDAA) showed that the differences are less pregnant compared to DP and F_A. The inhibitory effect is increasing with decreasing pH as two series of measurements on chitinase A at pH 5.4 and 7.4 indicated. At pH 5.4 the free amino groups of D units are stronger protonated than at pH 7.4. Consequently, ionic interactions between D units and ionic amino acid residues become stronger. The inhibitory effect for chitinase B is generally higher than for chitinase A due to the closer structure of its tunnel-like catalytic domain.

Additionally to the inhibitory experiments, hydrolysis studies with chitooligosaccharides on chitinase A and B were performed employing MALDI-TOF MS. The studies showed that the chitooligosaccharides are most stable, which have a D unit bound to subsite –1 of the family 18 chitinase. These experiments allow splitting the inhibition potency of a chitooligosaccharide into two distinct effects: The binding affinity of the chitooligosaccharide to the enzyme and its biostability. The affinity of an chitooligosaccharide to a family 18 chitinase is mainly determined by the number of A units interacting with the exposed aromatic residues of the odd numbered subsites of the catalytic and chitin binding domains of the protein whereas the biostability depends on the binding of a D unit to subsite -1.

Two DP6 isomers showed different IC_{50} concentrations (DDADAA 21.1 μM; DADDAA 15.9 μM) inhibiting chitinase A. This difference is explained by the affinities of the isomers to the binding site of chitinase A. Regarding only alignments of the sequences to the binding site of chitinase A where all core subsites -4 to +2 are bound to a monosaccharide unit, DADDAA shows more interactions with the hydrophobic subsites of chitinase A (-3, -1, +1) than DDADAA. The stability of both sequences against hydrolysis by chitinase A is comparable as DDADAA and DADDAA are not hydrolysed in the -4 → +2 binding mode

and generally hydrolysis occurs to a minor extend during the inhibition assay running time. Therefore, the observed IC_{50} concentrations reflect differences in affinities rather than stabilities against hydrolysis (biostabilities).

The concepts of affinity and biostability that are based on experimental data allow to predict the inhibitory effects of chitooligosaccharides with a given sequence, which is important for the design of family 18 chitinase inhibitors based on chitooligosaccharides. Chitinase inhibitors are important for the development of antifungal and antimalarial agents. Family 18 chitinases are models for human chitolectins so that affinities of chitooligosaccharides to chitinase A and B can be transferred to family 18 chitolectins like HC gp-39.

Binding of Heterochitooligosaccharides to the 39-kDa Human Cartilage Glycoprotein

HC gp-39 is a chitolectin evolved from active family 18 chitinases and shows a high homology with them (e.g. human chitotriosidase 53%). The chitin-binding domain of this protein shows subsites from -6 to +3 with core subsites from -3 to +3. The groove-like binding domain is locked beyond the +3 subsite. The protein binds to chitin oligomers with dissociation constants in the range of μM. It is under discussion whether subsites -5 and -6 represent a distinct binding domain for chitooligomers with DP < 4. The binding of chitin oligomers to HC gp-39 causes a strong conformational change of the whole protein, which could be the key of the modulating effect of chitin oligomers on the signalling pathways of HC gp-39. The protein is involved in signalling cascades initiating MAP kinase and PI-3K leading to the phosphorylation of ERK1/ERK2 and AKT, which is consistent with a role in the propagation of mitogenic signals.

HC gp-39 is over expressed under pathological conditions of several severe diseases like rheumatoid and osteoarthritis as well as colon and breast cancer. Putatively the binding of chitin oligosaccharides could down regulate the expression of HC gp-39.

As the human body contains active family 18 chitinases and additionally aggressive body fluids chitin oligomers are easily cut in the human body. The introduction of D units into the oligosaccharide chain enhances biostability. It is the scope of the present work to investigate how the introduction of D units influences the affinity between chitooligosaccharides and HC gp-39. The affinities of a series of DP6 homologs decrease with decreasing F_A. The introduction of 50% D units into the chitin oligosaccharide like for D_3A_3 recovers 27% of the maximal affinity (A_6 100%). Like for active family 18 chitinases the affinities to HC gp-39 increase with increasing DP of the chitooligosaccharide with a limitation according to the number of subsites. In conclusion, it was proved that heterochitooligosaccharides bind with affinities of the same order to HC gp-39 as chitin oligomers but offer the advantage of

increased biostability. A_6 is rapidly hydrolysed by chitinase B whereas DDADAA (D_3A_3) is stable against hydrolysis. The similarity of affinities indicates that heterochitooligomers like chitin oligomers will induce a conformational change of HC gp-39.

Identification of a High-Affinity Binding Oligosaccharide by (+) Nanoelectrospray Quadrupole Time-of-Flight Tandem Mass Spectrometry of a Non-Covalent Enzyme-Ligand Complex

The molecular mechanisms of the biological actions of heterochitooligosaccharides remain essentially unknown. This is due to a lack of structural information and to the fact that pure ligands are not available. The present mass spectrometric method is employed for detection and structural analysis of non-covalent protein-carbohydrate complexes providing information on the binding stoichiometry and identification of the ligand by fragmentation. A fraction of heterochitooligosaccharides was separated by GPC from an enzymatic hydrolysate. Analysis by (+) nanoESI MS revealed a mixture of nine components, oligomers and homologs, among which D_1A_3 and D_2A_3 are major compounds. Additionally, each homolog represents a mixture of isomers. The mixture was incubated with chitinase B from *Serratia marcescens* for 5, 90 and 180 min. After 5 min, complexes between chitinase B and D_1A_3 and D_2A_3 are detected. After 90 min, a third complex is detected for chitinase B and D_1A_2 resulting from a partial fragmentation of D_1A_3 and D_2A_3. After 180 min, a kinetic equilibrium of the species in the solution is observed.

The complex between chitinase B and D_2A_3 was selected in the quadrupole of the mass spectrometer followed by application to a top-down CID experiment. Two events, namely the breakdown of the protein-sugar complex and fragmentation of the released isomeric D_2A_3 ligand took place.

10 isomeric sequences of D_2A_3 exist. The CID MS/MS provided diagnostic fragment ions that can be used to deduce the sequence of the pentameric ligand that was stably bound to chitinase B. The sequence was identified to be DADAA. In case that DADAA occupies subsites -3 to +2, a D position is found in the crucial -1 subsite and a highly favourable A unit in subsite -2 as well as in subsite +1, resulting in high-affinity, non-productive binding.

In a different experiment the composition of the mixture of D_2A_3 isomers was determined by vMALDI-LTQ MS giving 57% DADAA, 15% ADDAA and 26% DDAAA. This result supports the thesis that DADAA is the stably binding D_2A_3 isomer as DDAAA will be hydrolysed to DDA and AA, and for ADDAA no A unit is found in subsite -2 (presuming a -3 to +2 binding mode).

In summary, the present work demonstrates that a carbohydrate binding enzyme selects high affinity binding ligands from a complex mixture of closely related oligosaccharides (i. e. especially isomers). Top-down sequencing in combination with sequence analysis is a feasible method for the identification of a heterochitooligosaccharide in a non-covalent protein-ligand complex. The mechanism of enzyme inhibition is deduced by combination of the mechanism of catalysis in structure identification of a high affinity binding oligosaccharide ligand. NanoESI-MS and fragmentation of the specific sequence of the bound ligand by CID MS/MS is presented as a powerful tool of general applicability in functional proteomics and glycomics.

5.0 References

1. M. G. Peter in *Biopolymers, Vol. 6: Polysaccharides II* (Ed.: A. Steinbüchel), Wiley-VCH, Weinheim, **2002**, 481.

2. S. Bahrke, J. M. Einarsson, J. Gislason, S. Haebel, M. C. Letzel, J. Peter-Katalinić, M. G. Peter, *Biomacromol.* **2002**, *3*, 696.

3. P. Sikorski, B. T. Stokke, A. Sørbotten, K. M. Vårum, S. J. Horn, V. G. H. Eijsink, *Biopolym.* **2005**, *77*, 273.

4. B. C. R. Zhu, R. A. Laine in *Chitin Handbook* (Eds.: R. A. A. Muzzarelli, M. G. Peter), Atec, Grottammare, **1997**, 147.

5. URL: http://pages.usherbrooke.ca/rbrzezinski/general1.htm

6. R. A. A. Muzzarelli in *Chitin Handbook* (Eds.: R. A. A. Muzzarelli, M. G. Peter), Atec, Grottammare, **1997**, 153.

7. G.-J. Wu, G.-J. Tsai in *Advances in Chitin Science* (Eds.: H. Struszczyk, A. Domard, M. G. Peter, H. Pospieszny), Poznań, Institute of Plant Protection, **2005**, 461.

8. A. B. V. Kumar, L. R. Gowda, R. N. Tharanathan, *Eur. J. Biochem.* **2004**, *271*, 713.

9. A. Domard, N. Cartier, *Int. J. Biol. Macromol.* **1989**, *11*, 297.

10. E. Belamie, A. Domard, M.-M. Giraud-Guille, *J. Polym. Sci. A : Polym. Chem.* **2000**, *35*, 3181.

11. G. G. Allan, M. Peyron in *Chitin Handbook* (Eds.: R. A. A. Muzzarelli, M. G. Peter), Atec, Grottammare, **1997**, 175.

12. K. L. B. Chang, M.-C. Tai, F.-H. Cheng, *J. Agric. Food Chem.* **2001**, *49*, 4845.

13. J. Defaye, A. Gadelle, C. Pedersen, *Carbohydr. Res.* **1994**, *251*, 267.

14. S. Nishimura, H. Kuzuhara, Y. Takiguchi, K. Shimahara, *Carbohydr. Res.* **1989**, *194*, 223.

15. H. Kuyama, T. Ogawa in *Chitin Handbook* (Eds.: R. A. A. Muzzarelli, M. G. Peter), Atec, Grottammare, **1997**, 181.

16. P. H. Seeberger in *Solid Support Oligosaccharide Synthesis and Combinatorial Carbohydrate Libraries* (Ed.: P. H. Seeberger), Wiley-VCH, Weinheim, **2001**, 1.

17. H. A. Orgueira, A. Bartolozzi, P. H. Schell, P. H. Seeberger, *Angew. Chem. Int. Ed.* **2002**, *41*, 2128.

18. C.-H. Wong, Z. Zhang, I. Ollmann, T. Baasov, X.-S. Ye, **2003**, US Patent 6538117.

19. A. Kobayashi, H. Kuwata, M. Kohri, R. Izumi, T. Watanabe, S.-I. Shoda, *J. Carbohydr. Chem.* **2006**, *25*, 533.

20. F. Nanjo, K. Sakai, M. Ishikawa, K. Isobe, T. Usui, *Agr. Biol. Chem.* **1989**, *53*, 2189.

21. G. Perugino, *Trends in Biotechnology* **2003**, *22*, 31.

22. A. Sørbotten, S. J. Horn, V. G. H. Eijsink, K. M. Vårum, *FEBS Journal* **2005**, *272*, 538.

23. S. J. Horn, A. Sørbotten, B. Synstad, P. Sikorski, M. Sørlie, K. M. Vårum, V. G. H. Eijsink, *FEBS Journal* **2006**, *273*, 491.

24. S. Aiba, *Carbohydr. Res*. **1994**, *265*, 323.

25. S. Aiba, *Carbohydr. Res.* **1994**, *261*, 297.

26. K. B. Hicks, P. C. Lim, M. J. Haas, *J. Chromatogr*. **1985**, *319*, 159.

27. K. Tokuyasu, H. Ono, M. Ohnishi-Kameyama, K. Hayashi, Y. Mori, *Carbohydr. Res.* **1997**, *303*, 353.

28. D. Koga, M. Mitsutomi, M. Kono, M. Matsumiya, *EXS (Chitin and Chitinases)* **1999**, *87*, 111.

29. M. Mitsutomi, M. Isono, A. Uchiyama, N. Nikaidou, T. Ikegami, T. Watanabe, *Biosci. Biotechnol. Biochem.* **1998**, *62*, 2107.

30. K. M. Vårum, O. Smidsrød, *Adv. Chitin Sci.* **1997**, *2*, 168.

31. T. Fukamizo, A. Ohtakara, M. Mitsutomi, S. Goto, *Agric. Biol. Chem.* **1991**, *55*, 2653.

32. K. Akiyama, K. Kawazu, A. Kobayashi, *Carbohydr. Res.* **1995**, *279*, 151.

33. C. Bosso, A. Domard, *Org. Mass Spectrom.* **1992**, *27*, 799.

34. H. Zhang, Y. G. Du, X. J. Yu, M. Mitsutomi, S. Aiba, *Carbohydr. Res.* **1999**, *320*, 257.

35. B. Domon, C. E. Costello, *Glycoconjugate J.* **1988**, *5*, 397.

36. K. M. Vårum, M. W. Antonsen, H. Grasdalen, O. Smidsrød, *Carbohydr. Res.* **1991**, *217*, 19.

37. K. M. Vårum, M. W. Antonsen, H. Grasdalen, O. Smidsrød, *Carbohydr. Res.* **1991**, *211*, 17.

38. K. M. Vårum, O. Smidsrød, *Adv. Chitin Sci.* **1997**, *2*, 168.

39. T. Fukamizzo, A. Ohtakara, M. Mitsutomi, S. Goto, *Agric. Biol. Chem.* **1991**, *55*, 2653.

40. U. Danesch, *Zs. f. Orthomol. Med.* **2007**, *5*, 6.

41. B. Alberts in *Molecular Biology of the Cell* (Eds.: B. Alberts, D. Bray, J. Lewis), Garland Pbl., New York and London, **1994**, 1294.

42. J. Y. Lee, A. P. Spicer, Curr. Opin. Cell Biol. 2000, 12, 581.

43. M. Yoshida, N. Itano, Y. Yamada, K. Kimata, *J. Biol. Chem.* **2000**, *275*, 497.

44. T. Sugamori, H. Iwase, M. Maeda, Y. Inoue, H. Kurosawa, *J. Biomed. Mat. Res.* **2000**, *49*, 225.

45. H. Ueno, F. Nakamura, M. Murakami, M. Okumura, T. Kadosawa, T. Fujinaga, *Biomaterials* **2001**, *22*, 2125.

46. H. Ueno, M. Murakami, M. Okumura, T. Kadosawa, T. Uede, T. Fujinaga, *Biomaterials* **2001**, *22*, 1667.

47. S.-M. Hwang, C.-Y. Chen, S.-S. Chen, J.C. Chen, *Biochem. and Biophys. Res. Commun.* **2000**, *271*, 229.

48. A. R. Shikhman, K. Kuhn, N. Alaaeddine, M. Lotz, *J. Immunol.* **2001**, *166*, 5155.

49. K. Suzuki, T. Mikcami, Y. Oawa, A. Tokoro, S. Suzuki, M. Suzuki, *Carbohydr. Res.* **1986**, *151*, 403.

50. K. Tsukada, T. Matsumoto, K. Aizawa, A. Tokoro, R. Naruse, S. Suzuki, M. Suzuki, *Jpn. J. Cancer Res.* **1990**, *81*, 259.

51. B. J. Chae, K. N. Han, S. C. Choi, W. T. Kim, T. W. Han, I. K. Kwon, Kangwon National University **2003**.

52. P. Colombo, A. M. Sciutto, *Acta Toxicol. Ther.* **1996**, *17*, 287.

53. Y. Maezaki, K. Tsuji, Y. Nakagawa, Y. Kawai, M. Akimoto, T. Tsugita, W. Takekawa, A. Terada, H. Hara, T. Mitsuoka, *Biosci., Biotechnol. and Biochem.* **1993**, *57*, 786.

54. T. Kawasaki, M. Kawasaki, A. Notomi, K. Itoh, N. Ikeyama, *Kichin, Kitosan, Kenyu* **1998**, *4*, 316.

55. P. P. G. van der Holst, H. R. M. Schalaman, H. P. Spaink, *Current Opinion in Structural Biology* **2001**, *11*, 608.

56. C. E. Semino, M. L. Allende, *Int. J. Dev. Biol.* **2000**, *44*, 183.

57. J. Bakkers, C. E. Semino, H. Stroband, J. W. Kijne, P. W. Robbins, H. P. Spaink, *Proc. Natl. Acad. Sci. USA* **1997**, *94*, 7982.

58. B. Ernst, G. W. Hart, P. Sinaÿ, Eds. *Carbohydrates in Chemistry and Biology*, Part II, Vol. 4, Wiley-VCH, Weinheim, **2002**.

59. P. Vander, K. M. Vårum, A. Domard, N. E. El Gueddari, B. M. Moerschbacher, *Plant Physiol.* **1998**, *118*, 1353.

60. H. Inui, Y. Yamaguchi, S. Hirano, *Biosci. Biotechnol. Biochem.* **1997**, *61*, 975.

61. H. Kaku, N. Shibuya, P. Xu, A. P. Aryan, G. P. Fincher, *Physiol. Plant.* **1997**, *100*, 111.

62. W. K. Roberts, C. P. Selitrennikoff, *J. Gen. Microbiol.* **1988**, *134*, 169.

63. J. Dénarié, F. Debellé, J.-C. Promé, *Annu. Rev. Biochem.* **1996**, *65*, 503.

64. R. B. Mellor, D. B. Collinge, *J. Exp. Bot.* **1995**, *46*, 1.

65. G. W. Gooday, *Mycol. Res.* **1995**, *99*, 385.

66. A. Hodge, I. J. Alexander, G. W. Gooday, *Mycol. Res.* **1995**, *99*, 935.

67. M. L. Bade, A. Stinson, *Biochem. Biophys. Res. Commun.* **1978**, *84*, 381.

68. D. Koga, T. Funakoshi, K. Mizuki, A. Ide, K. J. Kramer, K. C. Zen, H. Choi, S. Muthukrishnan, *Insect Biochem. and Mol. Biol.* **1992**, *22*, 305.

69. G. J. H. Lindsay, *J. Fish Biol.* **1984**, *24*, 529.

70. F. D. C. Manson, T. C. Fletcher, G. W. Gooday, *J. Fish Biol.* **1992**, *40*, 919.

71. C. E. M. Hollak, S. van Weely, M. H. J. van Oers, J. M. F. G. Aerts, *J. Clin. Invest.* **1994**, *93*, 1288

72. J. M. Aerts, C. E. Hollak, *Baillieres Clin. Haematol.* **1997**, *10*, 691.

73. E. H. Choi, P. A. Zimmerman, C. B. Foster, S. Zhu, V. Kumaraswami, T. B. Nutman, S. J. Chanock, *Genes Immun.* **2001**, *2*, 248.

74. R. G. Boot, G. H. Renkema, M. Verhoek, A. Strijland, J. Bliek, T. M. A. M. O. Meulemeester, M. M. A. M. Mannens, J. M. F. G. Aerts, *J. Biol. Chem.* **1998**, *273*, 25680.

75. R. G. Boot, E. F. C. Blommaart, E. Swart, K. Ghauharali-van der Vlugt, N. Bijl, C. Moe, A. Place, J. M. F. G. Aerts, *J. Biol. Chem.* **2001**, *276*, 6770.

76. F. Fusetti, H. von Moeller, D. Houston, H. J. Rozeboom, B. W. Dijkstra, R. G. Boot, J. M. F. G. Aerts, D. M. F. van Aalten, *J. Biol. Chem.* **2002**, *277*, 25537.

77. J. A. Elias, R. J. Homer, Q. Hamid, *J. Allergy Clin. Immunol.* **2005**, *116*, 497.

78. Z. Zhu, T. Zheng, R. J. Homer, *Science* **2004**, *304*, 1678.

79. Z. Zhu, T. Zheng, R. J. Homer, Y. K. Kim, N. Y. Chen, L. Cohn, Q. Hamid, J. A. Elias, Sci. 2004, 304, 1678.

80. A. Ray, L. Cohn, *J. Clin. Invest.* **1999**, *104*, 985.

81. URL: http://www.cazy.org/fam/acc_GH.html

82. T. Tanabe, K. Morinaga, T. Fukamizo, M. Mitsutomi, *Biosci. Biotechnol. Biochem.* **2003**, *67*, 354.

83. M. Izume, S. Nagae, H. Kawagishi, M. Mitsutomi, A. Ohtakara, *Biosci. Biotechnol. Biochem.* **1992**, *56*, 448.

84. M. Mitsutomi, M. Isono, A. Uchiyama, N. Nikaidou, T. Ikegami, T. Watanabe, *Biosci. Biotechnol. Biochem.* **1998,** *62*, 2107.

85. H. Kimoto, H. Kusaoke, I. Yamamoto, Y. Fujii, T. Onodera, A. Taketo, *Biosci. Biotechnol. Biochem.* **2002**, *277*, 14695.

86. K. J. Fischer, N. N. J. Aronson, *J. Biol. Chem.* **1992**, *267*, 19607.

87. B. Henrissat, *Protein Sequences Data Anal.* **1990**, *3*, 523.

88. T. Watanabe, Y. Ito, T. Yamada, M. Hashimoto, S. Sekine, H. Tanaka, *J. Bacteriol.* **1994**, *176*, 4465.

89. B.Synstad, S. Gåseidnes, D. M. F. van Aalten, G. Vriend, J. E. Nielsen, V. G. H. Eijsink, *Eur. J. Biochem.* **2004**, *271*, 253.

90. N. N. J. Aronson, B. A. Halloran, M. F. Alexyev, L. Amable, J. D. Madura, L. Pasupulati, C. Worth, P. van Roey, *Biochem. J.* **2003**, *376*, 87.

91. T. Uchiyama, F. Katouno, N. Nikaidou, T. Nonaka, J. Sugiyama, T. Watanabe, *J. Biol. Chem.* **2001**, *276*, 41343.

92. F. Katouno, M. Taguchi, K. Sakurai, T. Uchiyama, N. Nikaidou, T. Nonaka, J. Sugiyama, T. Watanabe, *J. Biochem.* **2004**, *136*, 163.

93. K. A. Brameld, W. A. Goddard, III, *J. Am. Chem. Soc.* **1998**, *120*, 3571.

94. I. Tews, A. C. T. van Sheltinga, A. Perrakis, K. S. Wilson, B. W. Dijkstra, *J. Am. Chem. Soc.* **1997**, *119*, 7954.

95. K. A. Brameld, W. D. Shrader, B. Imperiali, W. A. Goddard, III, *J. Mol. Biol.* **1998**, *280*, 913.

96. A. Perrakis, I. Tews, Z. Dauter, A. B. Oppenheim, I. Chet, K. S. Wilson, C. E. Vorgias, *Structure*, **1994**, *2*, 1169.

97. N. N. Aronson, B. A. Halloran, M. F. Alexeyev, X. E. Zhou, Y. Wang, E. J. Meehan, L. Chen, *Biosci. Biotechnol. Biochem.* **2006**, *70*, 243.

98. T. Watanabe, A. Ishibashi, Y. Ariga, M. Hashimoto, N. Nikaidou, J. Sugiyama, T. Matsumoto, T. Nonaka, *FEBS Lett.* **2001**, *494*, 74.

99. G. Vaaje-Kolstad, D. R. Houston, F. V. Rao, M. G. Peter, B. Synstad, D. M. F. van Aalten, V. G. H. Eijsink, *Biochim. Biophys. Act.* **2004**, *1696*, 103.

100. D. M. F. van Aalten, B. Synstad, M. B. Brurberg, E. Hough, B. W. Riise, V. G. H. Eijsink, R. K. Wierenga, *PNAS* **2000**, *97*, 5842.

101. D. M. F. van Aalten, D. Komander, B. Synstad, S. Gåseidnes, M. G. Peter, V. G. H. Eijsink, *PNAS* **2001**, *98*, 8979.

102. A. Sørbotten, S. J. Horn, V. G. H. Eijsink, K. M. Vårum, *FEBS J.* **2005**, *272*, 538.

103. A. Germer, C. Mügge, M. G. Peter, A. Rottmann, E. Kleinpeter, *Chem. Eur. J.* **2003**, *9*, 1964.

104. F. Cederkvist, A. D. Zamfir, S. Bahrke, V. G. H. Eijsink, M. Sørlie, J. Peter-Katalinić, M. G. Peter, *Angew. Chem. Int. Edn.* **2006**, *45*, 2429.

105. K. L. B. Chang, G. Tsai, *J. Agric. Food Chem.* **1997**, *45*, 1900.

106. G. H. Renkema, R. G. Boot, A. O. Muijsers, W. E. Donker-Kopman, J. M. F. G. Aerts, *J. Biol. Chem.* **1995**, *270*, 2198.

107. Y. Papanikolau, G. Prag, G. Tavlas, C. E. Vorgias, A. B. Oppenheim, K. Petratos, *Biochem.* **2001**, *40*, 11338.

108. J. Kzhyshkowska, A. Gratchev, S. Goerdt, *J. Cell. Mol. Med.* **2006**, *10*, 635.

109. R. G. Boot, G. H. Renkema, A. Strijland, A. J. Zonneveld, J. M. F. G. Aerts, *J. Biol. Chem.* **1995**, *270*, 26252.

110. Y. Nishimoto, S. Sakuda, S. Takayama, Y. Yamada, *J. Antibiod.* **1991**, *44*, 716.

111. J. Kzhyshkowska, S. Mamidi, A. Gratchev, *Blood* **2006**, *107*, 3221

112. L. Sticher, J. Hofsteenge, A. Milani, J.-M. Neuhaus, F. Meins, Jr., *Sci.* **1992**, *257*, 655.

113. J. J. Beintema, FEBS Lett. 1994, 350, 159.

114. T. Ohno, S. Armand, T. Hata, N. Nikaidou, B. Henrissat, M. Mitsutomi, T. Watanabe, *J. Bacteriol.* **1996**, *178*, 5065.

115. T. Fukamizo, C. Sasaki, E. Schelp, K. Bortone, J. D. Robertus, *Biochem.* **2001**, *40*, 2448.

116. T. Hollis. Y. Honda, T. Fukamizo, E. Marcotte, P. J. Day, J. D. Robertus, *Arch. Biochem. Biophys.* **1997**, *344*, 335.

117. D. M. Chipman, V. Grisaro, N. Sharon, *J. Biol. Chem.* **1967**, *242*, 4388.

118. T. Fukamizo, T. Ohkawa, Y. Ikeda, T. Torikata, S. Goto, *Carbohydr. Res*. **1995**, *267*, 135.

119. K. A. Bramfeld, W. A. Goddard, III, *PNAS USA Biophys.* **1998**, *95*, 4276.

120. M. Pennybacker, B. Liessem, H. Moczall, C. J. Trifft, K. Sandhoff, R. L. Proia, *J. Biol. Chem.* **1996**, *271*, 17377.

121. S. J. Williams, B. Mark, D. J. Vocadlo, M. N. G. James, S. G. Withers, *J. Biol. Chem.* **2002**, *277*, 40055.

122. S. Drouillard, S. Armand, G. J. Davies, C. E. Vorgias, B. Henrissat, *Biochem. J.* **1997**, *328*, 945.

123. J-Y. Masson, F. Denis, R. Brzezinski, *Gene* **1994**, *140*, 103.

124. J.-Y. Masson, I. Boucher, W. A. Neugebauer, D. Ramotar, R. Brzezinski, *Microbiol.* **1995**, *141*, 2629.

125. URL: http//www.ncbi.nlm.nih.gov/entrez/viewer.cgi?val=AB041775.1

126. NCBI GenBank locus AL132973. *Streptomyces coelicolor* A3(2) secreted chitosanase. Gene "SCF91.37". (**2004**). Amino acid sequence translated from the genomic sequence.

127. Amino acid sequence translated from the genomic sequence of *Streptomyces coelicolor* A3(2). Cosmid 3a3. Gene SC3A3.02.

128. V. Parro, M. San Román, I. Galindo, B. Purnelle, A. Bolotin, A. Sorokin, R. P. Mellado, *Microbiol.* **1997**, *143*, 1321.

129. L.A. Rivas, V. Parro, M. Moreno-Paz, R.P. Mellado, *Microbiol.* **2000**, *146*, 2929.

130. K. Seki, H. Kuriyama, T. Okuda, Y. Uchida in *Advances in Chitin Science*, vol.II (Eds.: A. Domard, G. A. F. Roberts, K. M. Vårum), Jacques André Publ. Lyon, France, **1997**, 284.

131. NCBI GenBank locus AF160195. *Bacillus* sp. KFB-CO4 thermostable chitosanase gene (*cho*K). Submitted by H. G. Yoon, and H. Y. Cho, **2000**.

132. H.-G. Yoon, H.-Y. Kim, Y.-H. Lim, H.-K. Kim, D.-H. Shin, B.-S. Hong, H.-Y. Cho, *Appl. Environmental Microbiol.* **2000**, *66*, 3727.

133. Z. Lu, Y. Il, Q. Que, G. F. Kutish, D. L. Rock, J. L. van Etten, *Virology* **1996**, *216*, 102.

134. L. Sun, B. Adams, J. R. Gurnon, Y. Ye, J. L. van Etten, *Virology* **1999**, *263*, 376.

135. T. Yamada, S. Hiramatsu, P. Songsri, M. Fujie, *Virology* **1997**, *230*, 361.

136. NCBI locus 2626878

137. K. Akiyama, T. Fujita, K. Kuroshima, T. Sakane, A. Yokota, R. Takata, *J. Biosci. Bioengineering* **1999**, *87*, 383.

138. H-G. Yoon, K-H. Lee, H-Y. Kim, H-K. Kim, D-H. Shin, B-S. Hong, H-Y. Cho, *Biosci. Biotechnol. Biochem.* **2002**, *66*, 986.

139. NCBI GenBank locus ABO29336. *Burkholderia gladioli csn*A gene for chitosanase A, complete coding sequence. Submitted by M. Shimosaka, Y. Fukumori, X . Zhang, N. He, R. Kodaira, and M. Okazaki, **1999**.

140. M. Shimosaka, Y. Fukumori, X. Y. Zhang, N. J. He, R. Kodaira, M. Okazaki, *Appl. Microbiol. Biotechnol.* **2000**, *54*, 354.

141. A. Ando, K. Noguchi, M. Yanagi, H. Shinoyama, Y. Kagawa, H. Hirata, M. Yabuki, T. Fujii, *J. Gen. Appl. Microbiol.* **1992**, *38*, 135.

142. M. Shimosaka, M. Kumehara, X.-Y. Zhang, M. Nogawa, M. Okazaki, *J. Fermentation and Bioengineering* **1996**, *82*, 426.

143. NCBI GenBank locus ABO38996. *Aspergillus oryzae csn* gene for chitosanase, complete coding sequence. Submitted by X. Zhang, A. Dai, A. Shimosaka, and M. Okazaki, **2000**.

144. NCBI GenBank locus AF105078. *Aspergillus fumigatus csn* chitosanase mRNA, partial sequence. Submitted by T. H. Kang, J. Y. Chung, and K.C. Chung, **1998**.

145. S. E. Screen, R. J. St Leger, **2000** *Metarhizium anisopliae* var. *acridum* putative chitosanase. GI locus 9971106, accession number AJ293219.

146. J. K. Park, K. Shimono, N. Ochiai, K. Shigeru, M. Kurita, Y. Ohta, K. Tanaka, H. Matsuda, M. Kawamukai, *J. Bacteriol.* **1999**, *181*, 6642. See also database files: NCBI locus 3399693. DDBJ locus AB010493.

147. Y. Matsuda, Y. Iida, T. Shinogi, K. Kakutani, T. Nonomura, H. Toyoda, *J. Gen. Plant Pathol.* **2001**, *67*, 318. See also NCBI GenBank locus AB030253.

148. *Lectins* (Eds. : A. Pusztai, S. Bardocz), CRC, USA, **1995**.

149. V. Triguéros, M. Wang, D. Père, L. Paquereau, L. Chavant, D. Fournier, *Arch. Insect. Biochem. Physiol.* **2000**, *45*, 175.

150. D. Voet, J.G. Voet, C. W. Pratt in *Lehrbuch der Biochemie* (Eds.: A. G. Beck-Sickinger, U. Hahn), Wiley-VCH, Weinheim, **2002**, 232.

151. J. Shemer, D. LeRoith, *Neuropeptides* **1987**, *9*, 1.

152. G. Ponzio, A. Debant, J. O. Contreras, B. Rossi, *Cell Signal* **1990**, *2*, 377.

153. H. Haas, F. H. Falcone, G. Schramm, K. Haisch, B. F. Gibbs, J. Klaucke, M. Pöppelmann, W.-M. Becker, H.-J. Gabius, M. Schlaak, *Eur. J. Immunol.* **1999**, *29*, 918.

154. L. J. Halverson, G. Stacey, *Appl. Environ. Microbiol.* **1986**, *51*, 753.

155. P. Nangia-Makker, S. Baccarini, A. Raz, *Cancer and Metastasis Reviews* **2000**, *19*, 51.

156. F.-T. Liu, *Expert Opinion on Therapeutic Targets* **2002**, *6*, 461.

157. B. Volck, J. S. Johansen, M. Stoltenberg, C. Garbarsch, P. A. Price, M. Østergaard, K. Østergaard, P. Løvgreen-Nielsen, S. Sonne-Holm, I. Lorenzen, *Osteoarthritis and Cartilage* **2001**, *9*, 203.

158. K. Vos, P. Steenbakkers, A. M. M. Miltenburg, E. Bos, M. W. van den Heuvel, R. A. van Hogezand, R. R. P. de Vries, F. C. Breedveld, A. M. H. Boots, *Annals of the Reumatic Diseases* **2000**, *59*, 544.

159. J. S. Johansen, B. V. Jensen, A. Roslind, D. Nielsen, P. A. Price, *Cancer Epidemiol. Biomarkers Prev.* **2006**, *15*, 194.

160. M. K. Tanvar, M. R. Gilbert, E. C. Holland, *Cancer Res.* **2002**, *62*, 4364.

161. H. Dehn, E. V. S. Høgdall, J. S. Johansen, J. A. Price, M. Jørgensen, S. A. A. Engelholm, C. K. Høgdall, *Acta Obstetricia et Gynecologica Scandinavica* **2003**, *82*, 287.

162. J. S. Johansen, C. Cintin, M. Jørgensen, C. Kamby, P. A. Price, *European Journal of Cancer* **1995**, *31*, 1437.

163. L. Drivsholm, J. S. Johansen, *Lung Cancer* **1997**, *18*, 155.

164. C. Nojgaard, J. S. Johansen, E. Christensen, L. T. Skovgaard, P. A. Price, U. Becker, *J. Hepatol.* **2003**, *39*, 179.

165. I. E. Koutroubakis, E. Petinaki, P. Dimoulios, E. Vardus, M. Roussomoustakaki, A. N. Maniatis, E. A. Kouroumalis, *International Journal of Colorectal Disease* **2003**, *18*, 254.

166. C. Østergaard, J. S. Sørensen, T. Benfield, P. A. Price, J. D. Lundgren, *Clinical and Diagnostic Laboratory Immunology* **2002**, **9**, 598.

167. E. Vignon, *Joint Bone Spine* **2001**, *68*, 454.

168. B. Schmidt-Rohlfing, K. Gavenis, M. Kippels, U. Schneider, *Scandinavian Journal of Rheumatology* **2002**, *31*, 151.

169. B. Volck, P. A. Price, J. S. Johansen, O. Sørensen, H. J. Nielsen, J. Calafat, N. Borregaard, *Procedings of the Association of American Physicians* **1998**, *110*, 351.

170. J. S. Johansen, J. Hvolris, M. Hansen, V. Backer, L. Lorenzen, P. A. Price, *Br. J. Rheumatol.* **1996**, *35*, 553.

171. A. P. Cope, S. D. Patel, F. Hall, M. Congea, H. A. J. M. Hubers, G. F: Verheijden, A. M. H. Boots, M. Menon, M. Trucco, A. W. M. Runders, G. Sønderstrup, *Arthritis and Rheumatism* **1999**, *42*, 1497.

172. A. M. H. Boots, G. F. M. Verheijden, E. S. Bos, U.S. Patent 5636507, **1996**, 19.

173. J. S. Johansen, *Dan. Med. Bull.* **2006**, *53*, 172.

174. P. Nyirkos, E. E. Golds, *Biochem. J.* **1990**, *269*, 265.

175. L. M. Shackelton, D. M. Mann, A. J. T. Millis, *J. Biol. Chem.* **1995**, *270*, 13076.

176. R. B. Kirkpatrick, J. G. Emery, J. R. Connor, R. Dodds, P. G. Lysko, M. Rosenberg, *Exp. Cell Res.* **1997**, *237*, 46.

177. M. Rehli, S. W. Krause, R. Andreesen, *Genomics* **1997**, *43*, 221.

178. A. D. Recklies, C. White, H. Ling, Biochem. J. 2002, 365, 119.

179. B. Dozin, M. Malpeli, L. Camardella, R. Cancedda, A. Pietrangelo, *Matrix Biology* **2002**, *21*, 449.

180. J. R. Connor, R. A. Dodds, J. G. Emery, R. B. Kirkpatrick, M. Rosenberg, M. Gowen, *Osteoarthritis and Cartilage* **2000**, *8*, 87.

181. J. M. Einarsson, J. Gislason, M. G. Peter, S. Bahrke, WO Patent 03/026677, **2003**.

182. K. Kavamura, T. Shibata, o. Saget, D. Peel, G. J. Bryant, *Development* **1999**, *126*, 211.

183. A. Lahiji, A. Sohrabi, D. S. Hungerford, C. G. Frondoza, *J. Biomed. Mat. Res.* **2000**, *51*, 586.

184. A. C. Terwisscha van Scheltinga, K. H. Kalk, J. J. Beintema, B. W. Dijkstra, *Structure* **1994**, *2*, 1181.

185. T. Hollis, A. F. Mozingo, K. Bortone, S. Ernst, R. Cox, J. D. *Robertus, Protein Sci.* **2000**, *9*, 544.

186. G. H. Renkema, R. G. Boot, F. L. Au, W. E. Donker-Koopman, A. Strijland, A. O. Muijsers, M. Hrebiček, J. M. F. G. Aerts, *Eur. J. Biochem.* **1998**, *251*, 504.

187. D. R. Houston, A. D. Recklies, J. C. Krupa, D. M. F. van Aalten, *J. Biol. Chem.* **2003**, *278*, 30206.

188. F. Fusetti, T. Pijning, K. H. Kalk, E. Bos, B. W. Dijkstra, *J. Biol. Chem.* **2003**, *278*, 37753.

189. Zaheer-ul-Haq, P. Dalal, N. N. Aronson Jr., J. D. Madura, *Biochem. Biophys. Res. Comun.* **2007**, Artikle in Press.

190. A. Varki, *PNAS* **1996**, *93*, 4523.

191. C. E. Semino, C. A. Specht, A. Raimondi, P. W. Robbins, *PNAS* **1996**, *93*, 4548.

192. M. F. Meyer, G. Kreil, *PNAS* **1996**, *93*, 4543.

193. N.-C. A. Chang, S.-I. Hung, K.-Y. Hwa, I. Kato, J.-E. Chen, C.-H. Liu, A. C. Chang, *J. Biol. Chem.* **2001**, *276*, 17497.

194. C. Westling, U. Lindahl, *J. Biol. Chem.* **2002**, *277*, 49247.

195. K. Norgard-Sumnicht, A. Varki, *J. Biol. Chem.* **1995**, *270*, 12012.

196. H. F. Bigg, R. Wait, A. D. Rowan, T. E. Cawston, *J. Biol. Chem.* **2006**, *281*, 21082.

197. T. Sekine, K. Masuko-Hongo, T. Matsui, H. Asahara, M. Takigawa, K. Nishioka, T. Kato, *Ann. Rheum. Dis.* **2001**, *60*, 49.

198. T. Knorr, F. Obermayr, E. Bartnik, A. Zien, T. Aigner, *Ann. Rheum. Dis.* **2003**, *62*, 995.

199. M. Sakata, K. Masuko-Hongo, J. Tsuruha, *Clin. Exp. Rheumatol.* **2002**, *20*, 343.

200. J. H. Martens, J. Kzhyshkowska, M. Falkowski-Hansen, *J. Pathol.* **2006**, *208*, 574.

201. I. H. Lok, C. M. Briton-Jones, P. M. Yuen, *J. Assist. Reprod. Genet.* **2002**, *19*, 569.

202. B. Malette, Y. Paquette, Y. Merlen, G. Bleau, *Mol. Reprod. Dev.* **1995**, *41*, 384.

203. Y. J. Sun, N. C. A. Chang, S. I. Hung, A. C. Chang, C. C. Chou, C. D. Hsiao, *J. Biol. Chem.* **2001**, *276*, 17507.

204. P. F. Valera, A. S. Liera, R. A. Mariuzza, J. Tormo, *J. Biol. Chem.* **2002**, *277*, 13229.

205. A. K. Mohanty, G. Singh, M. Paramasivam, K. Saravanan, T. Jabeen, S. Sharma, S. Yadav, P. Kauer, P. Kumar, A. Srinivasan, T. P. Singh, *J. Biol. Chem.* **2003**, *278*, 14451.

206. M. Hennig, B. Schlesier, Z. Dauter, S. Pfeffer, C. Betzel, W. E. Hohne, K. S. Wilson, *FEBS Lett.* **1992**, *306*, 80.

207. B. Schlesier, V. H. Nong, C. Horstmann, M. Hennig, *J. Plant Physiol.* **1996**, *147*, 665.

208. M. Hennig, J. N. Jansonius, A. C. Terwisscha van Scheltinga, B. W. Dijkstra, B. Schlesier, *J. Mol. Biol.* **1995**, *254*, 237.

209. M. E. Taylor, K. Drickamer, *Introduction to Glycobiologie, 2-nd Edition*, Oxford University Press, Oxford **2006**, 33.

210. D. Voet, J. G. Voet, C. W. Pratt, *Lehrbuch der Biochemie*, Wiley VCH, Weinheim, **2002**, 223, 229 – 231.

211. A. Varki, *Proc. Natl. Acad. Sci. USA* **1996**, *93*, 4523.

212. C. E. Semino, C. A. Specht, A. Raimond, P. W. Robbins, *Proc. Natl. Acad. Sci. USA* **1996**, *93*, 4548.

213. URL: http://www.thermo.com File_146.exe (LTQ Animation).

214. K. Kurita, T. Sannan, Y. Iwakura, *Macromol. Chem*. **2003**, *178*, 3197.

215. S. V. Nemtsev, A. I. Gamzazade, S. V. Rogozhin, V. M. Bykova, V. P. Bykov, *Appl. Biochem. Microbiol*. **2002**, *38*, 521.

216. P. Ross, R. Mayer, M. Benziman, *Microbiol. Rev.* **1991**, *55*, 35.

217. D. Ciechanska, H. Struszczyk, K. Guzinsca, *Fibres & Textiles in Eastern Europe* **1998**, *6*, 61.

218. D. Ciechanska, *Fibres & Textiles in Eastern Europe* **2004**, *12*, 69.

219. D. Ciechanska, H. Struszczyk, J. Kazimierczak, K. Guzinsca, M. Pawlak, E. Kozlowska, G. Matusiak, M. Dutkiewicz, *Fibres & Textiles in Eastern Europe* **2002**, *10*, 27.

220. Y. J. Jeong, S. Y. Cha, W. R. Yu, W. H. Park, *Tex. Res. J.* **2002**, *72*, 71.

221. D. Ciechanska, A. Niekraszswicz, M. Kucharska, G. Strobin, M. Wiśniewska-Wrona, M. H. Struszczyk, *Adv. Chi. Sci.* **2007**, **10**, 306.

222. C. H. Grün, F. Hochstenbach, B. M. Humbel, A. J. Verkleij, J. H. Sietsma, F. M. Klis, J. P. Kamerling, J. F. G. Vliegenthart, *Glycobiol.* **2005**, *15*, 245.

223. M. B. Brurberg, I. F. Nes, V. G. H. Eijsink, *Microbiol.* **1996**, *142*, 1581.

224. T. Fukamizo, D. Koga, S. Goto, *Biosci. Biotech. Biochem.* **1995**, *59*, 311.

225. M. C. Letzel, E. Synstad, V. G. H. Eijsink, J. Peter-Katalinić, M. G. Peter, *Advan. Chitin Sci.* **2000**, *4*, 545.

226. F. H. Cederkvist, M. P. Parmer, K. M. Vårum, V. G. H. Eijsink, M. Sørlie, *Carbohydrate Polymers* 2008, Article in press.

227. URL: http://en.wikipedia.org/wiki/Binding_constant

228. URL: http://en.wikipedia.org/wiki/Dissociation_constant

229. P. Dalal, L. L. Thomas, K. Robertson, B. A. Halloran, N. N. Aronson Jr., J. D. Madura, Thermodynamic Properties of Chitinase Interaction with Oligosaccharides (**2004**).

230. B. E. Hakala, C. White, A. D. Recklies, *J. Biol. Chem.* **1993**, *268*, 25803.

231. J. S. Johansen, P.Christoffersen, S. Moller, P. A. Price, J. H. Henriksen, C. Garbarsch, F. Bendtsen, *J. Hepatol.* **2000**, *32*, 911.

232. F. de Ceuninck, S. Gaufillier, A. Bonnaud, M. Sabatini, C. Lesur, P. Pastoureau, *Biochem. Biophys. Res. Commun.* **2001**, *285*, 926.

233. S. Gay, R. E. Gay, U. Müller-Ladner, T. Pap, *Rheuma-Nachrichten der Rheumaklinik und Institut für physikalische Medizin*, ETH Zürich **1999**, *52*, 1.

234. D. Voet, J.G. Voet, C. W. Pratt in *Lehrbuch der Biochemie* (Eds.: A. G. Beck-Sickinger, U. Hahn), Wiley-VCH, Weinheim, **2002**, 223.

235. www. rheuma-info.de, Pfizer Pharma GmbH, **2007**.

236. F. V. Rao, D. R. Houston, R. G. Boot, J. M. F. G. Aerts, S. Sakuda, D. M. F. van Aalten, *J. Biol. Chem.* **2003**, *278*, 20110.

237. G. Vaaje-Kolstad, A. Vasella, M. G. Peter, C. Netter, D. R. Houston, B. Westereng, B. Synstad, V. G. H. Eijsink, D. M. F. van Aalten, *J. Biol. Chem.* **2004**, *279*, 3712.

238. T. Ikegami, T. Okada, M. Hashimoto, S. Sino, T. Watanabe, M. Shirakawa, *J. Biol. Chem.* **2000**, *275*, 13654.

239. A. Germer, C. Mügge, M. G. Peter, A. Rottmann, E. Kleinpeter, *Chem. Eur. J.* **2003**, *9*, 1964.

240. B. Ganen, *J. Am. Chem. Soc.* **1991**, *113*, 7818.

241. W. Wang, E. N. Kitova, J. S. Klassen, *Anal. Chem.* **2003**, *75*, 4945.

242. A. J. R. Heck, R. H. H. van der Heuvel, *Mass. Spectrom. Ref.* **2004**, *23*, 368.

243. K. Benkestock, G. Sundqvist, P. O. Edelund, J. J. Roeraade, *J. Mass. Spectrom.* **2004**, *39*, 1059.

244. H. Naumer, W. Heller in *Untersuchungsmethoden in der Chemie* (Eds.: H. Naumer, W. Heller), Georg Thieme Verlag, Stuttgart, **1997**, 367.

245. S. Haebel, S. Bahrke, M. G. Peter, *Anal. Chem.* **2007**, *79*, 5557.

246. K. Suzuki, N. Sugaeara, M. Suzuki, T. Uchiyama, F. Katouno, N. Nikaidou, T. Watanabe, *Biosci. Biotechnol. Biochem.* **2002**, *66*, 1075.

Appendix

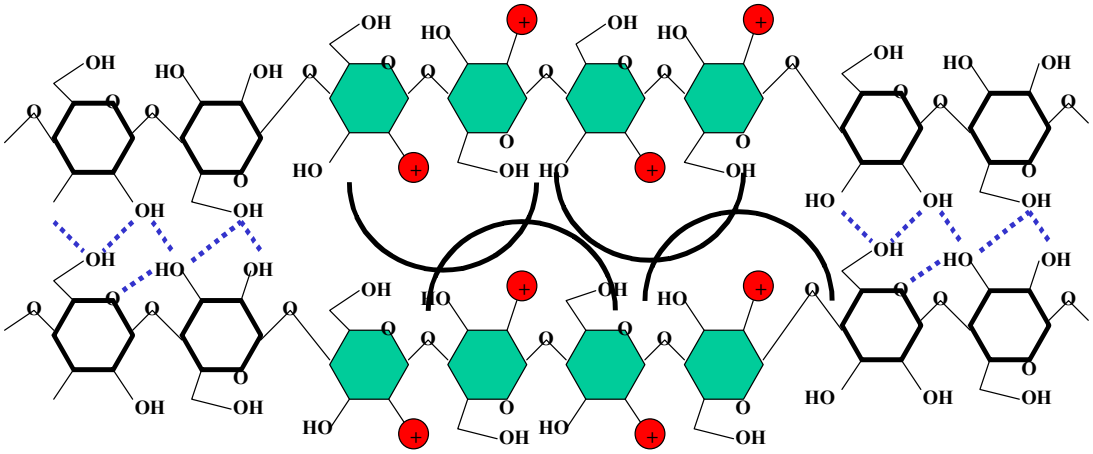

The cellulose areas are arranged in a crystalline form due to a network of hydrogen bonds. The glucose moieties possess little degrees of freedom. For areas of chito-oligomers the long-range ionic repulsion forces of the positively charged ammonium groups (red) of the glucosamine moieties (green) cover the short-range hydrogen bonds. Consequently, the glucosamine moieties possess an increased number of degrees of freedom leading to a twisting of the glucosamine units and a coil-like structure.

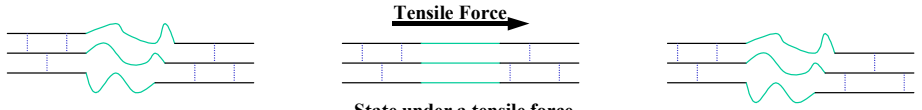

Relaxed state. The area of chito-oligomers green) is of higher disorder and thus higher entropic state than the cellulose area.

State under a tensile force along the polymer chains. The glucosamine units are aligned. The disorder and entropy is reduced.

State after reduction of the tensile force. The structure is flipping back into the relaxed state.

Figure S1. The elasticity of chitosan modified bacterial cellulose.

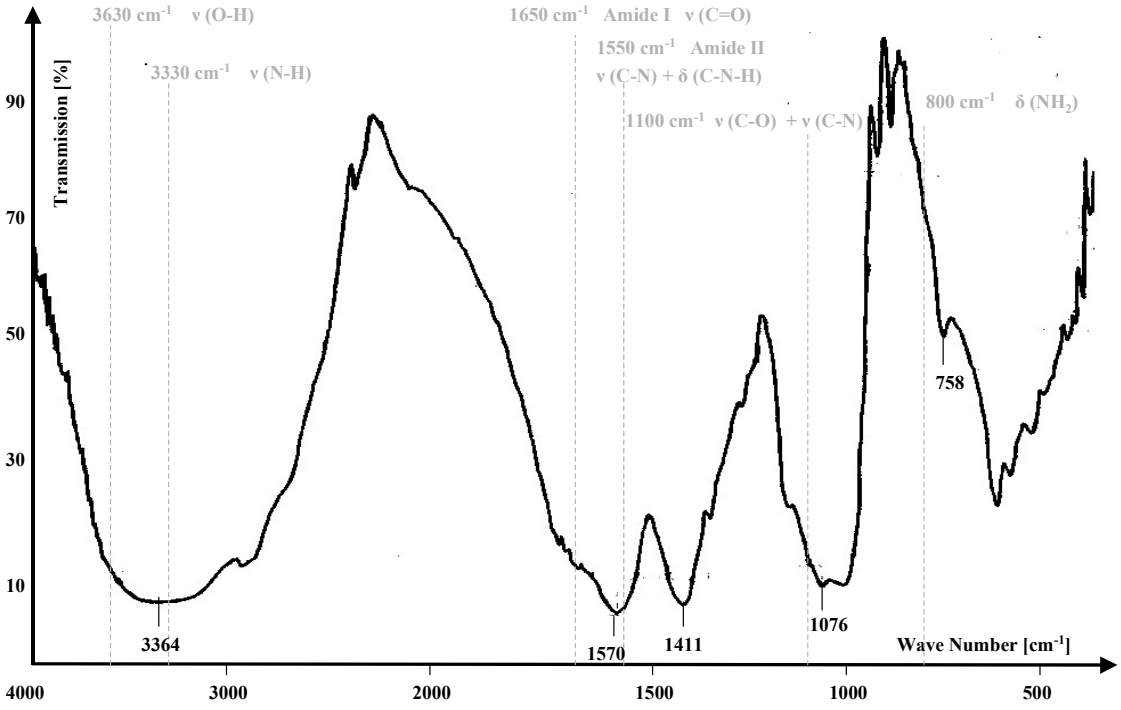

Figure S2. Infrared spectrum of chitosan modified bacterial cellulose.

Table S1. Assignment of the peaks of the infrared spectrum of the chitosan modified bacterial cellulose

Absorption Band Observed [cm^{-1}]	Absorption Band Literature [cm^{-1}]	Assignment	Species
3364	3330	υ (N-H)	Amine
	3630	υ (O-H)	Alcohole
1570	1550	Amide II ν (C-N) + δ (C-N-H)	Amide
	1650	Amide I ν (C=O)	Amide
1076	1100	ν (C-O)	Alcohole
	1100	ν (C-N)	Amine
758	800	δ (NH_2)	Amine

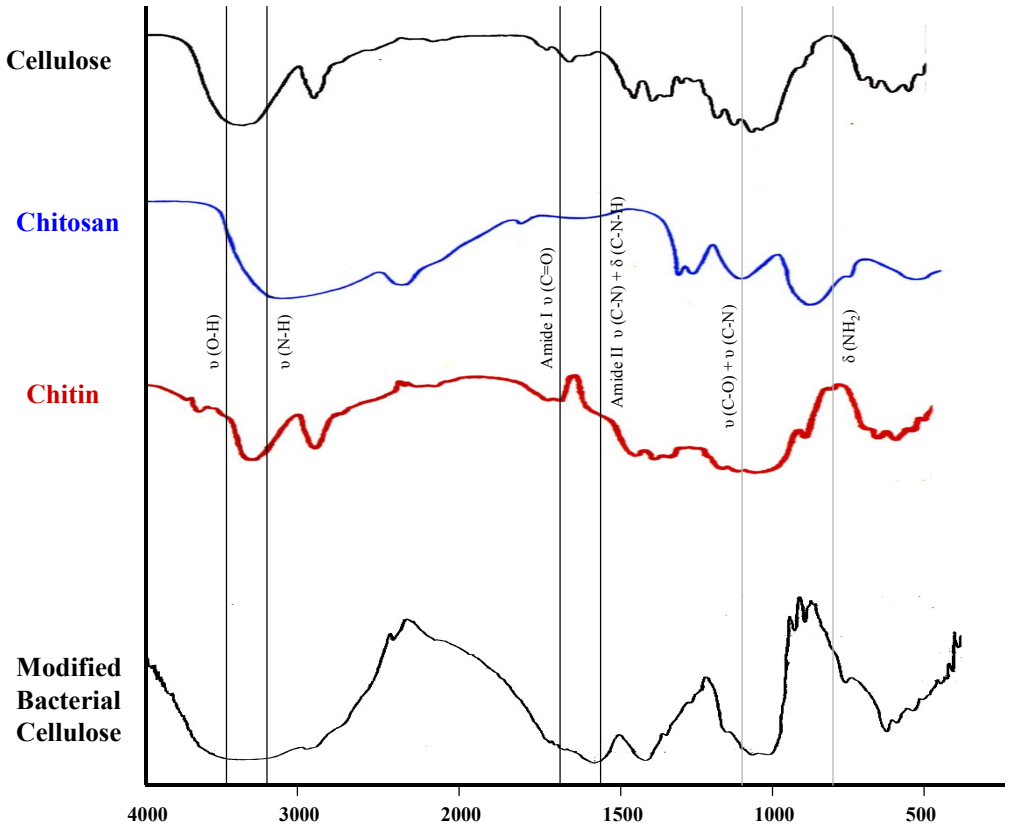

Figure S3. Comparison of the IR-spectra of modified bacterial cellulose and cellulose, chitosan, chitin.

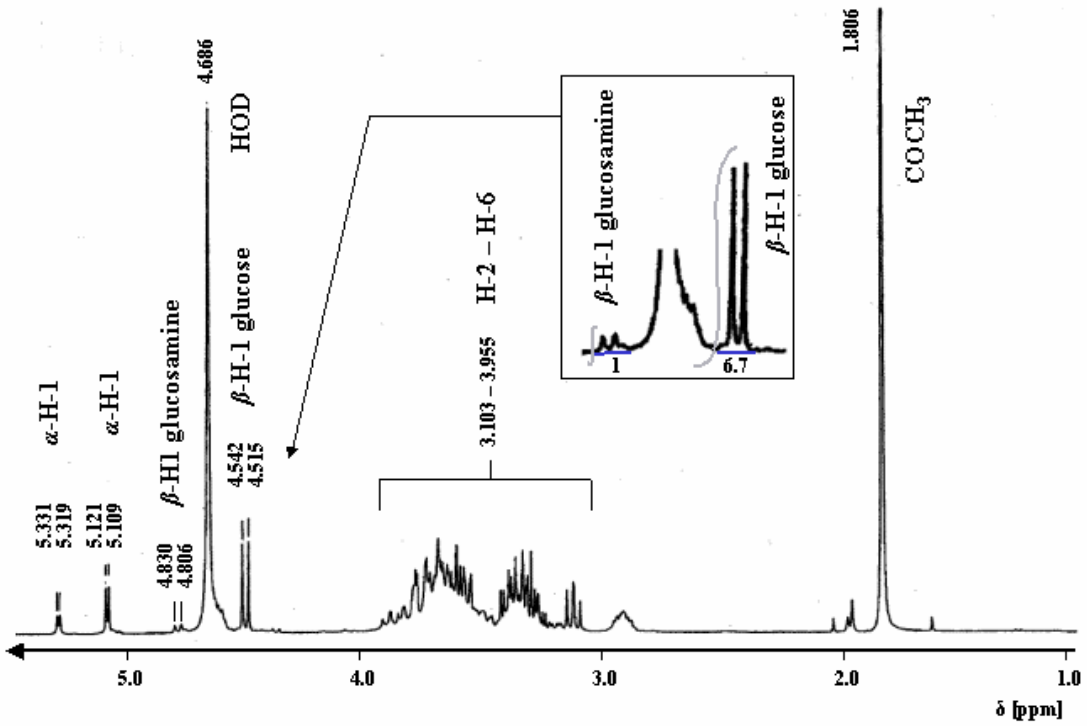

Figure S4. ^{1}H-NMR spectrum of chitosan modified bacterial cellulose in D_2O / DCl recorded at 300 MHz.

Table S2. Peak Assignment for the ^{1}H-NMR Spectrum of Chitosan Modified Bacterial Cellulose.

Chemical Shifts (reference HOD) [ppm]	Multiplett	Peak Assignment	Coupling Constants J [Hz]	Chemical Shifts References [ppm]	Coupling Constants References[Hz]
1.806	Singulett	-CO-C**H**$_3$			
3.103 – 3.955	Multiplett	-C**H**- (H-2 – H-6 glucose, glucosamine)		Chitobiose (A_2) (H-2 – H-6) 3.677 – 3.820 Cellobiose (H-2 – H-6) 3.19 – 4.03	
4.528	Dublett	-C**H**- (H-1 β-glucose)	$^3J_{(H1,H2)}$ = 8.1	Cellobiose (β-H-1 reducing end) 4.62 (β-H-1 non-reducing end) 4.50	
4.686	Singulett	**H**-O-D			
4.818	Dublett	-C**H**- (H-1 β-glucosamine)	$^3J_{(H1,H2)}$ = 8.0	Chitobiose (A_2) (β-H-1 reducing end) 4.700 (β-H-1 non-reducing end) 4.585	Chitobiose (A_2) $^3J_{(H1,H2)}$ = 8.7
5.115	Dublett	-C**H**- (H-1 α- sugar)	$^3J_{(H1,H2)}$ = 3.6	Chitobiose (A_2) (α-H-1 reducing end) 5.190 Cellobiose (α-H-1 reducing end) 5.30	Chitobiose (A_2) $^3J_{(H1,H2)}$ = 3.4
5.325	Dublett	-C**H**- (H-1 α- sugar)	$^3J_{(H1,H2)}$ = 3.6		

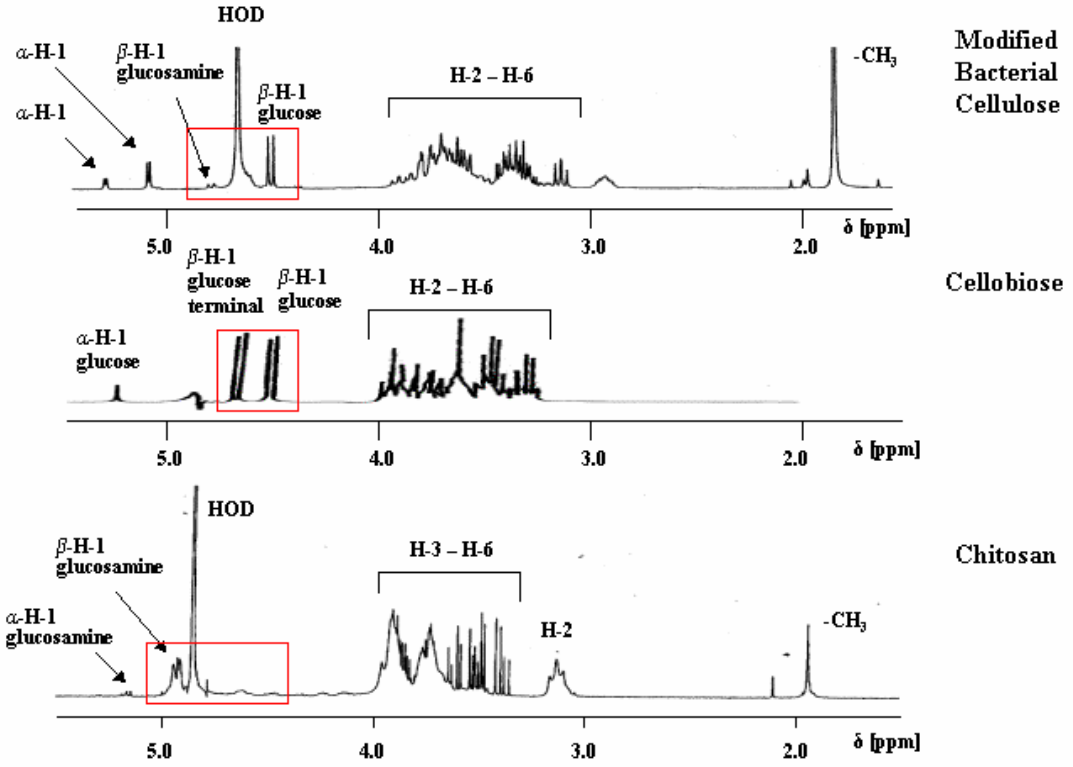

Figure S5. Comparison of the ^{1}H-NMR spectra of chitosan, cellobiose and modified bacterial cellulose.

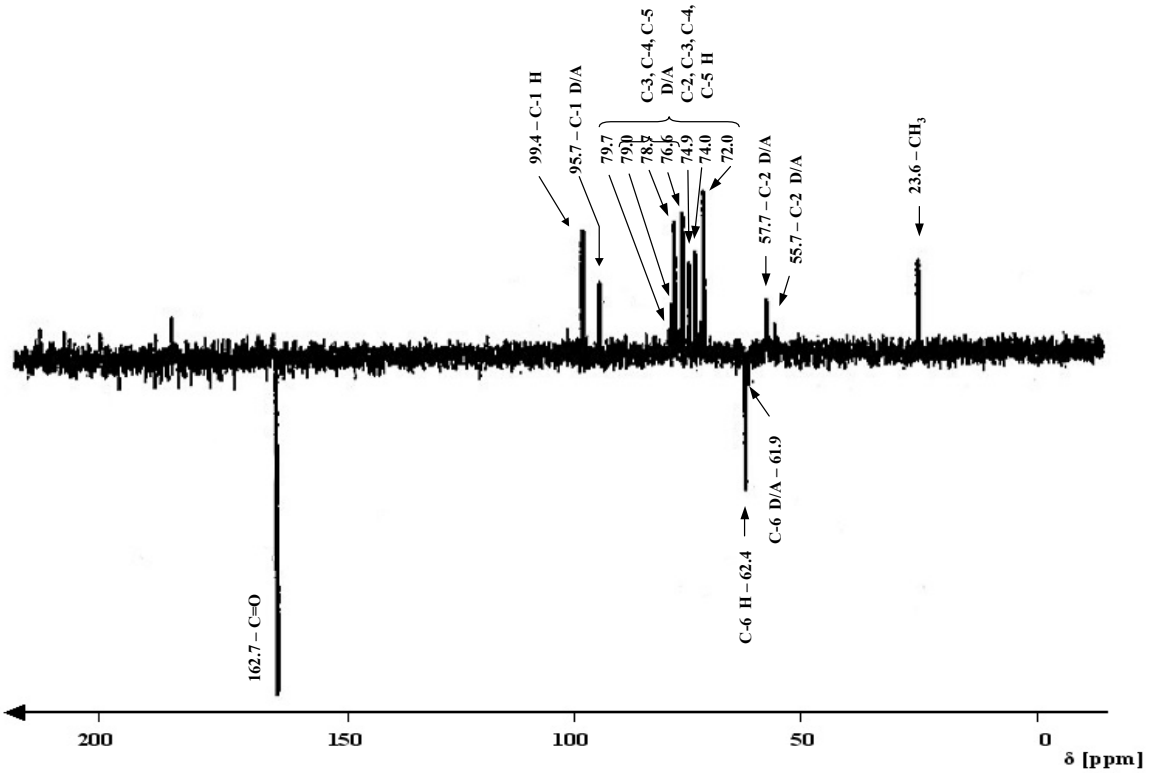

Figure S6. APT-^{13}C-NMR spectrum of chitosan modified bacterial cellulose (in D_2O / DCl, 300 MHz).

Table S3. Peak Assignment for the ^{13}C-NMR Spectrum of Chitosan Modified Bacterial Cellulose.

Chemical Shift [ppm]	Peak Assignment	Chemical Shifts References [ppm]
23.6	-CH_3	Chitosan Acetyl: 23.0
55.7	C-2 chitosan	Chitosan C-2: 55.8 A**A**A; 56.6 D**D**D
57.7	C-2 chitosan	Chitosan C-2: 57.5 DD**A** / DD**D**
61.9	C-6 chitosan	Chitosan C-6: 61.0 D**D**D; 61.1 DD**D**
62.4	C-6 cellulose	Cellobiose C-6: 62.4 H**H**; 61.8 **H**H Cellulose C-6: 60.6
72.0	C-3, C-4, C-5 chitosan C-2, C-3, C-4, C-5 cellulose	Chitosan C-3: 73.0 A**A**A; 71.0 D**D**D Chitosan C-4: 77.4 D**D**D; 80.0 A**A**A Chitosan C-5: 75.3 A**A**A; 75.7 D**D**D Chitobiose C-2: 74.7 H**H**; 75.7 **H**H Cellulose C-2: 75.2 Chitobiose C-3: 77.2 H**H**; 76.1 **H**H Cellulose C-3: 75.2 Chitobiose C-4: 71.1 H**H**; 80.1 **H**H Cellulose C-4: 73.1 H**H**; 80.0 **H**H Chitobiose C-5: 77.2 H**H**; 75.7 **H**H Cellulose C-5: 75.2
74.0		
74.9		
76.6		
78.7		
79.0		
79.7		
95.7	C-1 chitosan	Chitosan C-1: 93.5 DD**D**; 98.4 D**D**D
99.4	C-1 cellulose	Cellobiose C-1: 97.1 H**H**; 103.9 **H**H
162.7	-C=O	Chitosan Carbonyl: 175.6 DD**A**

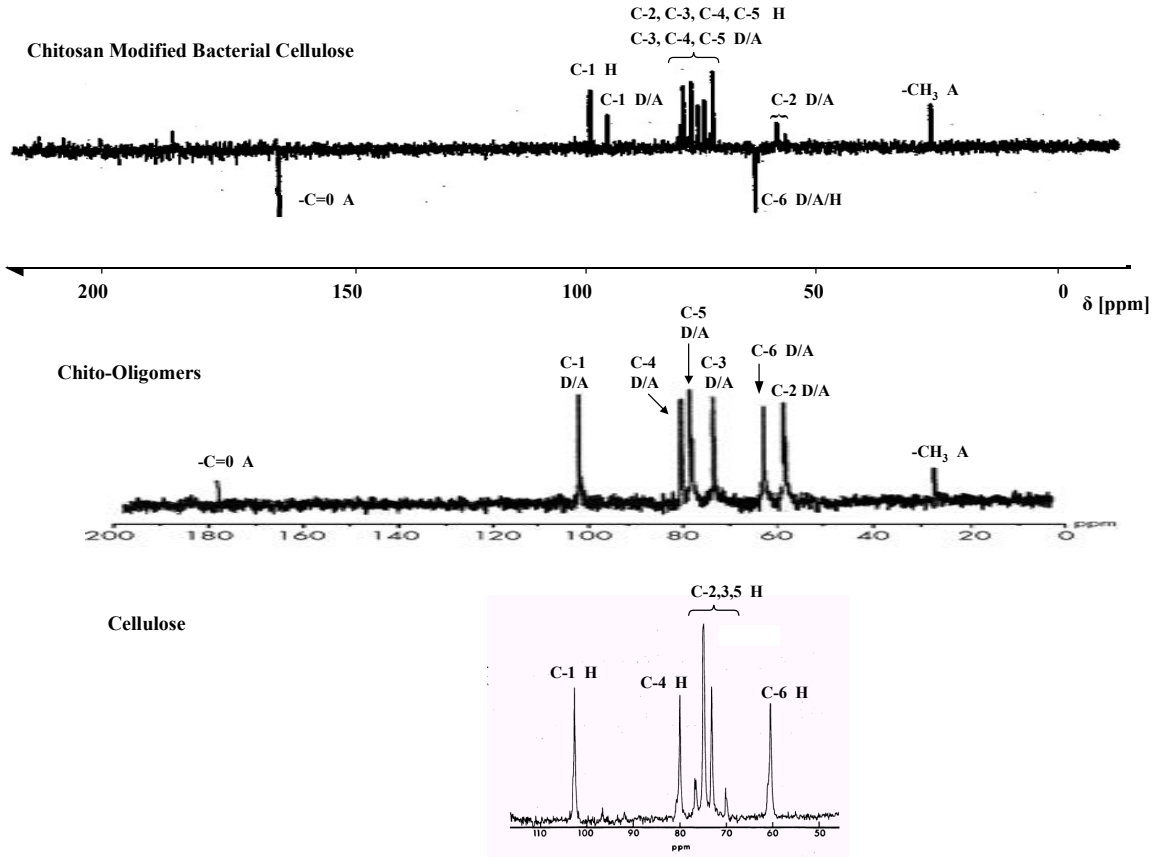

Figure S7. Comparison of the ^{13}C-NMR-spectra of chitosan modified bacterial cellulose, a mixture of chito-oligomers and cellulose.

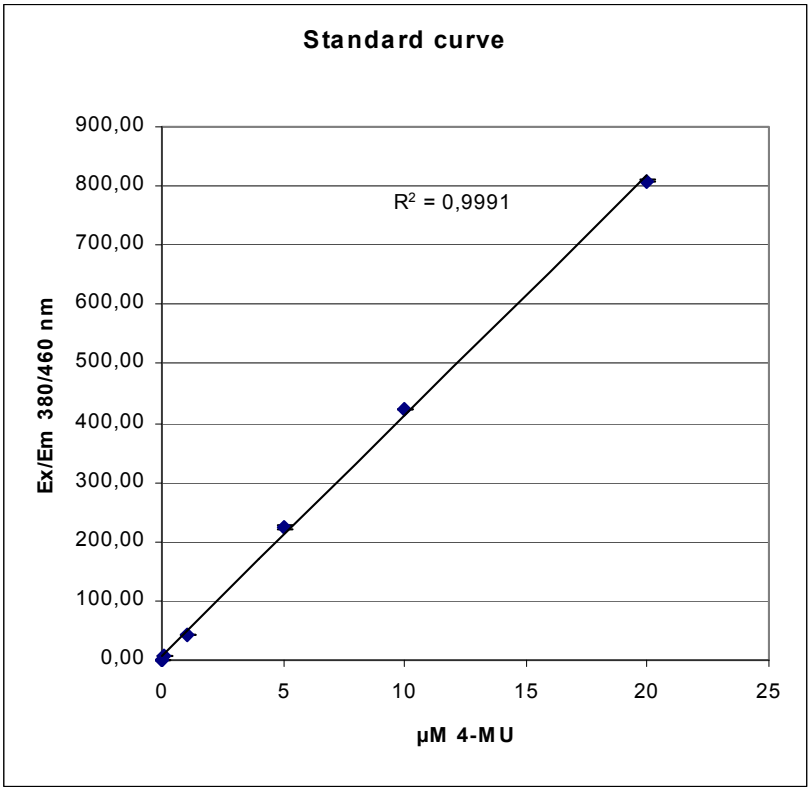

Figure S8. Standard curve of 4-MU release. Dependency of the fluorescence signal (excitation at 380 nm, emission at 460 nm) from the concentration of 4-MU.

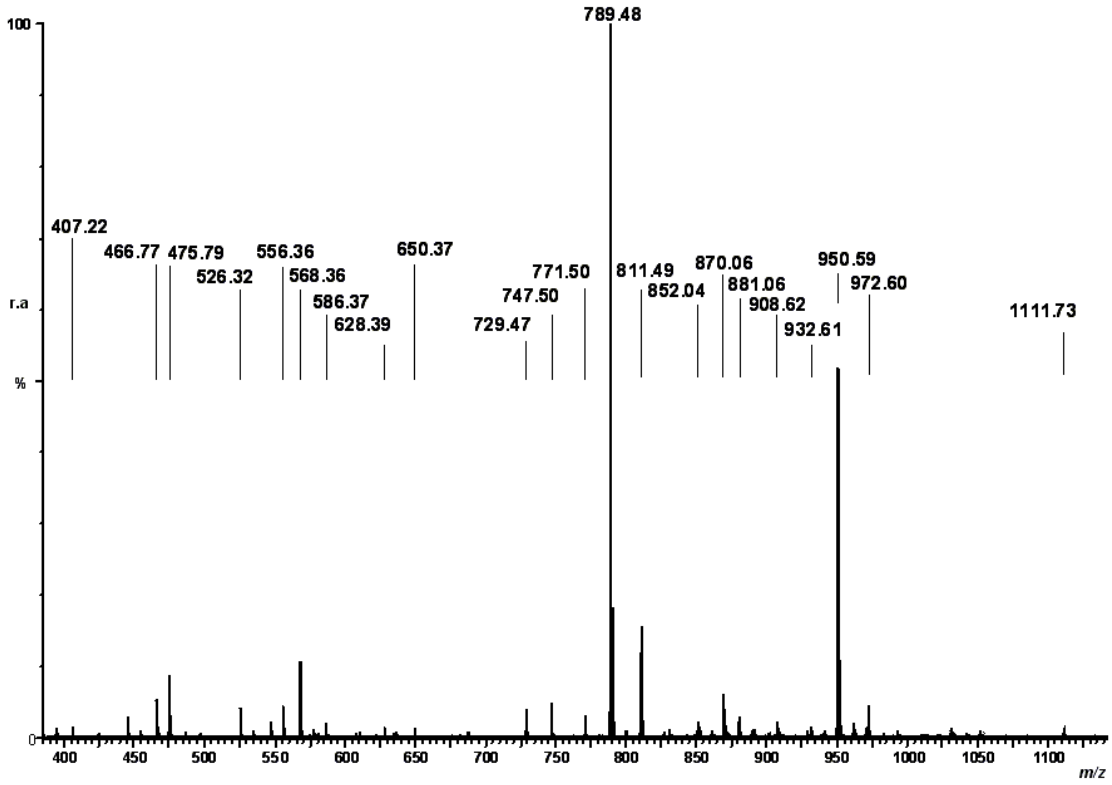

Figure S9. (+) nano ESI Q TOF MS of the chitooligosaccharide fraction used for incubation with ChiB.

Table S4. Oligomers and homologs present in the heterochitooligosaccharide fraction.

m/z	**assignment**
407.22 $[M\text{-}H_2O+2H]^{2+}$	A_4
526.32 $[M\text{-}H_2O+2H]^{2+}$	D_4A_2
586.37 $[M+H]^+$; 608.46 $[M+Na]^+$	D_1A_2
628.39 $[M+H]^+$; 650.37 $[M+Na]^+$	A_3
747.50 $[M+H]^+$; 729.47 $[M\text{-}H_2O+H]^+$	D_2A_2
789.48 $[M+H]^+$; 811.49 $[M+Na]^+$	**D_1A_3**
908.62 $[M+H]^+$; 890.73 $[M\text{-}H_2O+H]^+$	D_3A_2
950.59 $[M+H]^+$; 972.60 $[M+Na]^+$; 475.79 $[M+2H]^{2+}$; 466.77 $[M\text{-}H_2O+2H]^{2+}$	**D_2A_3**
1111.73 $[M+H]^+$; 556.36 $[M+2H]^{2+}$	D_3A_3

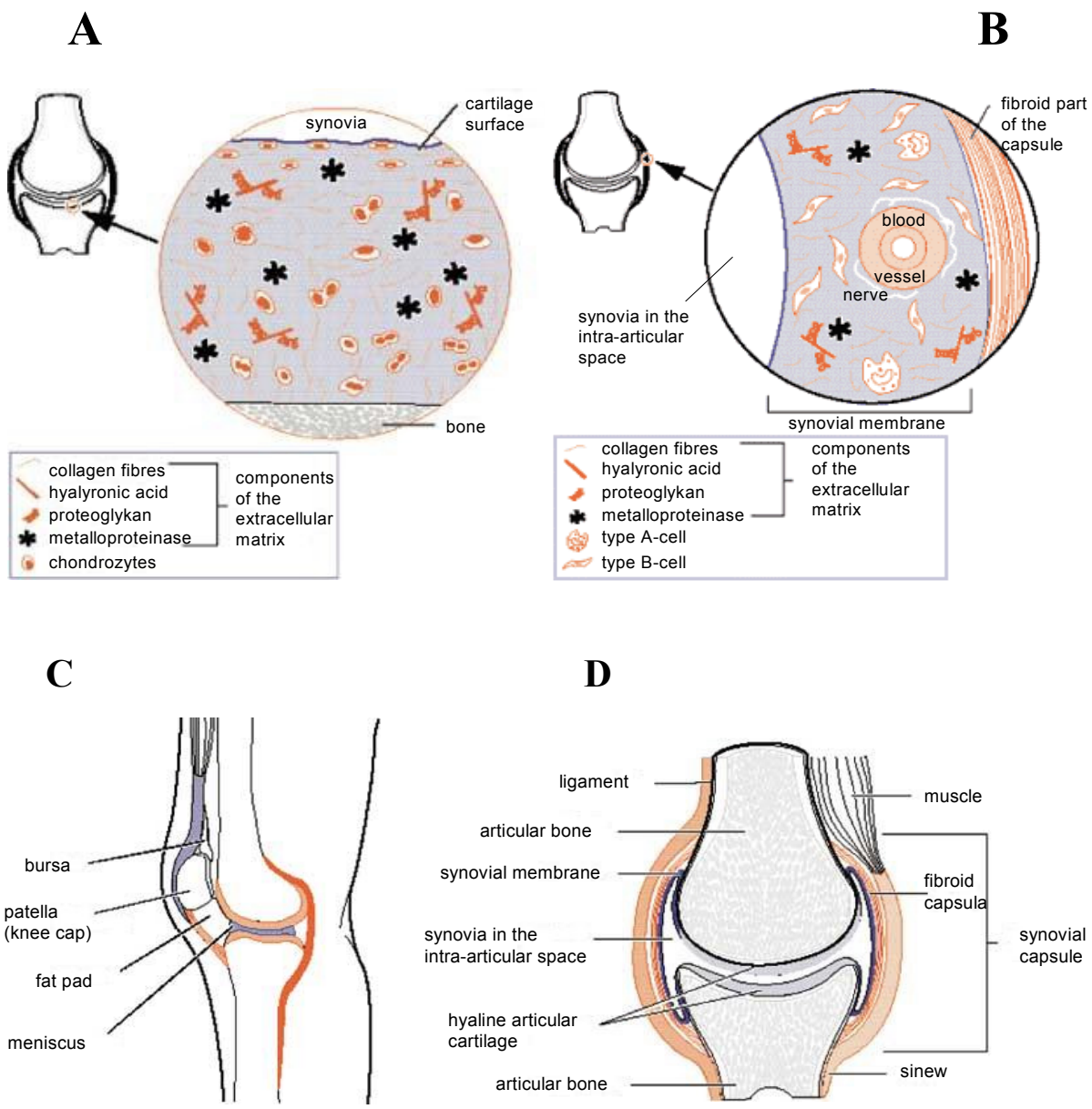

Figure S 10 A-D. Structure of the synovial joint. A, cut through the cartilage, which is located between the synovia and the bone. The cartilage contains collagen fibres, hyaluronic acid, proteoglycans and metalloproteinases. Chondrocytes are embedded in the cartilage matrix. B, cut through the joint capsule with the fibroid part, the cartilage part and the synovia. The cartilage part is intersected by blood vessels and nerves. C, cut through a knee joint. D, overview description of the parts of a synovial joint with the articular bone, the hyaline articular cartilage, the synovial membrane covering the synovia and the fibroid capsule which is covered by muscles and sinews. The figure was taken from literature [235].